ABSTRACT

Concentric bracing system is one of the most economical systems being used to provide lateral stability for steel structures during earthquake by inelastic behavior. Although inelastic response of structures is affected by their height and structural system, these issues are not considered for the design of concentrically braced frames (CBFs) in the current design codes. The previous research work on the economical comparison of steel bracing systems has compared their elastic response only, regardless of their plastic range. This work is aimed to study the inelastic behaviors and compare the weights of different CBFs (X-, V-, Inverted V- and Diagonal braced frames) in order to supply comprehensive information for design procedures.

Inelastic responses of the 4-, 8- and 12-story X-, V-, Inverted V- and Diagonal braced frames were assessed by the nonlinear static (pushover) analysis mainly based on FEMA 440 (2005). A new methodology was proposed for the economical comparison of the frames (subtracting the weight of a benchmark frame from the frame weights to calculate the pure bracing system weight) to overcome the inaccuracy of the procedures being used by the previous studies (using the total frame weight instead of the bracing system weight).

By conducting pushover analysis, it was found that the failure progress of all the frames was mainly due to the buckling of compression bracing members, but with some differences due to story height and frame type. Diagonal, Inverted V-, X- and V-braced frames generally have the highest to the lowest initial, elastic and post-

yield stiffness respectively. The changes in nonlinear responses of the frames due to the changes in the story height follow special and predictable rules and are generally has less effective on the results than the frame type. V-braced frame was found to have the highest target displacement point.

V-, Inverted V-, X- and Diagonal braced frames were found to be in order the lightest to the heaviest systems. The available economical comparison methodology for the bracing system was found to seriously undermine the differences among the results of the comparison whilst the methodology proposed in this work was observed to give more reliable results.

By estimating the energy dissipation per weight of all frames from the obtained results, it was observed that Inverted V-bracing system is the most efficient type for 4-story frames; V-bracing system is the most efficient for 12-story frames; X- and Diagonal bracing systems are the third and fourth efficient bracing systems respectively.

ÖZET

Deprem esnasında, esnek olmayan davranışı ile çelik yapılara yanal stabiliteyi en ekonomik bir şekilde sağlayabilen sistem Ortak Merkezli Destekleme sistemidir. Yapıların esnek olmayan davranışlarının yapı yükseklikleri ve yapı sisteminden etkilendiği bilinmekle birlikte bu konular günümüz tasarım kodlarında Ortak Merkezli Destekleme sistemleri için kullanılmamaktadır. Çelik bağlantı sistemlerinin ekonomik yönden karşılaştırması ile ilgili yapılmış geçmiş araştırmalar bu sistemlerin esnek davranışlarını incelemiş ve plastik davranışlarını gözardı etmiştir. Bu çalışmanın amacı farklı Ortak Merkezli Destekleme sistemlerinin (X-, V-, Ters V- ve Diagonal bağlanmış çerçevelerde) esnek olmayan davranışlarını inceleyerek tasarım kodlarına kapsamlı bilgi sağlamaktır.

Bu araştırmada 4-, 8- ve 12katlı, X-, V-, Ters V ve Diagonal bağlantılı çerçevelerin FEMA 440 (2005)'e göre linear olmayan statik (öteleme) analizi kullanılarak esnek olmayan davranışını incelemektir. Daha önce yapılan araştırmalarda görülen anomalilerden dolayı çerçevelerin ekonomik açıdan karşılaştırmaları için yeni bir yaklaşım önerilmiştir.

Öteleme analizi yaparken elde edilen sonuçlarda tüm çerçevelerin kırılmasının nedeni baskı altında olan bağlantı elemanlarının burkulması olduğu yönündedir, fakat bu kat tipi ve çerçeve tipine göre de farklılıklar gösterir. Diagonal, Ters V-, X- ve V- bağlantılı çerçeveler genelde sırası ile en yüksekten en düşüğe, ilk esneklik ve akma sonrası sertliğe sahipdirler. Çerçevelerin kat yükseklik değişiminden kaynaklanan ve linear olmayan davranışları özeldir ve tahmin edilebilir kuralları

takip eder ve bu davranışın sonuçlar üzerindeki etkisi çerçeve tipinin etkisinden azdır. V- bağlantılı çerçevenin en yüksek hedef sehim noktasına sahip olduğu anlaşılmıştır.

Sırası ile en hafiften en ağıra bağlantı sistemleri söyle sıralanabilir V-, Ters V-, X- ve Diagonal bağlantılar. Bağlantı sistemleri için bu güne kadar var olan ekonomik karşılaştırma metodlarının, karşılaştırma sonuçları arasındaki farklılıkları ciddi bir şekilde zayıflattığı, diğer yandan bu çalışmada önerilen yöntemin daha güvenilir sonuçlar verdiği görülmüştür.

Elde edilen sonuçlardan enerji dağılımının çerçeve ağırlığına olan dağılımı tahmin edilmiş ve 4 katlı çerçevelerde Ters V-, 12 katlı çerçevelerde de V- sisteminin en randımanlı bağlantı tipleri olduğu ve bunları daha düşük randımanlı olan X- ve Diagonal bağlantı sistemlerinin takip ettiği gözlemlenmiştir.

ACKNOWLEDGEMENTS

First and foremost, I would like to extend my deepest appreciation and gratitude to my family for being there for me all through my studies here. Their supports and encouragements are too numerous to mention.

I would also like to thank my supervisor, Asst. Prof. Dr. Murude Celikag for her contributions to the successful completion of this thesis. My thanks also go to the head of civil engineering department, Dr. Nilgun Hancioglu and all the instructors in the department and who have equally contributed to the success of this study.

Credits and appreciations are also given to the various individuals whose guidance helped in the actualization of this research work, especially Dr. Alireza Taghavi, Amir Ahmad Hedayat, Ehsan Yousefi, Siavash Sorooshian, Mohamad Sadri and Amin Asareh.

I would not forget to mention the invaluable supports of my friends, Mohamad Behnam, Shadi Radmehr, Obinna Onuaguluchi, Pedram Khajehhesameddin, Anoosheh Iravanian, Fatih Parlak, Saeid Kamkar, Amir Khanlou, Yasmin Chegini, Amin Abrishambaf, Milad Ebrahimi, Saman Esfandiarpour, Nasim Mosavat, Batu Ibrahimogullari, Temucin Yardimci, Sanaz Abbasi, Mana Behnam, Ahmad Haseeb Payab and Faruk Ibesevic, your friendship and exchange of ideas really helped in this thesis.

DEDICATION

I was able to fulfill my M.S. studies because of the efforts of several individuals.

To them, wherever they are, I dedicate this piece of work.

TABLE OF CONTENTS

ABSTRACT iii

ABSTRACT (TURKISH) v

ACKNOWLEDGEMENTS vii

DEDICATION viii

LIST OF FIGURES xvii

LIST OF TABLES xxiv

CHAPTER I: INTRODUCTION 1

1.1 Background 1

1.1.1 Preface 1

1.1.2 Literature Review 2

1.2 Objectives of the Study 8

1.3 Reasons for the Objectives 8

1.4 Guide to the Thesis 8

CHAPTER II: LITERATURE REVEIW 11

2.1 Types of Lateral Load Resisting Systems in Steel Structures 13

2.1.1 Steel Moment Frames 14

2.1.1.1 Fully Restrained Moment Frames 14

2.1.1.2 Partially Restrained Moment Frames 15

2.1.2 Steel Braced Frames 16

2.1.2.1 Concentrically Braced Frames 16

2.1.2.2 Eccentrically Braced Frames 19

2.1.2.3 Knee Braced Frames 20

2.1.3 Steel Plate Shear Walls 22

2.1.4 Steel Frames with Infills and Shear Cores 22
2.2 Structural Response Curve Evaluation Methods 22
2.2.1 Introduction 22
2.2.2 Structural Analysis Methods 23
2.2.3 Nonlinear Static (Pushover) Procedures 25
2.2.3.1 Introduction 25
2.2.3.2 Literature Review 27
2.2.3.3 Load Distribution in Pushover Analysis 28
2.2.3.3.1 Single-Mode Load Vectors 29
2.2.3.3.2 Multi-Mode Pushover Procedures 30
2.2.3.4 The Effects of Load Distribution in the Results of Pushover Analysis 33
2.2.3.5 Advantages and Disadvantages of Nonlinear Static Procedures 42
2.2.4 Nonlinear Dynamic Procedures 43
2.2.4.1 Introduction 43
2.2.4.2 Advantages and Disadvantages of Dynamic Procedures 43
2.3 A Background on Performance-based Engineering Procedures 46
2.3.1 Capacity-Spectrum Method of Performance Based Design 49
2.3.1.1 ATC-40 Capacity-Spectrum Method of Performance Based Design 49
2.3.1.2 FEMA 440 Evaluation of ATC-40 Capacity-Spectrum Procedure 53
2.3.1.3 FEMA 440 Improved Procedures for Equivalent of Linearization 55
2.3.2 Coefficient Method of Performance Based Design 56
2.3.2.1 FEMA 356 Coefficient Method 57
a) Rehabilitation Objectives 57
b) Structural Performance Levels and Ranges 58
c) Deformation-Controlled Versus Force-Controlled Behavior 60
d) Lateral Load Distribution 65

e) Idealized Force-Displacement Curve 65

f) Target Displacement 68

2.3.2.2 Evaluation of FEMA 356 Coefficient Method by FEMA 440 70

a) C_1 Evaluation 70

b) C_2 Evaluation 70

c) C_3 Evaluation 71

2.3.2.3 FEMA 440 Improved Procedures for Displacement Modification 71

a) C_1 Modification 71

b) C_2 Modification 72

c) C_3 Modification 72

2.3.3 Evaluation of Improved Nonlinear Static Procedures 72

2.3.3.1 Description of the Study 73

2.3.3.2 Results of the study 73

2.4 Inelastic Performance Assessment of Lateral Load Resisting Systems 75

2.5 Economical Comparison of Bracing Systems 81

2.6 Simultaneous Study on Weight and Inelastic Behavior of Bracing Systems 85

2.7 Conclusion 88

CHAPTER III: DESIGN OF MODEL STRUCTURES 90

3.1 Methodology of Design 90

3.1.1 Frame Geometry 90

3.1.1.1 Calculation of Weight of Bracing Members 92

3.1.1.2 Calculation of the Entire Frame Weight 93

3.1.1.3 Usage of Un-braced Benchmark Frames 93

3.1.1.4 Usage of X-braced Benchmark Frames Not Subjected to Lateral Loads 94

3.1.2 2-D versus 3-D Models 95

3.1.3 Design Criteria 97

3.1.4 Design Software 98
3.1.5 Design Material 98
3.1.6 Design Sections 99
3.1.7 Connections 100
3.1.8 Loading 100
3.1.9 Special V- and Inverted V-Bracing Shear Beam Considerations 101
3.2 Design Results 102
3.2.1 Design Results of 4-story frames 102
3.2.1.1 Design Results of 4-story X-braced Frame 102
3.2.1.2 Total Weight of 4-story X-braced Frame 103
3.2.1.3 Design Results of 4-story V-braced Frame 104
3.2.1.5 Design Results of 4-story Inverted V-braced Frame 105
3.2.1.6 Total Weight of 4-story Inverted V-braced Frame 105
3.2.1.7 Design Results of 4-story Diagonal braced Frame 106
3.2.1.8 Total Weight of 4-story Diagonal braced Frame 107
3.2.1.9 Design Results of 4-story Benchmark Frame 107
3.2.1.10 Total Weight of 4-story Benchmark Frame 108
3.2.2 Design Results of 8-story frames 109
3.2.2.1 Design Results of 8-story X-braced Frame 109
3.2.2.2 Total Weight of 8-story X-braced Frame 110
3.2.2.3 Design Results of 8-story V-braced Frame 110
3.2.2.5 Design Results of 8-story Inverted V-braced Frame 112
3.2.2.6 Total Weight of 8-story Inverted V-braced Frame 113
3.2.2.7 Design Results of 8-story Diagonal braced Frame 114
3.2.2.8 Total Weight of 8-story Diagonal braced Frame 115
3.2.2.9 Design Results of 8-story Benchmark Frame 116

3.2.2.10 Total Weight of 8-story Benchmark Frame 117
3.2.3 Design Results of 12-story frames 118
3.2.3.1 Design Results of 12-story X-braced Frame 118
3.2.3.2 Total Weight of 12-story X-braced Frame 120
3.2.3.3 Design Results of 12-story V-braced Frame 121
3.2.3.4 Total Weight of 12-story V-braced Frame 123
3.2.3.5 Design Results of 12-story Inverted V-braced Frame 124
3.2.3.6 Total Weight of 12-story Inverted V-braced Frame 126
3.2.3.7 Design Results of 12-story Diagonal braced Frame 127
3.2.3.8 Total Weight of 12-story Diagonal braced Frame 129
3.2.3.9 Design Results of 12-story Benchmark Frame 130
3.2.3.10 Total Weight of 12-story Benchmark Frame 132
CHAPTER IV: PUSHOVER ANALYSIS 134
4.1 Assessment of Nonlinear Behavior 134
4.2 Choice of the Method of Analysis 134
4.3 Choice of the Software for Computer Analysis 135
4.4 Pushover Load Pattern 136
4.5 Displacement-Based Pushover Analysis 136
4.6 Nonlinear Material Property 137
4.7 Failure Criteria 137
4.8 Plastic Hinge Properties 138
4.8.1 Column Hinge Properties 138
4.8.2 Brace Hinge Properties 139
4.8.3 Beam Hinge Properties 139
4.9 Idealization of Pushover Curve 139
4.10 Assessment of Bracing systems 140

CHAPTER V: RESULTS AND DISCUSSIONS 142
5.1 Pushover Curves and Failure Progresses 142
5.1.1 Pushover Curve and Failure Progress of 4-story X-braced Frame 142
5.1.2 Pushover Curve and Failure Progress of 4-story V-braced Frame 144
5.1.3 Pushover Curve and Failure Progress of 4-story Inverted V-braced Frame 145
5.1.4 Pushover Curve and Failure Progress of 4-story Diagonal braced Frame 146
5.1.5 Pushover Curve and Failure Progress of 8-story X-braced Frame 147
5.1.6 Pushover Curve and Failure Progress of 8-story V-braced Frame 148
5.1.7 Pushover Curve and Failure Pattern of 8-story Inverted V-braced Frame 150
5.1.8 Pushover Curve and Failure Progress of 8-story Diagonal braced Frame 151
5.1.9 Pushover Curve and Failure Progress of 12-story X-braced Frame 153
5.1.10 Pushover Curve and Failure Progress of 12-story V-braced Frame 155
5.1.11 Pushover Curve and Failure Progress of 12-story Inverted V-braced Frame ... 157
5.1.12 Pushover Curve and Failure Progress of 12-story Diagonal braced Frame 159
5.2 Categorizing the Pushover Curves by Number of Stories 160
5.2.1 Pushover Curves of 4-story Frames 161
5.2.2 Pushover Curves of 8-story Frames 162
5.2.3 Pushover Curves of 12-story Frames 163
5.3 Categorizing the Pushover Curves and Failure Patterns by Bracing System 164
5.3.1 Pushover Curves and Failure Patterns of X-braced Frames 164
5.3.2 Pushover Curves and Failure Patterns of V-braced Frames 166
5.3.3 Pushover Curves and Failure Patterns of Inverted V-braced Frames 167
5.3.4 Pushover Curves and Failure Patterns of Diagonal braced Frames 168
5.4 Idealized Pushover Curves 169
5.4.1 Idealized Response Curve of 4-story X-braced Frame 170
5.4.2 Idealized Response Curve of 4-story V-braced Frame 171

5.4.3 Idealized Response Curve of 4-story Inverted V-braced Frame 172
5.4.4 Idealized Response Curve of 4-story Diagonal braced Frame 173
5.4.5 Idealized Response Curve of 8-story X-braced Frame..... 174
5.4.6 Idealized Response Curve of 8-story V-braced Frame..... 175
5.4.7 Idealized Response Curve of 8-story Inverted V-braced Frame 176
5.4.8 Idealized Response Curve of 8-story Diagonal braced Frame 177
5.4.9 Idealized Response Curve of 12-story X-braced Frame..... 178
5.4.10 Idealized Response Curve of 12-story V-braced Frame..... 179
5.4.11 Idealized Response Curve of 12-story Inverted V-braced Frame 180
5.4.12 Idealized Response Curve of 12-story Diagonal braced Frame 181
5.5 Categorizing Idealized Pushover Curves by Number of Stories 182
5.5.1 Idealized Response Curves of 4-story Frames 183
5.5.2 Idealized Response Curves of 8-story Frames 184
5.5.3 Idealized Response Curves of 12-story Frames 186
5.6 Categorizing Idealized Pushover Curves by Bracing System 187
5.6.1 Idealized Response Curves of X-braced Frames..... 188
5.6.2 Idealized Response Curves of V-braced Frames..... 189
5.6.3 Idealized Response Curves of Inverted V-braced Frames 190
5.6.4 Idealized Response Curves of Diagonal braced Frames 191
5.7 Idealizing Disadvantageous Effects 191
5.8 Discussion on Weight Results 192
5.8.1 Weight Results comparison of 4-story Frames 193
5.8.2 Weight Results comparison of 8-story Frames 195
5.8.3 Weight Results comparison of 12-story Frames 197
CHAPTER VI: SUMMARY AND CONCLUSION 201
6.1 Summary..... 201

6.2 Major Findings 203
6.2.1 Failure Progresses 203
6.2.2 Actual Structural Response Curve Conclusions 204
6.2.3 Idealization Conclusions 205
6.2.4 The effect of number of stories 205
6.2.5 Economical Comparison 206
6.2.6 Overall Conclusions 206
6.3 Final Conclusion 207
6.4 Recommendations for Future Studies 208
REFERENCES 209
APPENDIX 223

LIST OF FIGURES

Figure 1.1: Variation of mean C_1 computed for the elastic perfectly plastic (EPP) model when subjected to ground motions recorded on site class *C* (Courtesy of Federal Emergency Management Agency). 5

Figure 1.2: Bilinear system with in-cycle negative post-elastic stiffness due to P- Δ effects (Courtesy of Federal Emergency Management Agency). 6

Figure 1.3: Comparison of responses for an oscillator with T = 0.2 s calculated using various procedures, response spectra scaled to the NEHRP spectrum, and values calculated for the NEHRP spectrum (Courtesy of Federal Emergency Management Agency). 7

Figure 2.1: 4-story X-braced frame. 17

Figure 2.2: 4-story concentric V-braced frame. 17

Figure 2.3: 4-story concentric Inverted V-braced frame. 18

Figure 2.4: 4-story diagonal braced frame. 18

Figure 2.5: 4-story Zipper-braced frame. 18

Figure 2.6: 4-story eccentric V-braced frame..... 20

Figure 2.7: 4-story eccentric Inverted V-braced frame. 20

Figure 2.7: 4-story knee-braced (a), X- (b), Diagonal (c), concentrically V- (d), eccentrically V (e), concentrically Inverted V (f) and eccentrically Inverted V- (g) braced frame frame. 21

Figure 2.8: Static and dynamic pushover analysis results for the regular frame structures (Courtesy of Mwafey & Elnashai, 2000). 35

Figure2.9a, b, c: Example results for displacements predicted by nonlinear static procedures (NSP) compared to nonlinear dynamic response-history analyses (NDA) (Courtesy of FEMA 440)..... 38

Figure 2.10.a,b: Dispersion in results for displacement for two levels of global drift. (Courtesy of FEMA 440)..... 40

Figure 2.11: Factors affecting seismic ground motion (Courtesy of FEMA 440). 44

Figure 2.12: Incremental dynamic analysis study for thirty ground motion records for a 5-story steel braced frame showing uncertainty in IDA due to dependency of the results on ground motion characteristics (Courtesy of Vamvatsikos & Cornell, 2002). 45

Figure 2.13: Schematic depiction of the use of inelastic analysis procedures to estimate forces and inelastic deformations for seismic ground motions and a nonlinear analysis model of the building (Courtesy of FEMA 440, 2005). 47

Figure 2.14: Graphical representation of the Capacity-Spectrum Method of equivalent linearization, as presented in ATC-40 (Courtesy of FEMA 440). 52

Figure 2.15: Mean error associated with the Capacity-Spectrum Method of ATC-40 for hysteretic behaviors types A, B, and C for site class C. 54

Figure 2.16: Component Force versus Deformation Curves (Courtesy of Federal Emergency Management Agency, FEMA 356). 62

Figure 2.17: Generalized Component Force- Deformation Relations for Depicting Modeling and Acceptance Criteria (Courtesy of FEMA 356). 63

Figure 2.18: Alternative Force-Deformation Curve (Courtesy of Federal Emergency Management Agency). 64

Figure 2.19: Idealized Force-Displacement Curves (Courtesy of Federal Emergency Management Agency). 67

Figure 2.20: Comparison of responses for an oscillator with T = 0.2 s calculated using various procedures (Courtesy of FEMA 440)..... 74

Figure 2.21: Comparison of responses for an oscillator with T = 0.5 s calculated using various procedures (Courtesy of FEMA 440)..... 74

Figure 2.22: Comparison of responses for an oscillator with T = 1.0 s calculated using various procedures (Courtesy of FEMA 440)..... 75

Figure 2.23: The effects of the type of bracing on the R value of the braced frames (Courtesy of Maheri & Akbari, 2003). 77

Figure 2.24: Comparison of the performance of commonly used steel frame systems (Courtesy of Huaung, Li & Chen, 2005). 78

Figure 2.25: Comparison of normalized weights of tall frames with different bracing systems against fixed support frame (Courtesy of Kameshki & Saka, 2001). 82

Figure 2.26: Inelastic response of a tension–compression concentrically braced steel frame (Courtesy of Tremblay 2002). 84

Figure 2.27: Pushover curves of the EBFs with shear yielding links (a) 9-storey frame (b) 3-storey frame (Courtesy of D. Ozhendekci & N. Ozhendekci, 2008). 86

Figure 2.28: Effects of the length of shear yielding links on the (a) normalized frame weights (b) normalized mean scale factors (c) coefficients of variation of scale factors (3-storey EBFs) (Courtesy of D. Ozhendekci & N. Ozhendekci, 2008). 87

Figure 3.1: X-braced 4-story frame. 96

Figure 3.2: X-braced 4-story frame. 96

Figure 3.3: Inverted V-braced 4-story frame. 97

Figure 3.4: Diagonal braced 4-story frame 97

Figure 3.5: Design Sections of 4-story X-braced frame. 103

Figure 3.6: Design Sections of 4-story V-braced frame. 104

Figure 3.7: Design Sections of 4-story Inverted V-braced frame. 105

Figure 3.8: Design Sections of 4-story Diagonal braced frame. 106

Figure 3.9: Design Sections of 4-story Benchmark frame. 108

Figure 3.10: Design Sections of 8-story X-braced frame. 109

Figure 3.11: Design Sections of 8-story V-braced frame. 111

Figure 3.12: Design Sections of 8-story Inverted V-braced frame. 113

Figure 3.13: Design Sections of 8-story Diagonal braced frame. 115

Figure 3.15.a: Design Sections of top 6 stories of 12-story X-braced frame. 119

Figure 3.15.b: Design Sections of bottom 6 stories of 12-story X-braced frame 120

Figure 3.16.a: Design Sections of top 6 stories of 12-story V-braced frame. 122

Figure 3.16.b: Design Sections of bottom 6 stories of 12-story V-braced frame 123

Figure 3.17.a: Design Sections of top 6 stories of 12-story Inverted V-braced frame. 125

Figure 3.17.b: Design Sections of bottom 6 stories of 12-story Inverted V-braced frame. 126

Figure 3.18.a: Design Sections of top 6 stories of 12-story Diagonal braced frame.... 128

Figure 3.18.b: Design Sections of bottom 6 stories of 12-story Diagonal braced frame. 129

Figure 3.19.a: Design Sections of top 6 stories of 12-story Benchmark frame..... 131

Figure 3.19.a: Design Sections of bottom 6 stories of 12-story Benchmark frame. 132

Figure 4.1: Lateral load–roof displacement relationship of a structure (Courtesy of Kim & Choi, 2005). 140

Figure 5.1: Pushover Curve of 4-story X-braced frame. 143

Figure 5.2.a: Failure moment condition of 4-story X-braced frame. 143

Figure 5.2.b: Plastic hinge level descriptions. 143

Figure 5.3: Pushover Curve of 4-story V-braced frame. 144

Figure 5.5: Pushover Curve of 4-story Inverted V-braced frame. 145

Figure 5.6: Collapse moment conditions of 4-story Inverted V-braced frame..... 145

Figure 5.7: Pushover Curve of 4-story Inverted Diagonal braced frame. 146

Figure 5.8: Collapse moment conditions of 4-story Diagonal braced frame. 146

Figure 5.9: Pushover Curve of 8-story X-braced frame. 147

Figure 5.10: Failure moment condition of 8-story X-braced frame. 148

Figure 5.11: Pushover Curve of 8-story V-braced frame. 149

Figure 5.12: Collapse moment conditions of 8-story V-braced frame. 149

Figure 5.13: Pushover Curve of 8-story Inverted V-braced frame. 150

Figure 5.14: Collapse moment conditions of 8-story Inverted V-braced frame..... 151

Figure 5.15: Pushover Curve of 8-story Inverted Diagonal braced frame. 152

Figure 5.16: Collapse moment conditions of 8-story Diagonal braced frame. 152

Figure 5.17: Pushover Curve of 12-story X-braced frame. 153

Figure 5.18: Failure moment condition of 12-story X-braced frame. 154

Figure 5.19: Pushover Curve of 12-story V-braced frame. 155

Figure 5.20: Collapse moment conditions of 12-story V-braced frame. 156

Figure 5.21: Pushover Curve of 12-story Inverted V-braced frame. 157

Figure 5.22: Collapse moment conditions of 12-story Inverted V-braced frame..... 158

Figure 5.23: Pushover Curve of 12-story Inverted Diagonal braced frame. 159

Figure 5.24: Collapse moment conditions of 12-story Diagonal braced frame. 160

Figure 5.25: Pushover Curves of 4-story Frames. 161

Figure 5.26: Pushover Curves of 8-story Frames. 162

Figure 5.27: Pushover Curves of 12-story Frames. 163

Figure 5.28: Force-Displacement pushover curves of X-braced frames. 165

Figure 5.29: Force-Global Drift pushover curves of X-braced frames. 165

Figure 5.30: Force-Displacement pushover curves of V-braced frames. 166

Figure 5.31: Force-Global Drift pushover curves of V-braced frames. 166

Figure 5.32: Force-Displacement pushover curves of Inverted V-braced frames..... 167

Figure 5.33: Force-Global Drift pushover curves of Inverted V-braced frames. 168

Figure 5.34: Force-Displacement pushover curves of Diagonal braced frames. 168

Figure 5.35: Force-Global Drift pushover curves of Diagonal braced frames. 169

Figure 5.36: Idealized and real structural response curve of 4-story X-braced frame. 171

Figure 5.37: Idealized and real structural response curve of 4-story V-braced frame. 172

Figure 5.38: Idealized and real structural response curve of 4-story Inverted V-braced frame. 173

Figure 5.39: Idealized and real structural response curve of 4-story Diagonal braced frame. 174

Figure 5.40: Idealized and real structural response curve of 8-story X-braced frame. 175

Figure 5.41: Idealized and real structural response curve of 8-story V-braced frame. 176

Figure 5.42: Idealized and real structural response curve of 8-story Inverted V-braced frame. 177

Figure 5.43: Idealized and real structural response curve of 8-story Diagonal braced frame. 178

Figure 5.44: Idealized and real structural response curve of 12-story X-braced frame.179

Figure 5.45: Idealized and real structural response curve of 12-story V-braced frame.180

Figure 5.46: Idealized and real structural response curve of 12-story Inverted V-braced frame. 181

Figure 5.47: Idealized and real structural response curve of 12-story Diagonal braced frame. 182

Figure 5.48: Idealized response curve of 4-story frames. 183

Figure 5.49: Idealized response curve of 8-story frames. 184

Figure 5.50: Idealized response curve of 12-story frames. 186

Figure 5.51: Idealized response curves of X-braced frames. 188

Figure 5.52: Idealized response curves of V-braced frames. 189

Figure 5.53: Idealized response curves of Inverted V-braced frames. 190

Figure 5.54: Idealized response curves of Diagonal braced frames. 191

Figure 5.55: Gross Weight of 4 story Frames (2nd Weight Comparison Method). 193

Figure 5.56: Normalized Gross Weight of 4 story Frames (2nd Weight Comparison Method). 194

Figure 5.57: Net Bracing Weight of 4-story Frames (4th Weight Comparison Method). 194

Figure 5.58: Normalized Net Bracing Weight of 4-story Frames (4th Weight Comparison Method). 195

Figure 5.59: Gross Weight of 8 story Frames (2nd Weight Comparison Method). 195

Figure 5.60: Normalized Gross Weight of 8 story Frames (2nd Weight Comparison Method). 196

Figure 5.61: Net Bracing Weight of 8-story Frames (4th Weight Comparison Method) 196

Figure 5.62: Normalized Net Bracing Weight of 8-story Frames (4th Weight Comparison Method)..... 197

Figure 5.63: Gross Weight of 12 story Frames (2nd Weight Comparison Method).... 197

Figure 5.64: Normalized Gross Weight of 12 story Frames (2nd Weight Comparison Method). 198

Figure 5.65: Net Bracing Weight of 12-story Frames (4th Weight Comparison Method). 198

Figure 5.66: Normalized Net Bracing Weight of 12-story Frames (4th Weight Comparison Method)..... 199

LIST OF TABLES

Table 2.1: Damage Control and Structural Performance Levels for Steel Braced Frames According to FEMA 356 (2000)..... 60

Table 3.1: Total weight of 4-story X-braced Frame..... 103

Table 3.2: Detailed weight information of 4-story X-braced Frame..... 103

Table 3.3: Total Weight of 4-story V-braced Frame..... 104

Table 3.4: Detailed Weight information of 4-story V-braced Frame..... 105

Table 3.5: Total Weight of 4-story Inverted V-braced Frame..... 106

Table 3.6: Detailed Weight information of 4-story Inverted V-braced Frame..... 106

Table 3.7: Total Weight of 4-story Diagonal braced Frame 107

Table 3.8: Detailed Weight information of 4-story Diagonal braced Frame 107

Table 3.9: Total Weight of 4-story Benchmark Frame. 108

Table 3.10: Detailed Weight information of 4-story Benchmark Frame. 108

Table 3.11: Total Weight of 4-story X-braced Frame..... 110

Table 3.12: Detailed Weight information of 4-story X-braced Frame..... 110

Table 3.13: Total Weight of 8-story V-braced Frame..... 111

Table 3.14: Detailed Weight information of 8-story V-braced Frame..... 112

Table 3.15: Total Weight of 8-story Inverted V-braced Frame..... 113

Table 3.16: Detailed Weight information of 8-story Inverted V-braced Frame..... 114

Table 3.17: Total Weight of 8-story Diagonal braced Frame. 115

Table 3.18: Detailed Weight information of 8-story Diagonal braced Frame. 116

Table 3.19: Total Weight of 8-story Benchmark Frame. 117

Table 3.20: Detailed Weight information of 8-story Benchmark Frame. 118

Table 3.21: Total Weight of 12-story X-braced Frame..... 120

Table 3.22: Detailed Weight information of 12-story X-braced Frame. 121

Table 3.23: Total Weight of 12-story V-braced Frame. 123

Table 3.24: Detailed Weight information of 12-story V-braced Frame. 124

Table 3.25: Total Weight of 12-story Inverted V-braced Frame..... 126

Table 3.26: Detailed Weight information of 12-story Inverted V-braced Frame..... 127

Table 3.27: Total Weight of 12-story Diagonal braced Frame. 129

Table 3.28: Detailed Weight information of 12-story Diagonal braced Frame..... 130

Table 3.29: Total Weight of 12-story Benchmark Frame. 132

Table 3.30: Detailed Weight information of 12-story Benchmark Frame. 133

Table 5.1: Idealizing parameters of structural response curve of 4-story X-braced frame. 170

Table 5.2: Idealizing parameters of structural response curve of 4-story V-braced frame. 171

Table 5.3: Idealizing parameters of structural response curve of 4-story Inverted V-braced frame. 172

Table 5.4: Idealizing parameters of structural response curve of 4-story Diagonal braced frame. 173

Table 5.5: Idealizing parameters of structural response curve of 8-story X-braced frame. 174

Table 5.6: Idealizing parameters of structural response curve of 8-story V-braced frame. 175

Table 5.7: Idealizing parameters of structural response curve of 8-story Inverted V-braced frame. 176

Table 5.8: Idealizing parameters of structural response curve of 8-story D-braced frame. 177

Table 5.9: Idealizing parameters of structural response curve of 12-story X-braced frame. 178

Table 5.10: Idealizing parameters of structural response curve of 12-story V-braced frame. 179

Table 5.11: Idealizing parameters of structural response curve of 12-story Inverted V-braced frame. 180

Table 5.12: Idealizing parameters of structural response curve of 12-story Diagonal braced frame. 181

Table 5.13: Force and Displacement quantity of yield and target displacement points of 4-story frames 183

Table 5.14: Force and Displacement quantity of yield and target displacement points of 8-story frames 185

Table 5.15: Force and Displacement quantity of yield and target displacement points of 8-story frames 186

Table 5.16: Comparison of Normalized Weight Results with second methodology. .. 199

Table 5.17: Comparison of Normalized Weight Results with fourth methodology..... 200

Table 6.1: Normalized energy dissipation over weight of bracing systems. 207

Table A.1: Table 5-4 of FEMA 356 (Courtesy of Federal Emergency Management Agency). 223

Table A.2.a: Part one of Table 5-6 of FEMA 356 (Courtesy of Federal Emergency Management Agency). 224

Table A.2.b: Part two of Table 5-6 of FEMA 356 (Courtesy of Federal Emergency Management Agency). 225

Table A.2.c: Part three of Table 5-6 of FEMA 356 (Courtesy of Federal Emergency Management Agency). 226

Table A.2.d: Part four of Table 5-6 of FEMA 356 (Courtesy of Federal Emergency Management Agency). 227

CHAPTER I

INTRODUCTION

1.1 Background

1.1.1 Preface

Every now and then, thousands of people loose their lives due to earthquakes in different parts of the world. Lateral stability has always been a major problem of steel structures especially in the areas with high earthquake hazard. The problem is clearly exemplified in Kobe earthquake in Japan and Northridge earthquake in the USA. This issue has been studied and concentric (such as X, Diagonal and chevron), eccentric and knee bracing systems have been suggested and consequently used by civil engineers for several decades.

Inelastic performance is one of the main factors influencing the choice of bracing systems. The bracing system that has a more plastic deformation before collapse can absorb more energy during the earthquake.

Different types of bracing systems have different construction costs and performances which are being compared with each other by engineers when designing structures.

1.1.2 Literature Review

Nonlinear response of bracing systems has been studied during the recent decades and as a result, seismic behavior factor, R, overstrength factor, Ω, and displacement amplification factor, C_d, is introduced to loading codes of practice such as UBC (Uniform Building Code) and IBC (International Building Code) that are widely used in the USA and other parts of the world. Since dealing with the actual performace levels are hard for design engineers, these parameters have been introduced by the codes to take the inelastic behavior of the bracing systems into account. In earthquake load calculation of a structure, seismic behavior factor is the parameter showing the effect of nonlinear performance of the bracing system, which is mainly influenced by the ductility of the system. These factors are key parameters influencing the efficiency of bracing since they directly affect the reduction of the earthquake loads of the structure. According to the loading codes, specific R, Ω and C_d factors are introduced for different structural systems (showing the difference of their nonlinear behavior), such as concrete moment frame and steel moment frame with high, medium and low ductility, steel frames with concrete shear walls and steel braced frames.

Moreover, further research has been done on assessment of nonlinear response of different structures, such as Steel X-braced and knee-braced reinforced concrete building (Maheri & Akbari R, 2003), response evaluation of reinforced concrete frames strengthened with steel bracing (Tasnimi & Masoomi, 1999), pushover tests on concentric and eccentric steel braced reinforced concrete frames (Mahri & Kousari & Razazan, 2003), establishing R factor and C_d , the displacement amplification factor, for building seismic provisions (Uang, 1991), evaluation of

strength reduction factors for earthquake-resisting design (Miranda & Bertero, 1994), evaluation of behavior factors on the basis of ductility and overstrength studies (Kappos, 1999).

On the other hand, from economical point of view, different types of bracing systems have been compared by Kameshki and Saka (2001) using linear design procedures. This shows that the effect of different ductility rates has not been taken into consideration.

Although separate response modification factors are not mentioned for different steel concentric bracing systems in the loading codes, inelastic response varies from one type to another. This leads to neglecting the differences of nonlinear behavior among various types of bracing systems in design. The earthquake load applied on the structure is calculated from equation 1.1.

$$C = \frac{A.B.I}{R} \tag{1.1}$$

(Where A, B and I reflect the values for site seismicity, soil type and importance factor of the structure)

Thus, economical comparison of different bracing types will not be valid unless the individual ductility levels are taken into consideration. In other words, the systems which are designed and expected to perform nonlinearly are compared linearly.

It has been observed that structural and seismic engineering procedures have been subjected to great changes during the last decades. Changing the codes of practice and introduction of new reports from Federal Emergency Management Agency (FEMA) show some of these changes. Although the current design codes are based on the recent research findings, the fast speed of improvement in nonlinear structural analysis procedures leads to requirement of more studies based on the current analysis procedures in order to assess the nonlinear behavior of structural systems.

The influence of neglecting the inelastic response of different concentric braces is not only limited to the economical aspect. Figure 1.1 (FEMA 440) gives the effect of frame response modification factor on the Coefficient Method (FEMA 356) of performance-based design of structures.

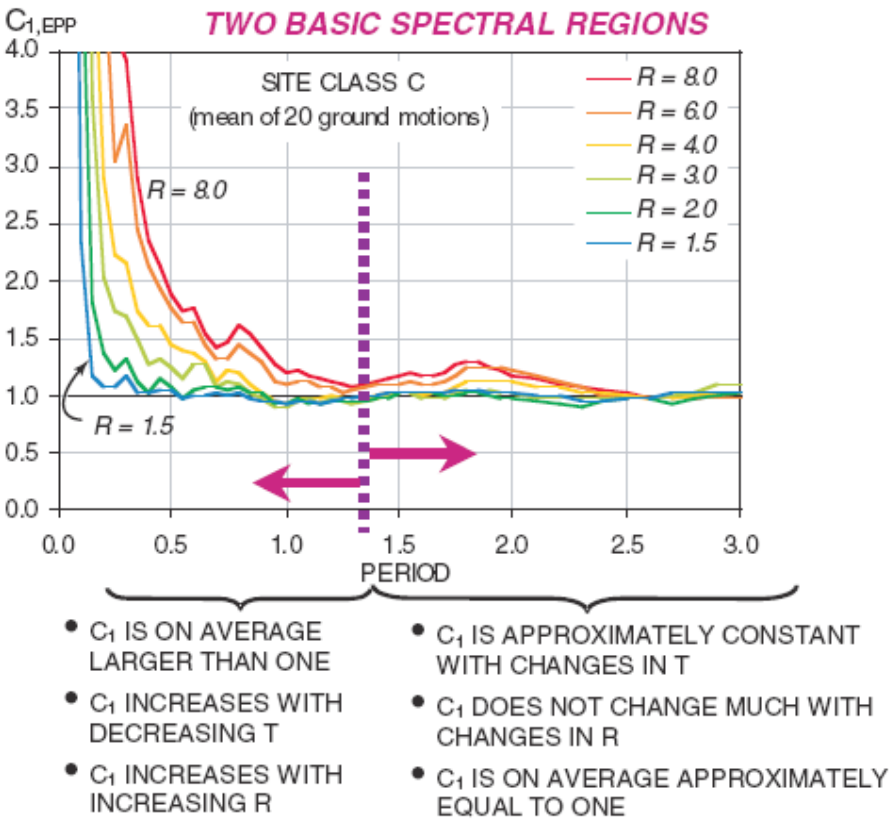

Figure 1.1: Variation of mean C_1 computed for the elastic perfectly plastic (EPP) model when subjected to ground motions recorded on site class *C* (Courtesy of Federal Emergency Management Agency).

Figure 1.1 simply shows the effect of ductility on Coefficient Based performance-based engineering procedure of FEMA 356 because of the resulting change in C_1 Coefficient due to the change in *R*.

Moreover, Coefficient C_3 is also affected by *R* as shown in Figure 1.2.

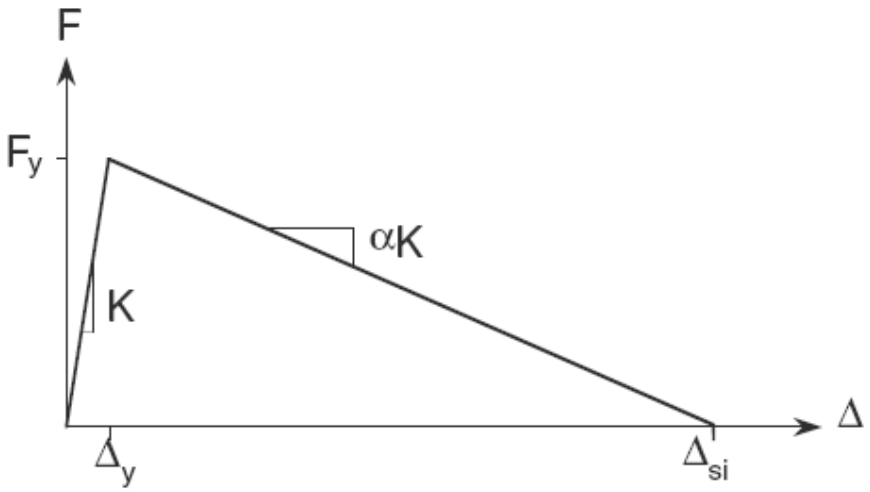

Figure 1.2: Bilinear system with in-cycle negative post-elastic stiffness due to *P*- Δ effects (Courtesy of Federal Emergency Management Agency).

Performance-based engineering procedures of FEMA 356 (Coefficient Method), ATC-40 (ADRS) and FEMA 440 (Modified Coefficient Method and MADRS) are described in the literature review.

After studying several nonlinear oscillators by different static and dynamic procedures, the following results in Figure 1.3 were achieved, as it was predicted by the information from Figures 1.1 and 1.2.

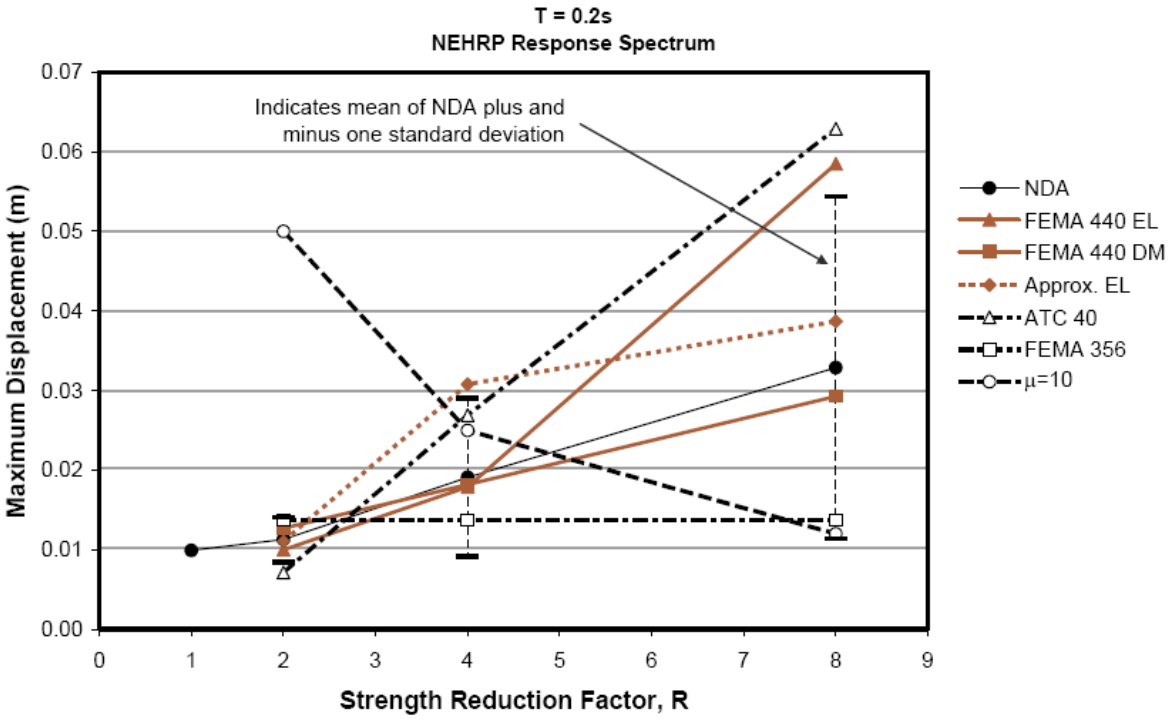

Figure 1.3: Comparison of responses for an oscillator with $T = 0.2$ s calculated using various procedures, response spectra scaled to the NEHRP spectrum, and values calculated for the NEHRP spectrum (Courtesy of Federal Emergency Management Agency).

FEMA 440 also states that "The results obtained using nonlinear dynamic analysis (NDA) indicate that for short-period oscillators, the maximum displacement response amplitude increases with decreasing strength (increasing *R*), while for longer-period oscillators the peak displacement response is less sensitive to strength", while according to Maheri and Akbari (2003), *R* decreases as the building height (and period) increase. This fact also necessitates the variability of R factors introduced according to the building height (in addition to the bracing type) in order to reach more accurate results in Performance Based Design of structures.

1.2 Objectives of the Study

This study aims to do a quantitative comparison between ductility levels of different steel bracing systems and compare the results from the economical point of view which is mainly based on the most recent research findings in the field of nonlinear structural analysis. By studying both weight and performance of the bracing systems simultaneously, the project states a more realistic comparison between them.

1.3 Reasons for the Objectives

All of the steel framed structures being designed and constructed require bracing system. Economy and performance are the two parameters influencing the type of structural systems to be used, especially bracing systems. By comparing these two parameters, this research can form the basis for new methods of evaluation for bracing systems.

On the other hand, accurate information about nonlinear behavior of different structural systems leads to higher quality in their design.

1.4 Guide to the Thesis

This study is comprised of six chapters.

Chapter two includes literature review, being divided into six sections. The first section (section 2.1) is devoted to the introduction of different types of lateral load resisting systems for steel structures such as bracing systems. Concentric bracing system is then described as one of the major steel bracing systems. Section 2.2

introduces different methods of evaluation of structural response curve. These methods (nonlinear static and nonlinear dynamic procedures) are comprehensively described with their history, usage, advantages and disadvantages in this section. In section 2.3, FEMA 356 (Coefficient Method), ATC-40 (ADRS) and FEMA 440 (Modified Coefficient Method and MADRS) Performance-based engineering procedures are described. Then, a comparison of all of these procedures is given from FEMA440. Sections 2.4, 25 and 2.6 are devoted to review of past research on the characteristics of bracing systems. They review the research being carried out on inelastic performance assessment, economical comparison and on both inelastic performance and economy of bracing systems simultaneously, respectively.

Chapter three is devoted to design of the model frames. The methodology of design of the structures and economical comparison of the bracing systems are first introduced in section 3.1. Then, the results of design of the frames including frame sections and weights are given in section 3.2.

Methodology of pushover analysis, evaluation of the actual pushover curve, idealizing the response curve is given in chapter four.

Chapter five includes results and discussion. This chapter is divided into eight sections. Actual pushover curves of the frames are given in section 5.1. Their failure progress is also explained explicitly in this section. The actual capacity curves are categorized by number of stories and bracing system in sections 5.2 and 5.3. Idealized response curves are given in section 5.4. At the next step, these curves are categorized by number of stories and bracing system in sections 5.5 and 5.6. Section 5.7 discusses the disadvantages of idealization. Economical comparison of bracing systems is given in section 5.8.

Chapter six includes summary and conclusion. A summary of what has been done and the consequential findings are given in sections 6.1 and 6.2 respectively. The final conclusion of the thesis is included in section 6.3. Section 6.4 introduces recommendations for future studies.

CHAPTER II

LITERATURE REVIEW

Different kinds of lateral load resisting systems commonly used in steel structures, such as, Steel Moment Frames, Steel Braced Frames, Steel Frames with steel plate shear wall, Steel Frames with infills and shear cores are introduced in section 2.1. A review on common methods of evaluation of structural response curve is done in section 2.2. Performance-based engineering procedures are reviewed in section 2.3. Then, the past research on inelastic performance assessment (section 2.4), economical comparison (section 2.5) and on assessing ductility and doing economical comparison of bracing systems simultaneously (section 2.6) are given in this chapter.

FEMA and ATC are cited in this chapter for many times. Thus, short description of them are given here.

On March 1, 2003, the Federal Emergency Management Agency (FEMA) became part of the U.S. Department of Homeland Security (DHS). The primary mission of the Federal Emergency Management Agency is to reduce the loss of life and property and protect the Nation from all hazards, including natural disasters (a hurricane, an earthquake, a tornado, a flood, a fire or a hazardous spill), acts of terrorism, and other man-made disasters, by leading and supporting the Nation in a risk-based, comprehensive emergency management system of preparedness, protection, response, recovery, and mitigation (http://www.fema.gov/about/index.shtm). Since earthquake is one of the greatest

natural disasters, FEMA has released different reports and documents regarding earthquake. FEMA 440 (2005), *Improvement of Nonlinear Static Seismic Analysis Procedures*, FEMA 273 and 274 (1997), *NEHRP*[1] *provisions and commentary for the seismic rehabilitation of buildings*, FEMA 356 (2000), *Prestandard and Commentary for the Seismic Rehabilitation of Buildings*, FEMA P695 (2009), Quantification of Building Seismic Performance Factors, FEMA-368 (2001), *NEHRP recommended provisions for seismic regulations for new buildings and other structures*, FEMA-445 (2006), *Next-Generation Performance-Based Seismic Design Guidelines Program Plan for New and Existing Buildings*, FEMA 355 (2000), *State of the Art Report on Systems Performance of Steel Moment Frames Subject to Earthquake Ground Shaking* are mainly used in this study. Full bibliographic information of these documents is available in the references.

"The Applied Technology Council (ATC) is a nonprofit, tax-exempt corporation established in 1973 through the efforts of the Structural Engineers Association of

---

[1] National Earthquake Hazards Reduction Program. NEHRP has four main goals:

- "Develop effective practices and policies for earthquake loss reduction and accelerate their implementation.
- Improve techniques for reducing earthquake vulnerabilities of facilities and systems.
- Improve earthquake hazards identification and risk assessment methods, and their use.
- Improve the understanding of earthquakes and their effects."

(http://www.nehrp.gov/about/index.htm)

California." ATC aims to develop and promote state-of-the-art, user-friendly engineering resources and applications for use in mitigating the consequences of natural and other hazards on the built environment. ATC identifies and encourages needed research and develops consensus opinions on structural engineering issues. ATC is guided by a Board of Directors consisting of representatives chosen by the American Society of Civil Engineers (ASCE), the National Council of Structural Engineers Associations, the Structural Engineers Association of California (SEAOC), the Western Council of Structural Engineers Associations, and four at-large representatives concerned with the practice of structural engineering. Project management and administration are done by a full-time Executive Director and support staff. Project work of ATC incorporates the experience of many individuals from academia, research, and professional practice who would not be available from any single organization (http://www.atcouncil.org/purpose.shtml). ATC has released different documents regarding earthquake engineering among which is ATC-40, *Seismic Evaluation and Retrofit of Concrete Buildings*. This document is mainly used in this study.

2.1 Types of Lateral Load Resisting Systems in Steel Structures

Steel frames are usually categorized by their lateral load resisting system, such as, Steel Moment Frames, Steel Braced Frames, Steel Frames with steel plate shear wall, Steel Frames with infills (reinforced concrete or masonry) and shear cores. Each of these systems has been studied by a great number of researchers.

Huaung, Li and Chen (2005) divide steel frames into four categories; moment resisting, concentrically braced, eccentrically braced and knee braced frame.

2.1.1 Steel Moment Frames

The key parameter affecting the linear and nonlinear behavior of steel moment-resisting frames is generally the connection configuration and detailing (FEMA 356). Therefore, various connection types and acceptance criteria for them are provided in different standards and reports, such as, Table 5-4 of FEMA 356 [Appendix] or AWS D.1.1. FEMA 356 divides steel moment frames into two categories as fully and partially restrained moment frames.

2.1.1.1 Fully Restrained Moment Frames

FEMA 356 (2000) introduces Fully Restrained (FR) moment frames as those moment frames with connections that are identified as FR in its Table 5-4 [Appendix]. The connections should be checked using this table.

Moment frames with connections that are not included in Table 5-4 of FEMA 356 [Appendix] are suggested to be defined as FR by this report if the following two conditions are applicable:

- The deformations of the joints (without panel zone deformation) do not contribute more than 10% to the total frame lateral deflection.
- The connection is necessarily as strong as (or stronger than) the weaker of the two members it is connecting.

Fully restrained moment frames are divided into Special Moment Frames and Ordinary Moment Frames by AISC (1997) Seismic Provisions.

2.1.1.2 Partially Restrained Moment Frames

FEMA 356 (2000) introduces Partially Restrained (PR) connections in its Table 5-4 [Appendix] and defines Partially Restrained (PR) moment frames as moment frames with connections identified as PR in the above mentioned table. Moment frames with connections that are not included in Table 5-4 [Appendix] are suggested to be defined as PR if one or two of the two following conditions are applicable:

- The beam-to-column joint deformations contribute more than 10% to the total frame lateral deflection.

- The connection strength is less than the strength of the weaker of the two members they join. For a PR connection with two or more failure modes, the weakest failure mechanism is suggested to be considered to govern the joint behavior.

Overall, the moment resisting frames have a disadvantage of proper energy dissipation but also high construction cost. These costs are especially increased because those sections passing strength checks are usually subject to increase in weight due to drift checks. These facts are stated by a number of past researches.

Huaung, Li and Chen (2005) describe MRF as an excellent energy dissipating system but they continue to add that in order to meet the drift requirements, the frame members have to be designed with uneconomically large sections in this system.

Kameshki and Saka (2001) state that moment resisting connection alone is generally not adequate for stiffening tall buildings due to its high cost. Lateral drift of high rise structures increases exponentially by the increase in the building height and so does

the amount of steel needed to resist lateral drift. They introduced lightweight columns and beams connected with bolted joints, which cannot transmit moments, with internal bracings as alternatives to provide an economical solution to the lateral drift problem instead of this system.

2.1.2 Steel Braced Frames

FEMA 356 (2000) describes steel braced frames as those frames that develop seismic resistance primarily through components of axial forces. These components are called bracing members. Steel braced frames are mainly categorized as: Concentrically Braced Frames (CBFs), Eccentrically Braced Frames (EBFs) and Knee Braced Frames (KBFs).

2.1.2.1 Concentrically Braced Frames

FEMA 356 (2000) define concentrically braced frames (CBF) as braced frames where the intersection of the component worklines are at a single point in a joint, or at multiple points such that the distance between points of intersection (eccentricity) is at least equal to the width of the smallest member that is connected at the joint.

CBFs are mainly divided into two as ordinary concentrically braced frames (OCBFs) and special concentrically braced frames (SCBFs). SCBFs have especial connection checklist that should be checked from AISC 1999. In this system, the bracing members resist the lateral load with the aid of the semi rigid connections.

Concentrically braced frames are geometrically categorized as:

- X-braced frames (Figure 2.1)
- Concentric V-braced frames (Figure 2.2)

- Concentric Inverted V-braced frames (Figure 2.3)

- Diagonal braced frames (Figure 2.4)

- Others –that are not of the same importance and usage compared to the above named ones. These systems could be exemplified by truss systems being used for lateral load resistance (such as zipper-braced frames shown in Figure 2.5).

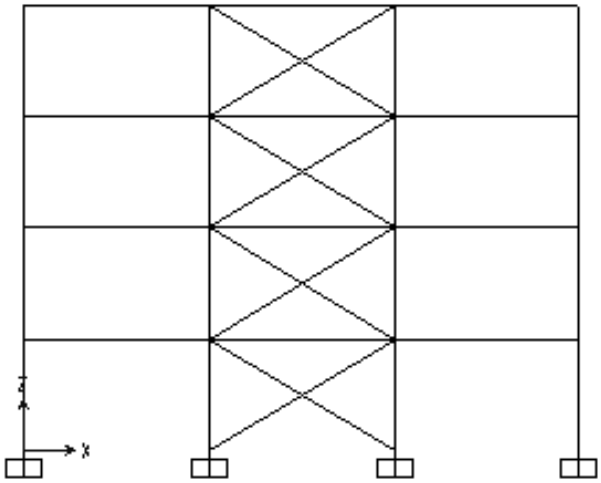

Figure 2.1: 4-story X-braced frame.

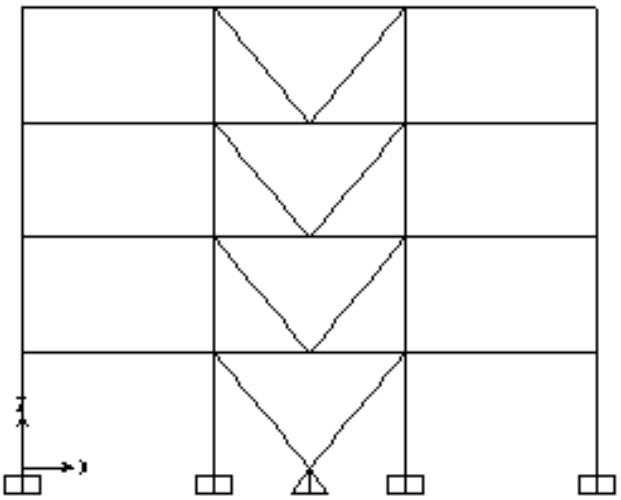

Figure 2.2: 4-story concentric V-braced frame.

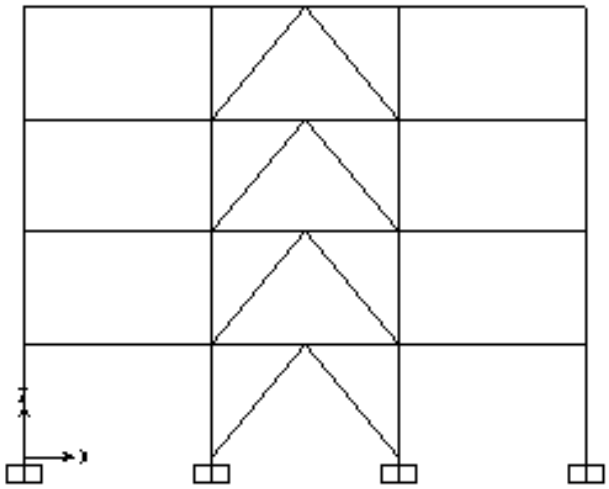

Figure 2.3: 4-story concentric Inverted V-braced frame.

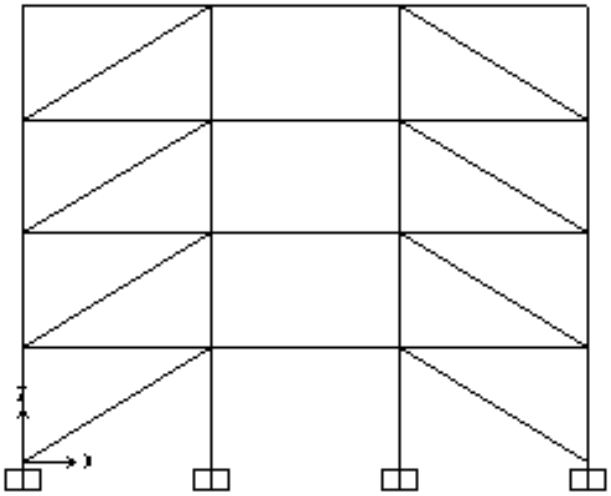

Figure 2.4: 4-story diagonal braced frame.

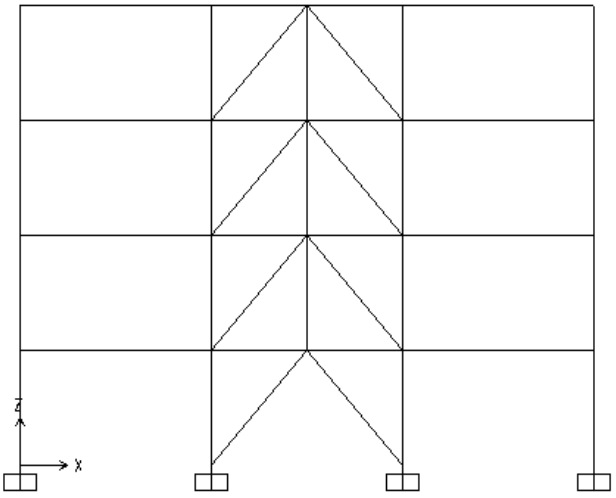

Figure 2.5: 4-story Zipper-braced frame.

One of the characteristics of CBFs is their little drift comparing to their strength. While a bracing system design should be checked for both strength and drift control, especially for tall buildings, after designing tall buildings with different concentric bracing systems, Kameshki and Saka (2001) state that the drift constraints are not the dominant parameter for bracing design of stories less than 14 for any kind of CBF. The dominant parameter is only strength. This is not correct for MRFs as it was mentioned in section 2.1.1. It is very likely that a MRF passes strength check while it still needs to be strengthened for passing drift limits.

2.1.2.2 Eccentrically Braced Frames

FEMA 356 (2000) defines Eccentric Braced Frames (EBF) as braced frames where the worklines of the components do not intersect at a single point and the distance between points of intersection, named eccentricity (*e*), exceeds the width of the smallest member that is connected at the joint. The component segment between these points is usually called shear link with a span equal to the eccentricity (*e*).

According to Huaung, Li and Chen (2005), EBF demonstrates sufficient stiffness and also excellent ductility by setting the brace eccentrically to the beam and forming a shear link. The frame provides reliable buckling protection due to the shear link yielding in a severe earthquake. However, they have a major problem. The beam should not be severely damaged, as the major part of a frame, because of the cost and difficulties required for structural rehabilitation due to the damage in the beam. Eccentric V and Inverted V are the most common eccentric bracing systems which are shown in Figures 2.6 and 2.7.

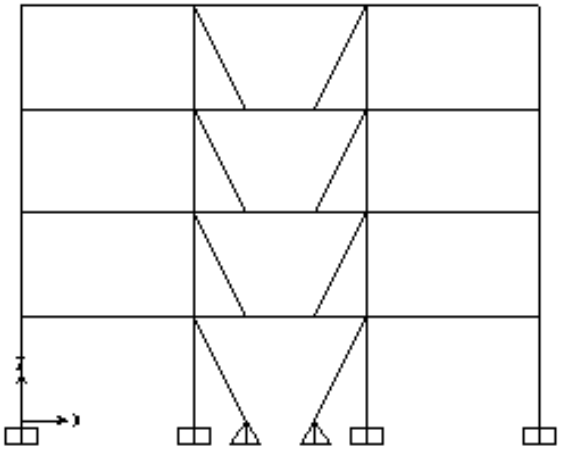

Figure 2.6: 4-story eccentric V-braced frame.

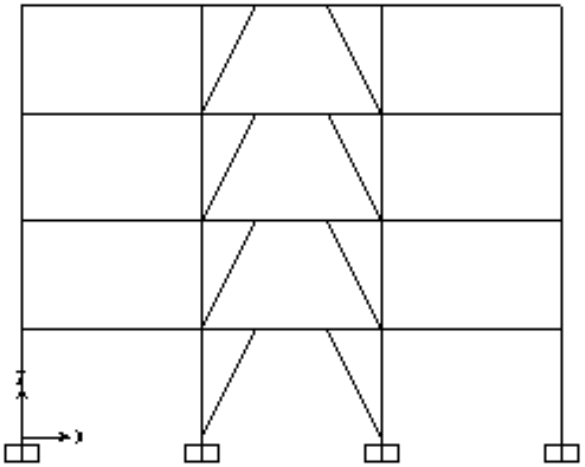

Figure 2.7: 4-story eccentric Inverted V-braced frame.

2.1.2.3 Knee Braced Frames

Knee bracing was presented by Aristizabal-Ochoa (1986) and investigated by Sam *et al*. (1995), Mofid and Khosravi (2000), Balendra *et al*. (2001) and William *et al*. (2002). According to Huaung, Li and Chen (2005), the KBF uses a secondary structural member to yield and absorb energy as "structural fuse" (the knee member) instead of the shear link. This is to ensure enough ductility and also achieve excellent lateral stiffness supplied by the diagonal brace. The major parts of the structure are safe by limiting the plastic hinges formed in the knee only. This makes the rehabilitation process easier. The knee element will yield first during a severe

earthquake as the structural fuse of the frame so that no damage occurs to the major structural members and the rehabilitation is easy and economical. Although having lots of advantages, knee-bracing system is newer and more complicated than other bracing systems. Due to this reason, it is not commonly used in steel frames. Figure 2.7 shows a typical knee, diagonal, X-, concentrically V-, eccentrically V, concentrically Inverted V and eccentrically Inverted V-braced frame.

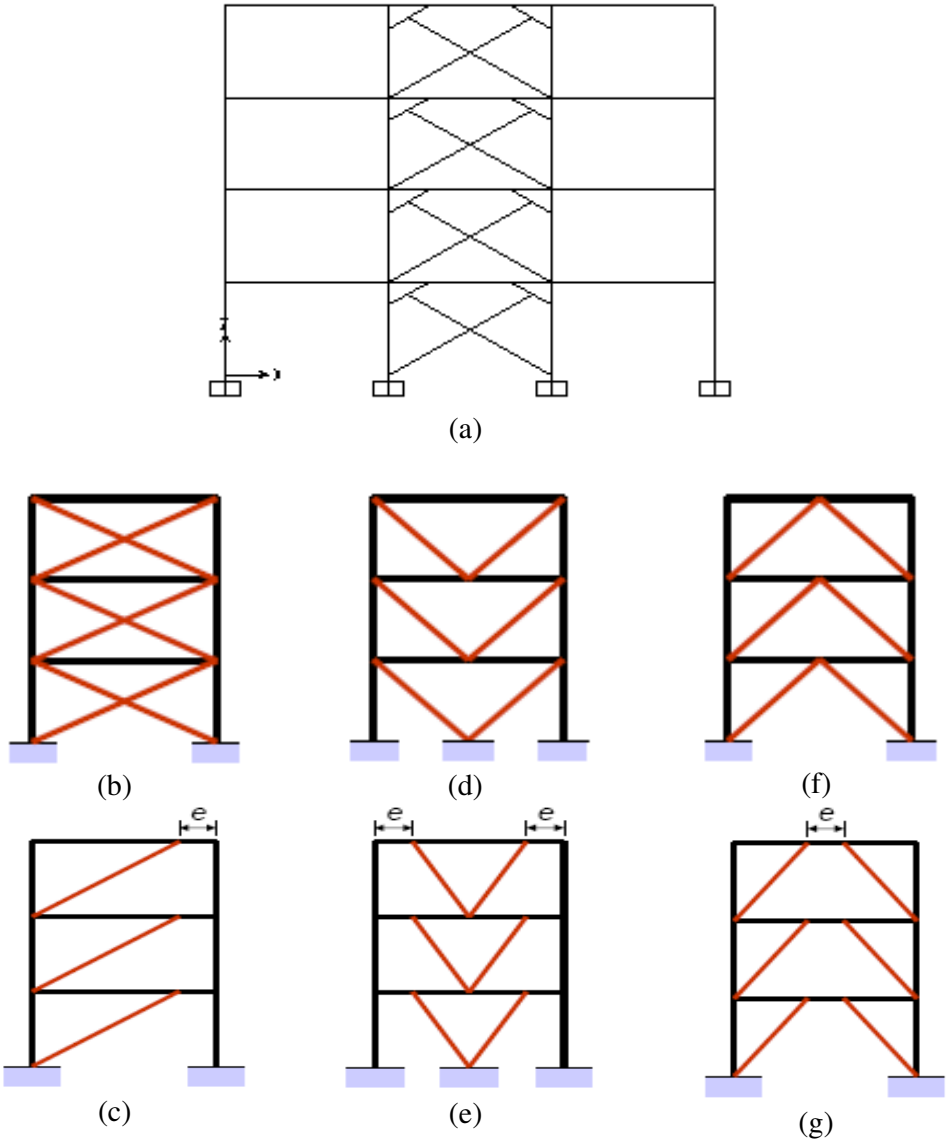

Figure 2.7: 4-story knee-braced (a), X- (b), Diagonal (c), concentrically V- (d), eccentrically V (e), concentrically Inverted V (f) and eccentrically Inverted V- (g) braced frame frame.

2.1.3 Steel Plate Shear Walls

According to FEMA 356 (2000), a Steel plate Shear Wall (SSW) should be provided with boundary members on all four sides. It should be welded to these elements. The steel plate walls can be designed to resist seismic loads alone or together with other existing lateral load resisting elements. This report states that a SSW develops its seismic resistance through shear stress.

Steel plate walls are not common but they have been used for rehabilitation of a few structures. The steel plate walls attract most of the seismic shear due to their stiffness (FEMA 356).

2.1.4 Steel Frames with Infills and Shear Cores

According to FEMA 356 (2000), steel frames with partial or complete infills of reinforced concrete or reinforced or unreinforced masonry should be evaluated by considering the stiffness of both the steel frame and infill material. This is a composite action and the relative stiffness of each element should be considered separately until complete failure of the walls has occurred.

Steel frames with infills (reinforced concrete or masonry) are not directly in the category of steel lateral load resisting systems. Therefore, they are not discussed any more in this chapter.

2.2 Structural Response Curve Evaluation Methods

2.2.1 Introduction

In order to assess the inelastic response of a structure, its response curve should be evaluated. The methods of evaluation of response curves of structures are two of the

more precise structural analysis methods. Thus, a short review on different types of structural analysis methods are given below and the ones which can be used for structural response curve evaluation are described in more detail.

2.2.2 Structural Analysis Methods

Structural analysis methods are mainly linear or nonlinear and static or dynamic. As a result, there are four main types of structural analysis; linear static, linear dynamic, nonlinear static and nonlinear dynamic analysis methods.

Linear Static Procedure (LSP) is the simplest structural analysis method. According to FEMA 356 (2000), while using this method, buildings shall be modeled with linearly elastic stiffness and damping values, at or near yield level. The calculations are done by pseudo lateral load in this method. This report continues to state that if the building's response to the design earthquake is inelastic (as it is often the case) then the actual internal forces that would develop during the yielding of the building will be different when compared to the values calculated by this method. Thus, the internal forces calculated are different than those developed in the actual building. This is due to inelastic response of components and elements.

Linear Dynamic Procedure (LDP) is the second analysis method explained in this review which is more accurate than linear static procedure. According to FEMA 356 (2000) as in the case of LSP, buildings shall be modeled with linearly elastic stiffness and damping values, at or near yield level for this method. Modal spectral analysis should be done by using linearly elastic response spectra that are not modified to take the anticipated nonlinear response into account. LDP produces displacements and internal forces that approximate the values that would be obtained in a yielding building (similar to LSP).

FEMA 356 (2000) gives the two methods of Response Spectrum and Time History for LDP. The Response Spectrum Method is based on using peak modal responses that are calculated from dynamic analysis of a mathematical model. The modes that contribute significantly to the response are only needed to be considered. Modal responses are combined for estimating the total building response quantities. The Time History Method involves "time-step-by-time-step" building response evaluation, using natural or synthetic earthquake records.

According to Powell (2007), it is now more than half a century that engineers are using linear procedures for structural analysis and design and the reason of this broad usage is their simplicity. On the other hand, they have a disadvantage that they do not have appropriate precision.

According to FEMA 356 (2000), linear procedures are only permitted for buildings which do not have an irregularity. It also gives the method to determine limitations on use of linear procedures by determining whether or not the structure is in its elastic response and does not allow the usage of linear procedures for post-elastic region of structures.

According to FEMA 440 (2005), "In general, linear procedures are applicable when the structure is expected to remain nearly elastic." But as the performance objective of the structure is associated with greater inelastic demands, the uncertainty with linear procedures increases. "Inelastic procedures facilitate a better understanding of actual performance." This results in a design that focuses on the critical aspects of the building and leads to more reliable and efficient solutions.

According to FEMA 440 (2005), "Knowledgeable engineers have long recognized that the response of buildings to strong ground shaking caused by earthquakes

results in inelastic behavior." However, until recently, linear procedures were mainly used for most structural analyses in order to predict the seismic behavior of buildings. This document continues to add that with the publication of the ATC-40 Report (1996), the FEMA 273 Report (1997), and the FEMA 356 Report (2000), nonlinear static analysis procedures became available to engineers. They provide efficient and transparent tools for predicting seismic behavior of structures.

Linear procedures (LSP and LDP), although being widely used by engineers, can not be used for evaluation of structural response curve since they are good predictor of the linear behavior of structures only, while structural response curve also includes its inelastic response. Thus, among the four mentioned analysis procedures, only the nonlinear approaches are appropriate for evaluation of structural response curve. This fact has also been stated by Maheri and Akbari (2003). These methods are nonlinear static (pushover) procedures (NSP) and nonlinear dynamic procedures (NDP) that are explained below.

2.2.3 Nonlinear Static (Pushover) Procedures

2.2.3.1 Introduction

According to Bruneau, Uang and Whittaker (1998), a pushover analysis is an incremental plastic analysis. In this analysis, the monotonically increasing lateral loads of constant relative magnitude are applied to a structure and increased until a target displacement is reached. The gravity loads should be kept constant during the analysis. Thus, the structure is actually pushed over. The aim of the analysis is mainly to determine its ultimate lateral load resistance capacity and also sequence and magnitude of plastifications when reaching target displacement point.

Bruneau M., *et al.* (1998) describe that invention of pushover analysis has taken place when many engineers have achieved this procedure by running repeated linear elastic structural analyses by computer programs and modified the model of the structure for the progressive changes in each increment in the structure.

According to FEMA 440 (2005), in pushover analysis, the nonlinear structural model is subject to progressive step by step increase in the lateral forces to generate a pushover or capacity curve (response curve) that represents the relationship between the applied lateral force and the global drift or displacement at the roof or some other control point.

According to FEMA 356 (2000), in NSP, a detailed mathematical model of the nonlinear load-deformation characteristics of the building shall be subjected to incremental lateral loads that represent inertia forces in an earthquake until a target displacement is reached. It continues to add that the target displacement represents the maximum displacement that is expected to be experienced by the structure during the design earthquake. The calculated internal forces of elements will be reasonable approximations of those expected during the design earthquake because the mathematical model takes the effects of material inelastic response into account.

Mwafy and Elnashai (2001) mention that another usage of pushover analysis is the highlighting of the potentially weak areas in the structure. NSP is applying a lateral load with a predefined pattern distributed along the building height. The lateral forces are then incrementally increased with a displacement control point at the top of the building until a specific level of deformation is reached. The drift corresponding to structural collapse may be the deformation expected in the design earthquake for assessment purposes or the roof displacement in case of designing a

new structure. NSP also demonstrates the sequence of yielding and failure on the structural elements and the structure and also the pattern of the overall response curve of the structure.

2.2.3.2 Literature Review

More than two decades ago, pushover analysis was developed by Saiidi and Sozen (1981) for reinforced concrete buildings.

Fajfar and Gaspersic (1996) state that pushover analysis is a "comprehensive, though relatively simple, non-linear method" for the seismic analysis of RC frames. They conclude that the method gives results of reasonable accuracy if the oscillation of the structure is mainly in the first mode.

Bracci, Kunnath and Reinhorn (1997) studied a one-third scale model, three-story reinforced concrete frame building that was subjected to repeated shaking table excitations and later retrofitted and tested again at the same intensities. They state that the procedure can give acceptable results of story demands versus capacities for use in seismic performance evaluation and rehabilitation of structures.

Applied Technology Council (ATC), released ATC-40 report (Seismic Evaluation and Retrofit of Concrete Buildings) in 1996. In 1997, Federal Emergency Management Agency (FEMA) released FEMA-273 and FEMA-274 reports (NEHRP provisions and commentary for the seismic rehabilitation of buildings) which were modified later on as FEMA 356 and FEMA 440. This was a great step in popularization of pushover analysis by structural engineers.

In 2000, Structural Engineers Association of California 'SEAOC' (Vision 2000) accepted pushover analysis as one of the methods among the other analysis

procedures with various level of complexity. According to Mwafy and Elnashai (2001), NSP is selected for its applicability to performance-based seismic design approaches. Its other advantage is that it can be used at different design levels to reach special performance targets. It was also mentioned that according to the recent discussions in European code-drafting committees, NSP is likely to be recommended in future building codes of practice. For more information about performance-based design approaches, the most practical and well-known ones are described in section 2.3.

Totally, pushover analysis is becoming a very popular nonlinear analysis method with a dramatic pace. The reports being released every few years by FEMA and the great number of technical papers being published about or using NSP is a proof of the popularity and importance of this method.

2.2.3.3 Load Distribution in Pushover Analysis

According to FEMA 440 (2005), the behavior of a multi-story structure that has multiple degrees of freedom (MDOF) subject to earthquake ground motion can be estimated from the performance of a single degree of freedom (SDOF) oscillator by pushover analysis. As pushover analysis has evolved, one of the main questions regarding this method which has been accounted by a great number of researchers is the load distribution pattern in the height of the building as it highly affects the results of the analysis. As a result, different patterns have been invented and examined and a summary of these are given in this chapter.

According to FEMA 440 (2005), the force distribution on the structure changes continuously during an actual earthquake. There is no problem within the elastic range because the response comprises contributions from multiple modes of

vibration. It is very difficult to assess the actual distribution because it is dramatically influenced by the dynamic characteristics of the earthquake ground motion and inelasticity of the materials of the structural element. "The combined deviations of the actual distribution of forces and deformations from those associated with the equivalent SDOF system and the assumed load vector are termed MDOF effects. Inelastic response of components or elements may differ from the SDOF model predictions due to MDOF effects in NSP.

FEMA 440 (2005) divides the pushover load patterns into two categories as single-mode load vectors and multi-mode pushover procedures which are described below.

2.2.3.3.1 Single-Mode Load Vectors

a) Concentrated Load: This is the simplest assumption for a load vector. It is a single concentrated load which is usually located at the roof level of the structure.

b) Uniform (rectangular): It is the load pattern in which the acceleration in the building model (MDOF) is the same value over its height.

c) (Inverted) Triangular: This pattern is based on the assumption that the acceleration increases linearly from zero at the base level to a maximum at the top of the MDOF model similar to an inverted triangle.

d) Code Distribution: This load pattern is very similar to triangular pattern but varies for periods less than 0.5 s and greater than 2.5 s to account for higher-mode effects (similar to the earthquake load distribution pattern used in the codes of practice).

e) First Mode: The first-mode load pattern is based on application of accelerations proportional to the first mode shape of the elastic MDOF model.

f) Adaptive: In adaptive procedure, lateral forces are applied in proportion to the amplitude of an evolving first-mode shape and the mass at each level within the MDOF model that is changed from the first mode load vector by the stiffness reduction due to the softening of the pushover curve.

g) **SRSS**: This technique (Square-Root-of-the-Sum-of-the-Squares) is based on SRSS combination of the elastic range modal story shears that results in a shear profile, referred to as the SRSS story shears. It should be noted that the elastic spectral amplitudes and modal properties are used. Generally, the number of modes having at least 90% of the mass participation is included.

2.2.3.3.2 Multi-Mode Pushover Procedures

According to FEMA 440 (2005), contrary to the single load vectors, Multi-mode pushover analysis procedures take into account of the response in several modes. In recent years, these procedures have been presented by different researchers, such as Sasaki, Freeman and Paret (1998), Reinhorn (1997), Chopra and Goel (2002), and Jan, Liu and Kao (2004). A brief review on the MPA is provided in this section. There have been a great number of studies on this issue and only the ones with the greatest importance which are also cited by FEMA 440 (2005) are chosen to be referred to in this study.

Chopra and Goel (2001a) achieved a great progress in this approach. They described a method in which NSPs are conducted independently in each mode that uses lateral-

force profiles representing the response in each of the modes from the first one up to the one which is desired to be taken into account. This method determines the response values at the target displacement which is associated with each modal pushover analysis. Response quantities that are obtained from each modal pushover are normally combined together using the SRSS method. The mode shapes and lateral force profiles are assumed to be invariant and usually based on elastic characteristics of the model despite the fact that the response in each mode might become nonlinear and variant due to stiffness degradation. Application of one of the displacement modifications or equivalent linearization procedures (which will be described comprehensively in section 2.3) to an elastic spectrum for an equivalent SDOF system, representing each mode, should be carried out for the computation of the target displacement values. After studying a nine-story steel moment-frame building, Chopra and Goel (2001a) concluded that MPA provided good estimates of story drift and floor displacement, but not plastic hinge rotations with acceptable accuracy.

In order to estimate the interstory drifts, Chintanapakdee and Chopra (2003) have applied the MPA procedure to frames with 3, 6, 9, 12, 15, and 18 stories. They concluded that the precision of interstory drift estimation is influenced by the degree of inelasticity and story level. The best accuracy was for shorter buildings and also for the lower and middle stories when the technique was applied to taller buildings. Contrarily, the MPA procedure was not capable of providing a reasonable estimate of the interstory drift for many ground motions for the upper stories of tall frames. This procedure was not used for estimating the bending moment, axial and shear force, or component deformation.

Yu *et al.* (2002) studied a 13-story steel building using the original and the two modified versions of MPA. They reported that when the target displacements were calculated by using the displacement Coefficient Method (explained later) to the median elastic response spectrum, the MPA method underestimated story drifts in the upper stories but overestimated drifts in the lower stories; this is while plastic hinge rotations of columns and beams were often overestimated, but the deformations of the panel zones were well estimated.

Chopra *et al.* (2004) compared interstory drift estimates of generic frames and SAC[2] frames that were obtained by using the original and modified MPA procedures. They concluded that the modified MPA method is a good alternative to the original one, since it gives a higher estimate for the seismic demand and improves the precision of the MPA results in some cases.

An improved MPA procedure that includes P-Δ effects in all considered modes was used by Goel and Chopra (2004). They studied 9- and 20-story moment-resisting frames and they found that this procedure has low accuracy in the estimation of plastic hinge rotation.

Jan *et al.* (2004) proposed an alternative technique in which potentially inelastic contributions from the first two modal pushover analyses are added together. This

---

[2] "SAC is a joint venture of the Structural Engineers Association of California (SEAOC), the Applied Technology Council (ATC), and California Universities for Research in Earthquake Engineering (CUREe), formed specifically to address both immediate and long-term needs related to solving performance problems with welded, steel moment-frame connections discovered following the 1994 Northridge earthquake" FEMA 355 (2001).

was the only technique that could provide reasonable estimates of the severity and location of plastic hinge rotations in 2-, 5-, 10-, 20- and 30-story steel moment frames.

Hernández-Montes *et al.* (2004) described a pushover procedure based on energy methods.

Aydinoglu (2003) defined a MPA with incremental response-spectrum. The multiple mode contributions are considered in an incremental pushover analysis in this procedure. The nature of this incremental analysis allows the effects of stiffness to decrease due to inelasticity in one mode to be taken into account for the other modes. An example was used in this study in order to illustrate the application of this method while the gravity loads and P-Δ effects were neglected. After comparing the results with nonlinear dynamic analysis, there was good agreement for interstory drift, story shear, floor displacement, floor overturning moment and beam plastic hinge rotation. Despite the good results obtained by this method FEMA 440 (2005) states that "Further study is required to establish the generality of the findings and potential limitations of the approach."

2.2.3.4 The Effects of Load Distribution in the Results of Pushover Analysis

According to Krawinkler and Seneviratna (1998), the load pattern influences the performance evaluation of structures more critically rather than the accurate determination of the target displacement point (which is going to be described in section 2.3). The load pattern selected for NSP is expected to represent and bound the inertia force distributions in a design earthquake. The distribution of inertia forces vary with the time duration and severity of the earthquake. This is an

indicator of the extent of inelastic deformations. By applying a constant load pattern, the procedure is based on the assumptions that the inertia force distribution is approximately constant throughout the earthquake duration. If this assumption turns out to be correct, the maximum deformations obtained from this constant load pattern will be comparable to those expected in the design earthquake.

They continue to state that uniform load pattern overestimates the demand in the lower stories compared to upper stories and also undermines the relative importance of overturning moments compared to story shear forces. The load pattern issue has been the weak point of the NSP at the time that this research has been carried out. Invariant patterns may mislead the predictions, especially for structures with long periods and localized mechanisms of yielding.

After that, FEMA 356 (2000) and ATC-40 (1996) chose their way of load pattern selection which will be discussed in section 2.3.

In 2001, in a research being carried out by Mwafy A.M. and Elnashai A.S., the applicability and validity of NSP were evaluated by comparing with "dynamic pushover" idealized envelopes that were obtained from incremental dynamic analysis as study benchmark. 12 reinforced concrete buildings with different characteristics were analyzed in this study by using natural and artificial ground motions. The results of over one hundred inelastic dynamic analyses were used to compare the static pushover results with different load patterns. Good correlation was obtained between static pushover results and the "dynamic pushover" idealized envelopes. They examined eight and twelve story buildings by multimodal, code and uniform load pattern which are explained in the previous section. They stated that

the use of the uniform load shape might shed light on the possibility of soft storey mechanism.

They realized that the variation of the results obtained from different methods observed for some buildings is mainly in the post-elastic range, and is due to the spread of yielding and member failure in the structure. The structural stiffness decreases, the fundamental period elongates and the inertia force distribution along the building changes progressively as a result of such mechanisms.

The results which are relevant to this research (regular frames without concrete shear walls) are shown in Figure 2.8.

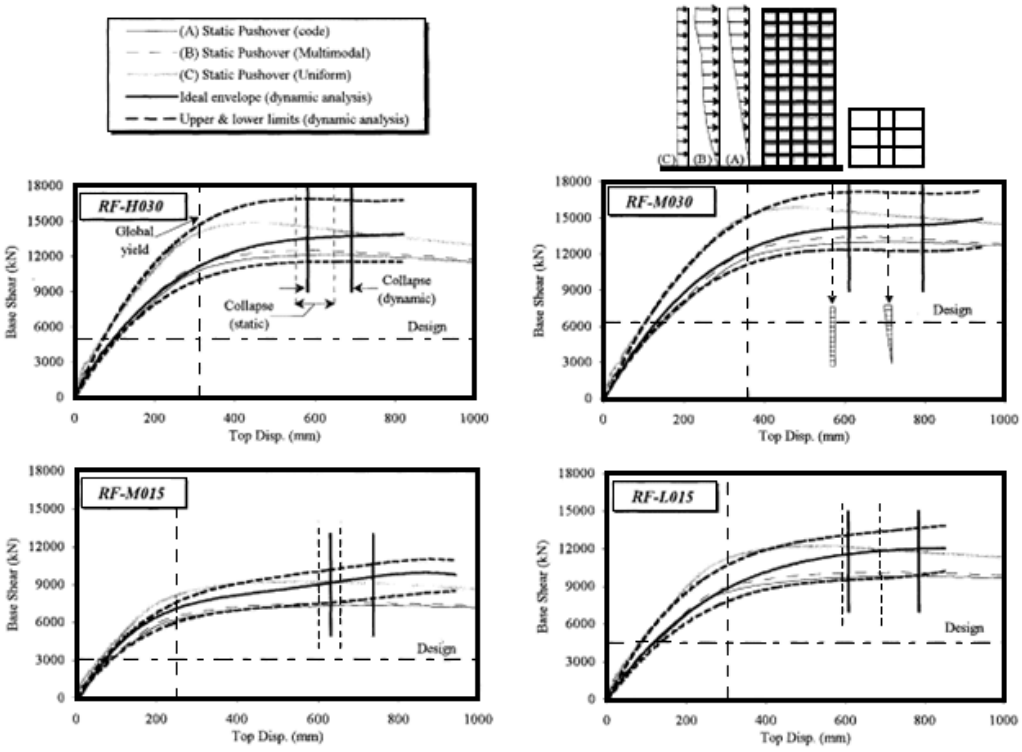

Figure 2.8: Static and dynamic pushover analysis results for the regular frame structures (Courtesy of Mwafey & Elnashai, 2000).

They conclude that the response of the frames is influenced by the lateral load distribution shape. The change is dramatically greater when moving from the code

and the multimodal load shapes to the uniform load pattern. They state that the difference between load shape A of Figure 2.8 (the code load pattern) and load shape B (load shape from multimodal analysis) is very small. The multimodal analysis load pattern did not show a great ability to predict the effects of higher modes although these effects are taken into account in the response of the second and the third group of buildings since its load shape only considers the elastic modal superposition while the amplification of higher mode effects are mainly in the plastic phase. The uniform load distribution is conservative from the design aspect. The difference between triangular and the multimodal distribution results was less than 4%. After comparing these two distributions with Dynamic Analysis, they reached the conclusion that the triangular distribution is the best one matching the characteristics of their models.

After five years of advancement, in a more detailed and greater research, which is still the most comprehensive study regarding this issue, FEMA 440 (2005) examining five different buildings with Triangular, Uniform, Code, First mode, Adaptive, SRSS and Multi-mode pushover patterns, reaches the following conclusions about the load distribution patterns in pushover analysis.

All of NSPs (nonlinear static procedures) estimated the results in reasonable evaluation of peak displacements over the height of the frames comparing to the nonlinear dynamic response-history analysis. Detailed information is given in Figure 2.9 and Figure 2.10. “Estimates made using the first-mode, triangular, and adaptive load vectors were best. A multiple mode procedure may be warranted for structures in which displacement response is suspected to be predominantly in a higher mode”, FEMA 440 (2005).

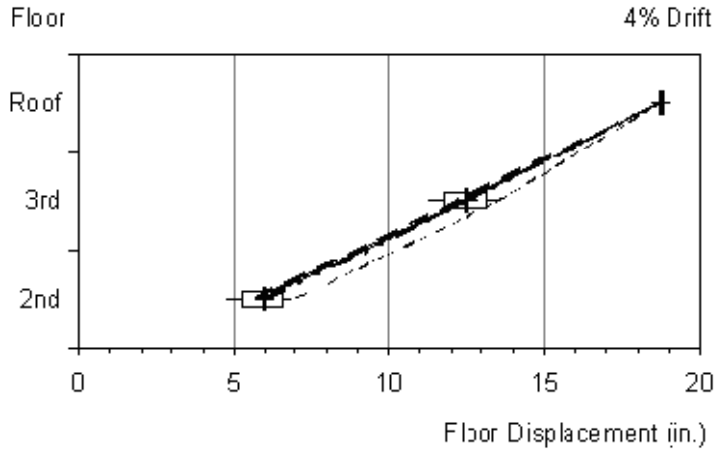

(a) Three-story frame building at 4% drift

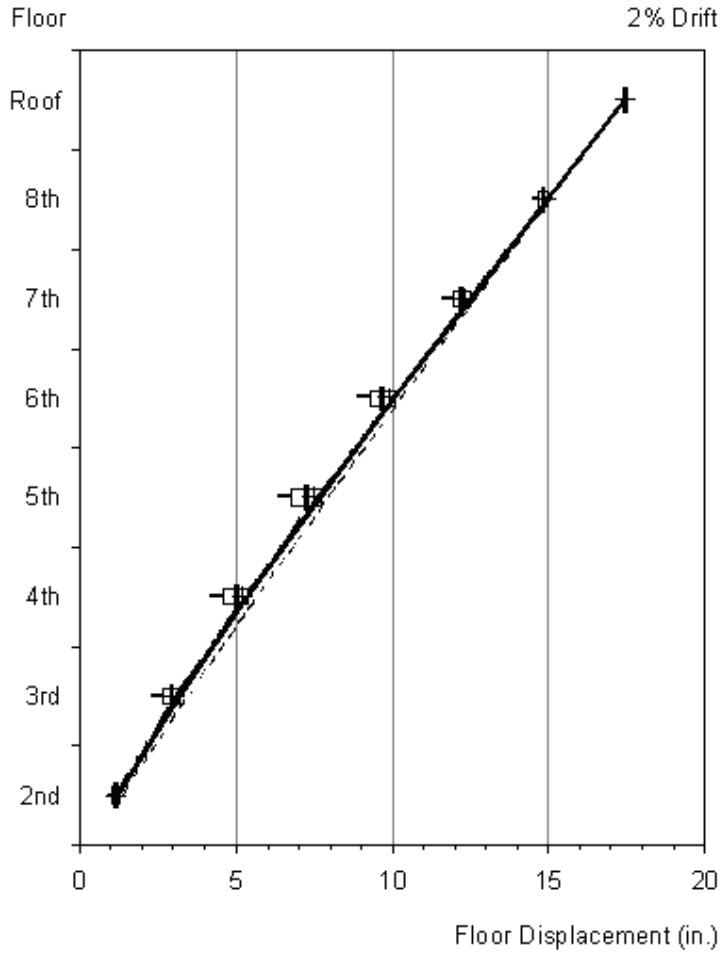

(b) Eight-story wall building at 2% drift

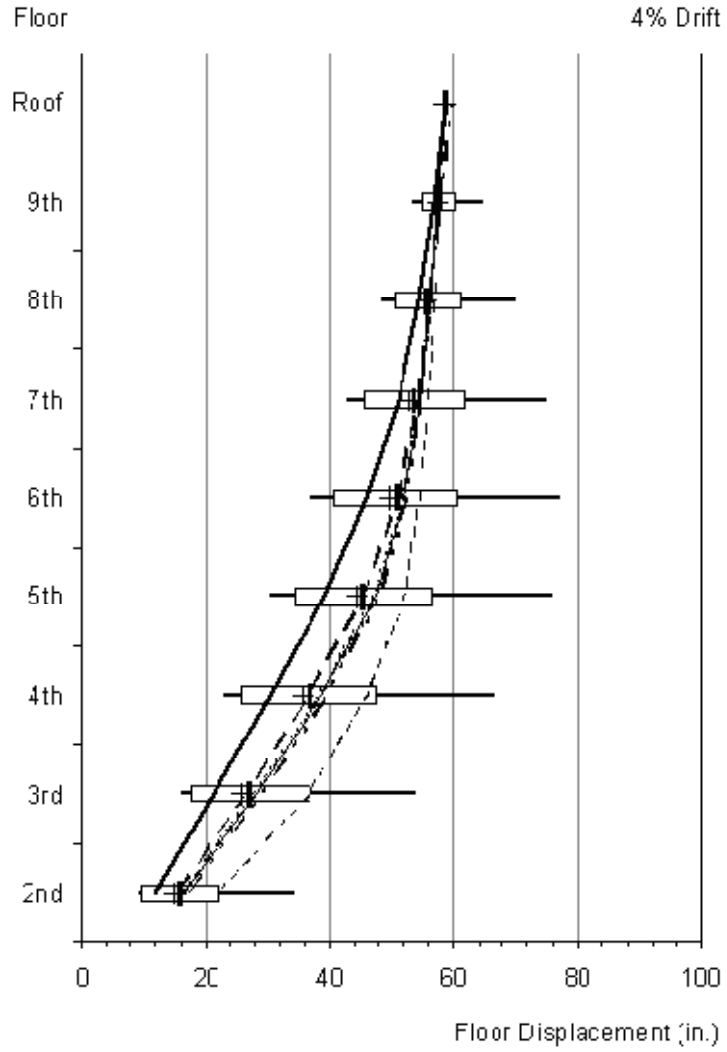

(c) Nine-story frame at 4% drift

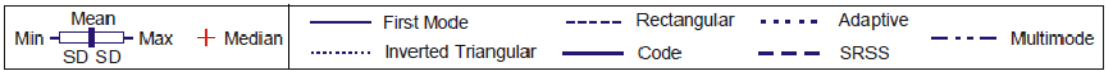

Figure2.9a, b, c: Example results for displacements predicted by nonlinear static procedures (NSP) compared to nonlinear dynamic response-history analyses (NDA) (Courtesy of FEMA 440).

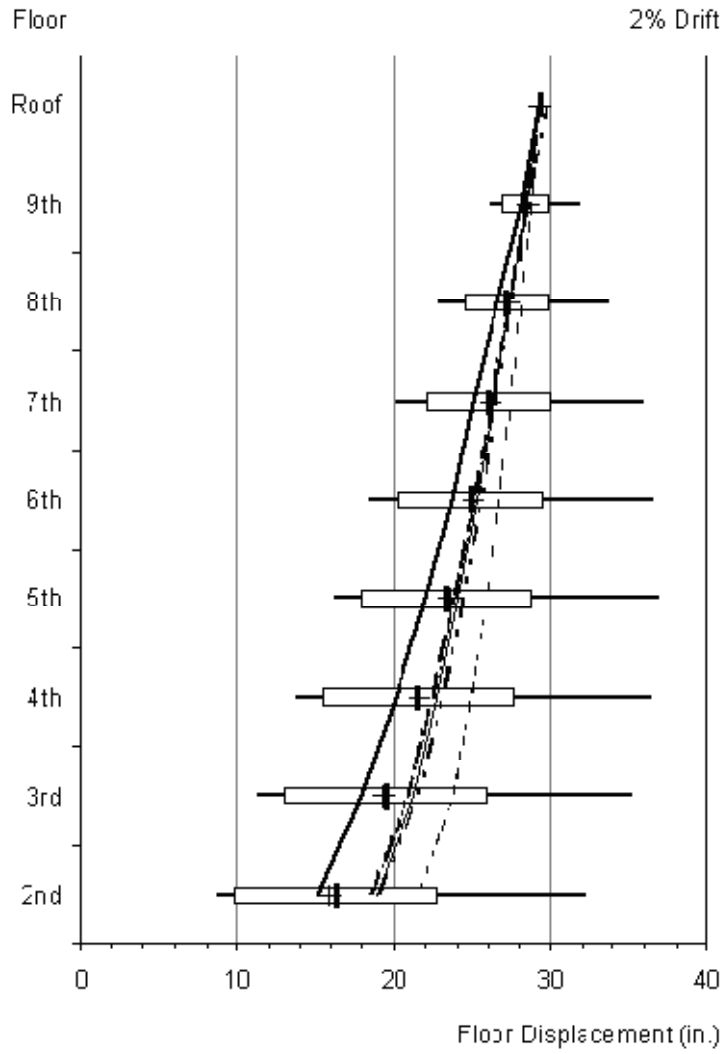

(a) Nine-story weak story frame at 2% drift

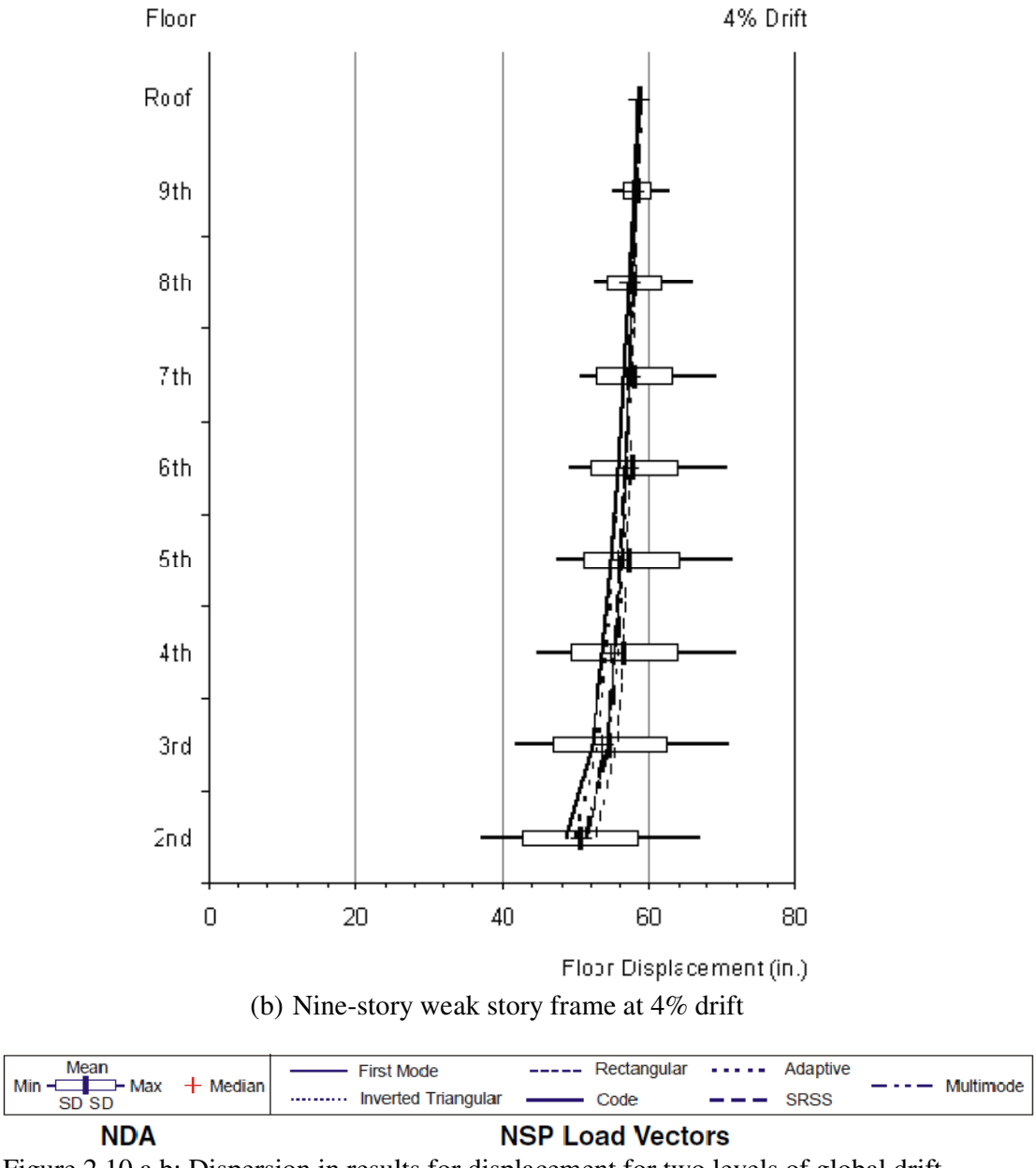

(b) Nine-story weak story frame at 4% drift

Figure 2.10.a,b: Dispersion in results for displacement for two levels of global drift. (Courtesy of FEMA 440).

It also states that dispersion in their results was observed for a weak story frame building.

The interstory drift was obtained reasonably over the height of the three-story frames and eight-story wall by using the first-mode, triangular, code, adaptive, and SRSS load vectors, and also with the modified MPA procedure.

The maximum interstory drift over the height of each building model, being determined by all single mode load patterns excluding the uniform load vector, was a reasonable estimate of the maximum interstory drift occurring in the nonlinear dynamic analyses. However, the modified MPA procedure was a better estimator.

The story shear and overturning moment were underestimated by using the single load vectors and overestimated by using the modified MPA procedure. The SRSS combinations of these quantities can exceed limits of development of inelastic mechanism. This is the probable reason for the overestimation of the results by modified MPA procedure.

After the above mentioned conclusions, FEMA 440 directly states that "The first-mode load vector is recommended because of the low error obtained for displacement estimates made with this assumption and to maintain consistency with the derivations of equivalent SDOF systems". "A single first-mode vector is sufficient for displacement estimates". This report states that the code distribution and the triangular vectors can also be used as alternatives, but with little increase in the error.

By using the adaptive load vector, the mean and maximum errors might probably become smaller or larger. This method requires more computational effort and might fail if the system exhibits dramatic changes in tangent stiffness.

When compared with the first-mode load vector, the SRSS load vector led to small improvements in overturning moment and story shear, had mixed effects for interstory drift, and sometimes worse results for displacement estimates. This procedure "requires greater computational effort for inconsistent improvements.

The uniform load vector is not recommended since it had dramatically worse errors for all of the response quantities, relative to the first-mode load vector.

This report states that multi-mode pushover analysis is a better choice than single load vector when estimating interstory drift. But it mentions that the choice between multi-mode and single load vector is influenced by the required parameter to be estimated (e.g., drift, plastic hinge rotation, force), the specific procedure details and the structure characteristics.

2.2.3.5 Advantages and Disadvantages of Nonlinear Static Procedures

Mwafey and Elnashai (2000), state that the main usage of the NSP is to estimate the seismic capacity (not seismic demand) of structures. This method is less applicable for prediction of seismic demands when the structure is subject to a special ground motion. But this disadvantage is not applicable for the current study since it does not want to define the target displacement point (term from FEMA 356 or performance point from ATC-40) on the pushover curve of the frames related to a specific ground motion.

According to FEMA 440 (2005),

- NSP is usually a reliable estimator of maximum floor and roof displacements.
- However, it is not an accurate predictor of maximum interstory drifts, particularly within the structures with high flexibility.
- NSP is a poor estimator of story forces such as overturning moments and shears.

- For estimation of interstory drifts over the heights of the buildings, multi-mode pushover analysis produces better results.

2.2.4 Nonlinear Dynamic Procedures

2.2.4.1 Introduction

According to FEMA 356 (2000), when the Nonlinear Dynamic Procedure (NDP) is applied for seismic analysis of the building, a mathematical model of the frame should be subjected to earthquake shaking which is represented by ground motion time histories. This model should account for the nonlinear load-deformation characteristics of individual components and elements of the building.

This report adds that Time History Analysis is used for the response calculations. With the NDP, the design displacements are determined directly through dynamic analysis using ground motion time histories instead of using a target displacement.

2.2.4.2 Advantages and Disadvantages of Dynamic Procedures

According to FEMA 440 (2005), during an earthquake, the amplitude, phasing, and frequency content of the shaking are highly influenced by source characteristics such as magnitude, rupture mechanism, fault plane orientation with respect to site, the source, attenuation, and site effects, which are depicted schematically in Figure 2.11 affect the character of ground shaking.

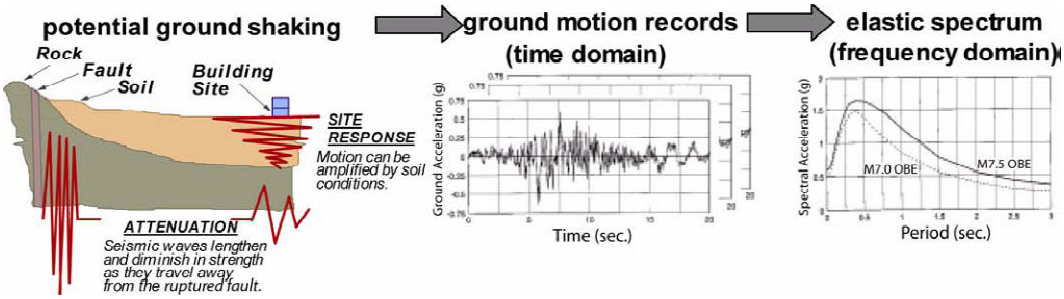

Figure 2.11: Factors affecting seismic ground motion (Courtesy of FEMA 440).

Krawinkler and Seneviratna (1998) state that NDP predicts the forces and cumulative deformation (damage) demands in every element of the structural system with sufficient reliability and is the final solution for structural analysis. But they continue to add that the solution implementation needs the availability of a set of ground motion records for accounting the uncertainties and differences in severity, frequency characteristics, and duration because of distances and rupture characteristics of the various faults that may cause motions at the site.

Mwafy and Elnashai (2001) state that NDP is a powerful tool for structural seismic response study. Accurate estimation of the anticipated seismic performance of structures can be reached by a set of carefully selected ground motion records. But they continue to state its disadvantage as the great sensitivity of the calculated inelastic dynamic response to the characteristics of the input motions. And as a solution to this problem, they describe that evaluation of the strength capacity in the post-elastic range can simply be done by NSP.

FEMA 356 mentions that "Calculated response can be highly sensitive to characteristics of individual ground motions" for nonlinear dynamic procedures.

Although FEMA 440 (2005) firstly states that nonlinear dynamic analysis is able to produce results with relatively low uncertainty by using the combination of ground

motion records, it continues to mention that in the real world, great dispersion in engineering demand parameters is resulted by the ground motion variability. It gives Figure 2.12 for better clarification of this problem which shows the results of a series of nonlinear dynamic analyses (Vamvatsikos & Cornell, 2002). It is shown in this figure that the dispersion increases with shaking intensity increase. This figure explicitly describes the dependence of the result of the dynamic analysis on the earthquake ground motions being chosen for the analysis which itself is a function of site characterizations.

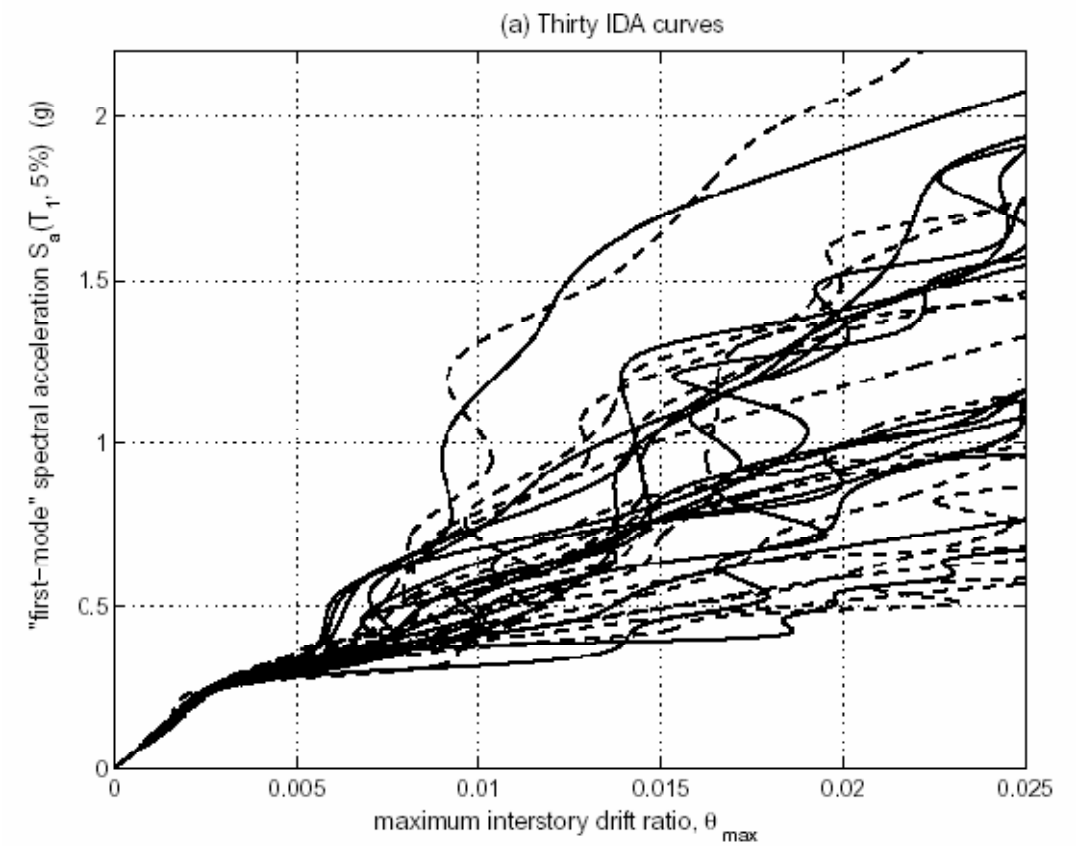

Figure 2.12: Incremental dynamic analysis study for thirty ground motion records for a 5-story steel braced frame showing uncertainty in IDA due to dependency of the results on ground motion characteristics (Courtesy of Vamvatsikos & Cornell, 2002).

2.3 A Background on Performance-based Engineering Procedures

As it will be described later in this chapter, after reaching a pushover curve, its yield and target displacement point needs to be calculated. These parameters are estimated by performance-based engineering (PBE) procedures. On the other hand, PBE procedures have lead to a greater usage and improvement of pushover analysis during the past decade. Due to these reasons, PBE procedures are reviewed in this section.

According to Krawinkler and Seneviratna (1998), NSP aims to evaluate the expected performance of a structure. It evaluates the strength and deformation demands of the structure in design earthquakes by means of nonlinear static analysis and compares them to available capacities at the performance levels of interest. This procedure assesses important performance parameters such as global drift, interstory drift, inelastic element deformations, deformations between elements, and element and connection forces. The pushover analysis provides information on many response characteristics which cannot be evaluated by a dynamic or elastic static analysis, such as the realistic force demands, including axial force demands on columns, force demands on brace connections, moment demands on beam-to-column connections, shear force demands, interstory drifts, deformation demands for inelastically deformed elements, consequences of the strength deterioration, the critical regions in which the deformation demands are expected to be high, the strength discontinuities in elevation or plan, etc.

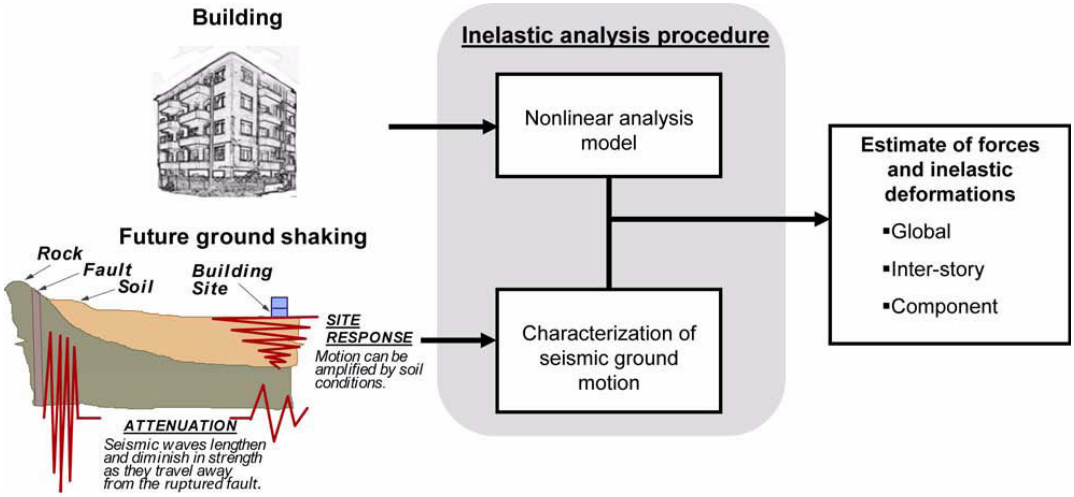

Figure 2.13: Schematic depiction of the use of inelastic analysis procedures to estimate forces and inelastic deformations for seismic ground motions and a nonlinear analysis model of the building (Courtesy of FEMA 440, 2005).

According to FEMA 356 (2000), the aim of PBE is to predict the performance of the structures to inform decisions regarding safety and risk. Thus, PBE provides estimates of performance in terms of expected damage to structural and nonstructural elements. Linear (traditional) design and analysis procedures can not predict performance explicitly because after any structural damage, the frame behaves inelastically. Contrarily, the inelastic seismic analysis procedures aim to directly evaluate the magnitude of inelastic deformations and distortions.

According to FEMA 440 (2005), great improvement has been made in PBE procedures relying on NSPs during the past decade. In 1996, ATC (Applied Technology Council) published the ATC-40 report (Seismic Evaluation and Retrofit of Concrete Buildings). In a larger project which was funded by FEMA (Federal Emergency Management Agency), ATC prepared the FEMA 273 report (Guidelines for the Seismic Rehabilitation of Buildings) and its commentary (FEMA 274) in 1997. Three years later, the American Society of Civil Engineers (ASCE) provided the FEMA 356 report (Prestandard and Commentary for the Seismic Rehabilitation

of Buildings) which introduces the second generation of FEMA 273/274 procedures, (published by FEMA) in 2000. Similar procedures are presented in all of these reports. FEMA-273, -274 and FEMA 356 detail the Coefficient Method, where displacement demand is calculated by displacement demand of the elastic predictions modification (explained in section 2.3.2). ATC-40 uses Capacity-Spectrum Method, where the modal displacement demand is estimated from the intersection of a pushover curve with a demand curve consisting of the smoothened response spectrum that represents the design ground motion, and is modified to take hysteretic damping effects into account (described in section 2.3.1). Both of these approaches are the same in generating a "pushover" curve to represent the inelastic force-deformation behavior of a structure. However, their difference is in the methods they use to calculate the inelastic displacement demand. FEMA 440 insists on the fact that the usage of pushover analysis in engineering practice has been accelerated after the publication of ATC-40 and FEMA 356 reports.

In 2005, Federal Emergency Management Agency released a new document, FEMA 440, Improvement of Nonlinear Static Seismic Analysis Procedures evaluating and improving both of the previous methods. It says that both of the ATC-40 and FEMA 356 documents present similar PBE methods relying on NSPs for structural demands prediction by generating a pushover (capacity) curve to estimate the inelastic force-deformation of structural behavior.

FEMA 440 states that after the publishing of the above mentioned reports and the consequent increase in the usage of NSPs by engineers, they have reported different evaluations of displacement demand for the same building by the two procedures. The differences reported are often for the displacement demand of the same ground

motion and same SDOF oscillator. Aschheim, Maffei and Black (1998), Chopra and Goel (1999a, 1999b, 2000), Albanesi, Nuti, and Vanzi (2000), Kunnath and Gupta (2000), Lew and Kunnath (2000), Yu, Heintz and Poland (2001), Zamfirescu and Fajfar (2001) and MacRae and Tagawa (2002) are some of the researchers who carried out such comparative work and reported the results.ATC and FEMA decided to conduct a study to determine the reasons for these variations in the results and also to develop improved application of these two procedures for practicing engineers. Then, these two authorities released FEMA 440 (2005) to cover the gap between these two methods and the differences between their results. This document was released for evaluation and improvement of the application of NSPs for use with PBE methods for seismic design, evaluation, and upgrading of structures (FEMA 440, 2005); some of the reasons of producing such a report are to recognize the applicability, limitations and reliability of nonlinear static procedures.

In this review, for each method, first of all the original document is reviewed. FEMA 440 evaluation and modifications are given after the description of each method. Finally, a comparison of all of the methods is given.

2.3.1 Capacity-Spectrum Method of Performance Based Design

This method has mainly been introduced in ATC-40 report and evaluated and modified later by FEMA 440.

2.3.1.1 ATC-40 Capacity-Spectrum Method of Performance Based Design

According to FEMA 440 (2005), different researchers have noticed that the inelastic displacement response of structures is often very similar to the displacement

response of elastic oscillators that have the same period for many years. This fact caused the invention of "equal displacement approximation."

According to Krawinkler and Seneviratna (1998), this procedure is based on the assumption that the response of the frame is related to the response of an equivalent single degree-of-freedom oscillator. It is also based on the incorrect assumptions that the response is governed by a single mode, and this mode shape is constant during the time history response. Although both of these assumptions are incorrect, they give relatively good estimates of the maximum seismic response of structures that their response is governed by one single mode.

According to FEMA 440 (2005), the basic assumption in equivalent linear methods (such as ATC-40) is that the maximum displacement of a nonlinear single-degree-of-freedom (SDOF) system can be estimated from the maximum displacement of another SDOF system that is linear elastic and has a period and a damping ratio of larger than those of the original nonlinear system. The elastic SDOF system being used to evaluate the maximum inelastic displacement of the original nonlinear system is named as the equivalent or substitute system and its period of vibration and damping ratio is called equivalent period and equivalent damping ratio, respectively.

Jacobsen (1930), the pioneer of this procedure, presented the concept of equivalent viscous damping. Afterwards, the concept of equivalent viscous damping was extended to yielding SDOF systems by Jacobsen (1960). This was followed by numerous research works done in this regard. The most noticeable ones are mentioned by FEMA 440, such as, Jennings (1968), Iwan and Gates (1979), Hadjian (1982), Fardis and Panagiatakos (1996), Miranda and Ruiz-García (2003). The work

of Freeman, Nicoletti and Tyrell (1975) is the primary basis of ATC-40 Capacity Spectrum Method. In all of these methods, the equivalent period and equivalent damping ratio are computed from the initial period of vibration and damping ratio of the nonlinear system and from the maximum displacement ductility ratio, μ and their differences are from the functions they have used in order to calculate the equivalent period and equivalent damping ratio, FEMA 440 (2005).

On a summary of ATC-40 capacity-spectrum method of equivalent linearization, FEMA 440 (2005) states that in the Capacity-Spectrum Method of ATC-40, the force-deformation relationship generation process of the structure is similar to the Coefficient Method of FEMA 356 (explained in section 2.3.2) but the results are plotted in acceleration- displacement response spectrum (ADRS) format (Figure 2.14) instead of base-shear-versus-roof-displacement relationship. The result is called a capacity curve for the structure. The seismic ground motion should also be converted to ADRS format in the next step. Then the capacity curve can be plotted on the same axes as the seismic demand so that they can be compared together.

In this procedure, it is assumed that the equivalent damping of the system is proportional to the area that is enclosed by the capacity curve. It is also assumed that T_{eq} (the equivalent period), is the secant period at which the seismic ground motion demand, is intersecting the ADRS capacity curve. The solution to determine the maximum inelastic displacement (i.e., performance point) is iterative since the equivalent period and damping are both functions of the system displacement, FEMA 440 (2005).

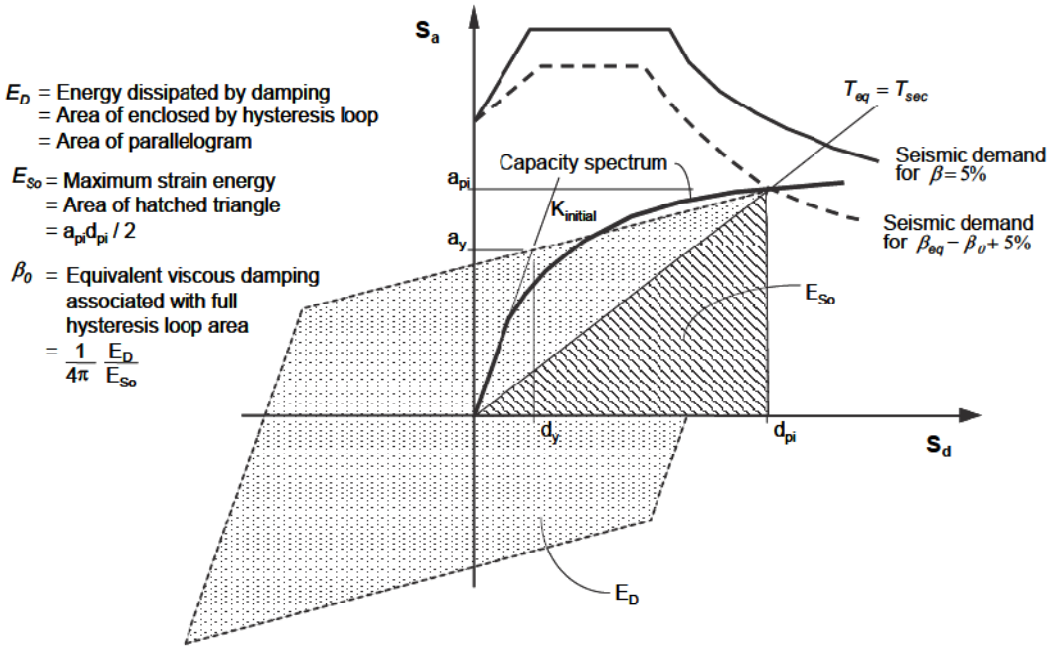

Figure 2.14: Graphical representation of the Capacity-Spectrum Method of equivalent linearization, as presented in ATC-40 (Courtesy of FEMA 440).

Calculation of equivalent period and equivalent damping of ATC-40 is as follows (equations 2.1, 2.2):

$$T_{eq} = T_0\sqrt{\frac{\mu}{1+\alpha\mu-\alpha}} \tag{2.1}$$

$$\beta_{eq} = \beta_{eff} = 0.05 + \frac{2}{\pi}\frac{(\mu-1)(1-\alpha)}{\mu(1+\alpha\mu-\alpha)} \tag{2.2}$$

T_0: the initial period of vibration of the nonlinear system

α: the post-yield stiffness ratio

κ: adjustment factor to approximately account for changes in hysteretic behavior in reinforced concrete structures

ATC-40 procedure is based on using three equivalent damping levels that change with the system hysteretic behavior. These behaviors are named as type A, B and C hysteretic behaviors in this document.

Lateral Load Distribution

The first mode load shape is the first recommendation of this report while below mentioned patterns are secondary load shape choices:

1. Concentrated load

2. Code distribution

3. First mode

4. Adaptive

5. Multi-mode pushover

(The description of these patterns are given in section 2.2.3.3)

2.3.1.2 FEMA 440 Evaluation of ATC-40 Capacity-Spectrum Procedure

After the decision on studying the shortages of ATC-40 method, the evaluation of this procedure was started by FEMA 440. In this evaluation, approximate results of Capacity-Spectrum procedure for hysteretic behavior types of A, B and C were compared with response-history analysis results that were computed with the EPP hysteretic model as benchmarks. Figure 2.15 (courtesy of FEMA 440) demonstrates the mean errors corresponding to ground motions recorded in site class C and for hysteretic behaviors type A, B, and C. According to the complete results which are not given in this study, ATC-40 Capacity-Spectrum Method was found to give very

large overestimations of the maximum displacement for relatively short-period systems up to approximately larger than twice the RHA benchmark displacements. The same results are also previously reported by Miranda and Ruiz-García, 2003; Akkar and Miranda, 2005 (FEMA 440, 2005), for some other equivalent linearization methods.

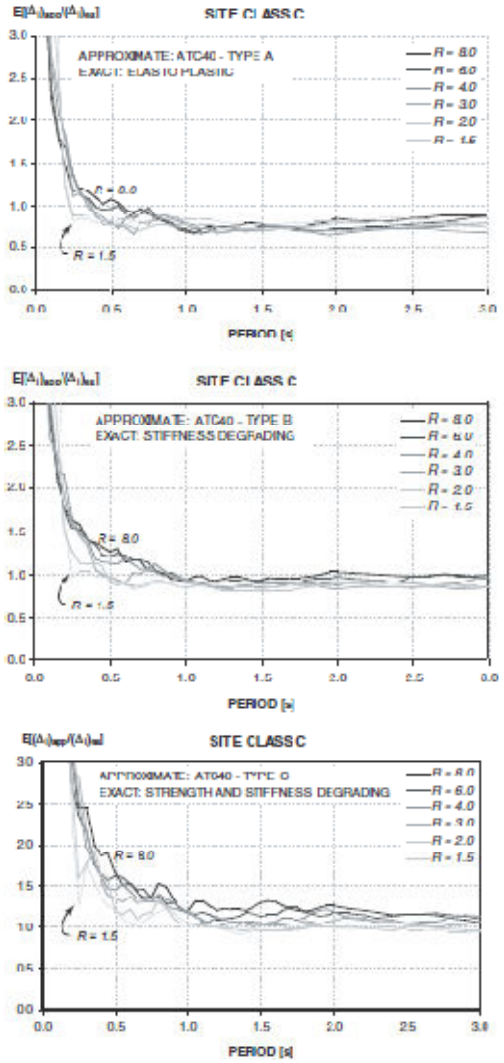

Figure 2.15: Mean error associated with the Capacity-Spectrum Method of ATC-40 for hysteretic behaviors types A, B, and C for site class C.

According to the complete results mentioned in FEMA 440, the Capacity- Spectrum Method behavior type A underestimates the maximum displacements for periods longer than about 0.6 s. The ATC-40 method tends to underestimate displacements

for systems with ATC-40 hysteretic behavior type B and periods longer than about 0.8 s. The approximate ATC-40 procedure tends to overestimate inelastic displacements in the case of systems with hysteretic behavior type C.

For periods of smaller than about 0.5 s dispersion of the error is very large while it is moderate and approximately constant for periods longer than 0.5 s. Detailed results of dispersion for site classes B, C, and D and behavior types A, B and C are not presented in this study since the main aim of this section was to summarize the evaluation of ATC-40 procedure.

2.3.1.3 FEMA 440 Improved Procedures for Equivalent of Linearization

FEMA 440 has made a number of modifications on ATC-40 procedure. They are mainly as follows:

Effective damping can be calculated from the equations 2.3, 2.4 and 2.5 which are optimized for application to any capacity curve:

For $1.0 < \mu < 4.0$,

$$\beta_{eff} = 4.9\,(\mu - 1)^2 - (\mu - 1)^3 + \beta_0 \tag{2.3}$$

For $4.5 < \mu < 6.5$,

$$\beta_{eff} = 14 + 0.32\,(\mu - 1) + \beta_0 \tag{2.4}$$

For $6.5 < \mu$,

$$\beta_{eff} = 19\left[\frac{0.64\,(\mu-1)-1}{[0.64\,(\mu-1)]^2}\right]\left(\frac{T_{eff}}{T_0}\right) + \beta_0 \tag{2.5}$$

Effective period can be estimated from equations 2.6, 2.7 and 2.8.

For 1.0 < μ < 4.0,

$$T_{eff} = [G(\mu - 1)^2 + H(\mu - 1)^3 + 1]\, T_0 \quad (2.6)$$

For 4.0 < μ < 6.5,

$$T_{eff} = [I + J(\mu - 1) + 1]\, T_0 \quad (2.7)$$

For 6.5 < μ,

$$T_{eff} = \{K\left[\sqrt{\frac{(\mu-1)}{1+L(\mu-2)}} - 1\right] + 1\}\, T_0 \quad (2.8)$$

G, H, I, J and K values should be extracted from tables of FFMA 440. Equivalent Linearization PBE procedure is explained in a comprehensive manner in ATC-40, FEMA 440 and numerous recent studies. However, this study will not give any further information regarding Equivalent Linearization PBE (contrary to Coefficient based procedure) since it is not going to be used by this study.

2.3.2 Coefficient Method of Performance Based Design

According to FEMA-445 (2006), the first generation of coefficient method of performance based design was mainly introduced by FEMA 273 and FEMA 274, which was replaced by its second generation by the release of FEMA 356. Since the usage of FEMA 273 and 274 is not recommended any more after the release of FEMA 356 report (according to FEMA 445) and also due to the similarity of the methods, the former reports are not explained any further in this review. It should be noted that according to FEMA-445 (2006), researchers are currently working on the next (third) generation of performance based design but exact information about this study is not available at this time.

2.3.2.1 FEMA 356 Coefficient Method

According to Powell (2007), although FEMA 356 is developed for rehabilitation purposes; it can also be used for design or analysis of new structures. In this document, a knowledge factor, κ, is introduced to make it applicable for both rehabilitation of old structures and design and analysis of new structures. It is accounting for the level of uncertainty in the data collection for existing structures; those that are required to be studied for rehabilitation objectives (FEMA 356).

In this method, each goal should consist of a target Building Performance Level and an Earthquake Hazard Level. Building Performance Level is the extent of building damage, (FEMA 356, 2000).

a) Rehabilitation Objectives

According to FEMA 356, Reduced Rehabilitation (which is the rehabilitation that addresses the entire structural and nonstructural systems of the building, but uses a lower seismic hazard or lower target Building Performance Level) should be designed for one or more of the following objectives:

1. Life Safety Building Performance Level (3-C)

2. Collapse Prevention Building Performance Level (5-E)

3. Building Performance Levels 4-C, 4-D, 4-E, 5-C, 5-D, 5-E, 6-D, or 6-E (which are described more accurately later).

b) Structural Performance Levels and Ranges

According to FEMA 356, the Structural Performance of a structure that is going to be studied should be selected from the below given four discrete Structural Performance Levels and two intermediate Structural Performance Ranges:

"The discrete Structural Performance Levels are Immediate Occupancy (S-1), Life Safety (S-3), Collapse Prevention (S-5), and Not Considered (S-6)." And "The intermediate Structural Performance Ranges are the Damage Control Range (S-2) and the Limited Safety Range (S-4)." Interpolation between the Performance Levels should be done for obtaining Structural Performance Ranges.

- **Immediate Occupancy Structural Performance Level (S-1):** In this level, the post-earthquake damage should be in the level that the structure remains safe to occupy. It should necessarily retain its pre-earthquake design strength and stiffness and should be in accordance with the acceptance criteria specified in FEMA 356 for Structural Performance Level S-1, FEMA 356 (2000).

- **Damage Control Structural Performance Range (S-2):** This range is the continuous range of damage between the Life Safety Structural Performance Level (S-3) and the Immediate Occupancy Structural Performance Level (S-1), FEMA 356, (2000).

- **Life Safety Structural Performance Level (S-3):** In Life Safety level, the post-earthquake damage should be at the level that damage has happened to structural components but the structure retains a margin against onset of

collapse. It should be in accordance with the acceptance criteria specified in FEMA 356 for Structural Performance Level S-3. FEMA 356, (2000).

- **Limited Safety Structural Performance Range (S-4):** Limited safety ranges are noted as the range of damage that is between the Life Safety Structural Performance Level (S-3) and the Collapse Prevention Structural Performance Level (S-5) FEMA 356, (2000).

- **Collapse Prevention Structural Performance Level (S-5):** In the post-earthquake damage of this level, the building continues to support gravity loads but is not capable of retaining any more margin against collapse, FEMA 356, (2000).

- **Structural Performance Not Considered (S-6):** According to FEMA 356 (2000), this level is for a building in which rehabilitation does not address the structural performance.

FEMA 356 introduces damage control and structural performance levels for four levels of Collapse Prevention, Life Safety, Immediate Occupancy and Operational Level for different structural elements from which Braced Steel Frames have been chosen in Table C1-3. The information is described in Table 2.1 in this research.

Table 2.1: Damage Control and Structural Performance Levels for Steel Braced Frames According to FEMA 356 (2000).

Steel Braced Frame	Collapse Prevention (S-5)	Life Safety (S-3)	Immediate Occupancy (S-1)
Conditions	Extensive yielding and buckling of braces. Many braces and their connections may fail.	Many braces yield or buckle but do not totally fail. Many connections may fail.	Minor yielding or buckling of braces.
Drift	2% transient or permanent	1.5% transient; 0.5% permanent	0.5% transient; negligible permanent

According to FEMA 356, the usage of pushover analysis has limitation and can only be used for the structures with little higher mode effects. In order to determine the level of significance of higher modes in a structure, a modal response spectrum analysis should be done for the frame by using sufficient number of modes that captures 90% of the frame mass participation. Another response spectrum analysis should also be carried out by considering only the first mode. If the shear force in any story that is resulted from the first modal analysis exceeds 130% of the corresponding story shear by the second analysis (considering only the first mode response), then the higher mode effects should be considered significant and pushover analysis can not be used.

c) Deformation-Controlled Versus Force-Controlled Behavior

According to Krawinkler and Seneviratna (1998), it is usually essential to perform a displacement rather than force control analysis because the target displacement might be in a situation with very little or zero (or even negative) lateral stiffness due to the development of the P-delta effect mechanisms.

These types of pushover curves are explained in figure 2.16. (FEMA 356) The Type 1 curve of this figure represents ductile behavior where there is an elastic range from point 0 to point 1 which is followed by a plastic range from points 1 to 3 with a residual strength and ability to support gravity loads at point 3 that is non-negligible. The plastic range is associated with a strain hardening or softening range from points 1 to 2 and a sequential strength-degraded range from points 2 to 3. If the strain-hardening or strain softening range is such that $e > 2g$, then the primary component actions exhibiting this behavior should be classified as deformation-controlled. Otherwise, they should be classified as force-controlled, FEMA 356 (2000).

The Type 2 curve being demonstrated in Figure 2.16 represents ductile behavior where there is an elastic range from point 0 to point 1 on the curve and a plastic range from points 1 to 2, which is accompanied by loss of strength and capability of supporting gravity loads after point 2. If the plastic range is such that $e > 2g$, then the component actions that exhibit this behavior type should be categorized as deformation-controlled; otherwise, force-controlled, FEMA 356 (2000).

The Type 3 curve shown in Figure 2.16 represents a nonductile or brittle behavior with an elastic range from point 0 to point 1 on the curve that is accompanied by a loss of strength and capability to retain gravity loads after point 1. All of the component actions having Type 3 behavior should be classified as force-controlled, FEMA 356 (2000).

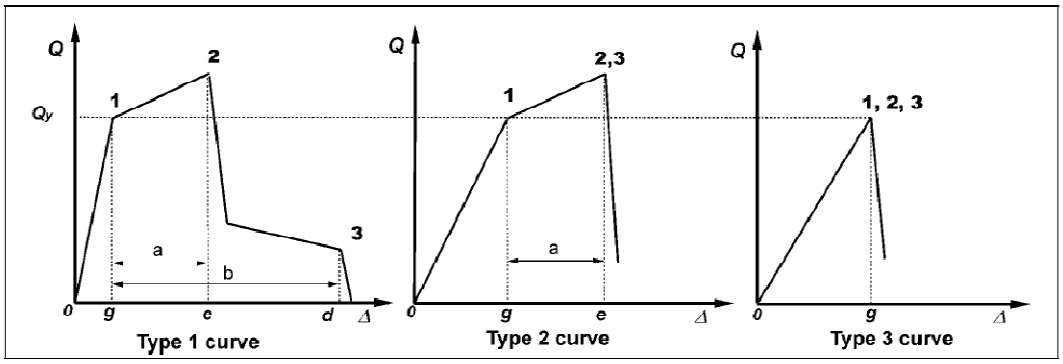

Figure 2.16: Component Force versus Deformation Curves (Courtesy of Federal Emergency Management Agency, FEMA 356).

This document gives more information on this issue on its figure C2-1 (Figure 2.17 of this research) stating that this figure shows the generalized force-deformation curves used in this document to demonstrate modeling of components and acceptance criteria for deformation-controlled actions. Linear response is between point *A* and an effective yield point (*B*). The slope from *B* to *C* usually represents strain hardening. *C* is the point at which significant strength degradation starts. After point *D*, the strength of the component is substantially reduced until point *E*. The component strength is essentially zero at deformations greater than point *E*.

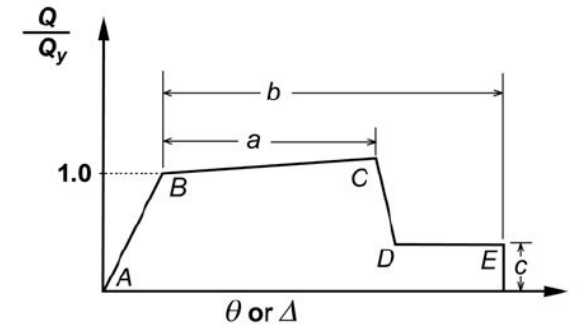

(a) Deformation

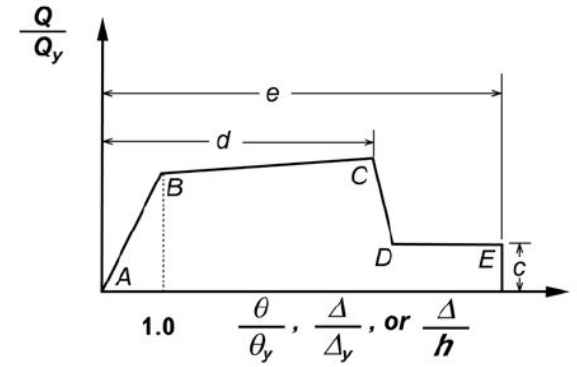

(b) Deformation ratio

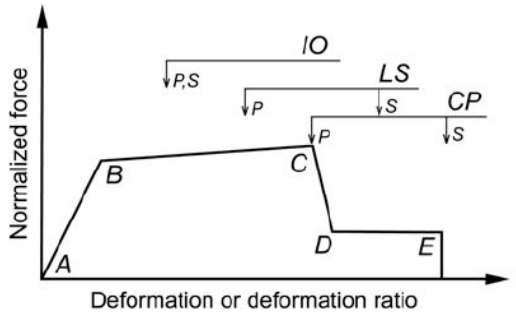

(c) Component or element deformation acceptance criteria

Figure 2.17: Generalized Component Force- Deformation Relations for Depicting Modeling and Acceptance Criteria (Courtesy of FEMA 356).

More information about the acceptance criteria for assemblies used in nonlinear procedures as:

- "Immediate Occupancy: the deformation at which permanent, visible damage occurred in the experiments but not greater than 0.67 times the deformation limit for Life Safety specified in 6.1.2.

- Life Safety: 0.75 times the deformation at point 2 on the curves.

- Collapse Prevention: The deformation at point 2 on the curves but not greater than 0.75 times the deformation at point 3."

An alternative force-deformation shape for the structure is also introduced in figure 2.18 from FEMA 356 (2000).

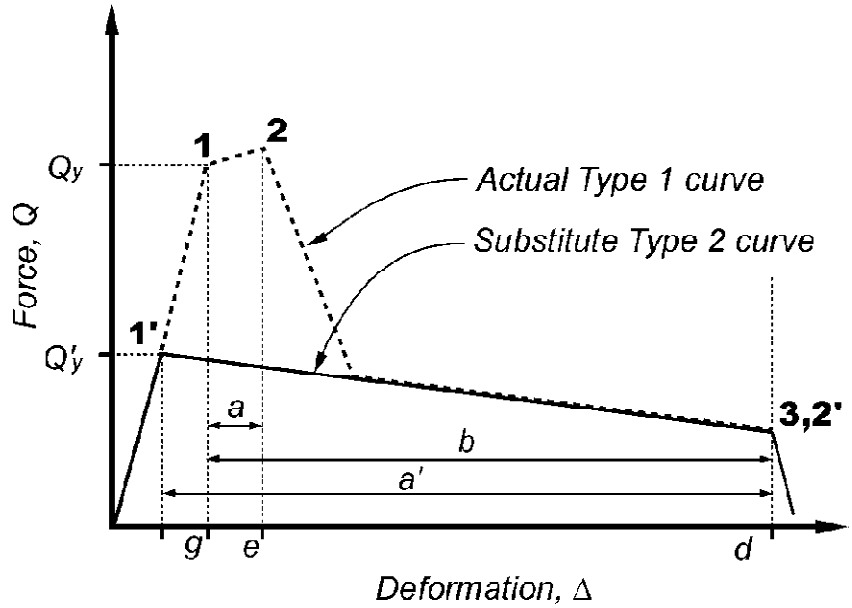

Figure 2.18: Alternative Force-Deformation Curve (Courtesy of Federal Emergency Management Agency).

According to FEMA 356 (2000), the control node of pushover analysis should be located at the mass center of the building roof.

In this document, two important key points are lateral load distribution (which has been problematic and further research into this area is given in the next parts of this

chapter) and idealization of Force-Displacement curve. These key points are explained here:

d) Lateral Load Distribution

According to FEMA 356, in each floor diaphragm, the lateral loads should be applied to the mathematical model in proportion to the inertia forces distribution.

In FEMA 356 procedure, two patterns, each from a separate category should be chosen and the more critical of the values should be used for rehabilitation objectives.

The first load pattern should be selected from the following list:

- Code distribution: Only if more than 75% of mass participates in first mode. In this way, the second vector must be the uniform distribution.
- First mode: Only if more than 75% of mass participation is in the first mode.
- SRSS: If $T_e > 1$ s.

The second load shape should be selected from the following list:

- Uniform distribution
- Adaptive load distribution

e) Idealized Force-Displacement Curve

FEMA 356 uses a coefficient method to calculate target displacement the older version of which was previously used in FEMA-273 and FEMA-274. In this method, the nonlinear capacity curve with its complexities should be replaced with

an idealized curve, in order to estimate the effective yield strength (V_y) and effective lateral stiffness (K_e) of the structure. The idealized curve is bilinear, with initial slope of K_e and post-yield slope of α. This bilinear curve should be estimated by cycles of trial and error with an approximate balance of the area under the actual and idealized curve. The effective lateral stiffness, K_e, is the secant stiffness which is calculated at a base shear force of 60% of V_y. The post-yield slope, α, is the slope of a line segment that connects the structural yield point to the target displacement located on the actual curve at the calculated point. In the cases of negative stiffness hardening, the effective yield strength should be necessarily greater than the maximum base shear force at the peak point of the actual curve. These parameters are illustrated in Figure 2.19.

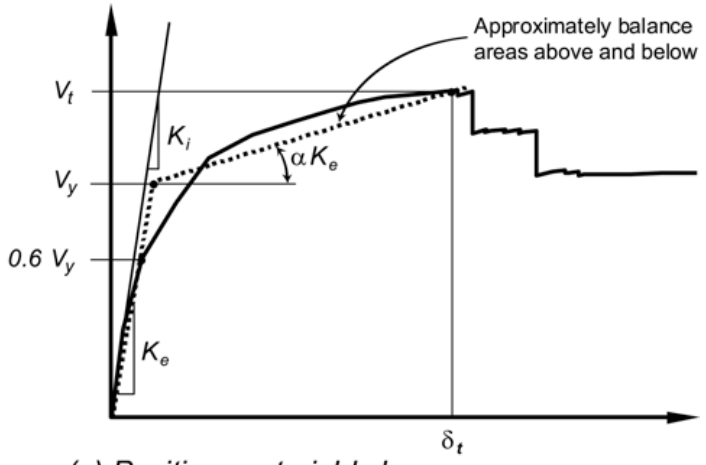

(a) Positive post-yield slope

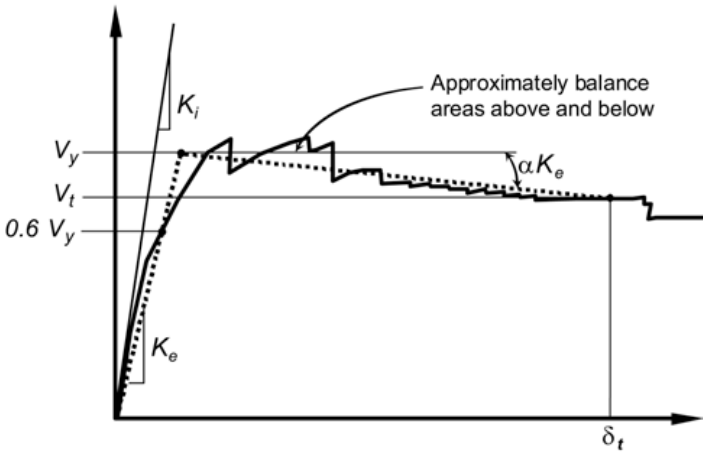

(b) Negative post-yield slope

Figure 2.19: Idealized Force-Displacement Curves (Courtesy of Federal Emergency Management Agency).

Period should be determined from equation 2.9.

$$T_e = T_i\sqrt{\frac{K_i}{K_e}} \tag{2.9}$$

Where:

T_i = Elastic fundamental period (in seconds) in the direction under consideration calculated by elastic dynamic analysis

f) Target Displacement

As it was explained in the previous sections, the estimation of target displacement point plays a significant role in the coefficient based performance-based method. Different documents and studies have mentioned various relationships for the calculation of target displacement point. FEMA 356 introduces the equations 2.10, 2.11, 2.12 and 2.13 for this task which are summarized in FEMA 440:

$$\delta_t = C_0\, C_1\, C_2\, C_3\, S_a\, \frac{T_e^2}{4\pi^2}\, g \qquad (2.10)$$

Where:

C_0: "Modification factor to relate spectral displacement of an equivalent SDOF system to the roof displacement of the building MDOF system". There are several ways of calculating C_0, the easiest of which is using the appropriate value from Table 3-2 of FEMA 356.

C_1: "Modification factor to relate expected maximum inelastic displacements to displacements calculated for linear elastic response" This coefficient should be calculated from the below equations:

$$\begin{cases} = 1.0 & T_e \geq T_s \\ = [1.0 + (R-1)\, Ts / Te] / R & T_e < T_s \end{cases} \qquad (2.11)$$

But not greater than

$$\begin{cases} 1.5 & T_e \geq T_s \\ 1.0 & T_e < T_s \end{cases}$$

Nor less than 1.0

T_e: "Effective fundamental period of the building in the direction under consideration, in seconds" which should be calculated in compliance with section 3.3.3.2.5 of FEMA 356.

T_s: "Characteristic period of the response spectrum, defined as the period associated with the transition from the constant-acceleration segment of the spectrum to the constant- velocity segment of the spectrum."

R: "Ratio of elastic strength demand to calculated yield strength coefficient"

$$R = \frac{S_a}{V_y/W} * C_m \tag{2.12}$$

C_2: "Modification factor to represent the effect of pinched hysteretic shape, stiffness degradation and strength deterioration on maximum displacement response." C_2 value should be obtained from table 3-3 of FEMA 356.

C_3: "Modification factor to represent increased displacements due to dynamic P-Δ effects."

$$C_3 = 1.0 + \frac{|\alpha|(R-1)^{3/2}}{T_e} \tag{2.13}$$

S_a: "Response spectrum acceleration, at the effective fundamental period and damping ratio of the building in the direction under consideration"

g: "acceleration of gravity"

α: "Ratio of post-yield stiffness to effective elastic stiffness, where the nonlinear force-displacement relation shall be characterized by a bilinear relation."

2.3.2.2 Evaluation of FEMA 356 Coefficient Method by FEMA 440

a) C_1 Evaluation

According to FEMA 440, the C_1 coefficient becomes independent of the structures lateral strength by the FEMA 356 C_1 capping that is imposed by structures with short periods of vibration. As a result, changes in the lateral displacement demands are not made due to the changes in R. The conclusions in this document (FEMA 440) are given below:

The value of C_1 is not influenced significantly with changes in R for periods longer than about 1.0 s (which is quite fair).

For structures with periods between 0.4 s and 1.0 s, the maximum displacement of the frame is underestimated. Underestimation increases with R.

Moreover, for structures with periods smaller than 0.4 s, sometimes, the use of capping on C_1 leads to great displacement underestimations.

Overall, it was observed in this study that the variations in C_1 due to the changes in period and lateral strength, as per FEMA 356, could be improved (FEMA 440).

b) C_2 Evaluation

The results given below are the conclusions drawn from FEMA 440:

The maximum displacements of stiffness-degrading (SD) oscillating models are totally smaller than the actual values, with minor exceptions. This is while the FEMA 356 C_2 coefficient increases lateral displacements in similar period ranges.

The lateral displacements of SD systems are generally larger than their actual ones for periods of vibration smaller than about 0.6 s. These differences increase with changes in R. For relatively strong SD systems, C_2 values in the period range specified in FEMA 356 are generally higher than those computed whilst they are smaller than those computed for weaker SD systems.

The simplified method in FEMA 356 overestimates displacements significantly for short periods of vibration and for periods of vibration larger that 1.0 s. Maximum displacement is overestimated for small values of R and underestimated for large values of R for short vibration periods.

c) C_3 Evaluation

FEMA 356 C_3 value sometimes leads to lateral dynamic instability of the model of the structure when the structure has negative stiffness hardening. This issue is not taken into account in this method properly.

2.3.2.3 FEMA 440 Improved Procedures for Displacement Modification

After the evaluation explained in section 2.3.2.2, the following modifications have been introduced into the FEMA 356 Displacement Modification method in order to lessen the mentioned problems.

a) C_1 Modification

The following is introduced by FEMA 440 for the coefficient C_1:

$$C_1 = 1 + \frac{R-1}{\alpha T_e^2} \tag{2.14}$$

Where, T_e (the effective fundamental period of the SDOF model of the structure) and R (the strength ratio) are computed as in the FEMA 356 method being explained in section 2.3.2.1. The constant α is 130, 90, and 60 for B, C, and D site classes, respectively. The coefficient C_1 for 0.2 s can be used for periods less than 0.2 s and can be assumed to be 1.0 for periods greater than 1.0 s (FEMA 440).

The FEMA 356 current C_1 is estimated to be inaccurate for the prediction of maximum displacements and is thus removed in FEMA 440.

b) C_2 Modification

The following suggestion is made by FEMA 440 for the coefficient C_2:

$$C_2 = 1 + \frac{1}{800}\left(\frac{R-1}{T}\right)^2 \tag{2.15}$$

The value of the coefficient C_2 for 0.2 s can be used again for periods less than 0.2 s and can be assumed equal to 1.0 for periods greater than 0.7 s. C_2 should only be used for the frames exhibiting great stiffness or strength degradation.

c) C_3 Modification

FEMA 440 has suggested that the FEMA 356 coefficient C_3 should be removed.

2.3.3 Evaluation of Improved Nonlinear Static Procedures

In this part, FEMA 440 compares results of nonlinear static procedures with results obtained by nonlinear response-history analyses (for a specific hazard level and site conditions).

2.3.3.1 Description of the Study

According to FEMA 440, sixteen ground motions and nine SDOF oscillators, with bilinear load-displacement relationships, five percent initial damping, post-elastic stiffness of five percent of elastic stiffness without strength or stiffness degradation, with three different yield strengths and three different periods and R values of 2, 4, and 8 were used for this study.

2.3.3.2 Results of the study

In Figures 2.21, 2.22 and 2.23 (courtesy of FEMA 440),

- NDA: The mean value of the maximum displacement response amplitudes (nonlinear dynamic analysis).
- FEMA 440 EL: The result of improved equivalent linearization method.
- FEMA 440 DM: The result of improved displacement modification.
- Approximate EL: The result of the section 6.5 of FEMA 440 approach.
- ATC-40 and FEMA 356 are the result of the mentioned methods.
- $\mu = 10$ corresponds to displacement ductility of 10.

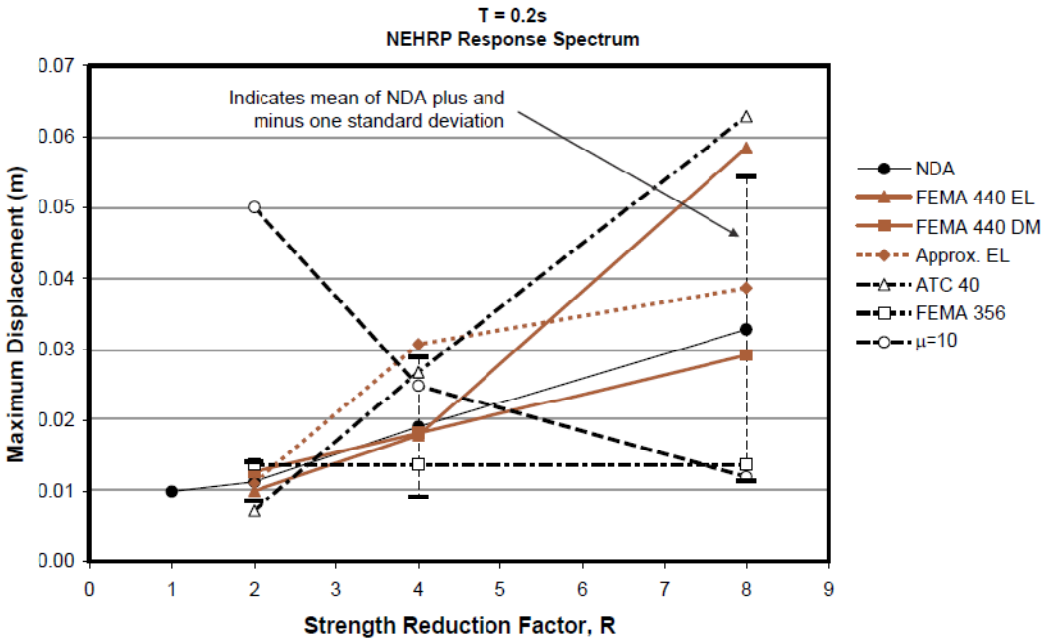

Figure 2.20: Comparison of responses for an oscillator with $T = 0.2$ s calculated using various procedures (Courtesy of FEMA 440).

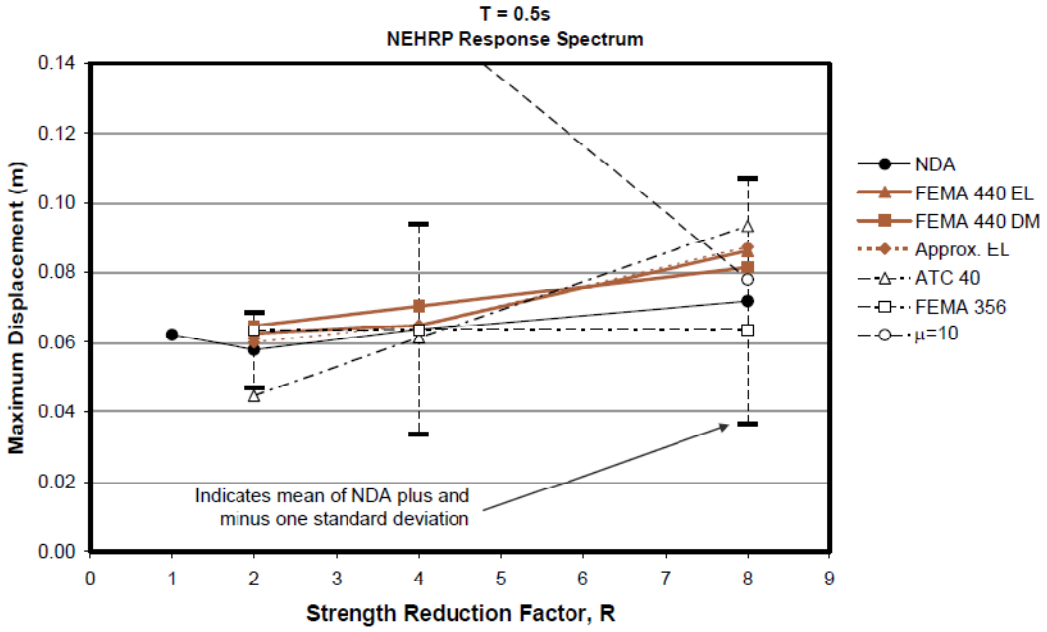

Figure 2.21: Comparison of responses for an oscillator with $T = 0.5$ s calculated using various procedures (Courtesy of FEMA 440).

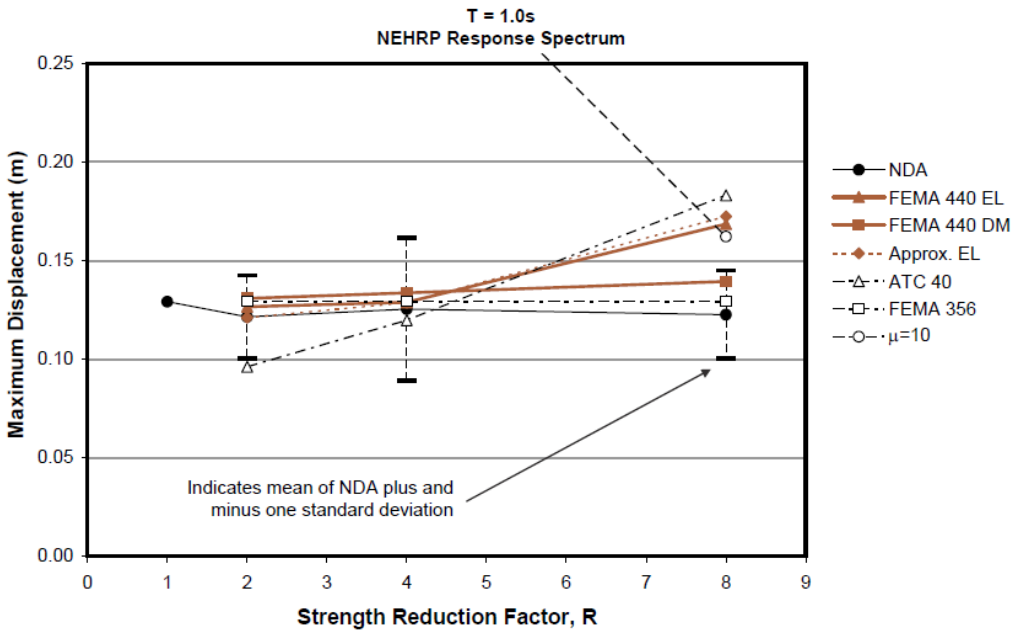

Figure 2.22: Comparison of responses for an oscillator with T = 1.0 s calculated using various procedures (Courtesy of FEMA 440).

This document states the following conclusions:

According to nonlinear dynamic analysis, short-period oscillators, being more sensitive to strength, the maximum displacement response amplitude increases as strength decreases. The improved procedures proposed by FEMA 440 generally follow the NDA observed mean trends with reasonable accuracies. The procedure of FEMA 356 is unable to estimate the displacement response increase with R for short-period oscillators and the ATC-40 procedure underestimates the displacement response when the R is small and overestimate the response when R is large.

2.4 Inelastic Performance Assessment of Lateral Load Resisting Systems

Assaf (1989) mentions that the number of bays in a structure has little effect on the R factor of the building. He also states that there is a decrease in the value of R factor due to an increase in the number of stories.

Mitchell and Paultere (1994) used force modification factors to review the codes approaches to treatment of ductility demand. They discussed how overstrength of structures could affect the factors influencing structural response. They concluded that the significance of structural overstrength on the ability of the structures to resist lateral load without collapse is demonstrated by the nonlinear analyses of RC frames.

Tremblay (2002) has tested the inelastic response of steel bracing members. The research assessed the inelastic response of diagonal steel bracing members which were subjected to cyclic inelastic loading. The aim was to collect data for the seismic design of CBFs since they require a ductile response under earthquakes. The buckling strength of the bracing members, the brace post-buckling compressive resistance, the brace maximum tensile strength, and the lateral deformations of the braces upon buckling were examined in this study. He states that there was a decrease in compressive strength as the plastic hinge formed near the brace mid-length after the buckling test of diagonal concentrically braced frames.

In 2003, Maheri and Akbari open a new chapter in inelastic response assessment of structures by calculating seismic behavior factor, R, for steel X-braced and knee-braced RC frames. By studying the effect of different parameters on ductility of 4, 8, and 12 story steel X-braced and knee-braced RC structures, such as, the type of bracing system and height (number of stories), they conclude that R generally decreases with an increase in the number of stories. Although this is not always the case, ductility-dependent component, R_μ, is subject to large variations with height variation. Moreover, the behavior factor provided by knee bracing is higher than the

one of X bracing system. This shows the dependency of bracing system type on the ductility of the frame. They are demonstrated in Figure 2.23.

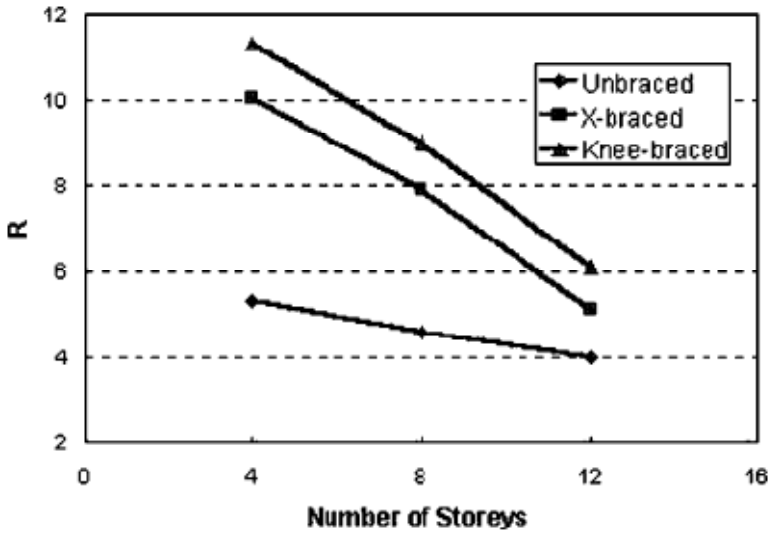

Figure 2.23: The effects of the type of bracing on the R value of the braced frames (Courtesy of Maheri & Akbari, 2003).

On a similar topic, Youssef, Ghaffarzadeh and Nehdi (2007) experimented the seismic performance of CBFs in reinforced concrete structures. They concluded that the braced frame resist higher lateral loads compared to the moment frame and provided sufficient ductility.

Huaung, Li and Chen (2005) provided a general review of concentrically braced frames in comparison with other steel lateral load resisting systems, ignoring the type of concentrically braced frame and its height (It should be noted that there are other researchers who has ignored the type of CBFs). This is given in the Figure 2.24. It can be observed from this figure that only one constant curve represents the behavior of all different CBFs undermining their type.

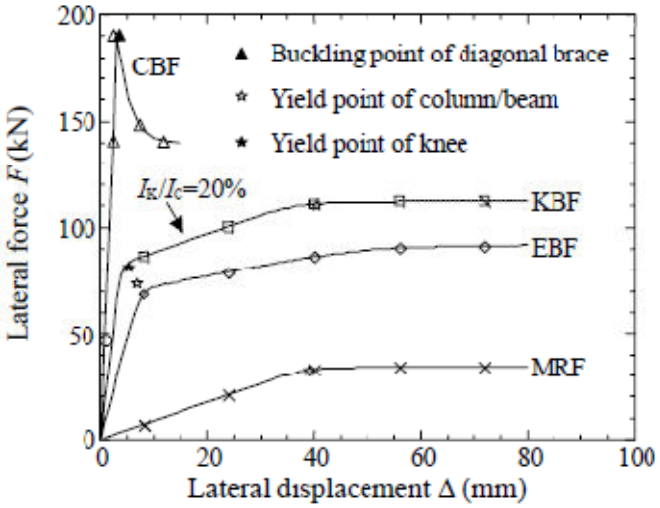

Figure 2.24: Comparison of the performance of commonly used steel frame systems (Courtesy of Huaung, Li & Chen, 2005).

Then they used pushover analysis to get the results and then suggested general design recommendations for knee bracing systems.

Kim and Choi, (2005) assessed the response modification factors of steel chevron braced frames, stating that although the seismic design codes prescribe one single modification factor value for all buildings with a specific structural system regardless of its earthquake load level and height, this parameter is dependent on the building period and applied load. They assess thirty concentrically inverted V braced frames with various numbers of stories and span lengths with pushover analysis, calculate their overstrength, ductility and response modification factors and verify their results with nonlinear dynamic analysis. According to their study, in an ordinary concentrically braced frame, after the elastic range of the building, the strength is reduced dramatically when the first compression brace buckles and the beams connected to the buckled brace yields consequently. Then, there is a slight increase in the structural lateral strength with further redistribution of loads, and another drop due to buckling of bracing members in other stories. They concluded

that there was an increase in both overstrength and ductility factors due to decrease in the frame height and the span length increase. The overstrength factors estimated are significantly smaller than the IBC code values. This outcome might cause unsafe design by underestimating the seismic force that is transferred to a critical element from the other elements of the lateral force resisting system. For all OCBF studied, the response modification factors were less than the code value. They state that some of the differences between their results and those of other researches are due to the difference in seismic load that is used in the structural design. They also compared their results with the nonlinear incremental dynamic analysis (IDA) and stated that the IDA results generally formed an upper bound to the NSP curves but the inelastic response obtained from both procedures were similar. At the end, they mention that the earthquake-resisting capacity of braced frames was less than the level specified in IBC 2000 design code. This is why these levels were reduced in FEMA-368 (2001), a few years after FEMA-302 (1997). They finally recommend other studies to be done on the assessment of inelastic response of concentrically braced frames in different seismic hazard levels, number of stories, target ductility ratios, etc in order to find more about the inelastic behavior of concentric braced frames. One of such studies might be the effect of the type of concentrically braced frames (which is the aim of the current study) since only chevron CBF has been studied in this research.

The findings of Jain SK, Navin R., indicates more necessity for further study on the inelastic performance of bracing systems. They state that the overstrength factor of structures vary with seismic zone, number of stories and design gravity load. Among these parameters, seismic zone plays the most critical role. The mean value of overstrength of the studied frames by this research is 2.84 and 12.7 in zones V and I of Indian code (with the highest and lowest seismicity), respectively. Moreover, this

parameter decreases with the increase in the number of stories. This means that overstrength factor of structures located in low-seismic regions are about five times of those located in regions with high seismicity. They claim that this is not currently taken into account in design codes.

Yang, Leon and DesRoches (2008) propose methodology for designing zipper-braced frames in order to achieve more ductile behavior. After designing three zipper braced frames, inelastic strength and deformation capacities for the entire structures were estimated by pushover analysis. The yielding and buckling sequences in the members were also assessed by this procedure. The inelastic performance of the frames was also evaluated by nonlinear dynamic analysis. They explain the pushover curve of a braced frame by a tri-linear curve having three stages. In the first stage, the behavior of the frame is linearly elastic until the first buckling occurs in a compressive bracing member. In the second stage, the capacities of compressive bracing members reach their minimum post-buckling strength. At this stage, the tension braces still attract load until their tension yield capacities. In the third stage, the tension braces yield and the base shear reaches its hardening range which is the ultimate base shear.

The inelastic response of steel structures with stainless steel (SS) has also been studied by Di Sarno, Elnashai and Nethercot, demonstrating the effect of steel properties on structural inelastic response. The results of the research they conducted in 2005, indicated that the use of stainless steel for the columns of the structure increased the system overstrength by 30% when compared to structures with mild steel. This clearly shows the effect of steel type being used on the response parameters of steel structures. In 2006, they did another study, leading to the

conclusion that usage of stainless steel for retrofitting of current structures leads to noticeable changes in nonlinear behavior of both CBFs and MRFs when compared to ones being retrofitted by mild steel. Finally, they (2008) studied the seismic performance of frames braced with stainless steel by using pushover and response inelastic history. Results show that the frames using stainless steel demonstrated greater plastic deformations and better energy absorption when compared with mild steel braced frames. Furthermore, the overstrength increases by about 40% in CBFs with SS braces and columns comparing to the frames made of mild steel. The use of stainless steel in the diagonals or in braces and links of eccentrically braced frames increases the global overstrength of the bracing system by 20%. When columns are also made out of SS, the increase in the overstrength can be as high as 50% in EBFs.

2.5 Economical Comparison of Bracing Systems

The increase in the construction of braced frames, especially CBFs, requires further studies on economical aspects of structures in order to achieve financial savings.

Brognoli, Gelfi, Zandonini and Zanella (1998) developed a software tool for optimal design of semi-rigid braced frames (braced frames with semi-rigid connections) by which economical comparison of semi-rigid braced frames has become conventional.

Kameshki and Saka (2001) studied the optimization of bracing system type for a fifteen story building by genetic algorithm. This method includes selection of beams, columns and bracing members from a set of sections for different bracing systems and calculation of the least weight of the frame. This study results showed that the X-bracing system with pinned beam to column connections provides the least steel weight comparing to other frames and V- and Z-bracing systems that are not as

efficient as the X-bracing system. It is also observed that the interstory drift constraints are dominant factors of design procedure in frames with rigid beam to column connections, and in frames with pinned beam to column connections with V or Z bracing systems. It should be noted that only one frame geometry with a constant height and number of stories was studied in this research. Figure 2.25 illustrates the results of this study (courtesy of Kameshki & Saka, 2001).

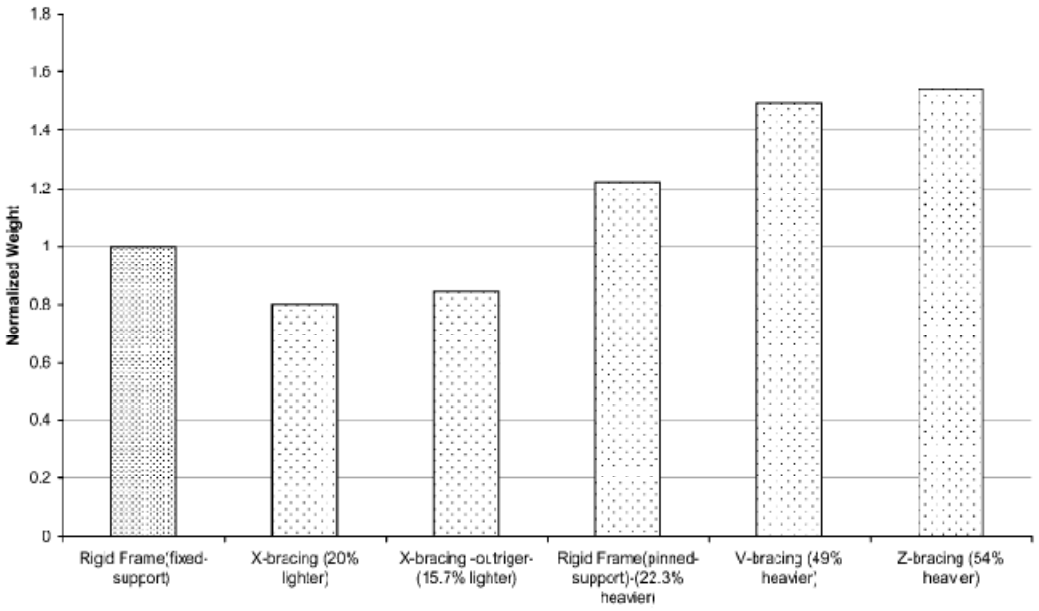

Figure 2.25: Comparison of normalized weights of tall frames with different bracing systems against fixed support frame (Courtesy of Kameshki & Saka, 2001).

They also explain that the effect of lateral forces in the frame is transferred to the shear links by bracing members in a V braced frame. These links are thus, subjected to larger forces compared with the other members. This fact affects the design of middle span beams. The methodology used in this research was based on linear elastic design of steel and drift check.

Columns are also affected by bracing system and thus, economical comparison of bracing systems should take their effect into account, as well the effect of the beams.

Tremblay (2002) explicitly describes the effect of nonlinear behavior of bracing on the column capacity: Under such large inelastic deformation levels of braced frames, strain hardening develops in the tension braces and the post-buckling capacity of the compression braces have reduced significantly and these changes result in a critical loading case for the column that should carry the gravity loads as well as the difference between the vertical components of the tension (stiffness hardened) and compression (buckled) bracing member forces (Figure 2.26).

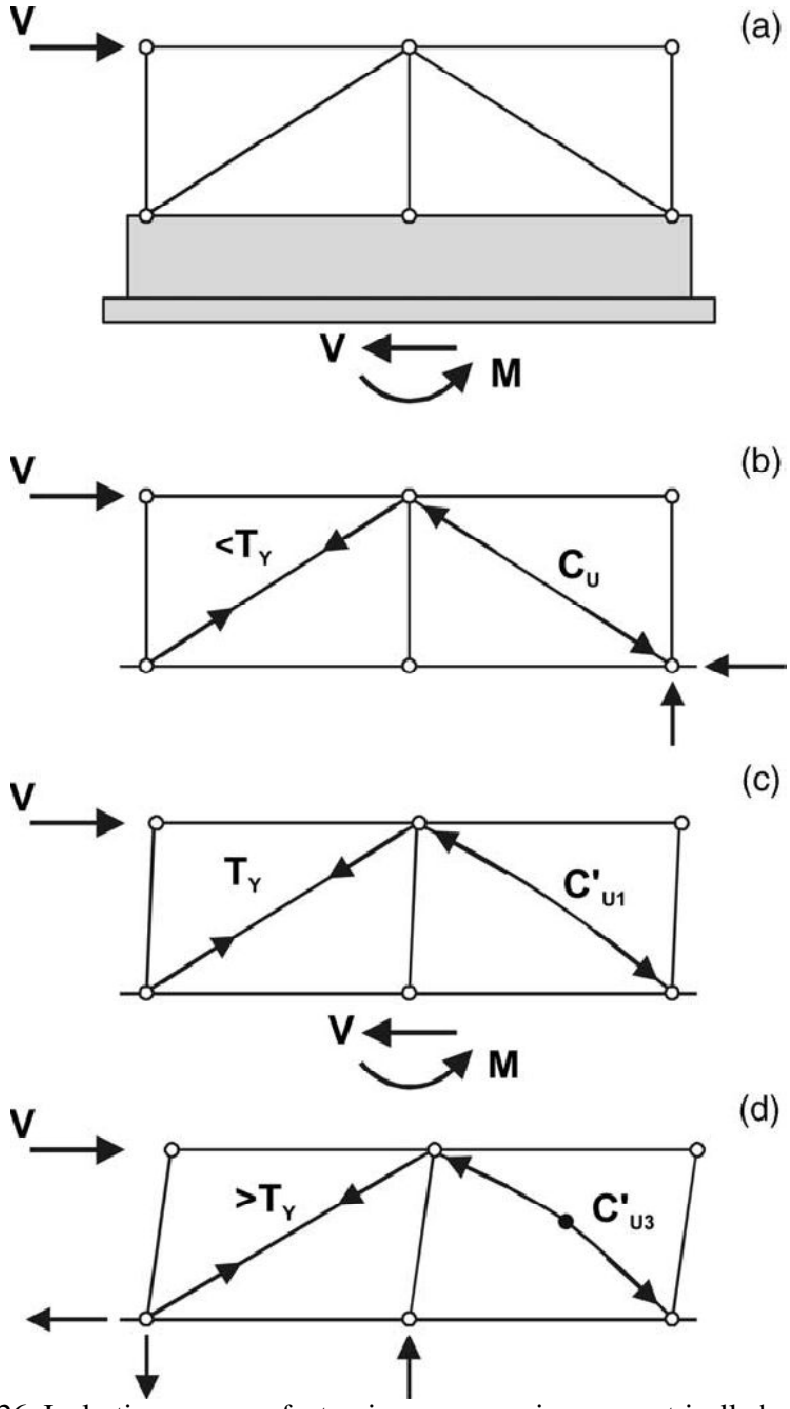

Figure 2.26: Inelastic response of a tension–compression concentrically braced steel frame (Courtesy of Tremblay 2002).

Similar results have been reported by Kim and Choi, (2005) but none of these two researches investigated the quantification of the effect of inelastic response of CBFs on seismic column demand.

Maher and Safari (2005) state that generally, design engineers determine the optimum positions of the bracing members by trial and error and develop topology optimization of steel bracing system for a two-dimensional steel frame by genetic algorithm.

Moghaddam, Hajirasouliha and Doostan (2005) state that the nonlinear response of lateral load resisting systems should be optimized. They presented a methodology for optimization of the dynamic response of CBFs, being subjected to earthquake load, which was based on the uniform distribution of deformations concept. This study has adopted an iterative optimization procedure in order to achieve the optimum distribution of structural properties. Inefficient materials are moved from the stronger to weaker parts of a frame in this approach in order to optimize the seismic design. This process continues to reach a state of uniform deformation.

2.6 Simultaneous Study on Weight and Inelastic Behavior of Bracing Systems

The review of the research work on inelastic behavior and economical aspects of bracing systems were given in the two previous sections. Although much has been done in each one of these fields, there was no research work studying both of them simultaneously until 2008.

D. Ozhendekci and N. Ozhendekci (2008) carried out a comprehensive research on "Effects of the frame geometry on the weight and inelastic behavior of eccentrically braced chevron steel frames". They state that parametric studies are still required about the effects of the frame geometry on the inelastic response and weight of the structures. The failure pattern of the shear link in EBFs is influenced by the level of eccentricity. 420 EBFs with shear yielding links, 105 EBFs with intermediate links, and 105 EBFs with flexural yielding links are designed in this research. One of the

reasons of the great number of models is due to the change in the eccentricity of braces. After doing the nonlinear analysis, they discuss the effects of frame geometry on the weight and global inelastic behavior of the frames for different categories of EBFs with different eccentricity. In this study, eccentrically braced chevron frames are categorized by the link element failure as shear yielding link, flexural yielding link and intermediate link frames. Due to the similarity of concentric chevron braces with the first category, some of its relevant figures are included in this section and in Figures 2.27 and 2.28 to demonstrate the research results more clearly.

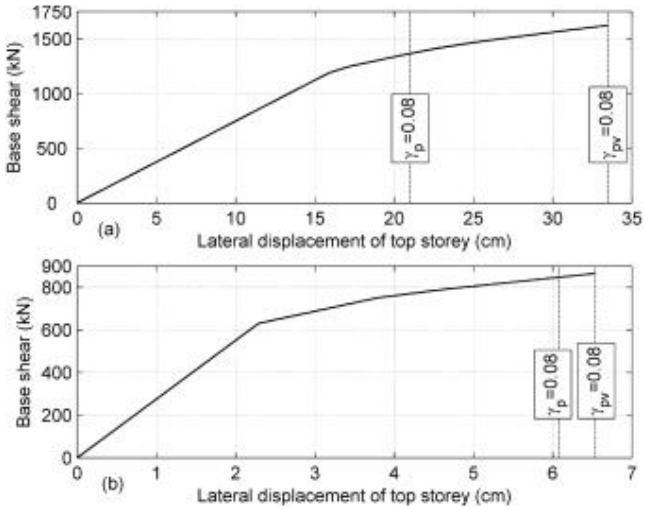

Figure 2.27: Pushover curves of the EBFs with shear yielding links (a) 9-storey frame (b) 3-storey frame (Courtesy of D. Ozhendekci & N. Ozhendekci, 2008).

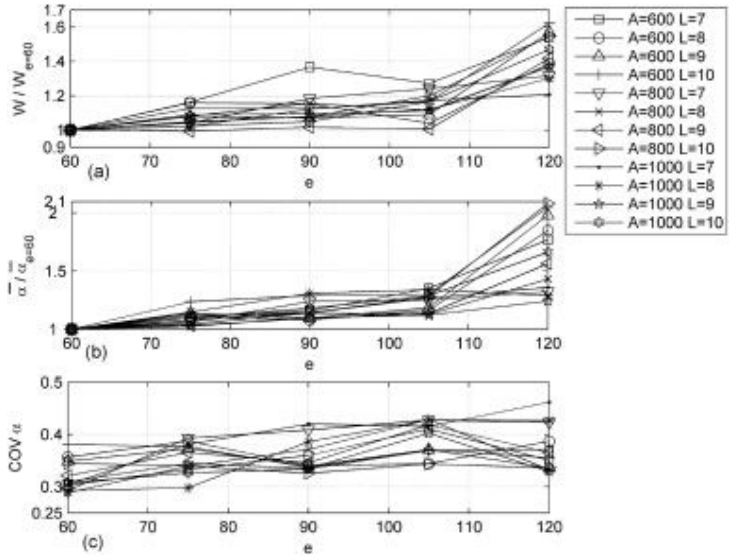

Figure 2.28: Effects of the length of shear yielding links on the (a) normalized frame weights (b) normalized mean scale factors (c) coefficients of variation of scale factors (3-storey EBFs) (Courtesy of D. Ozhendekci & N. Ozhendekci, 2008).

This research, although examining a great number of models and considering both inelastic behavior and weight simultaneously, is considering only the effect of eccentricity ratio of one type of EBF (chevron). Further research for different bracing systems is still lacking on this topic.

Richards (2009) studied the seismic column demand in steel ductile braced frames. This issue was noted and studied but not quantified in the economical comparison section by Tremblay (2002) and Kim and Choi (2005) that was reviewed in the previous section. In this research, "Seismic column demands were studied in buckling restrained braced frames, SCBFs, and EBFs with number of stories of 3, 9, and 18, by using nonlinear dynamic analysis. The axial force demands which were observed in this study were 55–70% of demands commonly used in design for columns at the base of 9- and 18-story BRBFs and EBFs. This shows potential cost savings on columns, base plates, anchor rods, and foundations in tall frames. On the other hand, column axial load demands were up to 100% more than those commonly

used in the design of low-rise SCBFs with braces in the 2-story X-braced frame, due to the force redistribution occurring after brace buckling. This research shows the effect of number of stories on seismic column demand but still seismic beam demand has not been studied.

2.7 Conclusion

In this chapter, different types of lateral load resisting systems (mainly bracing systems) in steel structures were introduced (section 2.1).Concentrically braced frames (section 2.1.2.1) are going to be studied further in this research. The methods of evaluation of structural response curve were described with their advantages and disadvantages in section 2.2. Nonlinear static (pushover) analysis is going to be used in this study. Different load patters of pushover analysis and their effects on the analysis results were also studied in section 2.2. First mode load pattern is chosen to be employed. A background on performance-based engineering procedures and an evaluation of them were given in section 3.3. FEMA 440 Improved Coefficient Method of performance-based engineering is employed. Reviews on the past research on assessment of inelastic performance of lateral load resisting systems and economical comparison of them were given in sections 2.4 and 2.5 respectively. Section 2.6 gives a review on simultaneous study on weight and inelastic behavior of bracing systems. Only two studies have been done on this topic (on 2008 and 2009). From the research works given in section 2.6, it could be concluded that recently, researchers are insisting that the economical study of a bracing system should necessarily be based on its nonlinear characteristics to have sufficient accuracy. Though, very few studies have been carried out on this topic. A

comprehensive study on weight and inelastic behavior of concentrically braced frames is still missing. This issue will be studied in this research.

CHAPTER III

DESIGN OF MODEL STRUCTURES

This chapter is divided into two sections. The methodology of design is described in section 3.1. Then, the results (design sections, weight of the sections and the total weights of the frames) are given in section 3.2.

The units of Kg, Kgf and meter are used in this study for mass, force and distance respectively.

3.1 Methodology of Design

The geometry of the frames that are going to be designed and analyzed in this study is defined in section 3.1.1. Four different methodologies of economical comparison of bracing systems are also given in this section. Choice of 2-D versus 3-D models are done in section 3.1.2. The criteria of design are chosen in section 3.1.3. Design software is selected and introduced in section 3.1.4. The design materials and the steel sections which are going to be used for designing the frames are given in sections 3.1.5 and 3.1.6. Sections 3.1.7, 3.1.8 and 3.1.9 are devoted to connections, loading of the frames and special considerations of shear beams in V- and Inverted V-braced frames.

3.1.1 Frame Geometry

For assessment of bracing systems, the first step is to design different models with different bracing systems to be assessed in the next step. The choice of models and

their geometry is very important for this study since they effect the results of frame inelastic behavior (Maheri & Akbari, 2003, Kappos, 1999, Assaf , 1989, Tremblay, 2002, Kim & Choi, 2005, D. Ozhendekci & N. Ozhendekci, 2008) and economical aspects (Kameshki & Saka, 2001, Tremblay, 2002, Maher & Safari, 2005, D. Ozhendekci & N. Ozhendekci, 2008, Richards, 2009). Thus, the frame geometry was decided to be chosen from the past well-known studies in similar topics. Among the available literature, this study is similar to that of Maheri and Akbari (2003). Therefore, the frame geometry chosen are the same as those used by Maheri and Akbari (2003) which were originally used by Mwafy and Elnashai (2001). Mwafy and Elnashai (2001) compared the results of analysis carried out on these frames by using nonlinear static (pushover) and dynamic procedures and found that NSP is excellent in evaluation of nonlinear behavior of these models. The use of similar models and analysis method with the above named studies also allows better verification of the models and usage of nonlinear static (pushover) procedure for this analysis.

The models geometry information is as follows:

- 4-, 8- and 12-storey frames representing the low to medium rise buildings are chosen (according to Maheri & Akbari, 2003 and Mwafy & Elnashai, 2001).

- Each frame has three bays with 5 meter span length as per the frame of Maheri and Akbari (2003) although the original frames had five bays with span lengths of 5 meters (Mwafy and Elnashai, 2001). The former had reduced the number of bays since according to Assaf (1998), number of spans has little effect on nonlinear response of the frames but reduction of bays increases the speed of frame analysis by computer. The use of three

bays is a very good choice for the efficient placement of the X-, V-, and inverted V- bracing systems within the frame central bay. Moreover, Diagonal bracing system can be located within the two perimeter bays at the corner.

- Height of all stories is 3 meters, as per the above mentioned references.

- Each frame is braced against lateral loading with four different concentric bracing systems (X-, V-, inverted V- and diagonal).

A braced frame that is not subjected to lateral loads is also required for each frame of the special number of stories to determine the added weight due to the lateral load. The reason for this requirement is the methodology of calculation of the economical effect of lateral load resisting system. Four methodologies were studied in order to be used for economical comparison of the frames. These methodologies are as follows:

3.1.1.1 Calculation of Weight of Bracing Members

If the effect was only on the bracing members, their weight could easily be calculated directly in order to find their economical effect. But according to the past researchers like Tremblay (2002) and Richards (2009), they also effect the seismic column demand (and consequently weight) and seismic beam demand (Kim & Choi, 2005). Thus, the weight of the bracing members can not be used as the whole effect of the bracing system on the structure.

3.1.1.2 Calculation of the Entire Frame Weight

The method that was used by Kameshki and Saka (2001) and D. Ozhendekci and N. Ozhendekci (2008) is to calculate the whole weight of the frames with different bracing systems. This method is more precise than the previous one but it also has a problem. The frame weight is not totally devoted to resist the lateral loads only. A part of steel is required to resist the vertical loads (with a fixed vertical load resisting system as in the case of this study) and the rest is devoted to resist the lateral loads. Considering the whole weight of the frame, the results are underestimated in this method since different weights of bracing system are added to a constant weight of vertical load resisting system.

3.1.1.3 Usage of Un-braced Benchmark Frames

This study has suggested another solution to this problem; to have an un-braced structure not being subjected to lateral load as a benchmark. Then, the weight of the un-braced benchmark structure can be calculated with the weight of braced structures so that the weight of bracing systems can be found. In this method, the effect of end conditions of columns is not taken into consideration. The bracing system affects the end conditions of columns, leading to reduction in the column demand for vertical loads in a frame. When the bracing system is removed, even if the structure is only subjected to the vertical loads, the column sections will increase. This will lead to an unwanted increase in the whole structure weight, affecting the results of the study.

3.1.1.4 Usage of X-braced Benchmark Frames Not Subjected to Lateral Loads

The last solution that has been suggested and used by this research is to have a braced frame as benchmark that is not subjected to any lateral load. In this way, the problem of the previous method is removed since the end conditions of the columns are the same for all of the models and the weight of the vertical load resisting system will become constant. The differences in the weights of the frames are then only related to lateral load resisting systems. In this way, the effect of the increase in seismic beam and column demand is taken into account, the undermining of the method used by the previous researchers has been eliminated, all of the columns are in the same ending conditions and the unwanted effect of column ending conditions on the bracing system weight is also removed. Theoretically, there is a problem in this method: the weight of the bracing system that has been used in the benchmark frame to equalize the ending conditions of the columns effect the weight of the frame both directly (their own weight) and indirectly (the effect of their weight on the whole frame weight, requiring heavier column sections). The first problem is removed by decreasing their weight from the steel weight of the benchmark frame. The second problem is only theoretical because the systems being used for ending conditions of the columns are too light to affect the column sizes indirectly.

The comparison of the mentioned methodologies can be found in chapter five.

In accordance with what is described above, there are fifteen models to be designed in this project:

- 4-story X-, V-, inverted V and diagonal braced frame subjected to earthquake load and a 4-story X-braced frame not subjected to any lateral load

- 8-story X-, V-, inverted V and diagonal braced frame subjected to earthquake load and an 8-story X-braced frame not subjected to any lateral load

- 12-story X-, V-, inverted V and diagonal braced frame subjected to earthquake load and a 12-story X-braced frame not subjected to any lateral load

3.1.2 2-D versus 3-D Models

The choice between 2-D or 3-D design and analysis is another factor affecting the computer analysis time. Different beliefs exist among different researchers about the choices. Usually, the decision is based on the degree of regularity of the structures. Mwafy and Elnashai (2001), as the first researchers using these models, declare that due to the regularity of the frames, 2-D frames can explicitly show the behavior of the structure and there is no need to use 3-D models that reduce analysis speed and require more time. Maheri and Akbari (2003) have also modeled the frames two dimensionally, verifying their choice by referring to the former reference. In this research, 2-D modeling has also been chosen in line with the two mentioned studies but further verification is brought by referring to FEMA 356, which has been chosen due to being widely accepted by other researchers. In this criterion, structures are allowed to be modeled 2 dimensional if it has the following two conditions:

- The structure has rigid diaphragms

- The horizontal torsion effects have been considered in the model

Since these two conditions exist in the frames of this study, the usage of 2-D rather than 3-D models is also in line with FEMA 356.

The 4-story model geometries are given in the Figures 3.1 to 3.4. The 8- and 12-story model geometries are similar to the 4-story frames with the difference in the number of stories.

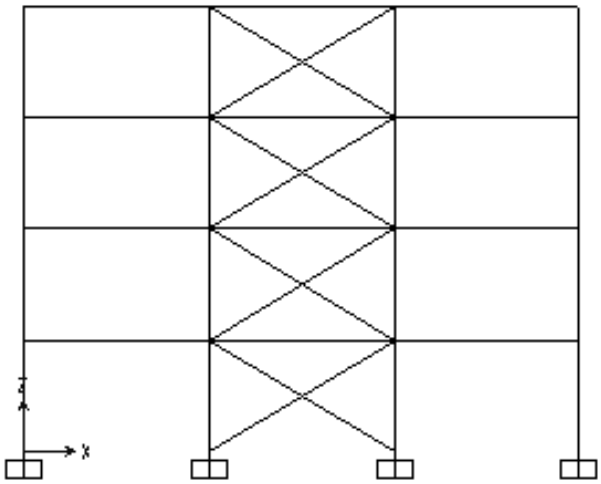

Figure 3.1: X-braced 4-story frame.

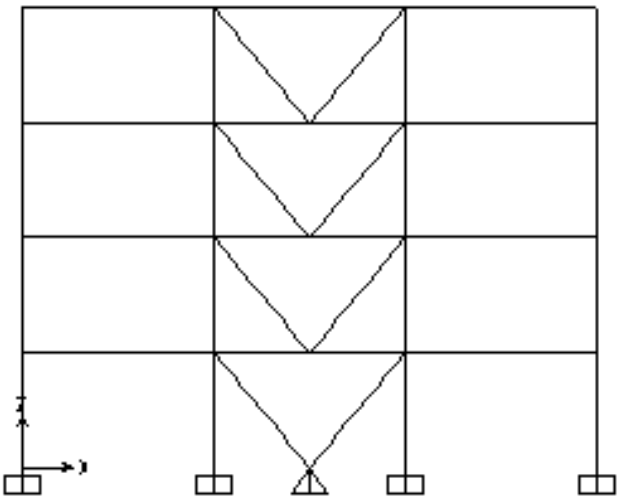

Figure 3.2: X-braced 4-story frame.

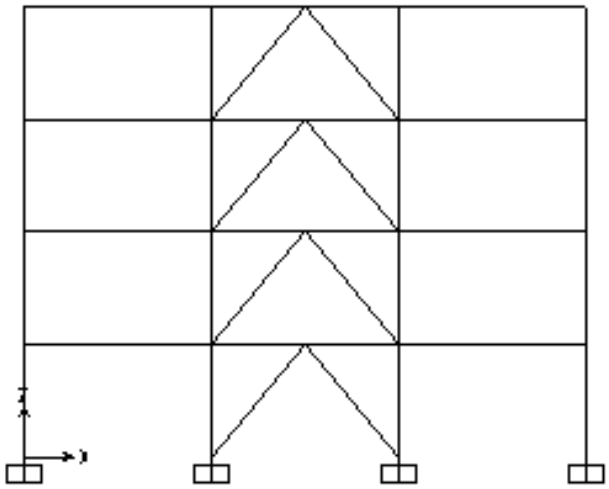

Figure 3.3: Inverted V-braced 4-story frame.

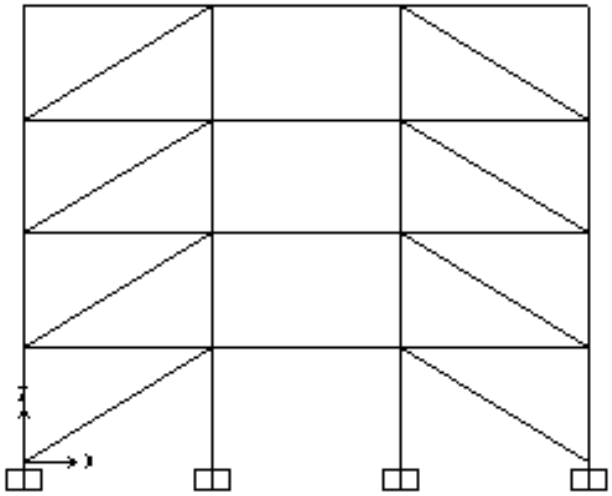

Figure 3.4: Diagonal braced 4-story frame.

The geometry of the 4-story X-braced frames that is not subjected to lateral load is not given separately due to its similarity to the X-braced frames in Figures 3.1.

3.1.3 Design Criteria

AISC (1999) is used as steel design code. IBC (2003) was used as loading code. Manual of Steel Construction, Load and Resistance Factor Design, LRFD, 2nd Edition (AISC 1994) was used for availability of materials and sections. ACI 318-05 (2005) was used to estimate the slab depths in order to calculate the dead load of

frames. In IBC (2003), Concentrically Braced Frames are divided into two as Ordinary and Special CBFs. SCBFs should pass the requirements of page 268 of IBC (for connections of members). Otherwise, the frames are categorized as OCBFs. This research studies the OCBFs.

3.1.4 Design Software

SAP 2000 version 11.0.4 has been used for the design of models as it is a powerful finite element computer program in design and analysis of the structures. SAP 2000 is produced by SCI Company in University of California at Berkeley. It is capable of doing linear and nonlinear, static and dynamic analyses. It has special practical features which have made it popular among the structural engineers.

3.1.5 Design Material

For steel material property, this study has referred to AISC 1994 steel construction manual, which is one of the most widely used steel construction manuals worldwide, Inel and Ozmen (2006) and CSI Analysis Reference Manual (2007), which is the reference of – SAP 2000, ETABS and SAFE – three of the most widely used structural computer programs. SAP 2000 has a default material property for steel and concrete which has been described in CSI Analysis Reference Manual (2007), (2006) and also previous versions of the manual. Inel and Ozmen (2006) has referred to the 2002 version of this manual and used the default material property of SAP 2000 for their study. After verification of the steel properties with Table 1.1 of AISC 1994 steel construction manual, it was observed that the material is a typical steel type being used in the United States that has appropriate characteristics as being defined by Kim and Choi (2005). The same material property is chosen to be used for this study, referring to the above named references.

The steel properties are given below:

- Modulus of Elasticity: E = 2.039E+10 kg/m^2
- Poisson's Ratio: ν = 0.3
- Weight per Unit Volume: 800.3801 kgf/m^3
- Mass per Unit Volume: 800.3801 kg/m^3
- Minimum Yield Stress: 38668829 kgf/m^2
- Effective Tensile Stress: 50269478 kgf/m^2

3.1.6 Design Sections

W sections are used for columns and beams and rectangular hollow sections are used for the bracing members from the sections available in 1994 AISC Constructional Steel Manual. This is in line with the works of D. Ozhendekci, D and N. Ozhendekci (2008), Yang, Leon and DesRoches (2008) and Kim and Choi (2005). Moghaddam, Hajirasouliha and Doostan (2005) have also used I-sections (IPE and IPB from DIN Sections) for beams and columns and rectangular hollow sections for braces.

For a building with I column sections, the earthquake is more critical in the direction which the columns are bent in their weak axes. In order to take this issue into account, in the drawing time, the columns were rotated 90 degrees so that the weaker axes are proportional to the lateral load direction, in order to study the more critical condition.

3.1.7 Connections

The beam-column connections are assumed to be pinned. The columns are continuous between the two story levels. The brace connections are pinned. These are all in line with Kim and Choi (2005). The column base plate connections are fixed in order to reduce the column sections according to Kameshki and Saka (2001).

3.1.8 Loading

Loading is in accordance with IBC (2003), one of the most frequently used loading codes worldwide. The frames are assumed to be residential which is defined as the Category II of Table 1604.5 of IBC 2003. Seismic factor of Category II should be taken 1.0 in accordance with page 272 of IBC (2003).

Live Load of the frames is 230 kg/m^2 from Table 1607.1 of page 275 of IBC (2003).

Dead Load is assumed to be 700 kg/m^2 on the assumption that the slab thickness will not exceed 15 cm.

In computer simulation of the frames, there are always a number of parameters varying for different possibilities of the frame situation, usage, etc. According to FEMA 440 (2005), "As detailed as these models may be, they inevitably introduce approximations and associated uncertainties into the analysis process. In most instances with inelastic analysis, it is preferable to base the model on the best estimate of the expected properties of the structure. In this manner, the overall analysis results in the estimate of central values (e.g., median or mean) of engineering demand parameters with minimum bias." In line with this reference, Site class was defined as C which is the median of "A – E" different site classes. It

stands for very dense soil and soft rock from 1615.1.1 of page 322 of IBC (2003). S_s and S_1 have then been chosen for site class C from Table 1615.1.2 of page 323 of IBC. Their values are

- $S_s = 1.0$
- $S_1 = 0.4$

System response parameters are not exactly known for each CBF separately at this moment since they are affected by the frame nonlinear response and this is one of the reasons of this study. In similar conditions, Maheri and Akbari (2003) first designed the frames according to the parameters given in the codes, and then analyzed the frames by pushover analysis. The same procedure is done in this study. OCBF response parameters according to IBC (2003) are

- $R = 5$ (from Table 1617.6.2 of page 334 of IBC)
- System Overstrength Factor: $\Omega_0 = 2$
- Deflection Amplification Factor: $C_d = 4.5$

3.1.9 Special V- and Inverted V-Bracing Shear Beam Considerations

According to AISC (1999), Bruneau, Uang and Whittaker (1998) and Kim and Choi (2005), in a V- or inverted V-braced frame, the shear beam should carry the vertical loads (dead, live, etc) without the braces. No proportion of vertical loads should be carried by the bracing members. While designing such frames in SAP 2000, it was observed that this is not considered by the software automatically and the design leads to wrongly designed lightweight beams. This problem was solved manually. The steel section of the beams in the benchmark frames which were not under

vertical load and without chevron bracing were noticed to be “W 16X26”. This section was introduced for chevron braced frames. It should be noted that even in the automatic beam choice, the beams designed for the spans without chevron bracing were also “W 16X26”. This shows the correctness of the beam design.

The base of first story V bracing was pinned on the ground in line with Bruneau, Uang and Whittaker (1998).

3.2 Design Results

After modeling the frames and their analysis, they were designed according to AISC (1999) and the results are given below in three different sections for 4, 8 and 12 story buildings.

3.2.1 Design Results of 4-story frames

These results are for the five different 4-story frames as follows:

3.2.1.1 Design Results of 4-story X-braced Frame

The sections are shown in Figure 3.5.

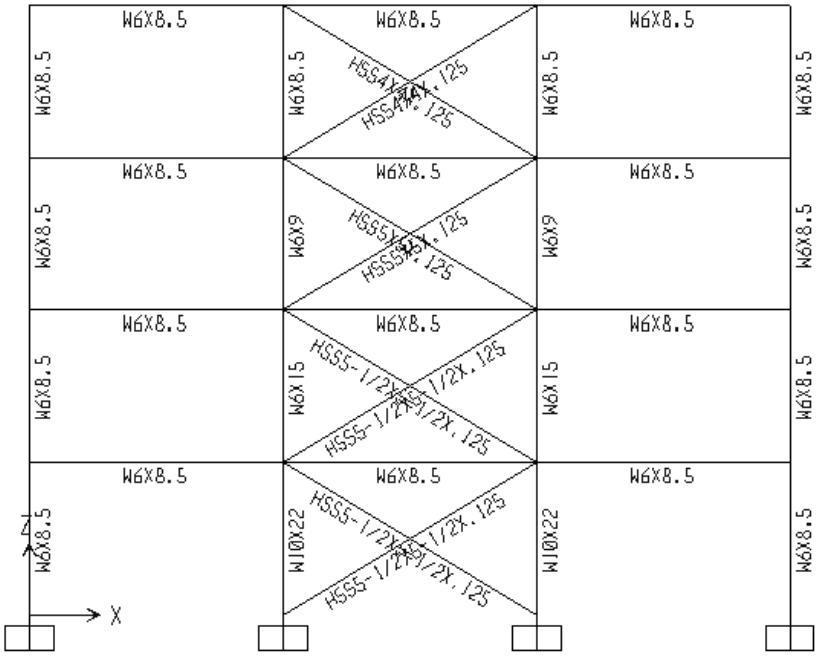

Figure 3.5: Design Sections of 4-story X-braced frame.

3.2.1.2 Total Weight of 4-story X-braced Frame

The weight information is given in Table 3.1 and Table 3.2

Table 3.1: Total weight of 4-story X-braced Frame.

Object Type	Material	Total Weight	Number of Pieces
		Kgf	Unitless
Frame	Steel	4483.2	36

Table 3.2: Detailed weight information of 4-story X-braced Frame.

Section	Object Type	Number of Pieces	Total Length	Total Weight
		Unitless	m	Kgf
W6X12	Frame	2	6.00	107.86
W6X15	Frame	6	18.00	405.62
W6X20	Frame	2	6.00	178.96
W8X24	Frame	2	6.00	215.11
W8X31	Frame	2	6.00	277.10
W14X43	Frame	2	6.00	382.83
W16X26	Frame	12	60.00	2333.44
HSS6X6X.125	Frame	4	23.32	318.89
HSS4-1/2X4-1/2X.125	Frame	2	11.66	118.11
HSS5-1/2X5-1/2X.125	Frame	2	11.66	145.27

3.2.1.3 Design Results of 4-story V-braced Frame

The sections are shown in Figure 3.6.

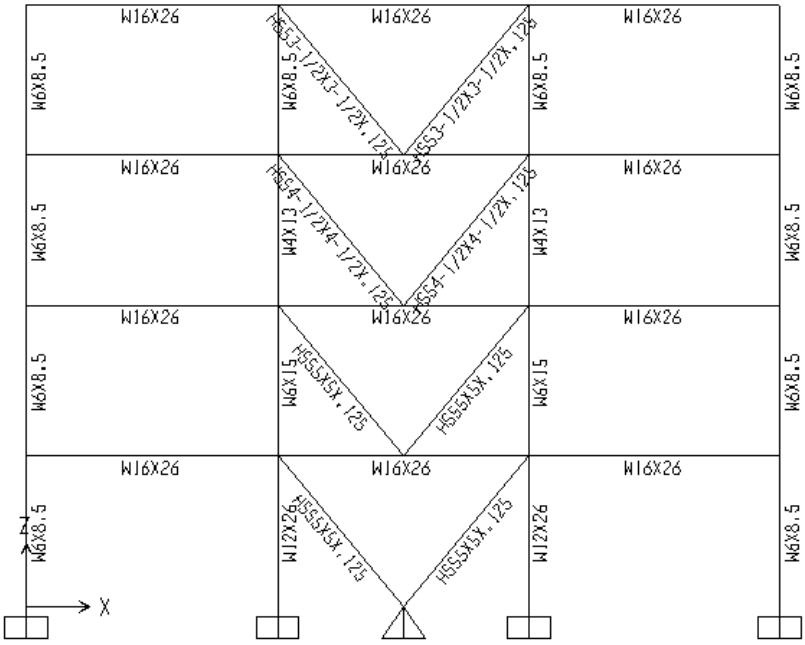

Figure 3.6: Design Sections of 4-story V-braced frame.

3.2.1.4 Total Weight of 4-story V-braced Frame

The weight information is given in Table 3.3 and Table 3.4.

Table 3.3: Total Weight of 4-story V-braced Frame.

Object Type	Material	Total Weight	Number of Pieces
		Kgf	Unitless
Frame	Steel	4271.72	36

Table 3.4: Detailed Weight information of 4-story V-braced Frame.

Section	Object Type	Number of Pieces	Total Length	Total Weight
		Unitless	m	Kgf
W6X12	Frame	2	6.00	107.86
W6X15	Frame	6	18.00	405.62
W6X20	Frame	2	6.00	178.96
W8X24	Frame	2	6.00	215.11
W10X33	Frame	2	6.00	295.02
W14X48	Frame	2	6.00	428.41
W16X26	Frame	12	60.00	2333.44
HSS3X3X.125	Frame	2	7.81	51.42
HSS4X4X.125	Frame	2	7.81	70.00
HSS6X6X.125	Frame	2	7.81	106.79
HSS4-1/2X4-1/2X.125	Frame	2	7.81	79.10

3.2.1.5 Design Results of 4-story Inverted V-braced Frame

The sections are shown in Figure 3.7.

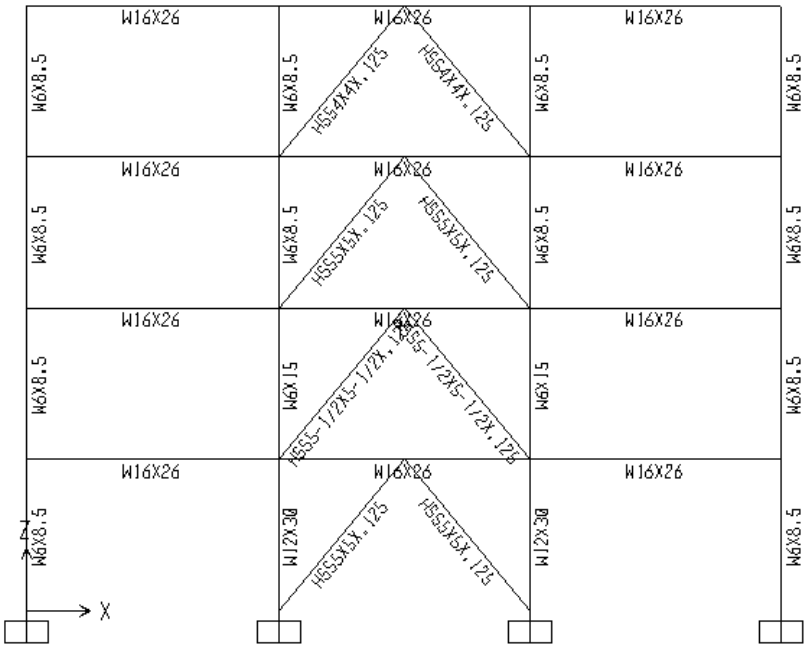

Figure 3.7: Design Sections of 4-story Inverted V-braced frame.

3.2.1.6 Total Weight of 4-story Inverted V-braced Frame

The weight information is given in Table 3.5 and Table 3.6

Table 3.5: Total Weight of 4-story Inverted V-braced Frame.

Object Type	Material	Total Weight	Number of Pieces
		Kgf	Unitless
Frame	Steel	4372.69	36

Table 3.6: Detailed Weight information of 4-story Inverted V-braced Frame.

Section	Object Type	Number of Pieces	Total Length	Total Weight
		Unitless	m	Kgf
W4X13	Frame	2	6.00	116.37
W6X12	Frame	2	6.00	107.86
W6X15	Frame	4	12.00	270.41
W6X20	Frame	4	12.00	357.92
W12X30	Frame	2	6.00	267.07
W16X26	Frame	12	60.00	2333.44
W21X48	Frame	2	6.00	428.41
HSS5X5X.125	Frame	2	7.81	88.20
HSS5X5X.1875	Frame	4	15.62	259.45
HSS5-1/2X5-1/2X.1875	Frame	2	7.81	143.57

3.2.1.7 Design Results of 4-story Diagonal braced Frame

The sections are shown in Figure 3.8.

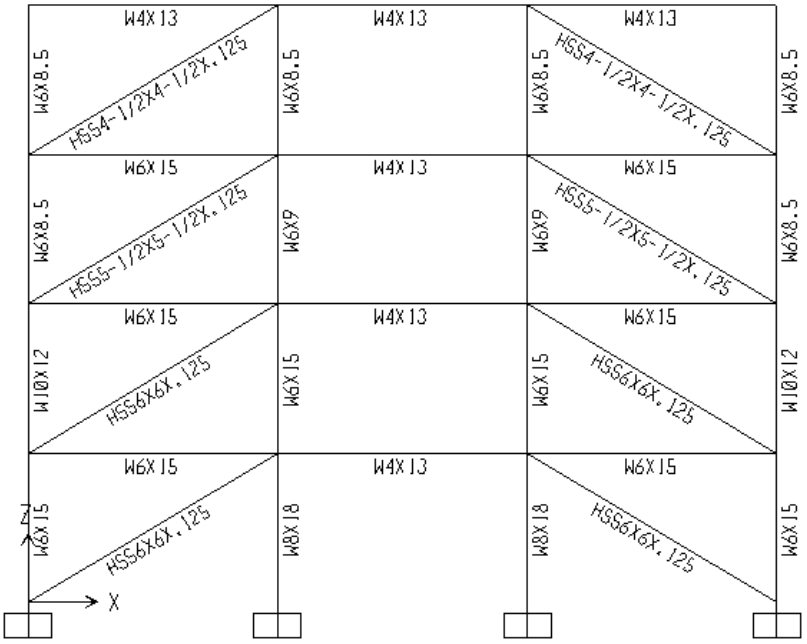

Figure 3.8: Design Sections of 4-story Diagonal braced frame.

3.2.1.8 Total Weight of 4-story Diagonal braced Frame

The weight information is given in Table 3.7 and Table 3.8

Table 3.7: Total Weight of 4-story Diagonal braced Frame

Object Type	Material	Total Weight	Number of Pieces
		Kgf	Unitless
Frame	Steel	5653.38	36

Table 3.8: Detailed Weight information of 4-story Diagonal braced Frame

Section	Object Type	Number of Pieces	Total Length	Total Weight
		Unitless	m	Kgf
W6X12	Frame	2	6.00	107.86
W6X15	Frame	4	12.00	270.41
W6X20	Frame	4	12.00	357.92
W8X28	Frame	2	6.00	250.36
W10X39	Frame	2	6.00	349.41
W12X30	Frame	2	6.00	267.07
W16X36	Frame	12	60.00	3220.64
HSS6X6X.1875	Frame	4	23.32	470.07
HSS5-1/2X5-1/2X.125	Frame	2	11.66	145.27
HSS5-1/2X5-1/2X.1875	Frame	2	11.66	214.37

3.2.1.9 Design Results of 4-story Benchmark Frame

Benchmark frame is the frame with X-bracing which is not subjected to any lateral load and it is for comparing the results only. The sections are shown in Figure 3.9.

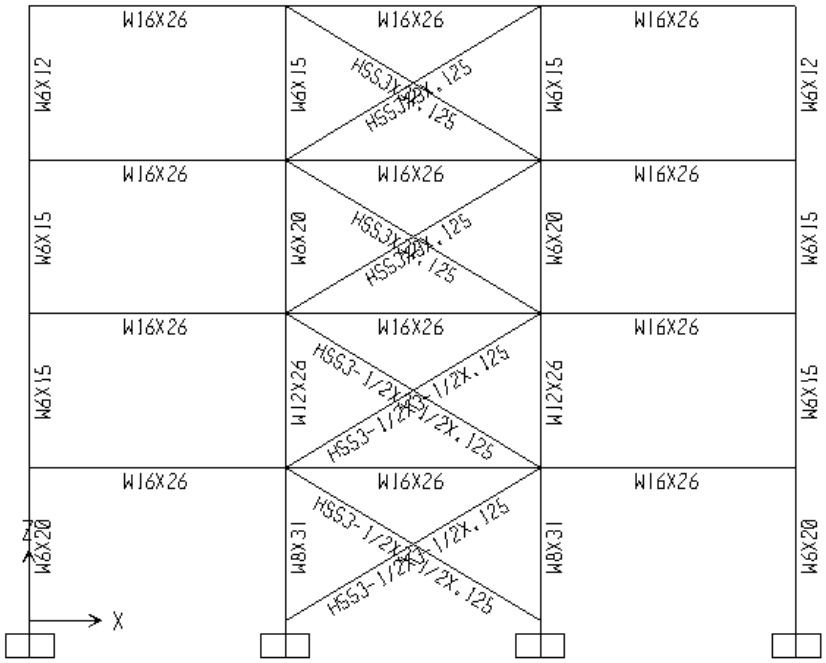

Figure 3.9: Design Sections of 4-story Benchmark frame.

3.2.1.10 Total Weight of 4-story Benchmark Frame

The weight information is given in Table 3.9 and Table 3.10.

Table 3.9: Total Weight of 4-story Benchmark Frame.

Object Type	Material	Total Weight	Number of Pieces
		Kgf	Unitless
Frame	Steel	4049.79	36

Table 3.10: Detailed Weight information of 4-story Benchmark Frame.

Section	Object Type	Number of Pieces	Total Length	Total Weight
		Unitless	m	Kgf
W6X12	Frame	2	6.00	107.86
W6X15	Frame	6	18.00	405.62
W6X20	Frame	4	12.00	357.92
W8X31	Frame	2	6.00	277.10
W12X26	Frame	2	6.00	232.43
W16X26	Frame	12	60.00	2333.44
HSS3X3X.125	Frame	4	23.32	153.54
HSS3-1/2X3-1/2X.125	Frame	4	23.32	181.89

3.2.2 Design Results of 8-story frames

These results are given for the five different 8-story frames as follows:

3.2.2.1 Design Results of 8-story X-braced Frame

The sections are shown in Figure 3.10.

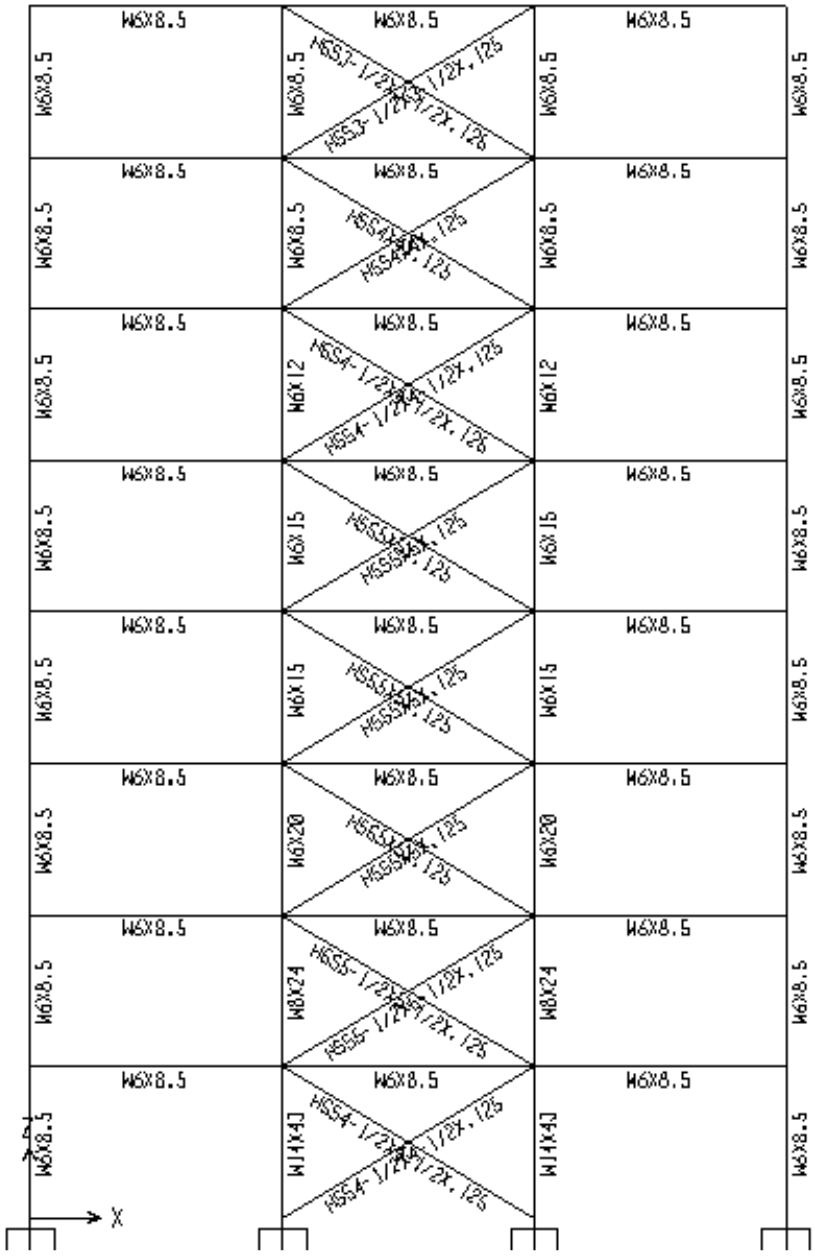

Figure 3.10: Design Sections of 8-story X-braced frame.

3.2.2.2 Total Weight of 8-story X-braced Frame

The weight information is given in Table 3.11 and Table 3.12.

Table 3.11: Total Weight of 4-story X-braced Frame.

Object Type	Material	Total Weight	Number of Pieces
		Kgf	Unitless
Frame	Steel	10486.81	72

Table 3.12: Detailed Weight information of 4-story X-braced Frame.

Section	Object Type	Number of Pieces	Total Length	Total Weight
		Unitless	m	Kgf
W6X12	Frame	2	6.00	107.86
W6X15	Frame	6	18.00	405.62
W6X20	Frame	4	12.00	357.92
W8X24	Frame	2	6.00	215.11
W8X28	Frame	4	12.00	500.72
W8X31	Frame	4	12.00	554.19
W8X35	Frame	2	6.00	312.95
W10X60	Frame	2	6.00	534.75
W12X45	Frame	2	6.00	398.02
W12X53	Frame	2	6.00	473.98
W16X26	Frame	24	120.00	4666.88
W27X84	Frame	2	6.00	753.51
HSS4X4X.125	Frame	2	11.66	104.53
HSS5X5X.125	Frame	2	11.66	131.69
HSS6X6X.125	Frame	4	23.32	318.89
HSS5-1/2X5-1/2X.125	Frame	6	34.98	435.82
HSS5-1/2X5-1/2X.1875	Frame	2	11.66	214.37

3.2.2.3 Design Results of 8-story V-braced Frame

The sections are shown in Figure 3.11.

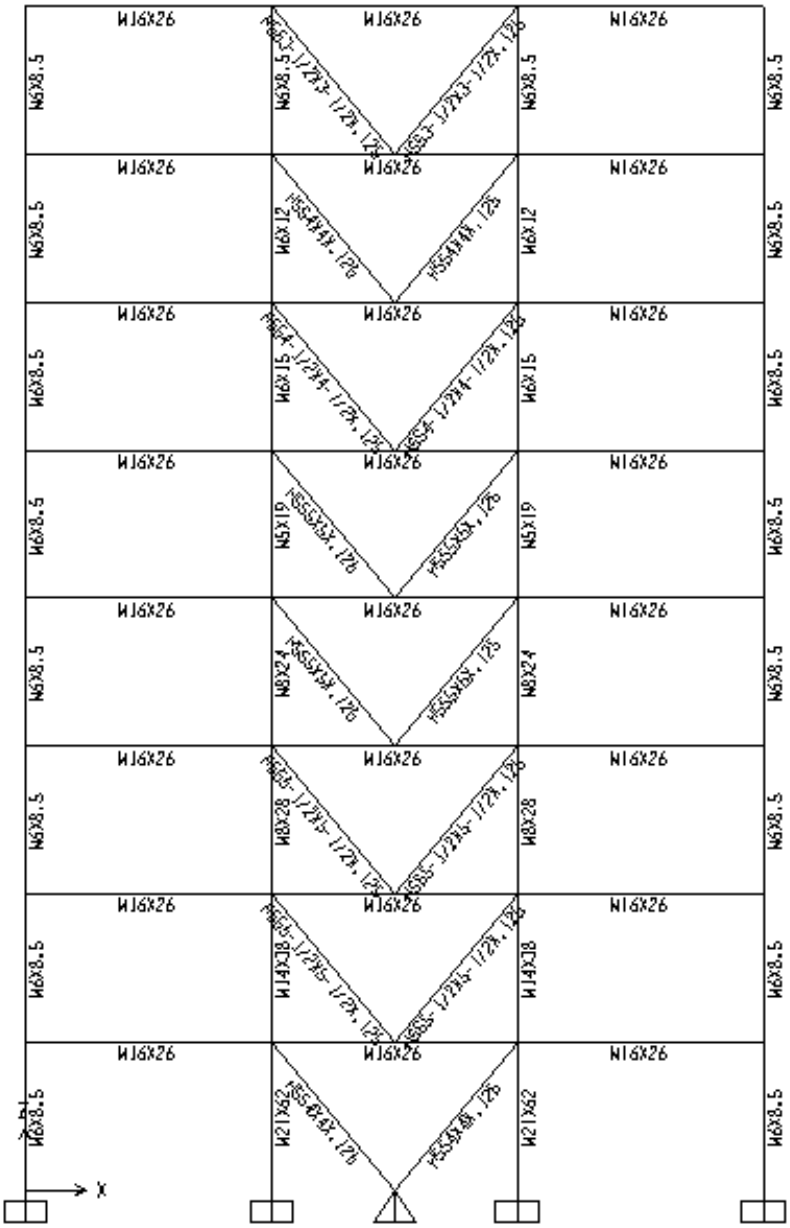

Figure 3.11: Design Sections of 8-story V-braced frame.

3.2.2.4 Total Weight of 8-story V-braced Frame

The weight information is given in Table 3.13 and Table 3.14.

Table 3.13: Total Weight of 8-story V-braced Frame.

Object Type	Material	Total Weight	Number of Pieces
		Kgf	Unitless
Frame	Steel	10356.65	72

Table 3.14: Detailed Weight information of 8-story V-braced Frame.

Section	Object Type	Number of Pieces	Total Length	Total Weight
Text	Text	Unitless	m	Kgf
W6X12	Frame	2	6.00	107.86
W6X15	Frame	6	18.00	405.62
W6X20	Frame	2	6.00	178.96
W8X24	Frame	4	12.00	430.23
W8X28	Frame	2	6.00	250.36
W8X31	Frame	6	18.00	831.29
W10X49	Frame	2	6.00	437.52
W10X60	Frame	2	6.00	534.75
W12X72	Frame	2	6.00	641.09
W14X43	Frame	2	6.00	382.83
W16X26	Frame	24	120.00	4666.88
W30X99	Frame	2	6.00	884.16
HSS4X4X.125	Frame	2	7.81	70.00
HSS5X5X.125	Frame	8	31.24	352.79
HSS2-1/2X21/2X.125	Frame	2	7.81	42.32
HSS3-1/2X3-1/2X.125	Frame	2	7.81	60.91
HSS4-1/2X4-1/2X.125	Frame	2	7.81025	79.10

3.2.2.5 Design Results of 8-story Inverted V-braced Frame

The sections are shown in Figure 3.12.

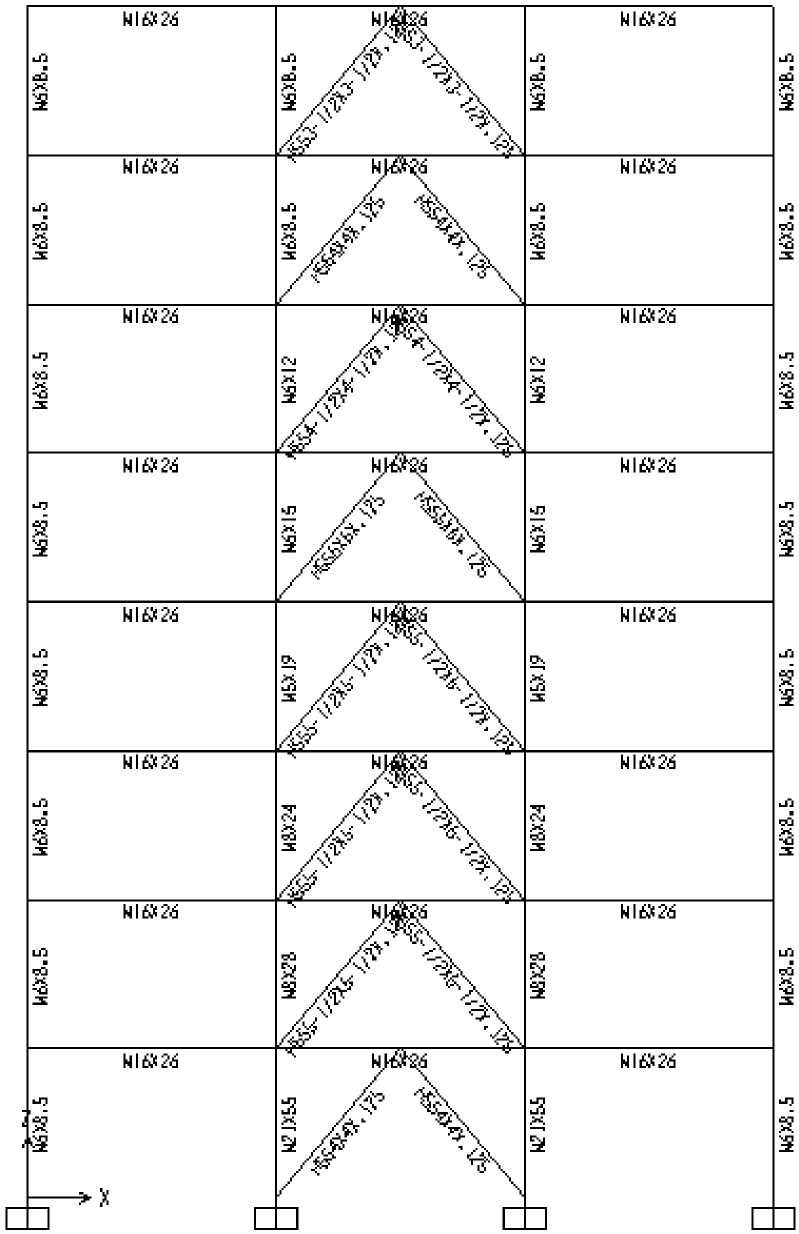

Figure 3.12: Design Sections of 8-story Inverted V-braced frame.

3.2.2.6 Total Weight of 8-story Inverted V-braced Frame

The weight information is given in Table 3.15 and Table 3.16.

Table 3.15: Total Weight of 8-story Inverted V-braced Frame.

Object Type	**Material**	**Total Weight**	**Number of Pieces**
		Kgf	Unitless
Frame	Steel	10369.77	72

Table 3.16: Detailed Weight information of 8-story Inverted V-braced Frame.

Section	Object Type	Number of Pieces	Total Length	Total Weight
		Unitless	m	Kgf
W4X13	Frame	2	6.00	116.37
W5X19	Frame	2	6.00	168.93
W6X12	Frame	2	6.00	107.86
W6X15	Frame	4	12.00	270.41
W6X20	Frame	2	6.00	178.96
W8X24	Frame	2	6.00	215.11
W8X28	Frame	4	12.00	500.72
W8X31	Frame	4	12.00	554.19
W8X35	Frame	2	6.00	312.95
W12X45	Frame	2	6.00	398.02
W12X53	Frame	2	6.00	473.98
W12X65	Frame	2	6.00	580.32
W16X26	Frame	24	120.00	4666.88
W30X99	Frame	2	6.00	884.16
HSS5X5X.1875	Frame	2	7.81	129.72
HSS6X6X.125	Frame	2	7.81	106.79
HSS4-1/2X4-1/2X.125	Frame	2	7.81	79.10
HSS5-1/2X5-1/2X.125	Frame	4	15.62	194.59
HSS5-1/2X5-1/2X.1875	Frame	6	23.43075	430.70

3.2.2.7 Design Results of 8-story Diagonal braced Frame

The sections are shown Figure 3.13.

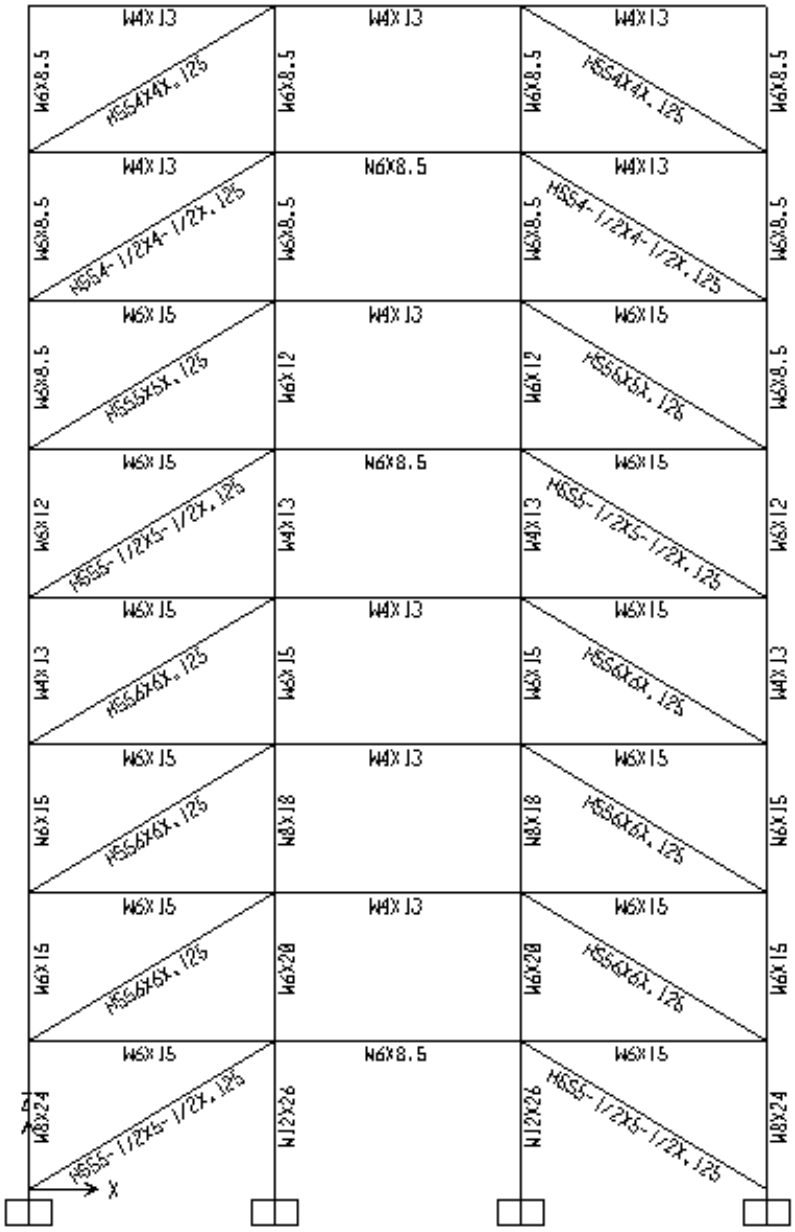

Figure 3.13: Design Sections of 8-story Diagonal braced frame.

3.2.2.8 Total Weight of 8-story Diagonal braced Frame

The weight information is given in Table 3.17 and Table 3.18.

Table 3.17: Total Weight of 8-story Diagonal braced Frame.

Object Type	Material	Total Weight	Number of Pieces
		Kgf	Unitless
Frame	Steel	12881.25	72

Table 3.18: Detailed Weight information of 8-story Diagonal braced Frame.

Section	Object Type	Number of Pieces	Total Length	Total Weight
		Unitless	m	Kgf
W6X12	Frame	2	6.00	107.86
W6X15	Frame	4	12.00	270.41
W6X20	Frame	4	12.00	357.92
W8X24	Frame	2	6.00	215.11
W8X31	Frame	4	12.00	554.19
W10X39	Frame	4	12.00	698.82
W10X49	Frame	2	6.00	437.52
W12X26	Frame	2	6.00	232.43
W12X45	Frame	2	6.00	398.02
W12X53	Frame	2	6.00	473.98
W14X48	Frame	2	6.00	428.41
W14X61	Frame	2	6.00	543.86
W16X36	Frame	24	120.00	6441.27
HSS5X5X.125	Frame	2	11.66	131.69
HSS6X6X.125	Frame	2	11.66	159.45
HSS6X6X.1875	Frame	8	46.64	940.15
HSS7X7X.1875	Frame	2	11.66	275.79
HSS5-1/2X5-1/2X.1875	Frame	2	11.66	214.37

3.2.2.9 Design Results of 8-story Benchmark Frame

Benchmark frame is the frame with X-bracing which is not subjected to any lateral load and it is for comparing the results only. The sections are shown in Figure 3.14.

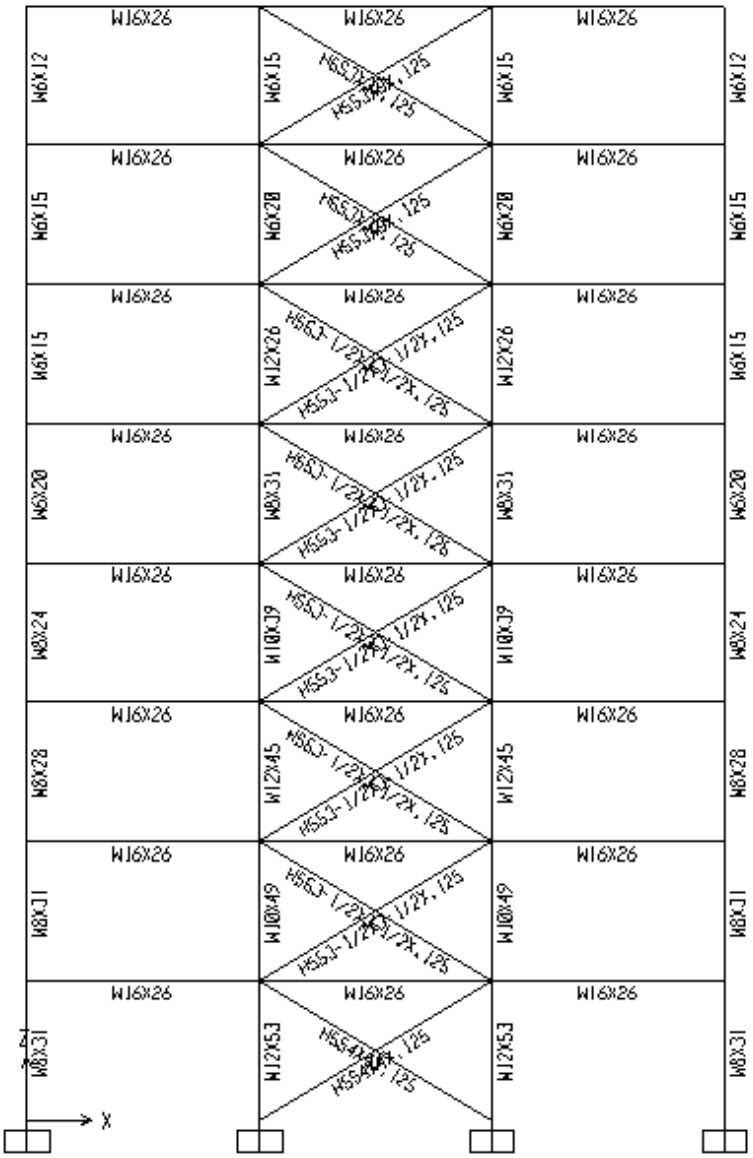

Figure 3.14: Design Sections of 8-story Benchmark frame.

3.2.2.10 Total Weight of 8-story Benchmark Frame

The weight information is given in Table 3.19 and Table 3.20.

Table 3.19: Total Weight of 8-story Benchmark Frame.

Object Type	Material	Total Weight	Number of Pieces
		Kgf	Unitless
Frame	Steel	9439.19	72

Table 3.20: Detailed Weight information of 8-story Benchmark Frame.

Section	Object Type	Number of Pieces	Total Length	Total Weight
		Unitless	m	Kgf
W6X12	Frame	2	6.00	107.86
W6X15	Frame	6	18.00	405.62
W6X20	Frame	4	12.00	357.92
W8X24	Frame	2	6.00	215.11
W8X28	Frame	2	6.00	250.36
W8X31	Frame	6	18.00	831.29
W10X39	Frame	2	6.00	349.41
W10X49	Frame	2	6.00	437.52
W12X26	Frame	2	6.00	232.43
W12X45	Frame	2	6.00	398.02
W12X53	Frame	2	6.00	473.98
W16X26	Frame	24	120.00	4666.88
HSS3X3X.125	Frame	4	23.32	153.54
HSS4X4X.125	Frame	2	11.66	104.53
HSS3-1/2X3-1/2X.125	Frame	10	58.30	454.72

3.2.3 Design Results of 12-story frames

These results are given for the five different 12-story frames as follows:

3.2.3.1 Design Results of 12-story X-braced Frame

The sections are shown in Figure 3.15.

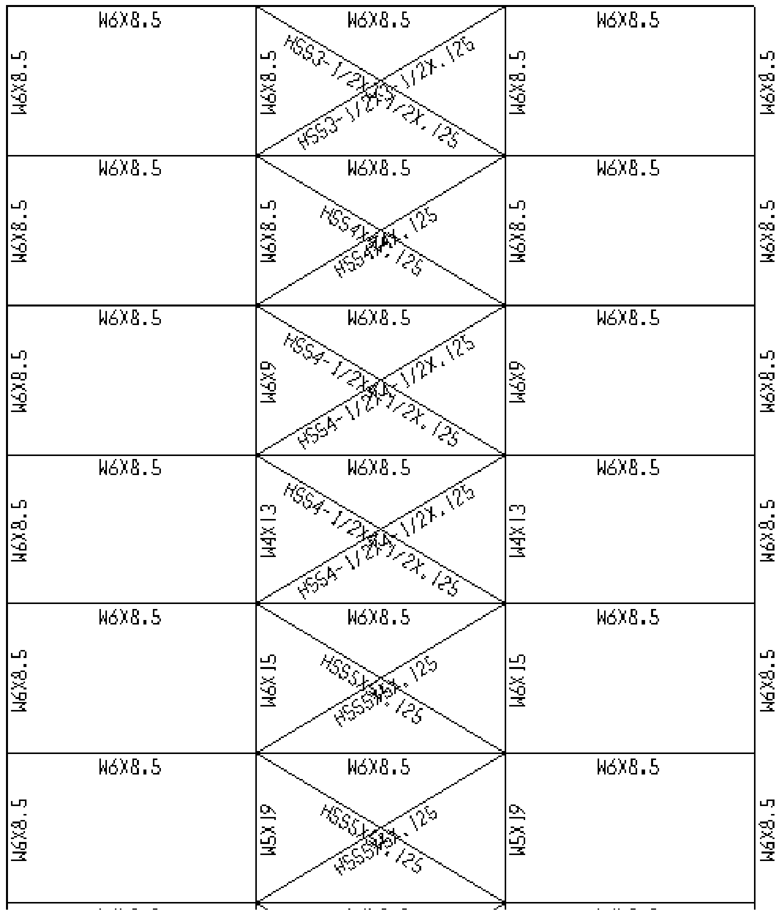

Figure 3.15.a: Design Sections of top 6 stories of 12-story X-braced frame.

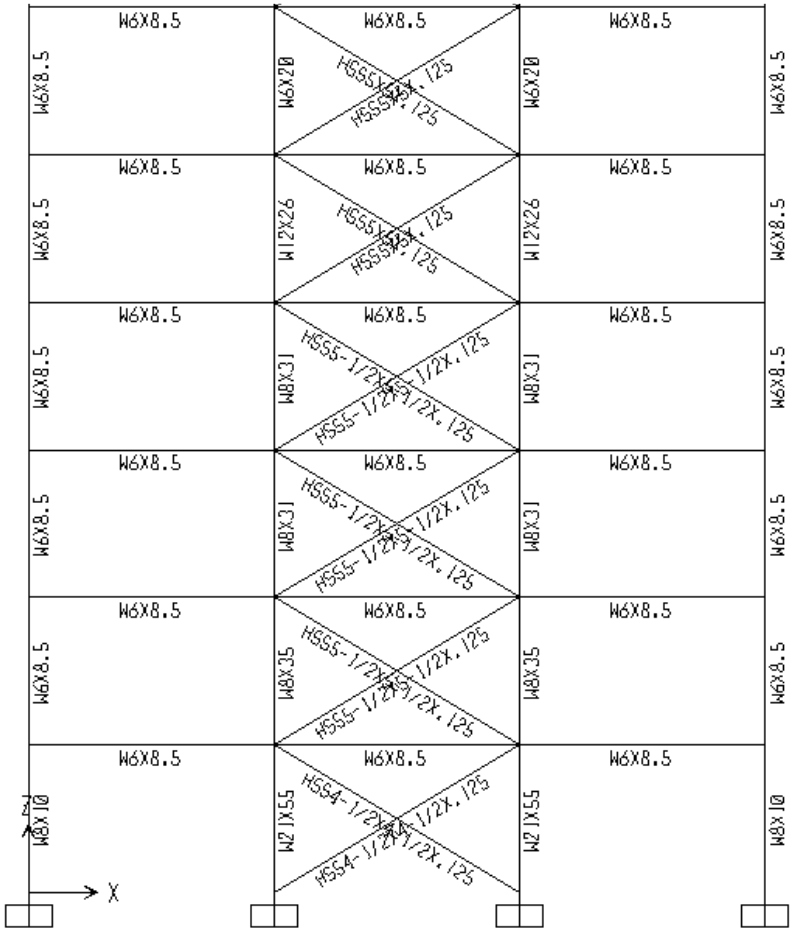

Figure 3.15.b: Design Sections of bottom 6 stories of 12-story X-braced frame.

3.2.3.2 Total Weight of 12-story X-braced Frame

The weight information is given in Table 3.21 and Table 3.22.

Table 3.21: Total Weight of 12-story X-braced Frame.

Object Type	Material	Total Weight	Number of Pieces
		Kgf	Unitless
Frame	Steel	18005.66	108

Table 3.22: Detailed Weight information of 12-story X-braced Frame.

Section	Object Type	Number of Pieces	Total Length	Total Weight
Text	Text	Unitless	m	Kgf
W6X12	Frame	2	6.00	107.86
W6X15	Frame	6	18.00	405.62
W6X20	Frame	4	12.00	357.92
W8X24	Frame	2	6.00	215.11
W8X28	Frame	4	12.00	500.72
W8X31	Frame	4	12.00	554.19
W8X40	Frame	2	6.00	355.49
W10X33	Frame	4	12.00	590.04
W10X39	Frame	2	6.00	349.41
W10X49	Frame	2	6.00	437.52
W12X45	Frame	2	6.00	398.02
W12X58	Frame	2	6.00	516.52
W12X65	Frame	2	6.00	580.32
W14X48	Frame	2	6.00	428.41
W14X90	Frame	2	6.00	805.16
W16X26	Frame	36	180.00	7000.32
W18X76	Frame	2	6.00	677.55
W18X86	Frame	2	6.00	768.70
W24X117	Frame	2	6.00	1045.19
HSS4X4X.125	Frame	2	11.66	104.53
HSS5X5X.125	Frame	6	34.98	395.08
HSS6X6X.125	Frame	6	34.98	478.34
HSS5-1/2X5-1/2X.125	Frame	4	23.32	290.55
HSS5-1/2X5-1/2X.1875	Frame	6	34.98	643.10

3.2.3.3 Design Results of 12-story V-braced Frame

The sections are shown in Figure 3.16.

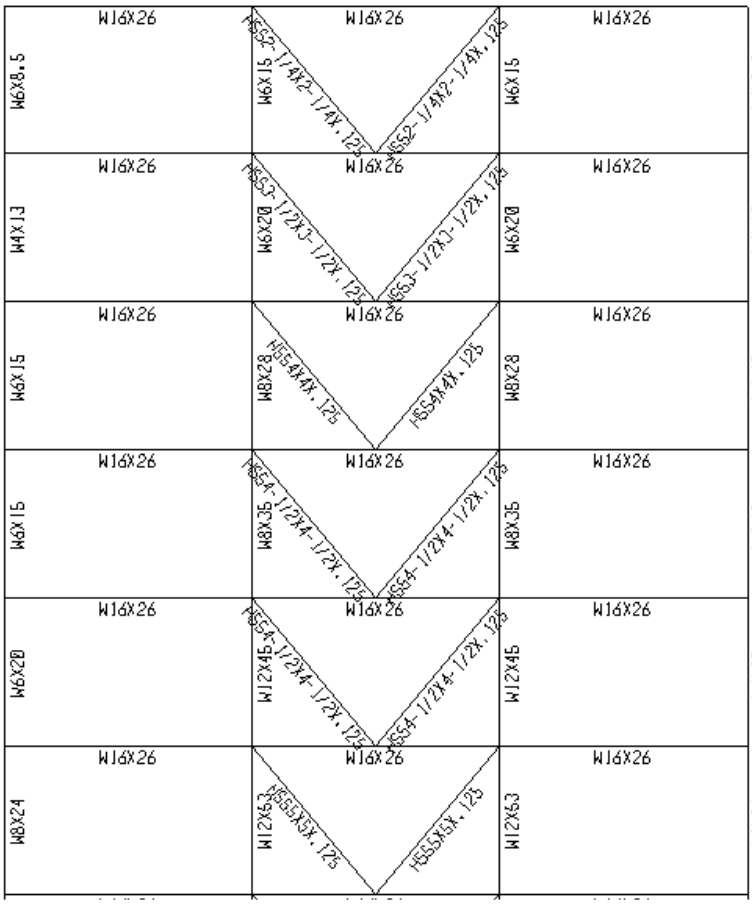

Figure 3.16.a: Design Sections of top 6 stories of 12-story V-braced frame.

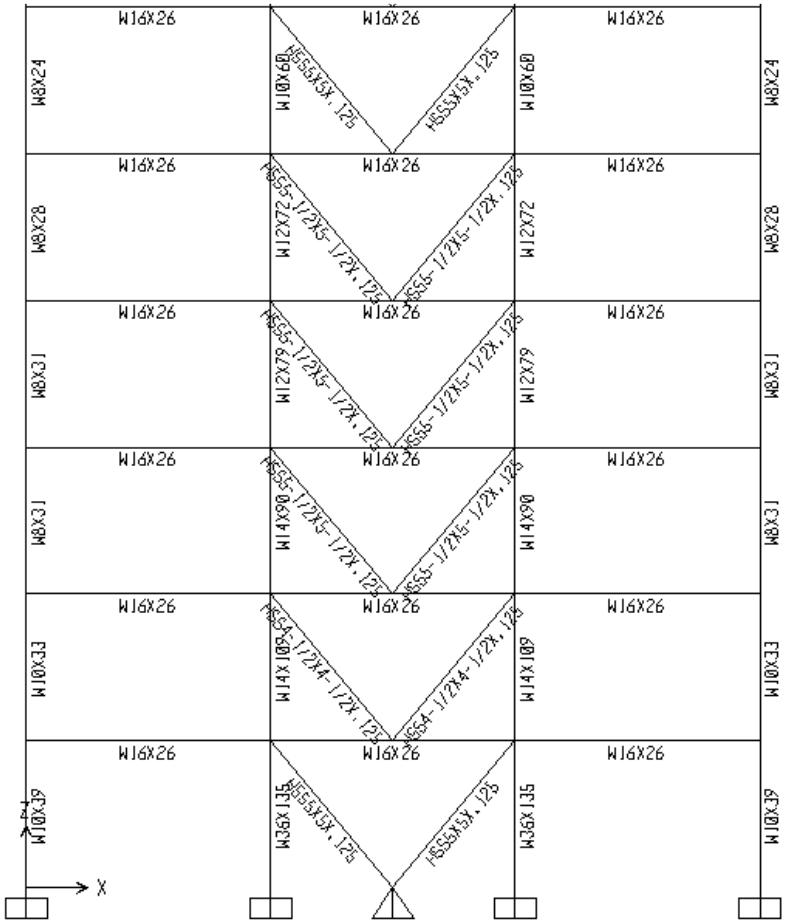

Figure 3.16.b: Design Sections of bottom 6 stories of 12-story V-braced frame.

3.2.3.4 Total Weight of 12-story V-braced Frame

The weight information is given in Table 3.23 and Table 3.24.

Table 3.23: Total Weight of 12-story V-braced Frame.

Object Type	Material	Total Weight	Number of Pieces
		Kgf	Unitless
Frame	Steel	18301.04	108

Table 3.24: Detailed Weight information of 12-story V-braced Frame.

Section	Object Type	Number of Pieces	Total Length	Total Weight
		Unitless	m	Kgf
W6X12	Frame	2	6.00	107.86
W6X15	Frame	6	18.00	405.62
W6X20	Frame	2	6.00	178.96
W8X24	Frame	4	12.00	430.23
W8X28	Frame	2	6.00	250.36
W8X31	Frame	6	18.00	831.29
W10X33	Frame	2	6.00	295.02
W10X39	Frame	2	6.00	349.41
W10X49	Frame	2	6.00	437.52
W12X40	Frame	2	6.00	355.49
W12X45	Frame	2	6.00	398.02
W12X58	Frame	2	6.00	516.52
W12X72	Frame	2	6.00	641.09
W12X79	Frame	2	6.00	704.89
W14X43	Frame	2	6.00	382.83
W14X90	Frame	2	6.00	805.16
W14X99	Frame	2	6.00	884.16
W16X26	Frame	36	180.00	7000.32
W24X117	Frame	2	6.00	1045.19
W27X146	Frame	2	6.00	1309.52
HSS4X4X.125	Frame	2	7.81	70.00
HSS5X5X.125	Frame	4	15.62	176.39
HSS2-1/4X2-1/4X.125	Frame	2	7.81	37.81
HSS3-1/2X3-1/2X.125	Frame	2	7.81	60.91
HSS4-1/2X4-1/2X.125	Frame	6	23.43	237.30
HSS5-1/2X5-1/2X.125	Frame	8	31.24	389.17

3.2.3.5 Design Results of 12-story Inverted V-braced Frame

The sections are shown in Figure 3.17.

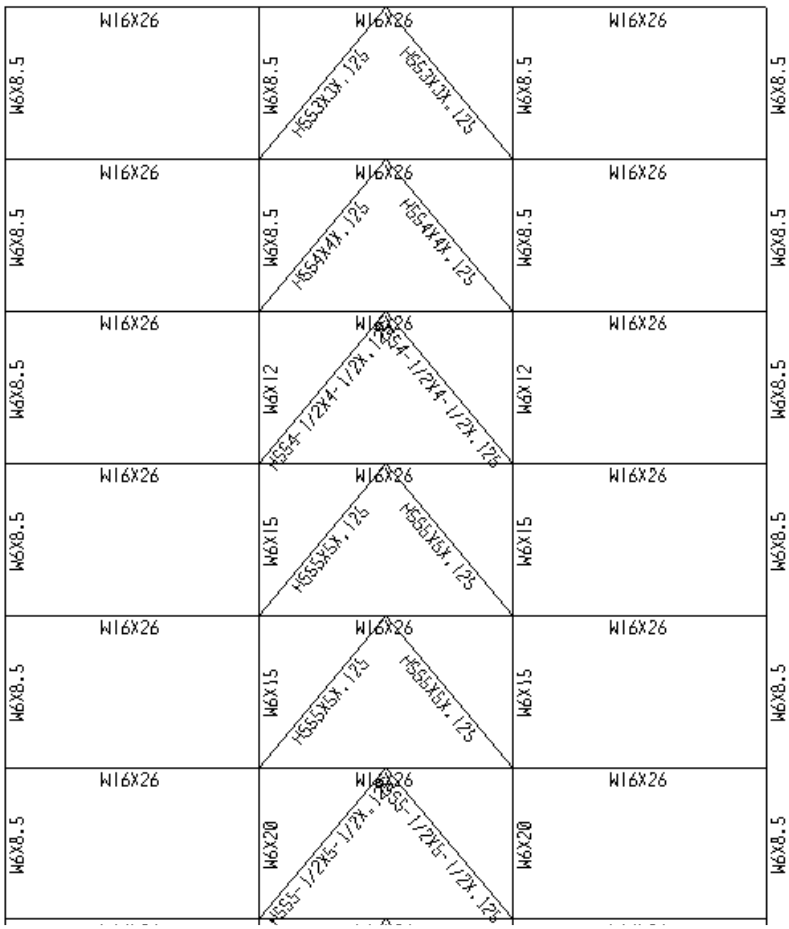

Figure 3.17.a: Design Sections of top 6 stories of 12-story Inverted V-braced frame.

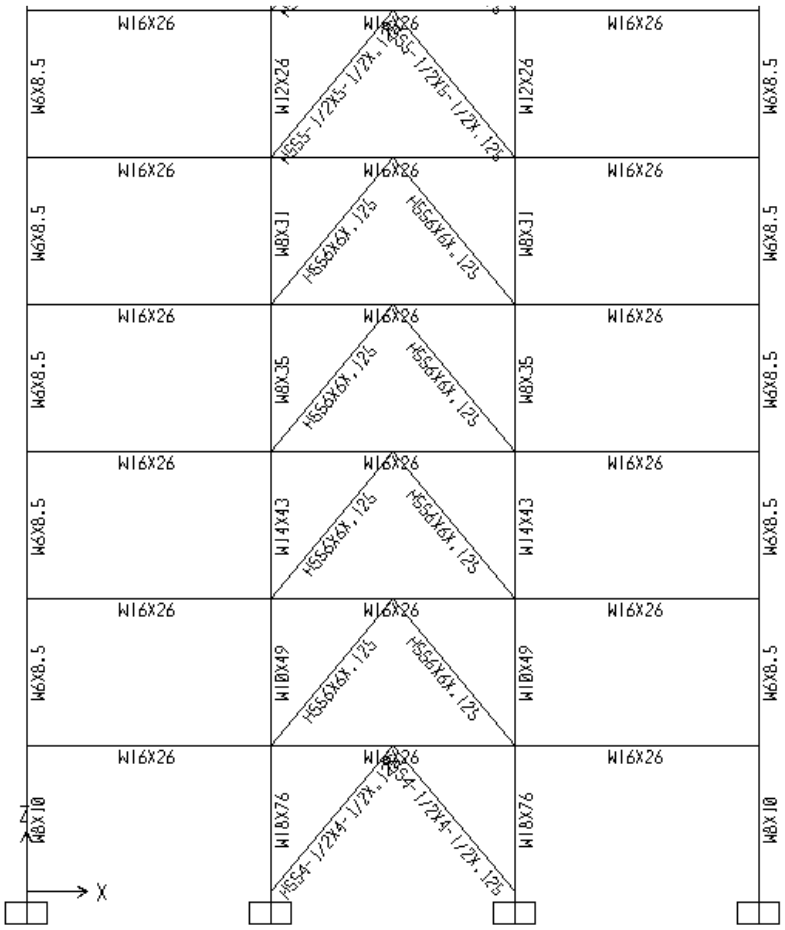

Figure 3.17.b: Design Sections of bottom 6 stories of 12-story Inverted V-braced frame.

3.2.3.6 Total Weight of 12-story Inverted V-braced Frame

The weight information is given in Table 3.25 and Table 3.26.

Table 3.25: Total Weight of 12-story Inverted V-braced Frame.

Object Type	Material	Total Weight	Number of Pieces
		Kgf	Unitless
Frame	Steel	18028.37	108

Table 3.26: Detailed Weight information of 12-story Inverted V-braced Frame.

Section	Object Type	Number of Pieces	Total Length	Total Weight
		Unitless	m	Kgf
W4X13	Frame	2	6.00	116.37
W5X19	Frame	2	6.00	168.93
W6X12	Frame	2	6.00	107.86
W6X15	Frame	4	12.00	270.41
W6X20	Frame	2	6.00	178.96
W8X24	Frame	2	6.00	215.11
W8X28	Frame	4	12.00	500.72
W8X31	Frame	4	12.00	554.19
W8X40	Frame	2	6.00	355.49
W10X33	Frame	4	12.00	590.04
W10X39	Frame	2	6.00	349.41
W12X45	Frame	4	12.00	796.04
W12X53	Frame	2	6.00	473.98
W12X72	Frame	2	6.00	641.09
W14X61	Frame	2	6.00	543.86
W14X90	Frame	2	6.00	805.16
W16X26	Frame	36	180.00	7000.32
W18X86	Frame	2	6.00	768.70
W24X104	Frame	2	6.00	929.73
W24X131	Frame	2	6.00	1169.76
HSS5X5X.125	Frame	2	7.81	88.20
HSS5X5X.1875	Frame	4	15.62	259.45
HSS6X6X.125	Frame	2	7.81	106.79
HSS4-1/2X4-1/2X.125	Frame	2	7.81	79.10
HSS5-1/2X5-1/2X.125	Frame	2	7.81	97.29
HSS5-1/2X5-1/2X.1875	Frame	12	46.86	861.40

3.2.3.7 Design Results of 12-story Diagonal braced Frame

The sections are shown in Figure 3.18.

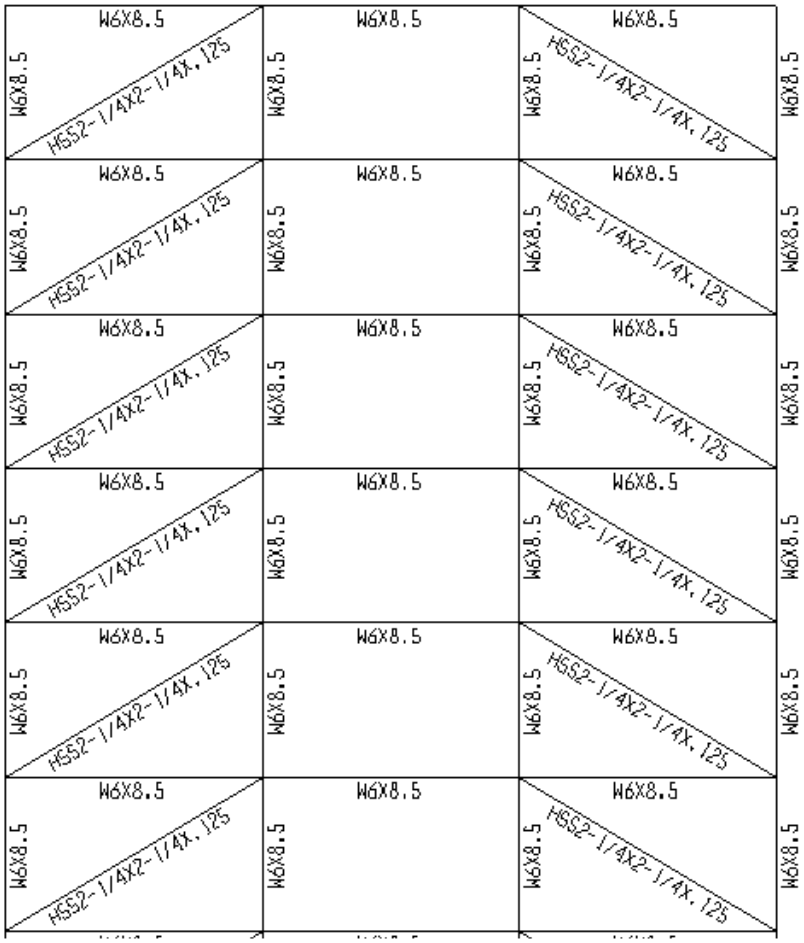

Figure 3.18.a: Design Sections of top 6 stories of 12-story Diagonal braced frame.

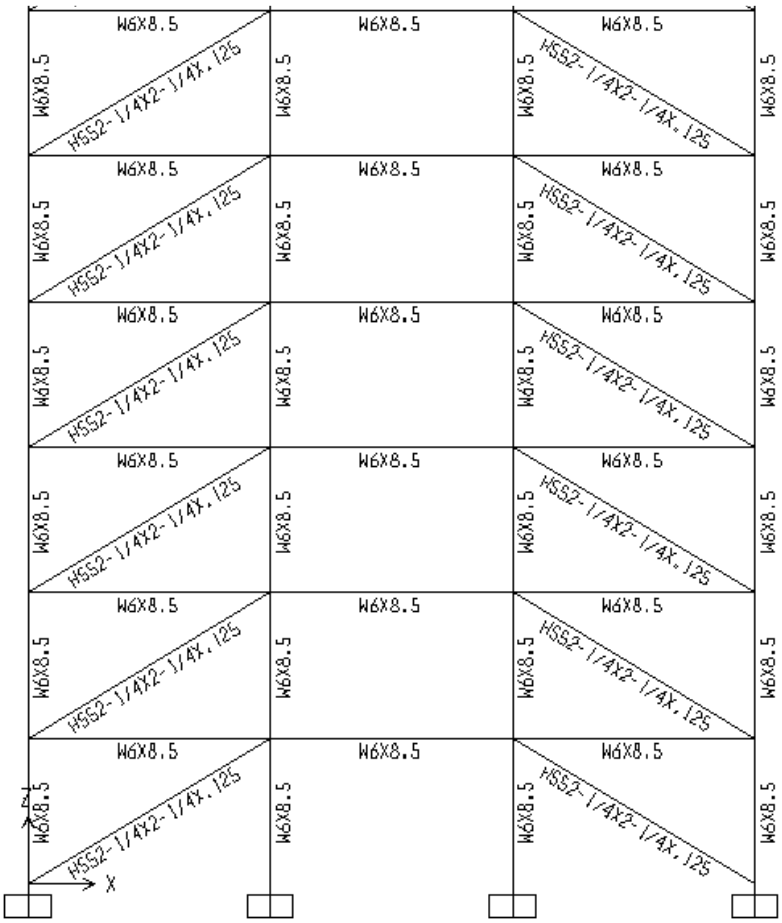

Figure 3.18.b: Design Sections of bottom 6 stories of 12-story Diagonal braced frame.

3.2.3.8 Total Weight of 12-story Diagonal braced Frame

The weight information is given in Table 3.27 and Table 3.28.

Table 3.27: Total Weight of 12-story Diagonal braced Frame.

Object Type	Material	Total Weight	Number of Pieces
		Kgf	Unitless
Frame	Steel	22024.19	108

Table 3.28: Detailed Weight information of 12-story Diagonal braced Frame.

Section	Object Type	Number of Pieces	Total Length	Total Weight
Text	Text	Unitless	m	Kgf
W5X19	Frame	2	6.00	168.93
W6X12	Frame	2	6.00	107.86
W6X15	Frame	4	12.00	270.41
W6X20	Frame	2	6.00	178.96
W8X24	Frame	4	12.00	430.23
W8X31	Frame	4	12.00	554.19
W8X35	Frame	4	12.00	625.90
W10X49	Frame	4	12.00	875.04
W10X60	Frame	2	6.00	534.75
W12X45	Frame	2	6.00	398.02
W12X53	Frame	2	6.00	473.98
W12X58	Frame	2	6.00	516.52
W12X65	Frame	4	12.00	1160.64
W12X72	Frame	2	6.00	641.09
W12X79	Frame	2	6.00	704.89
W14X38	Frame	1	5.00	283.58
W14X43	Frame	2	6.00	382.83
W14X90	Frame	2	6.00	805.16
W16X36	Frame	35	175.00	9393.52
W18X86	Frame	2	6.00	768.70
HSS5X5X.125	Frame	2	11.66	131.69
HSS6X6X.1875	Frame	8	46.64	940.15
HSS7X7X.1875	Frame	8	46.64	1103.14
HSS5-1/2X5-1/2X.125	Frame	2	11.66	145.27
HSS5-1/2X5-1/2X.1875	Frame	4	23.32	428.74

3.2.3.9 Design Results of 12-story Benchmark Frame

Benchmark frame is the frame with X-bracing which is not subjected to any lateral load and it is for comparing the results only. The sections are shown in Figure 3.19.

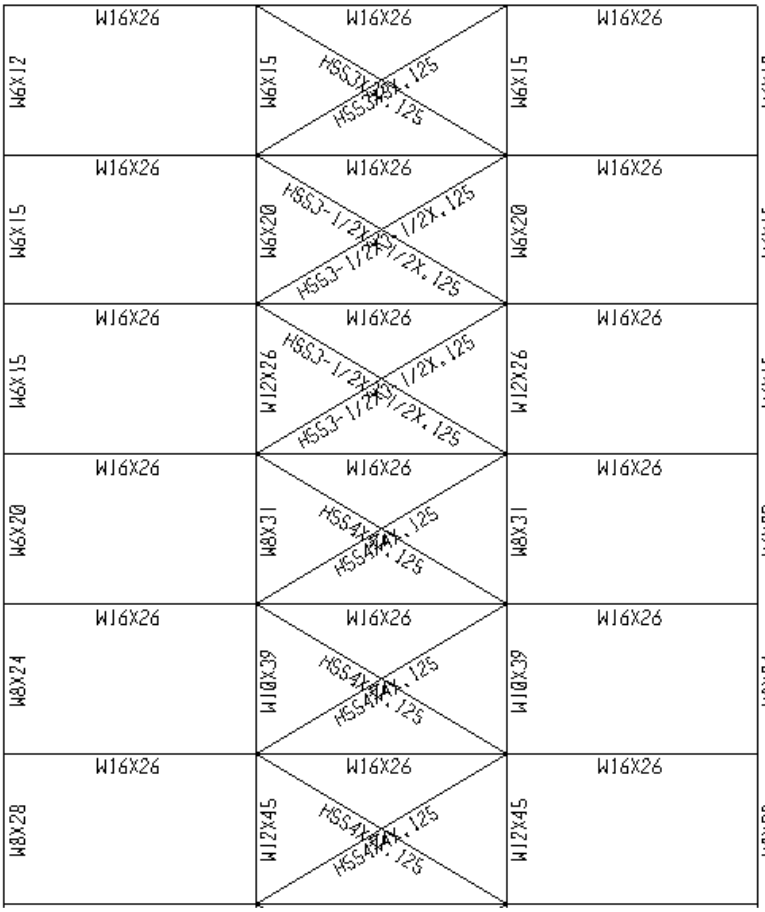

Figure 3.19.a: Design Sections of top 6 stories of 12-story Benchmark frame.

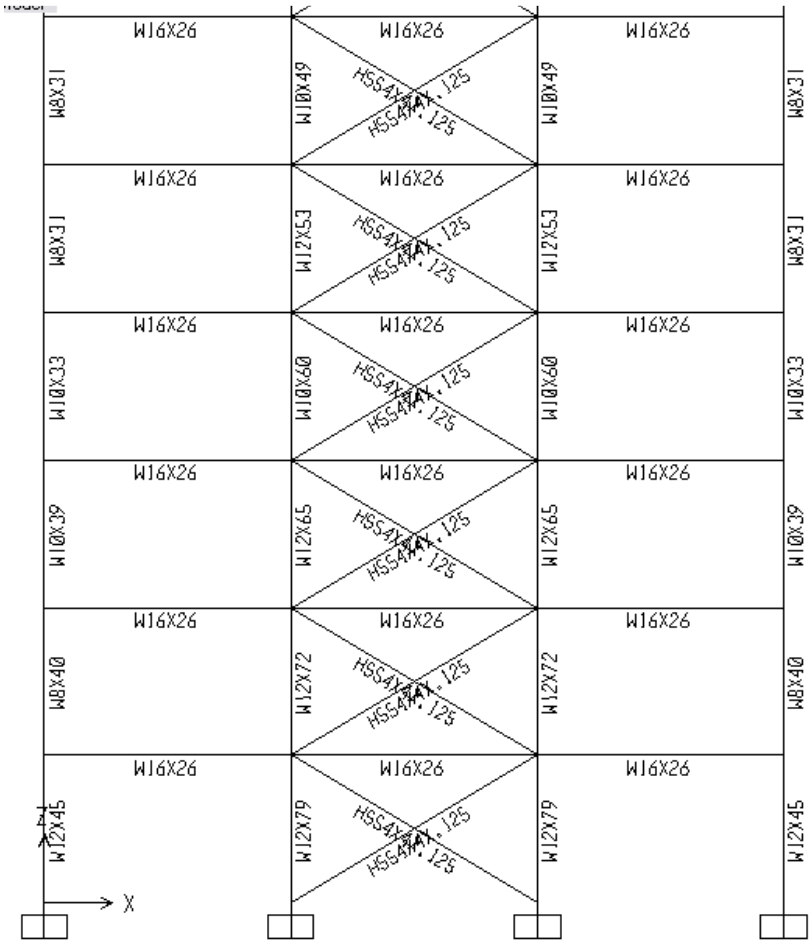

Figure 3.19.a: Design Sections of bottom 6 stories of 12-story Benchmark frame.

3.2.3.10 Total Weight of 12-story Benchmark Frame

The weight information is given in Table 3.29 and Table 3.30.

Table 3.29: Total Weight of 12-story Benchmark Frame.

Object Type	Material	Total Weight	Number of Pieces
		Kgf	Unitless
Frame	Steel	16118.23	108

Table 3.30: Detailed Weight information of 12-story Benchmark Frame.

Section	Object Type	Number of Pieces	Total Length	Total Weight
Text	Text	Unitless	m	Kgf
W6X12	Frame	2	6.00	107.86
W6X15	Frame	6	18.00	405.62
W6X20	Frame	4	12.00	357.92
W8X24	Frame	2	6.00	215.11
W8X28	Frame	2	6.00	250.36
W8X31	Frame	6	18.00	831.29
W8X40	Frame	2	6.00	355.49
W10X33	Frame	2	6.00	295.02
W10X39	Frame	4	12.00	698.82
W10X49	Frame	2	6.00	437.52
W10X60	Frame	2	6.00	534.75
W12X26	Frame	2	6.00	232.43
W12X45	Frame	4	12.00	796.04
W12X53	Frame	2	6.00	473.98
W12X65	Frame	2	6.00	580.32
W12X72	Frame	2	6.00	641.09
W12X79	Frame	2	6.00	704.89
W16X26	Frame	36	180.00	7000.32
HSS3X3X.125	Frame	2	11.66	76.77
HSS4X4X.125	Frame	18	104.95	940.74
HSS3-1/2X3-1/2X.125	Frame	4	23.32	181.89

CHAPTER IV

PUSHOVER ANALYSIS

4.1 Assessment of Nonlinear Behavior

As it was mentioned in section 2.2, structural response curve is the key point to evaluate the nonlinear parameters of a structure. These parameters (such as response modification factor, overstrength factor and displacement amplification factor) can all be extracted from the pushover curve of the frame with mathematical equations.

4.2 Choice of the Method of Analysis

Among the four methods of linear static, linear dynamic, nonlinear static and nonlinear dynamic analysis, the third one, nonlinear static (pushover) procedure, has been chosen. The reasons for this choice are explained below.

Linear procedures, either static or dynamic are not suitable for this study since they directly deal with the nonlinear behavior of the frames for ductility assessment. According to FEMA 356, explained in the Literature Review, linear procedures can only be used with acceptable precision when the structure behaves fully elastically.

With the conclusion that linear procedures can not be used for this study, the choice remains between the two alternatives of nonlinear static (pushover) and dynamic procedures. The former requires less computer analysis time, not considering the site characteristics of a special place directly, while the latter requires more computer analysis time, considering the site, fault and earthquake characters directly. It should

be noted that the aim of this study is to assess the overall bracing systems, regardless of the characterizations of the site, fault and earthquake in a special region. The research by Mwafy and Elnashai (2001) has shown that pushover analysis is highly capable of predicting the nonlinear behavior of regular frames if the lateral load distribution is chosen correctly. On a research similar to this study, Maheri and Akbari (2003) used pushover analysis for ductility assessment of regular frames from the work of Mwafy and Elnashai (2001).

As a result, the nonlinear static procedure has been chosen for this research where the models with the geometry of Maheri and Akbari (2003) were analyzed. The results of the pushover analysis have been verified before by Mwafy and Elnashai (2001). The pushover results of this study can also be easily verified by referring to the two named researches. The choice is also in line with the findings of Moghaddam and Hajirasouliha (2006), Kim and Choi (2005) and the methodology used by Kim and Choi (2005) for a research similar to this study.

4.3 Choice of the Software for Computer Analysis

Nowadays, different computer programs are capable of doing pushover analysis on frames. According to the statistics prepared by Federal Emergency Management Agency (given in FEMA 440), SAP 2000, DRAIN 2D-X and DRAIN 3D-X are the most widely used computer programs for this kind of analysis. According to the same reference, SAP 2000 was used for 35 percent of the research work carried out in the above mentioned statistics. SAP 2000. Version 11.0.4 - Advanced is chosen for this research due to the above verification, its high capabilities in nonlinear analysis of the frames and also idealization of the pushover curves based on the most recent methods. This is also in line with the decision of Inel, M; Ozmen, HB. (2006),

who studied DRAIN-2DX, DRAIN-3DX, PERFORM-2D, and SAP2000 and eventually choosed SAP 2000 for their study.

4.4 Pushover Load Pattern

As it was discussed in sections 2.4,3.1.1 and 4.2, Maheri and Akbari (2003) used inverted triangular load pattern referring to Mwafy and Elnashai (2001). But after that, FEMA 440 was released in 2005 stating that lateral load distribution proportional to the first mode of the frame gives the most accurate results for pushover analysis. Accordingly, first mode lateral load pattern was chosen which is also in line with similar research carried out by Kim and Choi (2005). It is explained in this chapter that global drift is used for failure check of the frames and according to FEMA 440, it is more appropriate to use first mode load vector for estimating global and SRSS load vector for interstory drift estimation.

4.5 Displacement-Based Pushover Analysis

Among Force-based and Displacement-based methods, the latter has higher precision but it can only be used for ductile frames. In a brittle frame, displacement-based pushover analysis can not be completed by the computer and thus, force-based analysis must be done although it has lower precision. Displacement-based procedure was used by 2% displacement increments in line with Maheri and Akbari (2003) and Powell (2007). It should be noted that the software will adjust the displacement increments in order to minimize the variation of the pushover curve with the real nonlinear structural response. Due to this reason, in the next chapter, it can be observed that the length of displacement increments vary from one to another specially when the structure changes from linear to nonlinear phase.

After the displacement-based pushover analysis, the pushover curve can easily be reached by connecting the analysis points together with line segments.

4.6 Nonlinear Material Property

The nonlinear material property was chosen as the SAP 2000 default since it demonstrates a ductile (and thus appropriate for nonlinear analysis) and widely used behavior according to 1994 AISC LRFD Manual of Steel Construction. This is also in line with Inel and Ozmen (2006). P-Δ effects were also considered for more accuracy according to Kim and Choi (2005).

4.7 Failure Criteria

There are different local (such as column hinging mechanism) and global (such as global or interstory drift) failure criteria for pushover analysis which have been studied in another research by Mwafy and Elnashai (2002). Maheri and Akbari (2003) referred to this study for failure criterion of the frames and chose global drift. This study also chooses the same criterion according to the mentioned studies. It should be noted that first mode load pattern is a better predictor of global and SRSS load pattern is a better predictor of interstory drift in pushover analysis. For the amount of global drift, Maheri and Akbari (2003) has referred to FEMA 273 and 274 (1997) but FEMA 356 has been released after those reports in 2000. According to this report, a CBF reaches its collapse at a global drift of 1.5% for life safety and 2% for collapse prevention. Later, it has been described to be 1.5% for ductility study of the system by Kim and Choi (2005). 1.5% is used by this study.

Another failure mode is a decrease of more than 20% in the lateral force in the idealized pushover curve of the frame according to FEMA 356 which has also been used by Inel and Ozmen (2006). This failure mode is also used in this study.

4.8 Plastic Hinge Properties

Federal Emergency Management agency has given thorough information about plastic hinge properties of all of the structural elements in its Table 5-6 [Appendix] which is widely used by other researchers. The information of this table is available as default hinge properties in SAP 2000 software. Inel and Ozmen (2006) state that for steel buildings, the difference between the results of pushover analysis by using default hinge and user defined properties is much less than reinforced concrete frames. They continue to say that even for RC frames, the difference is very little for new buildings and more for old ones (more appropriate for rehabilitation objectives). Since the aim of this study is assessing the nonlinear behavior of the bracing systems rather than rehabilitation of old building with specific hinge parameters, the default hinges of SAP 2000 are used in this study.

4.8.1 Column Hinge Properties

According to FEMA 356, a plastic hinge in a column is made on the interaction of axial force (P), moment in the stronger (M_2) and weaker (M_3) direction of the section. P-M_2-M_3 interaction was used for defining hinges at the beginning and ending points of the columns (the junctions with other structural elements where load is carried to columns) according to Table 5-6 of FEMA 356 [Appendix] in this study.

4.8.2 Brace Hinge Properties

According to Tremblay (2002), nonlinear behavior of brace elements can be best modeled by assuming a hinge (being made under pure axial load) in the middle of the elements. An axial load plastic hinge is modeled in the 0.5 relative distances of all bracing elements as per Table 5-6 of FEMA 356 [Appendix] in this study.

4.8.3 Beam Hinge Properties

In a V or inverted V braced frame, one or two plastic hinges occur in the shear link (the beam on which the brace elements are connected). The hinges are factors of shear, flexure or interaction of both of them, depending on the eccentricity ratio of the bracing system. According to Ricles and Popov (1994) and D. Ozhendekci and N. Ozhendekci (2008), plastic hinge mechanism is due to the shear in the chevron braces with low eccentricity. A shear load plastic hinge is modeled within the 0.5 relative distances of all shear beams (the place of connection of bracing elements with the beam) according to Table 5-6 of FEMA 356 [Appendix] in this study.

On the contrary with the MRFs, no plastic hinge exists at the beginning and ending points of beams in a braced frame since the beam to column connections are simply pinned. It should be noted that in a real CBF, the beam to column connections are not ideally pinned and resist a little amount of moment which is negligible compared to rigid connections. But the beam to column connections of this study has been assumed to be pinned in line with Kim and Choi (2005).

4.9 Idealization of Pushover Curve

For reaching the nonlinear behavior parameters of a frame, according to Kim and Choi (2005) and Maheri and Akbari (2003), all that has to be done on a pushover

curve is idealizing the real pushover curve by a bilinear curve. Comprehensive information is brought about idealization in FEMA 273, 356 and 440 coefficient-based methods of performance-based procedures. Kim and Choi (2005) have used FEMA 356 method in their research. But since FEMA 440 has modified the method later, the modified coefficient-based method of FEMA 440 is used in this study. Figure 4.1 shows the idealized bilinear versus real pushover curve of a frame. The parameters shown in Figure 4.1 are demonstrated and compared in chapter five.

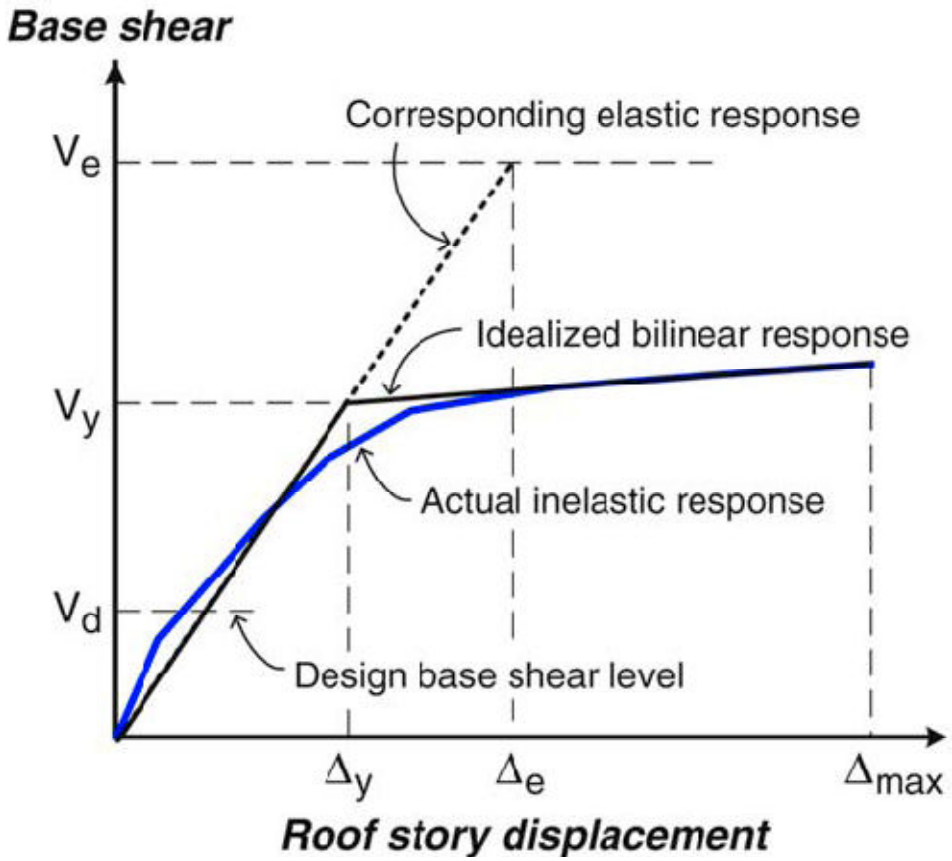

Figure 4.1: Lateral load–roof displacement relationship of a structure (Courtesy of Kim & Choi, 2005).

4.10 Assessment of Bracing systems

For assessment of inelastic performance of the frames, the pushover curves and failure progress of each frame is studied in section 5.1. Then, they are categorized by

their number of stories and bracing system in sections 5.2 and 5.3 respectively. In continue idealized response curves of the frames are given separately in section 5.4. Idealized curves are also idealized by their number of stories and bracing system similar to the actual response curves in sections 5.5 and 5.6.

Economical comparison of the bracing systems has been carried out in section 5.8 by the methodologies explained in chapter three.

The energy that each frame dissipates (evaluated in section 5.4) over the net weight of the bracing system (evaluated in section 5.8) is calculated for each frame separately. The normalized values of energy dissipation per net weight of the bracing systems are given in chapter six for conclusion.

CHAPTER V

RESULTS AND DISCUSSIONS

The results of analysis are presented in this chapter. Normal pushover curve of each frame is given with its failure reason. Then the push over curves of the frames with the same number of stories and the same bracing system are compared. The idealized curves are given and the weights of the frames are also compared.

5.1 Pushover Curves and Failure Progresses

In this part, pushover curves and failure patterns of each frame is given separately. The failure reason of the frame is also discussed.

5.1.1 Pushover Curve and Failure Progress of 4-story X-braced Frame

Figure 5.1 and 5.2.a show the pushover curve and failure pattern of the 4-story X-braced frame. Figure 2.2.b describes the signs that are used for showing the levels of plastic hinges in this chapter.

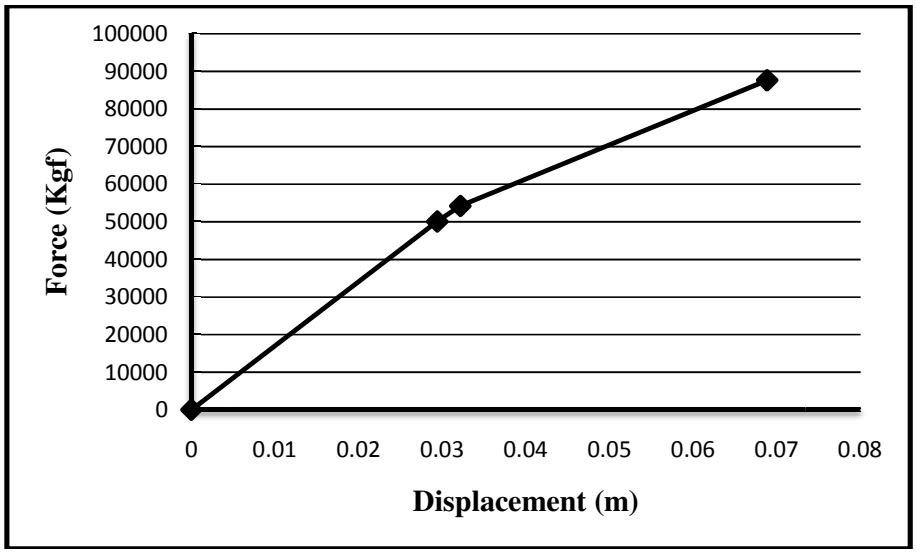

Figure 5.1: Pushover Curve of 4-story X-braced frame.

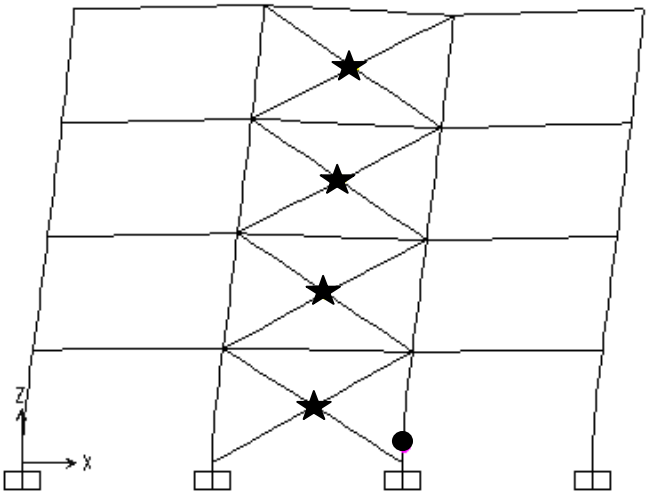

Figure 5.2.a: Failure moment condition of 4-story X-braced frame.

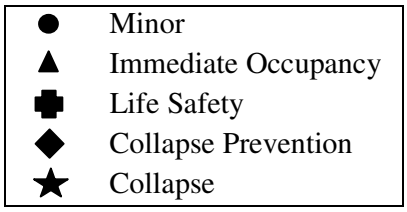

Figure 5.2.b: Plastic hinge level descriptions.

It can be observed that at the failure moment, all of the compressive braces are buckling and reaching a collapse level plastic hinge. A minor plastic hinge can also be seen on the first story column. Overall the reduction of the slope of the pushover

curve and consequent failure is due to the failure of the compressive members of the bracing system.

5.1.2 Pushover Curve and Failure Progress of 4-story V-braced Frame

Figure 5.3 and 5.4 show the pushover curve and failure pattern of the 4-story V-braced frame.

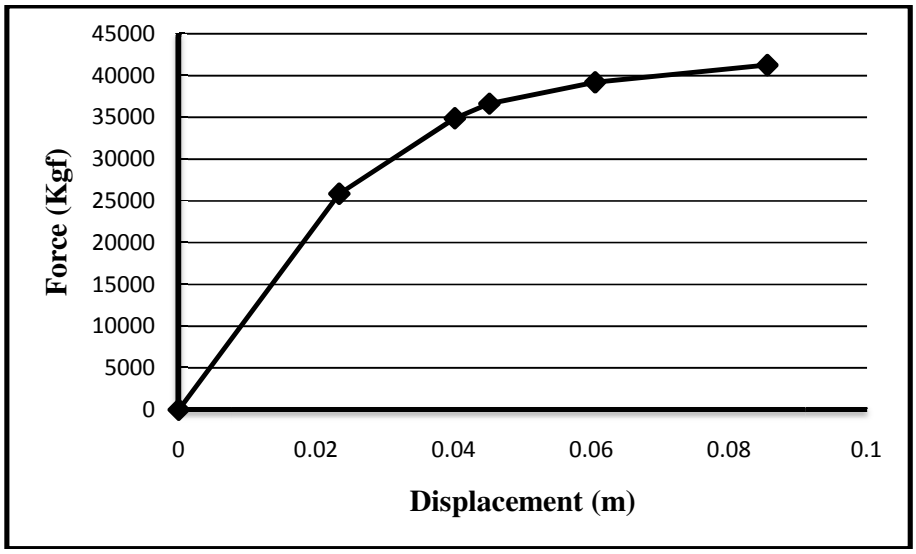

Figure 5.3: Pushover Curve of 4-story V-braced frame.

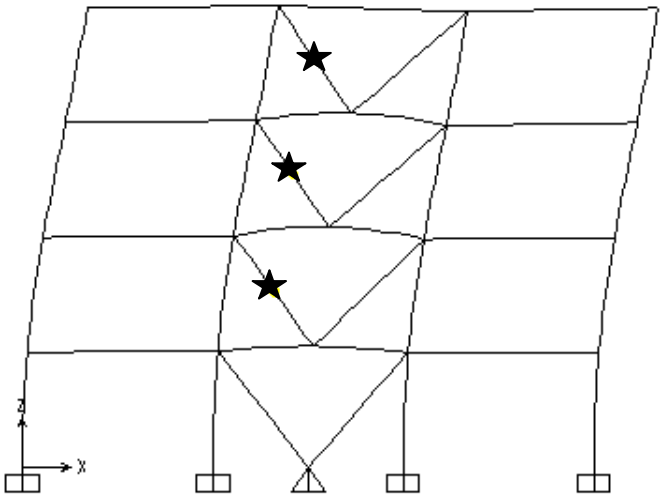

Figure 5.4: Collapse moment conditions of 4-story V-braced frame.

It could be noticed from Figures 5.3 and 5.4 that reason of the reduction of the slope of the pushover curve at each stage is the buckling of the compressive bracing members. At the failure stage, a plastic hinge at collapse level exists in compressive bracing members of all stories except the first story. No plastic hinge has occurred in beams or columns.

5.1.3 Pushover Curve and Failure Progress of 4-story Inverted V-braced Frame

Figure 5.5 and 5.6 show the pushover curve and failure pattern of the 4-story Inverted V-braced frame.

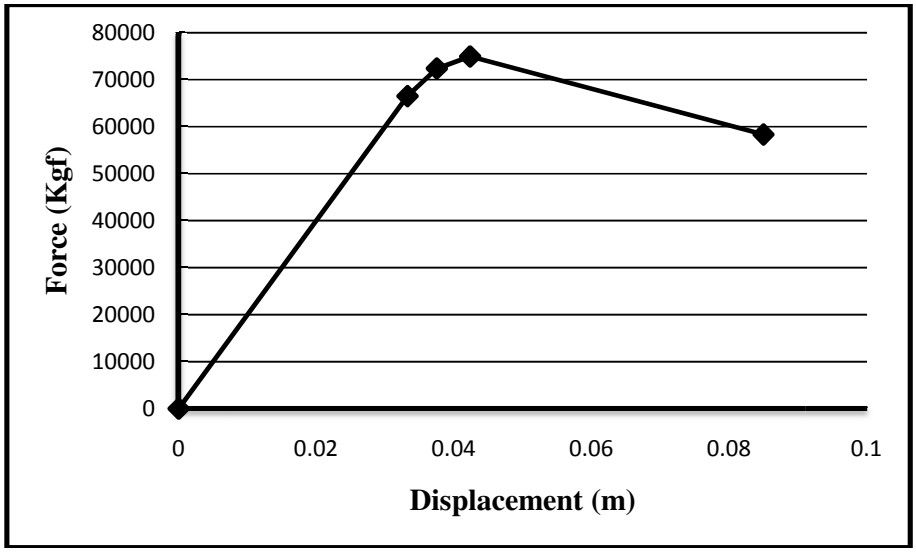

Figure 5.5: Pushover Curve of 4-story Inverted V-braced frame.

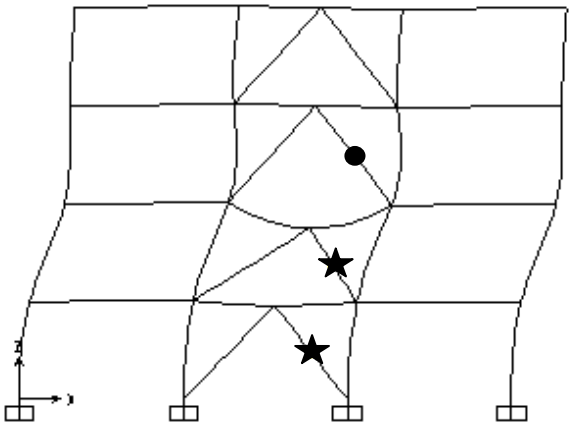

Figure 5.6: Collapse moment conditions of 4-story Inverted V-braced frame.

In this frame, collapse level plastic hinge in the compressive members of bracing system at first and second story and a minor plastic hinge in the compressive brace member of the third floor are the reasons of slope reduction in pushover curve and the failure. The shear beam has deflected dramatically in contrast with the V-braced frame because the bracing system is not connected to foundation in the first story.

5.1.4 Pushover Curve and Failure Progress of 4-story Diagonal braced Frame

Figure 5.7 and 5.8 show the pushover curve and failure pattern of the 4-story Diagonal braced frame.

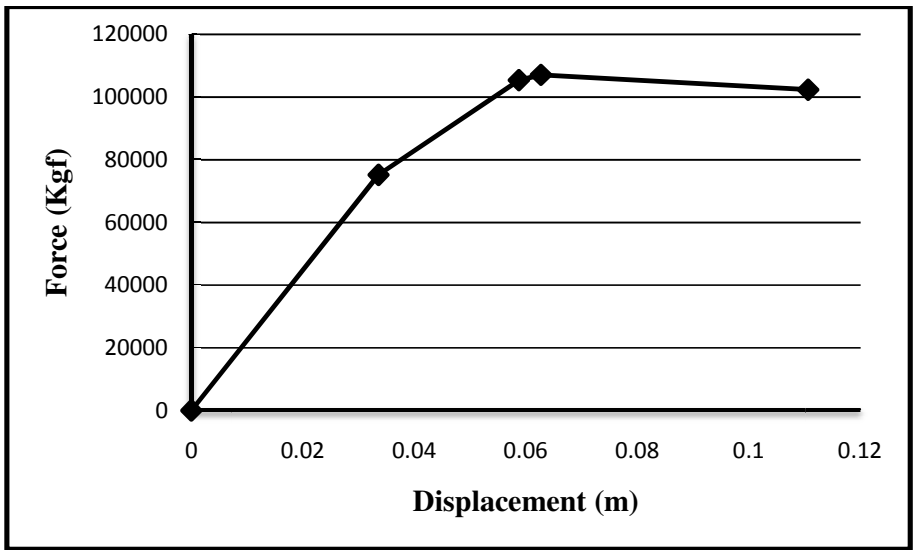

Figure 5.7: Pushover Curve of 4-story Inverted Diagonal braced frame.

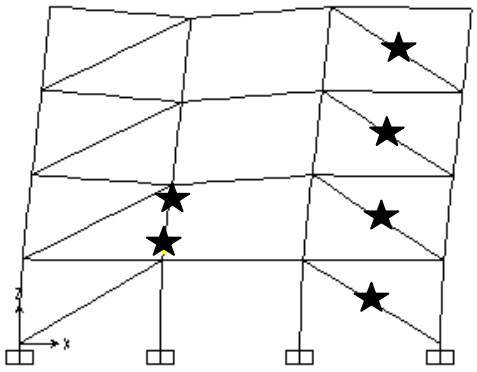

Figure 5.8: Collapse moment conditions of 4-story Diagonal braced frame.

In this frame, the plastic hinges in the compressive bracing members developed until they reached collapse level. At the last (failure) stage, two plastic hinges are also developed at the beginning and the end point of the second story column.

5.1.5 Pushover Curve and Failure Progress of 8-story X-braced Frame

Figure 5.9 and 5.10 show the pushover curve and failure pattern of the 8-story X-braced frame.

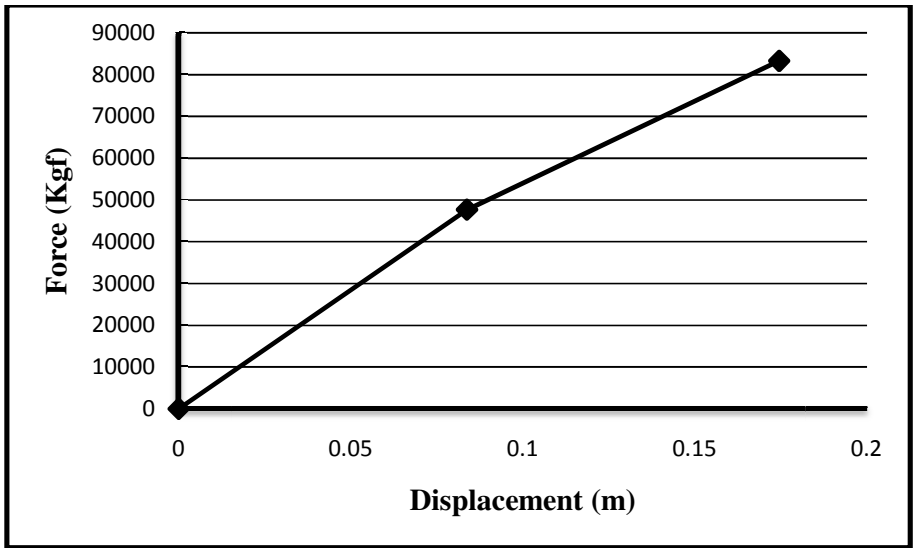

Figure 5.9: Pushover Curve of 8-story X-braced frame.

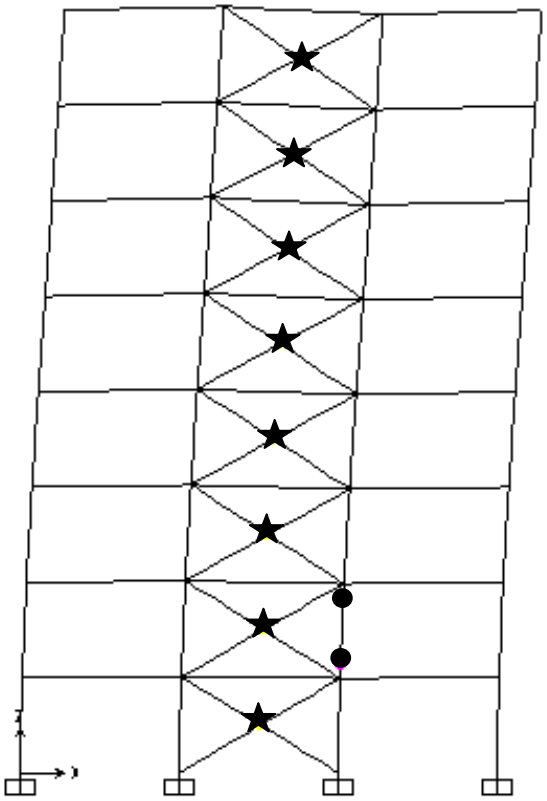

Figure 5.10: Failure moment condition of 8-story X-braced frame.

It can be observed that at the failure moment all the compressive braces are buckling and reaching to a collapse level plastic hinge. This is very similar to the performance of the same bracing system in 4-story frame. Though, this time, the minor plastic hinge is at the beginning and the end point of the second story column. The failure of the compressive members of the bracing system is the reason for the reduction of the slope of the pushover curve and consequent failure (as it was the case for 4-story X-braced frame).

5.1.6 Pushover Curve and Failure Progress of 8-story V-braced Frame

Figure 5.11 and 5.12 show the pushover curve and failure pattern of the 8-story V-braced frame.

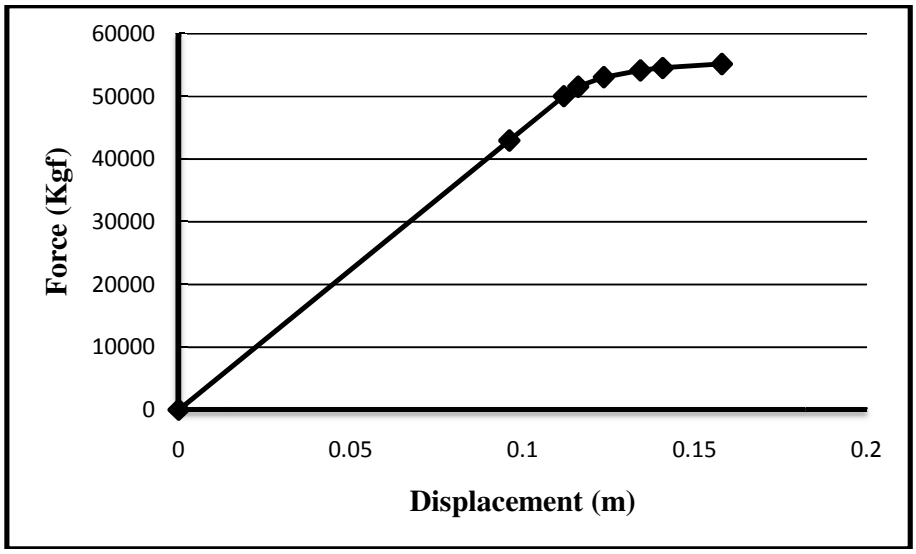

Figure 5.11: Pushover Curve of 8-story V-braced frame.

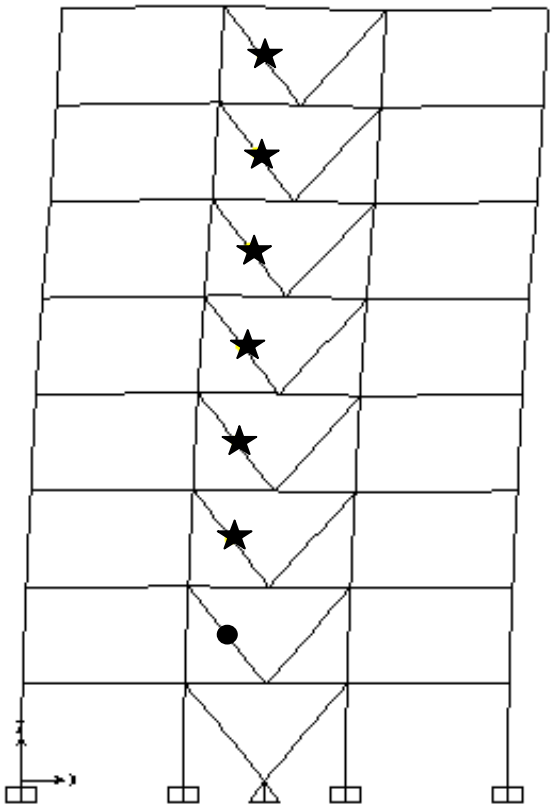
Figure 5.12: Collapse moment conditions of 8-story V-braced frame.

This frame has higher number of decreasing stages compared to the X-braced frame. It could be noticed from Figures 5.11 and 5.12 that reduction in the slope of the pushover curve at each stage is due to the buckling of compressive bracing

members. At the failure stage, a plastic hinge at collapse level exists in compressive bracing members of all stories excepting the first story which has no plastic hinge and the second story which has a minor plastic hinge. No plastic hinge has occurred in beams or columns.

5.1.7 Pushover Curve and Failure Pattern of 8-story Inverted V-braced Frame

Figure 5.13 and 5.14 show the pushover curve and failure pattern of the 8-story Inverted V-braced frame.

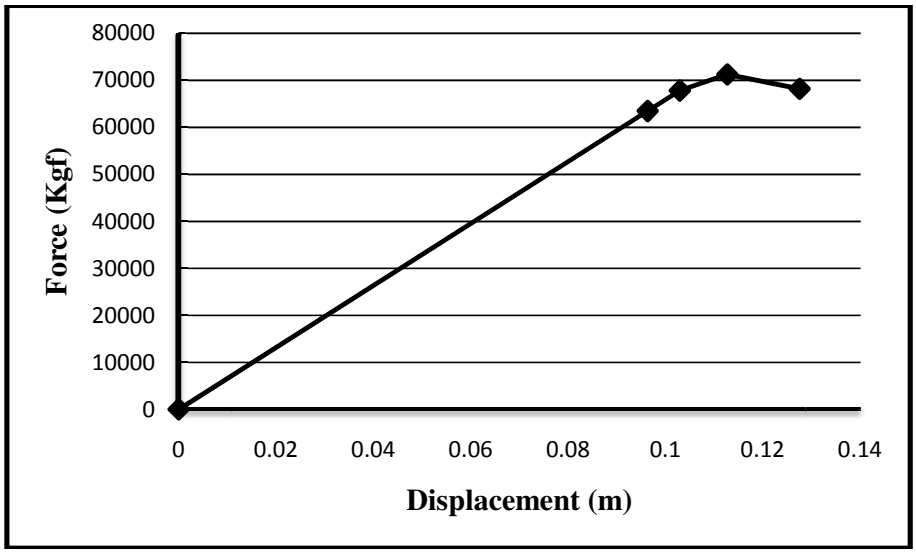

Figure 5.13: Pushover Curve of 8-story Inverted V-braced frame.

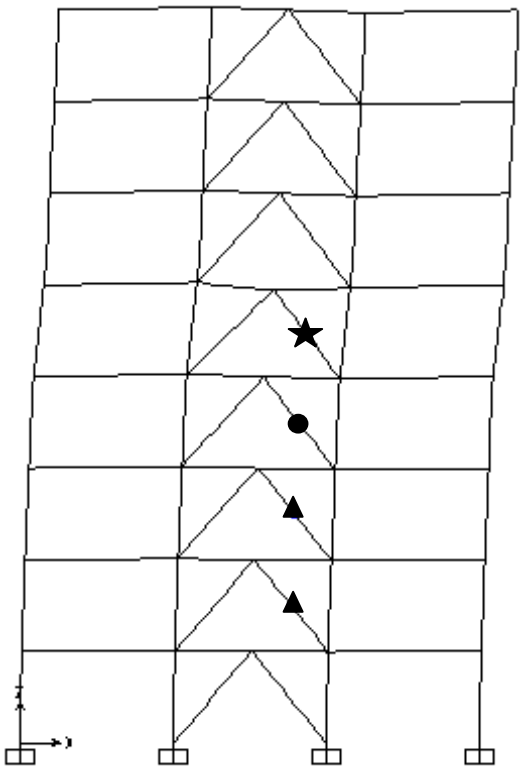

Figure 5.14: Collapse moment conditions of 8-story Inverted V-braced frame.

In this frame, the collapse level plastic hinge occurs at the compressive members of bracing system at fifth story and two Immediate Occupancy plastic hinges in the compressive brace member of the first and second floor. These are the reasons of slope reduction in the pushover curve and the failure. In this frame, the shear beam did not deflect dramatically in contrast with the 4-story Inverted V-braced frame.

5.1.8 Pushover Curve and Failure Progress of 8-story Diagonal braced Frame

Figure 5.15 and 5.16 show the pushover curve and failure pattern of the 8-story Diagonal braced frame.

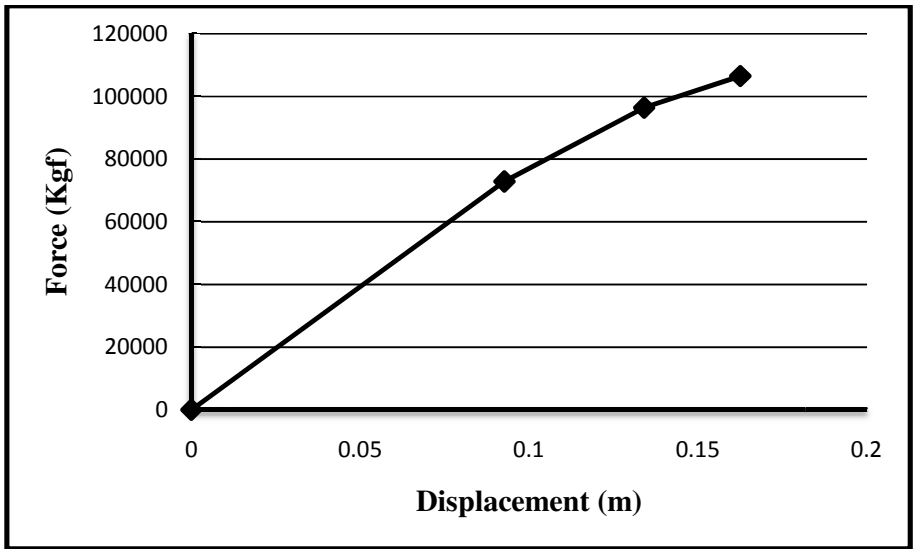

Figure 5.15: Pushover Curve of 8-story Inverted Diagonal braced frame.

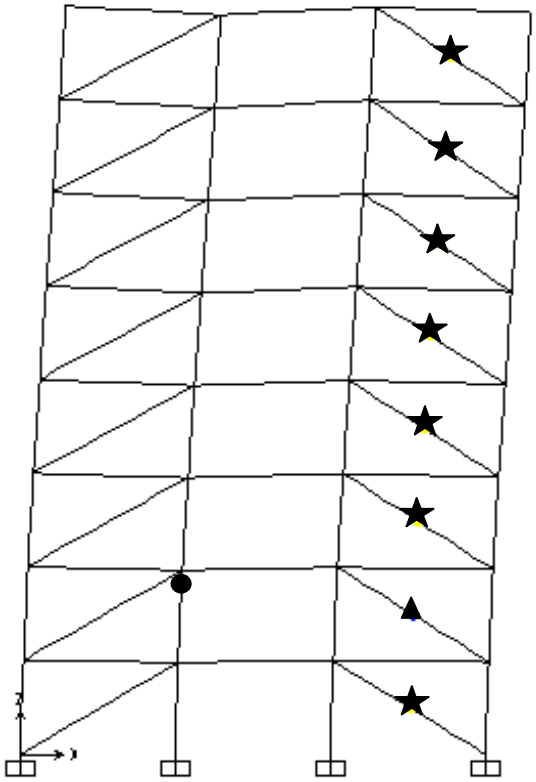
Figure 5.16: Collapse moment conditions of 8-story Diagonal braced frame.

In this frame, except for the minor and Immediate Occupancy plastic hinge in the compressive bracing members of the first and second story, plastic hinges developed in the compressive bracing members until they reached collapse level. At the last

(collapse) stage, a plastic hinge was also developed at the end point of the second story column which is similar to the case of the same bracing system in the 4-story frame.

5.1.9 Pushover Curve and Failure Progress of 12-story X-braced Frame

Figure 5.17 and 5.18 show the pushover curve and failure pattern of the 12-story X-braced frame.

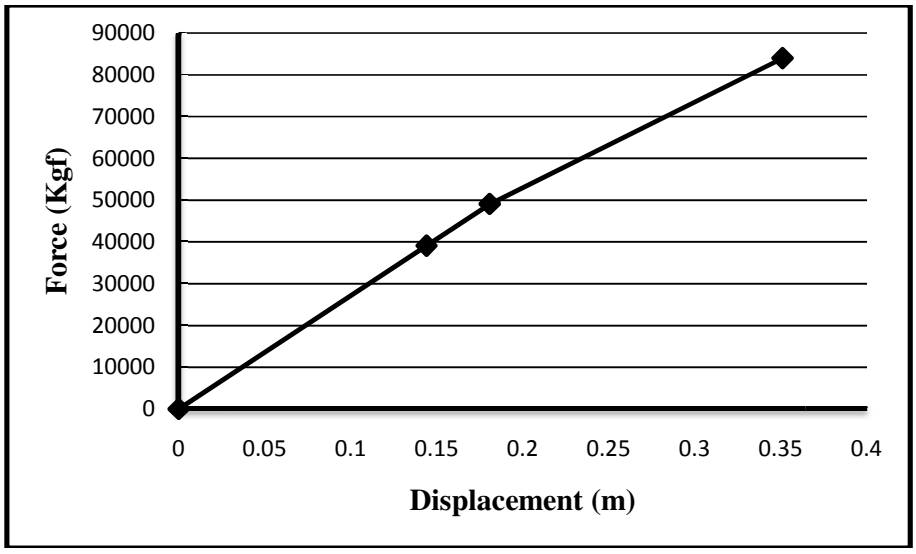

Figure 5.17: Pushover Curve of 12-story X-braced frame.

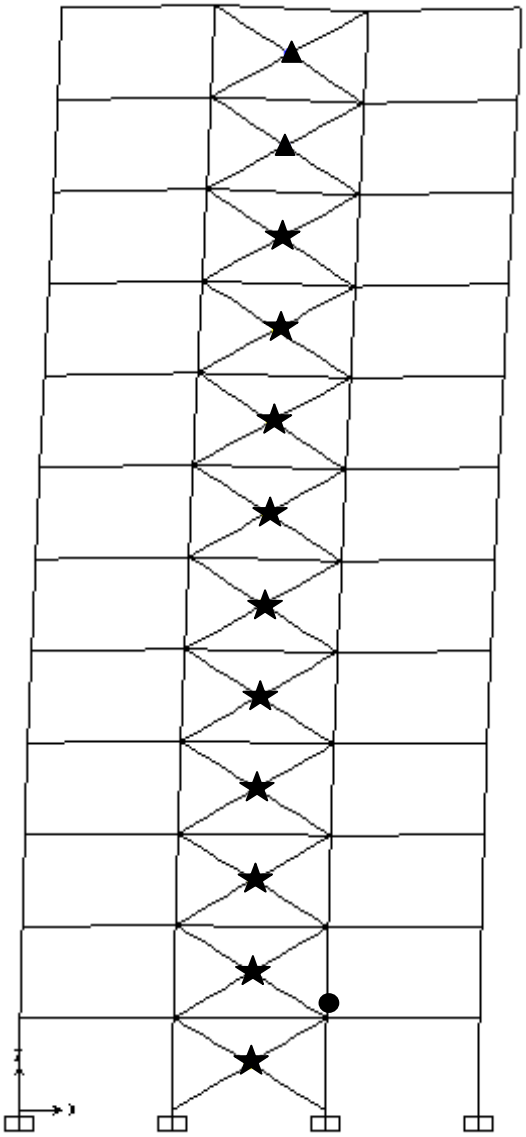

Figure 5.18: Failure moment condition of 12-story X-braced frame.

It can be observed that at the failure moment, all of the compressive braces are buckling and reaching a collapse level plastic hinge at stories one to ten and immediate occupancy level at stories eleven and twelve. This is similar to the performance of the same bracing system in shorter frames which was discussed before. Though, this time, the minor plastic hinge is at the beginning of the second story compressive column. Overall, the failure of the compressive members of the bracing system is the reason for the reduction of the slope of the pushover curve and

consequent collapse of the frame (as the case for 4- and 8-story X-braced frame). It can be seen that in an X-braced frame, the severity of plastification decreases in the higher story levels.

5.1.10 Pushover Curve and Failure Progress of 12-story V-braced Frame

Figure 5.19 and 5.20 show the pushover curve and failure pattern of the 12-story V-braced frame.

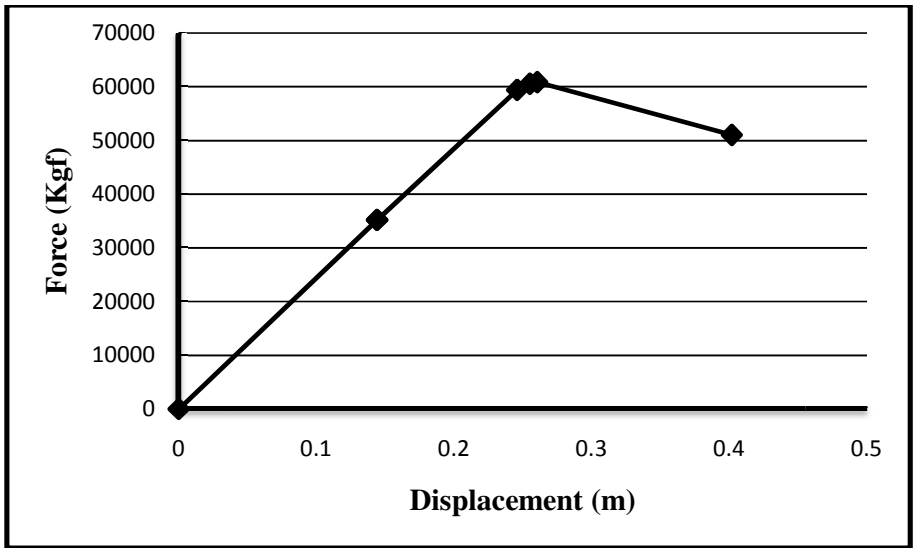

Figure 5.19: Pushover Curve of 12-story V-braced frame.

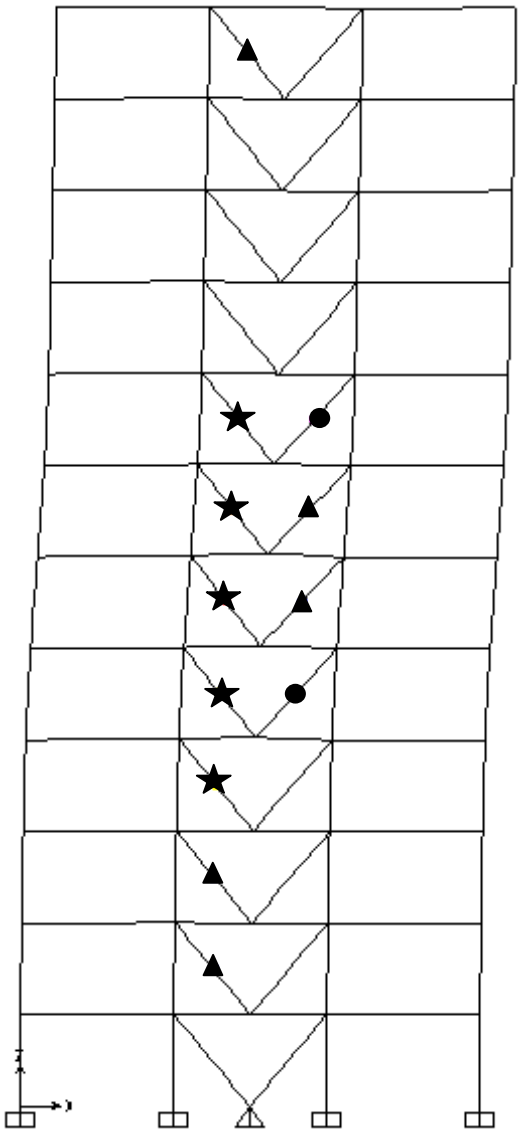

Figure 5.20: Collapse moment conditions of 12-story V-braced frame.

It could be noticed from Figures 5.19 and 5.20 that there is a dramatic reduction in the slope of the pushover curve in a very short stage due to the buckling of compressive bracing members mainly in the central and lower stories which has been accompanied with minor and immediate occupancy plastic hinges in tension bracing members of central stories at collapse stage. No plastic hinge has occurred in beams or columns. There is no plastic hinge in the first story bracing members.

This case is also similar to the performance of the same bracing system in shorter frames.

5.1.11 Pushover Curve and Failure Progress of 12-story Inverted V-braced Frame

Figure 5.21 and 5.22 show the pushover curve and failure pattern of the 12-story Inverted V-braced frame.

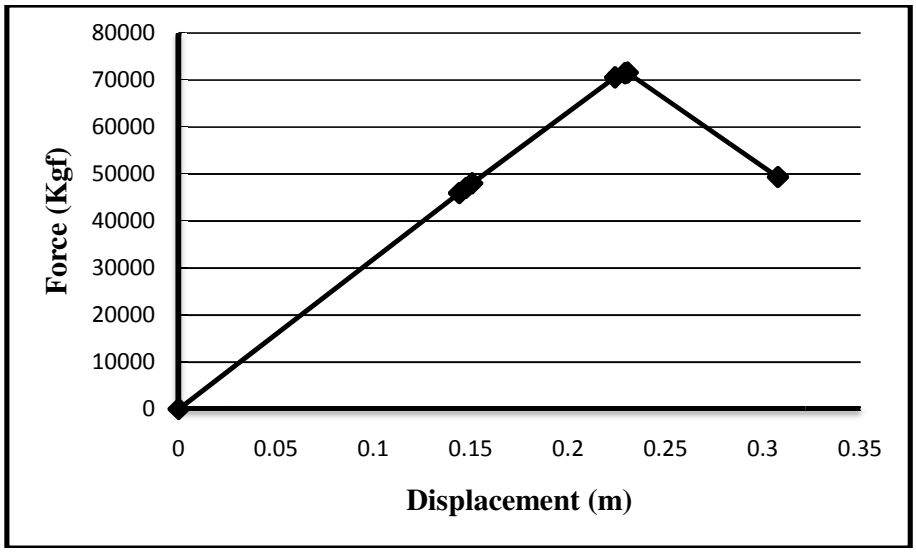

Figure 5.21: Pushover Curve of 12-story Inverted V-braced frame.

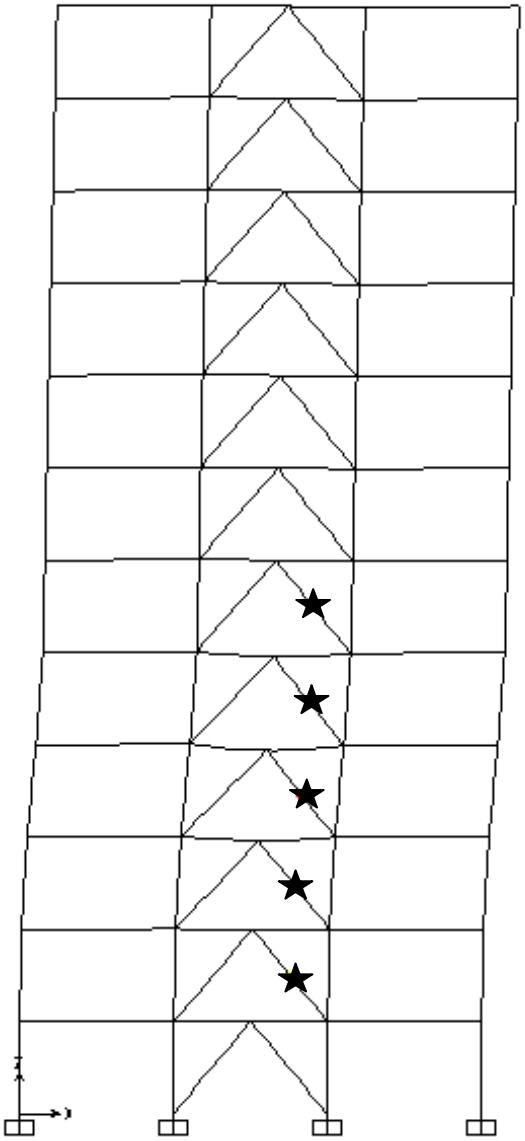

Figure 5.22: Collapse moment conditions of 12-story Inverted V-braced frame.

In this frame, similar to 12-story V-braced frame, there is a dramatic reduction in the slope of the pushover curve within a very short stage due to the buckling of compressive bracing members mainly in the lower six stories. In contrast with the V-braced frame, there is no plastic hinge in tension bracing members but in both cases, plastification is at its peak from second story up to the mid-height of the frame. In this frame, the shear beam has not deflected dramatically in contrast to 4-story and similar to 8-story Inverted V-braced frame.

5.1.12 Pushover Curve and Failure Progress of 12-story Diagonal braced Frame

Figure 5.23 and 5.24 show the pushover curve and failure pattern of the 8-story Diagonal braced frame.

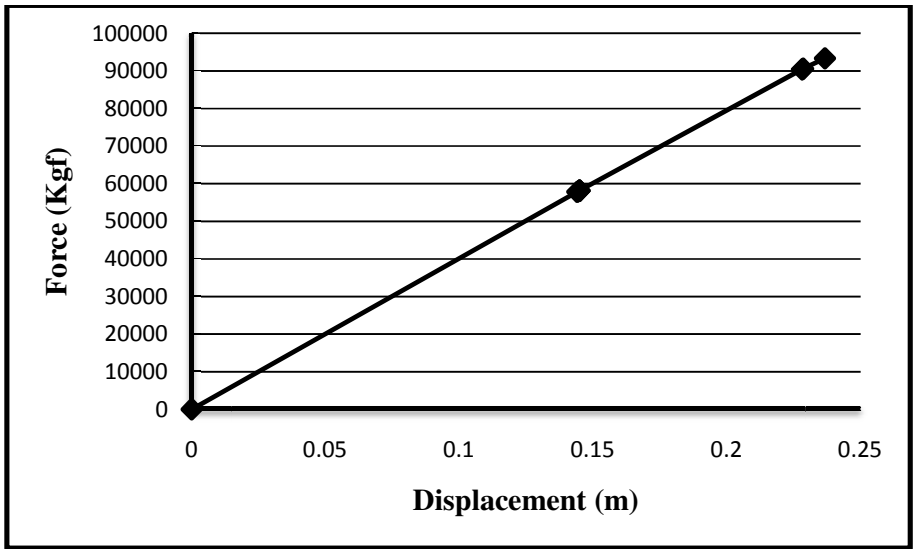

Figure 5.23: Pushover Curve of 12-story Inverted Diagonal braced frame.

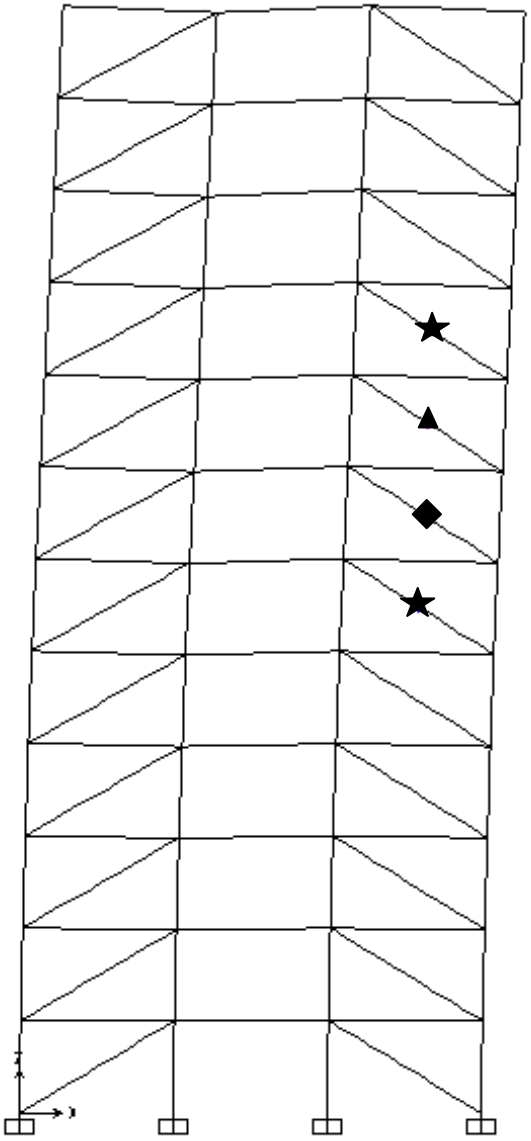

Figure 5.24: Collapse moment conditions of 12-story Diagonal braced frame.

The failure of the frame is due to the few plastic hinges in the compressive members of bracing system. This means that the frame does not have enough energy dissipation comparing to other ones. This will be discussed in more detail later.

5.2 Categorizing the Pushover Curves by Number of Stories

Separate structural response curves from pushover analysis were presented in the previous section with other details to demonstrate the failure pattern of each frame.

In this part, the pushover curves are categorized by their number of stories for better comparison of different bracing systems. In this way, behavior of each system can be compared with others in the group with the same number of stories. The frames are categorized in the groups of 4-, 8- and 12-story. Each group contains X-, V-, Inverted V- and diagonal braced frames. One figure is given for each group containing different structural response curves.

5.2.1 Pushover Curves of 4-story Frames

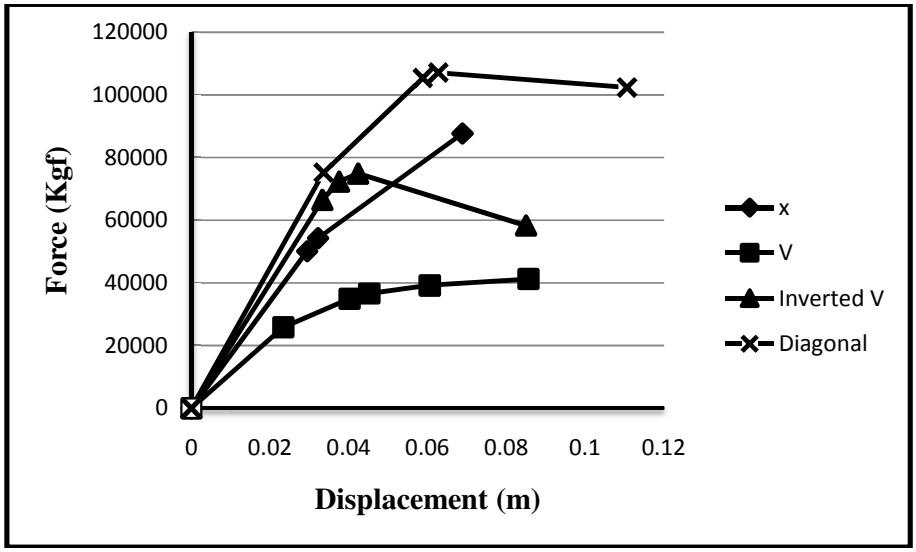

Figure 5.25: Pushover Curves of 4-story Frames.

It can be observed from figure 5.25 that the elastic stiffness of all of the bracing systems is not much different from each other. Diagonal, Inverted V-, X- and V-braced frames have respectively the highest to lowest elastic stiffness in four story buildings. On the contrary, in the post-elastic region, the differences are far beyond the simplification assumption made by the design codes. Diagonal braced frame has the highest values of shear capacity per displacement and also collapse point comparing to other frames in its entire structural response curve. But this can not be taken as a great advantage for this system since its design weight is more than the

other bracing systems. Inverted V-braced frame, having the highest elastic stiffness after the diagonal braced frame, faces a dramatic decrease in its post-elastic region, reaching lower stiffness values comparing to X-braced frame. V-braced frame has the least values of shear capacity per displacement comparing to other frames in its entire structural response curve. But this can not be taken as a great disadvantage for this system either since its design weight is less than the other systems. V-braced frame has the highest number of pushover steps, showing larger number of changes in the frame before collapse.

5.2.2 Pushover Curves of 8-story Frames

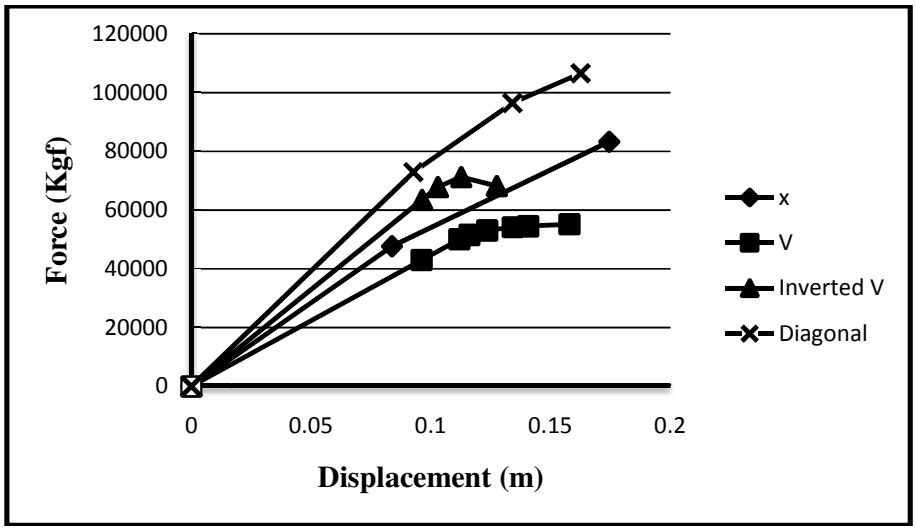

Figure 5.26: Pushover Curves of 8-story Frames.

The order of the curves of 8-storey frame is very similar to those of the 4-story frames. The order of change in the elastic stiffness of all of the bracing systems is similar to the one for four story frame but the actual stiffness values are lower. Diagonal, Inverted V-, X- and V-braced frames still have respectively the highest to the lowest elastic stiffness in these frames as in the case for four story buildings. This is while the behavior of the 4- and 8-story frames in the post-elastic area is also

very similar to each other with minor differences. Diagonal braced frame once again has the highest values of shear capacity per displacement and also collapse point comparing to other frames in its entire structural response curve. Inverted V-braced frame, having the highest elastic stiffness after the diagonal one, faced a dramatic decrease in its post-elastic region, but contrary to the 4-story frames, it does not reach to a lower stiffness comparing to X-braced frame. V-braced frame has the least values of shear capacity per displacement comparing to other frames in its entire structural response curve. It also has the highest number of pushover steps comparing to other frames, showing larger number of changes in the frame before collapse.

5.2.3 Pushover Curves of 12-story Frames

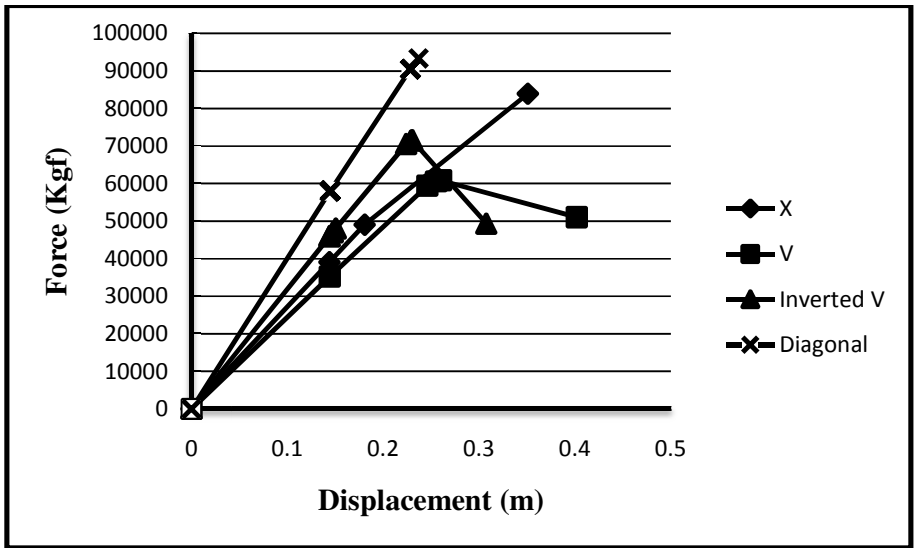

Figure 5.27: Pushover Curves of 12-story Frames.

The response curves are different for 12-story frames when compared to the two former ones, 4- and 8-story but still some of the characteristics mentioned are also governing herein. The elastic stiffness behavior is same as the other groups. The behavior of diagonal, X- and V-braced frames are also similar to the previous ones

but with more dramatic changes. The Inverted V-braced frame, having the most dramatic changes, falls below all of the bracing types in shear capacity per displacement in this group. The behavior of X-braced frame is similar to the formerly mentioned groups.

5.3 Categorizing the Pushover Curves and Failure Patterns by Bracing System

It is observed that performance of each bracing system is similar in some aspects in frames with different number of stories and differ in some other aspects. The similarities are mentioned as the characteristics of each special bracing system in this part. A generalized effect of frame height on the failure pattern is also tried to be given. It is observed that the failure patterns are more affected by the bracing system rather than the number of stories. Thus, failure patterns were not categorized by the number of stories of the frame in the previous part. In this part, pushover curves are also categorized in four different groups of X-, V-, Inverted V- and diagonal braced frames. Each group consists of three curves (being demonstrated in one figure) for different story numbers. The effect of number of stories (frame height) on each bracing system is highlighted. Because the frame heights differ in the curves of one group, stiffness of different bracing systems can not be compared directly on the basis of a Force-Displacement curve. To solve this problem, each Force-Displacement curve is accompanied by its equivalent Force-Drift (global drift) curve.

5.3.1 Pushover Curves and Failure Patterns of X-braced Frames

Structural response curves of 4-, 8- and 12-story X-braced frames are shown in Figure 5.28 and 5.29.

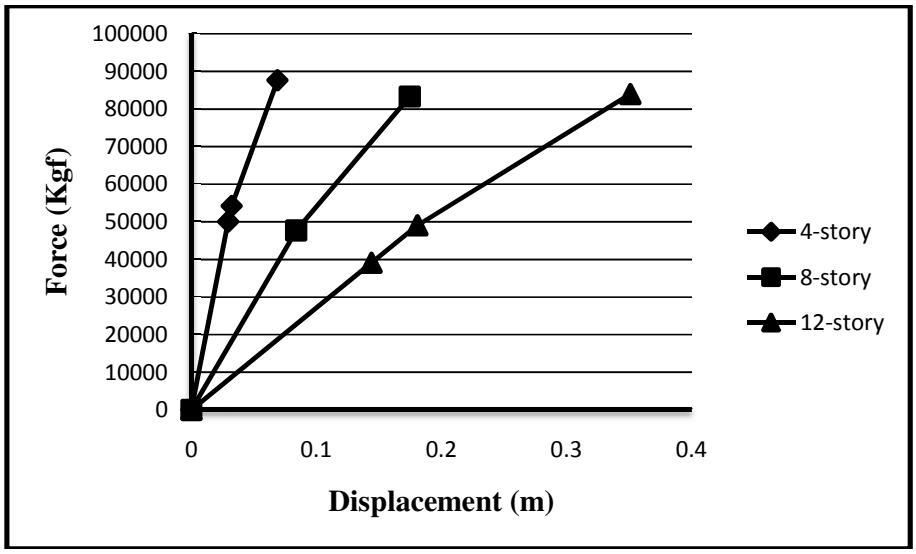

Figure 5.28: Force-Displacement pushover curves of X-braced frames.

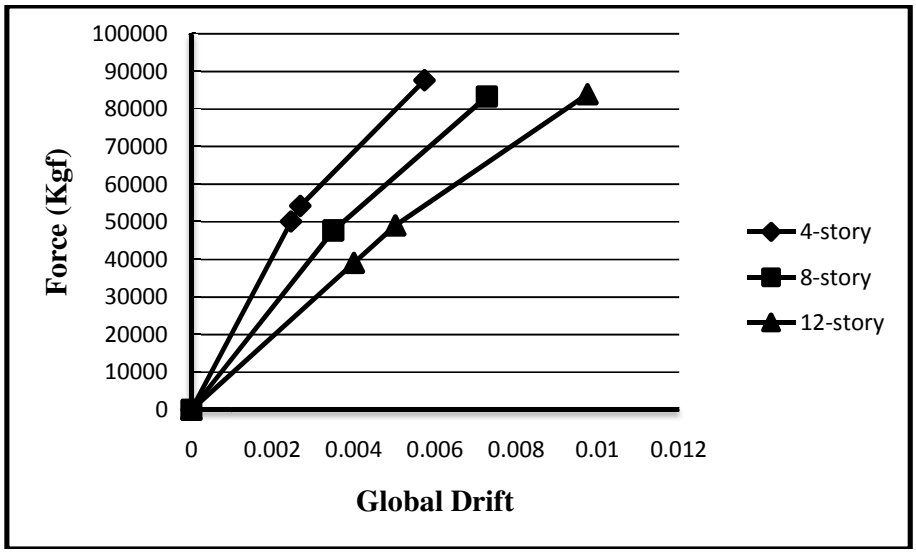

Figure 5.29: Force-Global Drift pushover curves of X-braced frames.

It can be observed from Figures 5.2, 5.10 and 5.18 that the typical failure pattern of X-braced frames are due to collapse level plastic hinges in the compressive members of bracing system which change into more minor hinges as the story level reaches to eleven and twelve. One or two minor plastic hinges are also observed in the first two story columns with the highest compressive seismic force. Figures 5.28 and 5.29 verify the discussed failure pattern by showing similar behavior in pushover curves for all three X-braced frames. They have similar initial stiffness behavior and the

stiffness values reduced after the first buckling in bracing members. Post-elastic responses are also very similar. Overall, in X-braced frames, both elastic and post-elastic stiffness decreases as the number of stories increase. It should also be noted that the frames have continuous positive stiffness for all of their response curve ranges.

5.3.2 Pushover Curves and Failure Patterns of V-braced Frames

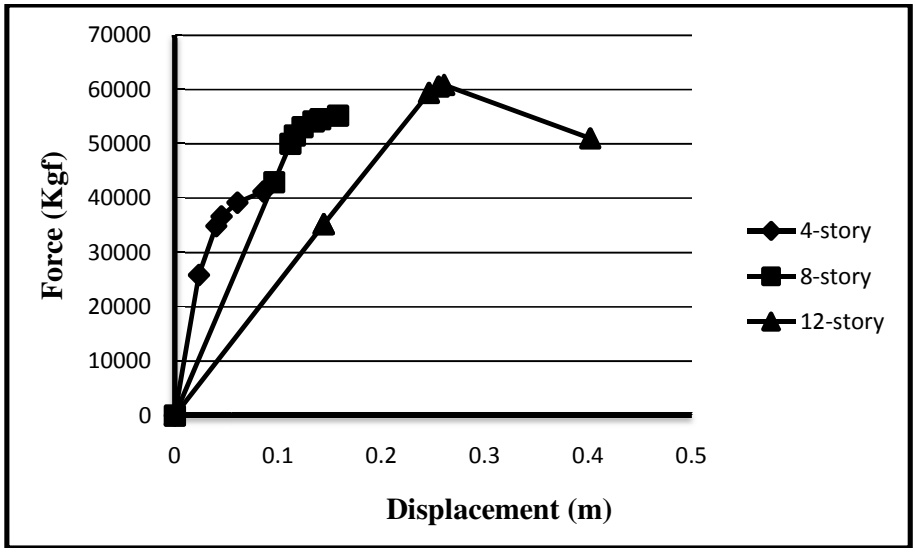

Figure 5.30: Force-Displacement pushover curves of V-braced frames.

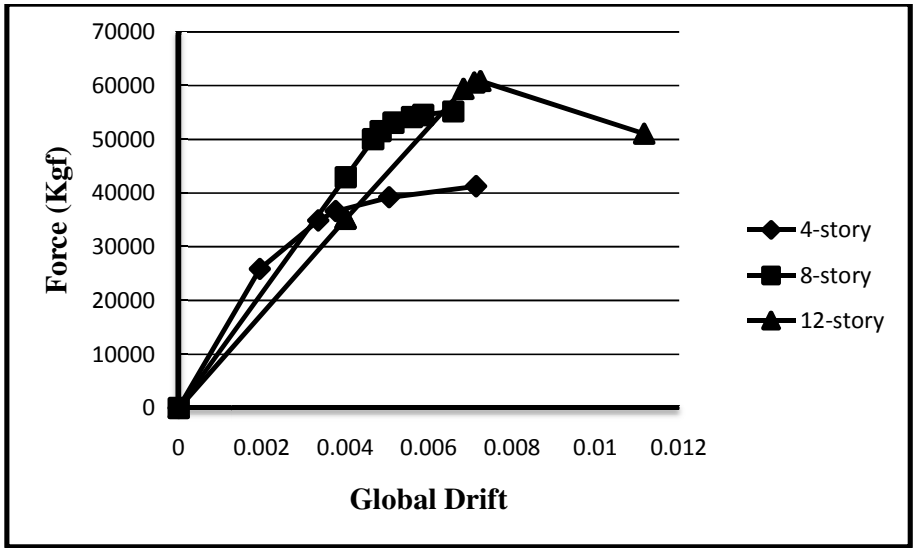

Figure 5.31: Force-Global Drift pushover curves of V-braced frames.

According to Figures 5.4, 5.12 and 5.20, the typical failure of V-braced frames are also due to the buckling of compressive members of bracing system. But in this case, no plastic hinge exists in the first story of the frame. A reason for this behavior might be the connection robustness of the first story bracing members to the ground. Another difference between this case and others is the existence of minor plastic hinges in the tensile bracing members before the failure. This leads to more efficient energy dissipation. As in the case of X-braced frames, the plasticity of the hinges decreases as the number of stories increases. This behavior is magnified in V-braced frames and this might be the reason for the noticeable difference between the taller (12-story) frame and the shorter ones (4- and 8-story) as shown in Figures 5.30 and 5.31. Similar to the X-braced frames, the highest elastic lateral stiffness decreases with an increase in the number of stories. Post-elastic stiffness is subject to greater changes and need more studying. Idealization results will be demonstrated for this issue.

5.3.3 Pushover Curves and Failure Patterns of Inverted V-braced Frames

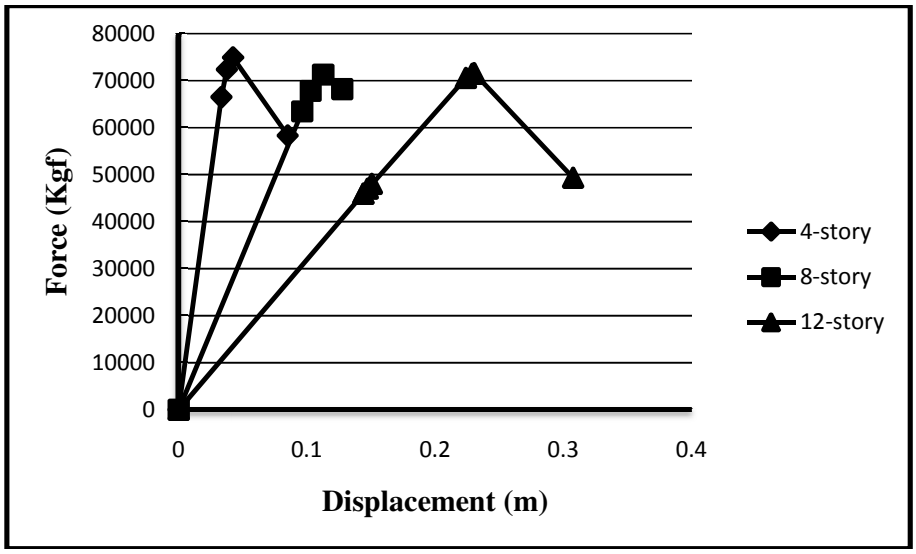

Figure 5.32: Force-Displacement pushover curves of Inverted V-braced frames.

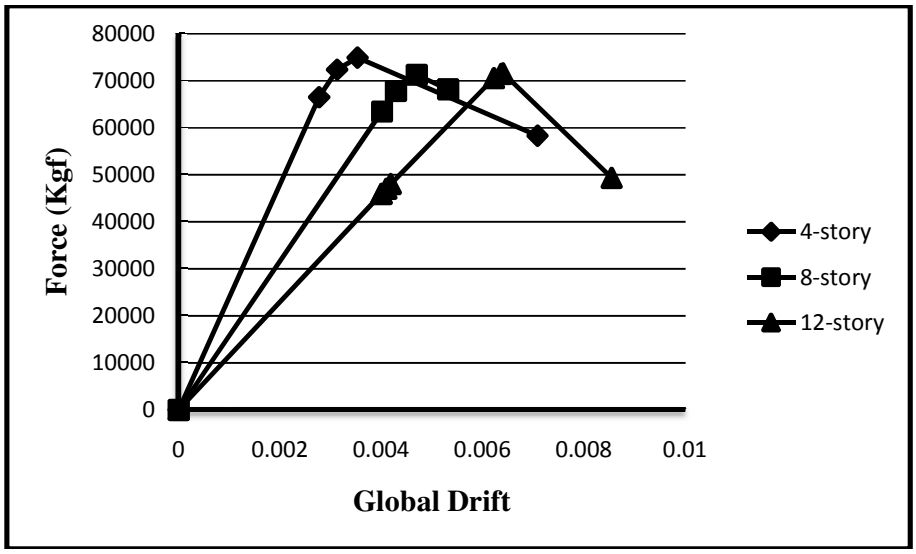

Figure 5.33: Force-Global Drift pushover curves of Inverted V-braced frames.

The change in the initial stiffness magnitude due to the differences in the number of stories is the same as other bracing systems (It decreases as the number of stories increases). The decrease in the post-elastic stiffness is more than the previously mentioned bracing systems (Figures 5.32 and 5.33). Typical failure pattern is due to buckling of the compressive braces. Buckling vulnerability of the compressive bracing members does not obey any strict rule but is generally similar to other cases.

5.3.4 Pushover Curves and Failure Patterns of Diagonal braced Frames

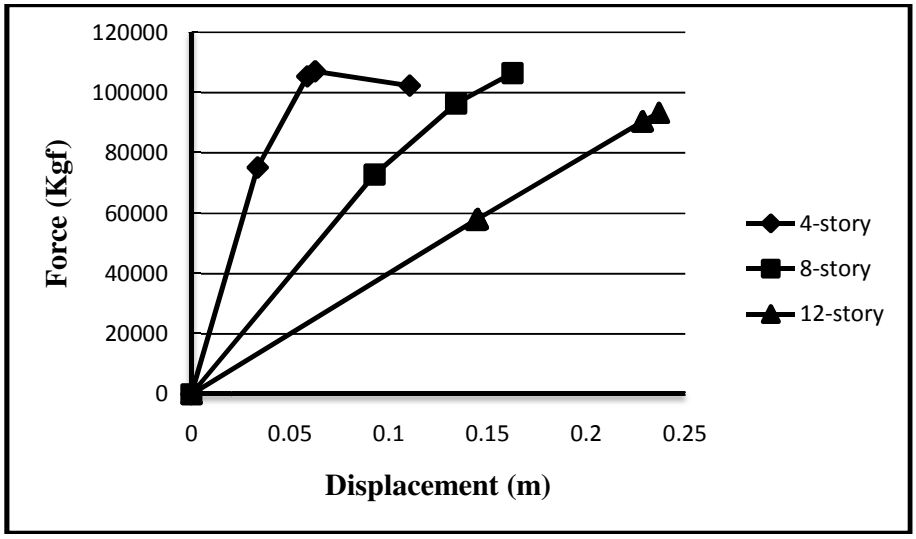

Figure 5.34: Force-Displacement pushover curves of Diagonal braced frames.

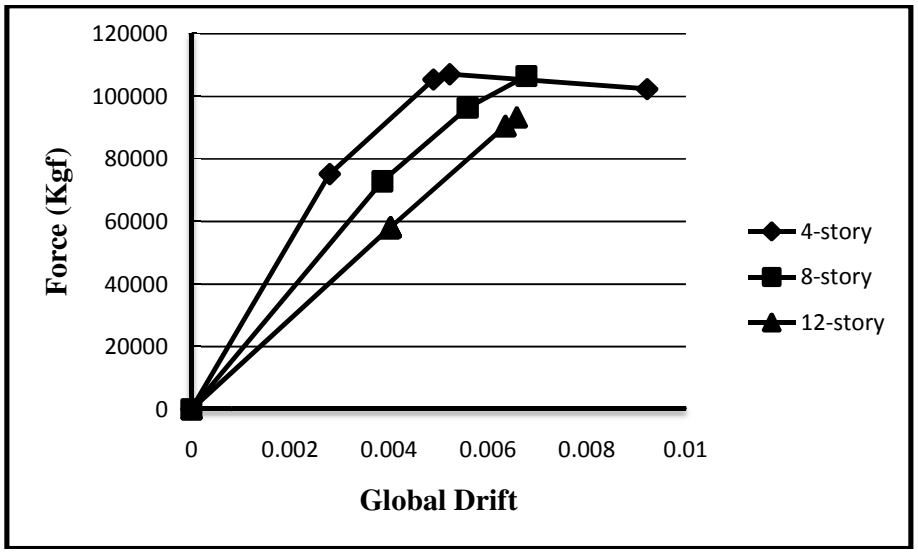

Figure 5.35: Force-Global Drift pushover curves of Diagonal braced frames.

It can be mentioned that as a general rule, initial stiffness decreases as the number of stories increase. The change in post-elastic stiffness will be discussed later after the idealization of the pushover curves. This makes quantitative analysis easier. Brace buckling vulnerability is low in the first story, increases in the second and third stories and decreases when reaching higher stories of 12-story frames. This pattern is observed to be general for all of the 12-story frames. Minor plastic hinges exist in the compressive columns of the first few stories.

5.4 Idealized Pushover Curves

As it was discussed in earlier sections, the initial stiffness of the frame is very easy to find from its structural response curve but numerical comparison on post-elastic stiffness is not possible to obtain in this way. By idealizing, elastic stiffness, post-elastic stiffness, yield point and target displacement point of the frame can be reached for quantitative comparison of different frames (discussed in the literature review). Mathematical calculations are done by Microsoft Excel according to the information in chapter two and the parameters obtained are given in the tables

below. In this part, idealized response curve of each frame is given together with its pushover curve in one figure and the related parameters are also given. In the next step, they will be categorized and discussed in similar manner that was done in sections 5.2 and 5.3.

5.4.1 Idealized Response Curve of 4-story X-braced Frame

Table 5.1: Idealizing parameters of structural response curve of 4-story X-braced frame.

Item	Value
C_0	0.8058
C_1	1.1116
C_2	1.0392
S_a	1
T_e	0.5578
T_i	0.5578
K_i (Kgf/m)	1702742.2
K_e (Kgf/m)	1702742.2
α	0.4858
R	4.1244
V_y (Kgf)	53527.56
D_y (m)	0.0314
Weight (Kgf)	220766.39
C_m	1

Target displacement point of the frame is at the point with displacement of 0.073 m and force of 87619.0 Kgf. Yield and target displacement point of the frame is shown on the idealized response curve of the frame in Figure 5.36.

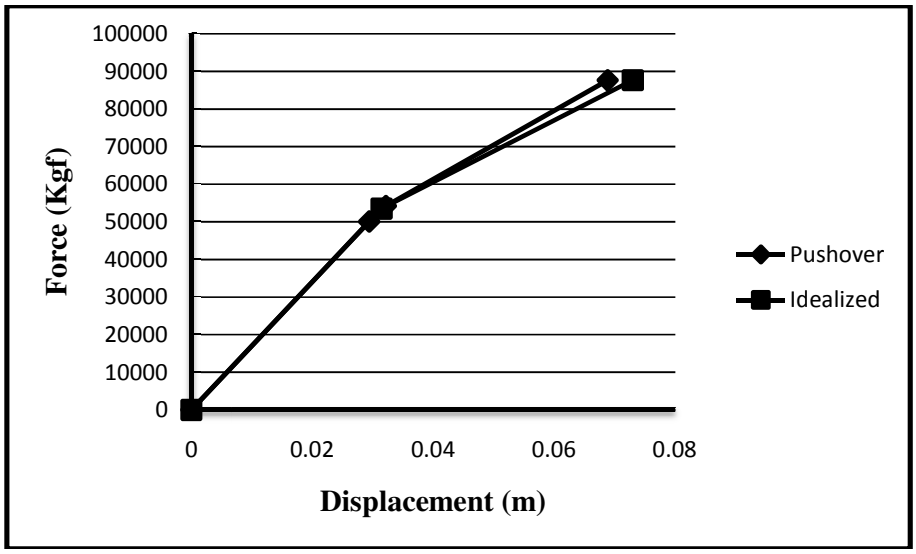

Figure 5.36: Idealized and real structural response curve of 4-story X-braced frame.

5.4.2 Idealized Response Curve of 4-story V-braced Frame

Table 5.2: Idealizing parameters of structural response curve of 4-story V-braced frame.

Item	Value
C_0	0.6858
C_1	1.0861
C_2	1
S_a	0.6541
T_e	0.8561
T_i	0.8561
K_i (Kgf/m)	1107893.4
K_e (Kgf/m)	1107893.4
α	0.1147
R	6.6787
V_y (Kgf)	33771.06
D_y (m)	0.0305
Weight (Kgf)	344807.6
C_m	1

Target displacement point of the frame is at the point with displacement of 0.089 m and force of 41232.1 Kgf. Yield and target displacement point of the frame is shown on the idealized response curve of the frame in Figure 5.37.

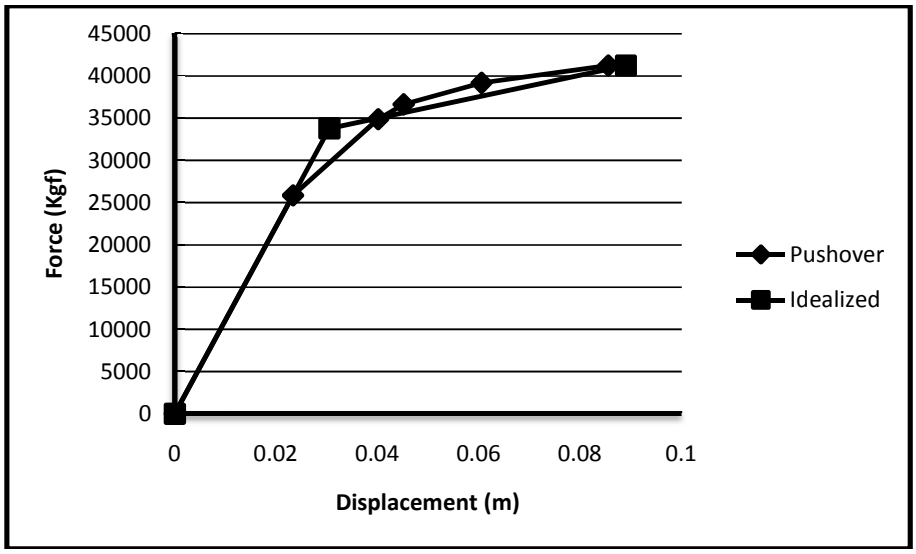

Figure 5.37: Idealized and real structural response curve of 4-story V-braced frame.

5.4.3 Idealized Response Curve of 4-story Inverted V-braced Frame

Table 5.3: Idealizing parameters of structural response curve of 4-story Inverted V-braced frame.

Item	Value
C_0	0.8318
C_1	1.0821
C_2	1.0263
S_a	0.9012
T_e	0.6214
T_i	0.6214
K_i (Kgf/m)	1999092.8
K_e (Kgf/m)	1999092.8
A	-0.186
R	3.8522
V_y (Kgf)	75856.54
D_y (m)	0.0379
Weight (Kgf)	324259
C_m	1

Target displacement point of the frame is at the point with displacement of 0.081 m and force of 60000.6 Kgf. Yield and target displacement point of the frame is shown on the idealized response curve of the frame in Figure 5.38.

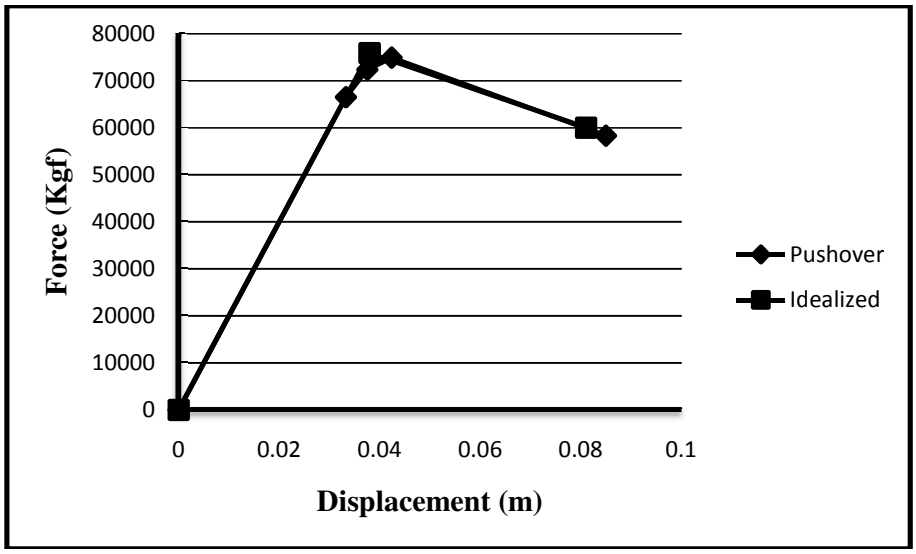

Figure 5.38: Idealized and real structural response curve of 4-story Inverted V-braced frame.

5.4.4 Idealized Response Curve of 4-story Diagonal braced Frame

Table 5.4: Idealizing parameters of structural response curve of 4-story Diagonal braced frame.

Item	Value
C_0	0.7658
C_1	1.1268
C_2	1.0252
S_a	1.0849
T_e	0.5899
T_i	0.5899
K_i (Kgf/m)	2239288.8
K_e (Kgf/m)	2239288.8
α	0.0896
R	3.6477
V_y (Kgf)	97011.84
D_y (m)	0.0433
Weight (Kgf)	326180.1
C_m	1

Target displacement point of the frame is at the point with displacement of 0.083 m and force of 105039.7 Kgf. Yield and target displacement point of the frame is shown on the idealized response curve of the frame in Figure 5.39.

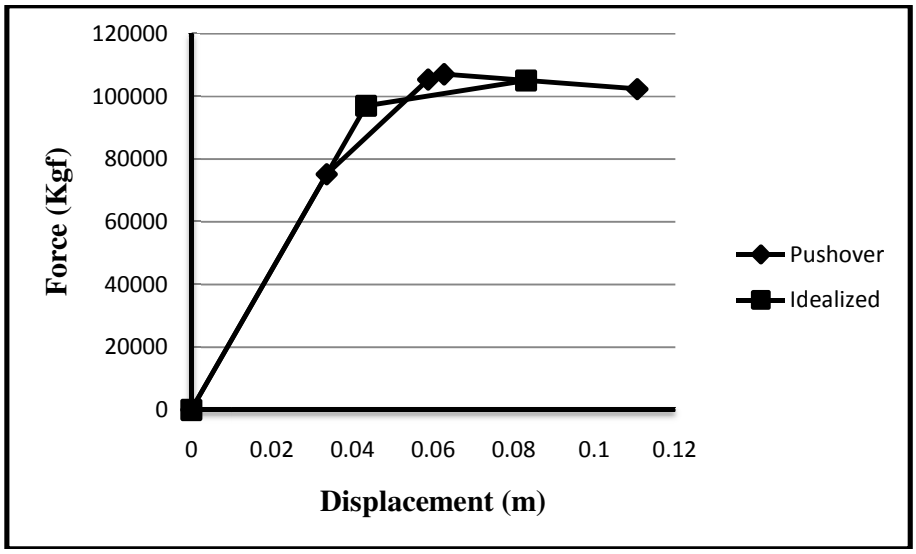

Figure 5.39: Idealized and real structural response curve of 4-story Diagonal braced frame.

5.4.5 Idealized Response Curve of 8-story X-braced Frame

Table 5.5: Idealizing parameters of structural response curve of 8-story X-braced frame.

Item	Value
C_0	0.6969
C_1	1
C_2	1
S_a	0.4552
T_e	1.2303
T_i	1.2303
K_i (Kgf/m)	569133.2
K_e (Kgf/m)	569133.2
α	0.6892
R	4.2447
V_y (Kgf)	47671.13
D_y (m)	0.0838
Weight (Kgf)	444573.6
C_m	1

Target displacement point of the frame is at the point with displacement of 0.12 m and force of 61893.7 Kgf. Yield and target displacement point of the frame is shown on the idealized response curve of the frame in Figure 5.40.

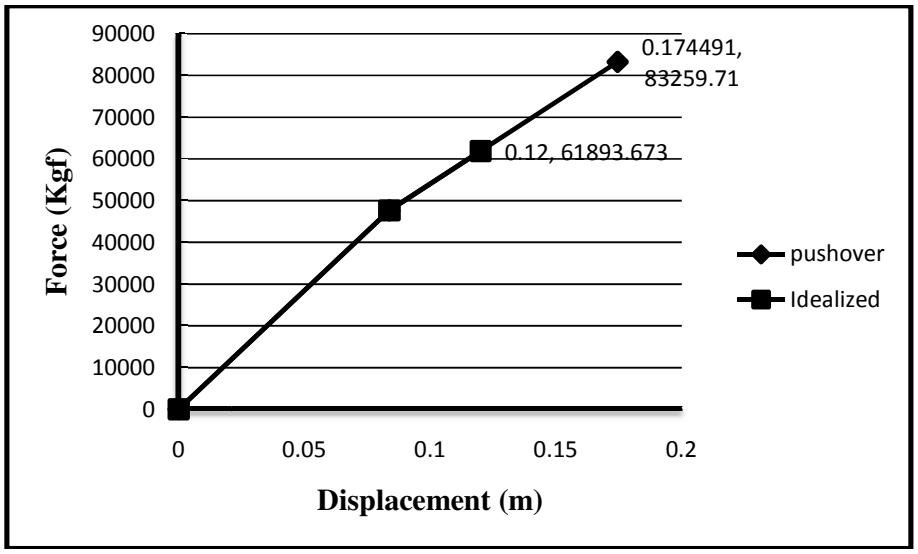

Figure 5.40: Idealized and real structural response curve of 8-story X-braced frame.

5.4.6 Idealized Response Curve of 8-story V-braced Frame

Table 5.6: Idealizing parameters of structural response curve of 8-story V-braced frame.

Item	Value
C_0	0.6761
C_1	1
C_2	1
S_a	0.3276
T_e	1.7096
T_i	1.7096
K_i (Kgf/m)	446913.1
K_e (Kgf/m)	446913.1
α	0.1128
R	4.0239
V_y (Kgf)	52989.63
D_y (m)	0.1186
Weight (Kgf)	650935
C_m	1

Target displacement point of the frame is at the point with displacement of 0.162 m and force of 55167.2 Kgf. Yield and target displacement point of the frame is shown on the idealized response curve of the frame in Figure 5.41.

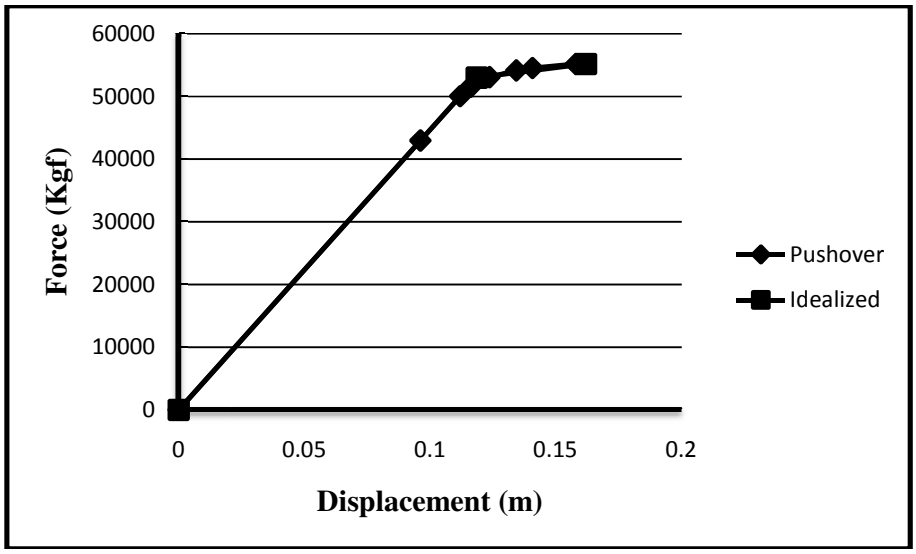

Figure 5.41: Idealized and real structural response curve of 8-story V-braced frame.

5.4.7 Idealized Response Curve of 8-story Inverted V-braced Frame

Table 5.7: Idealizing parameters of structural response curve of 8-story Inverted V-braced frame.

Item	Value
C_0	0.6765
C_1	1
C_2	1
S_a	0.4024
T_e	1.3918
T_i	1.3918
K_i (Kgf/m)	659383.4
K_e (Kgf/m)	659383.4
α	-0.1935
R	3.6787
V_y (Kgf)	71198.37
D_y (m)	0.108
Weight (Kgf)	650954.6
C_m	1

Target displacement point of the frame is at the point with displacement of 0.132 m and force of 68188.4 Kgf. Yield and target displacement point of the frame is shown on the idealized response curve of the frame in Figure 5.42.

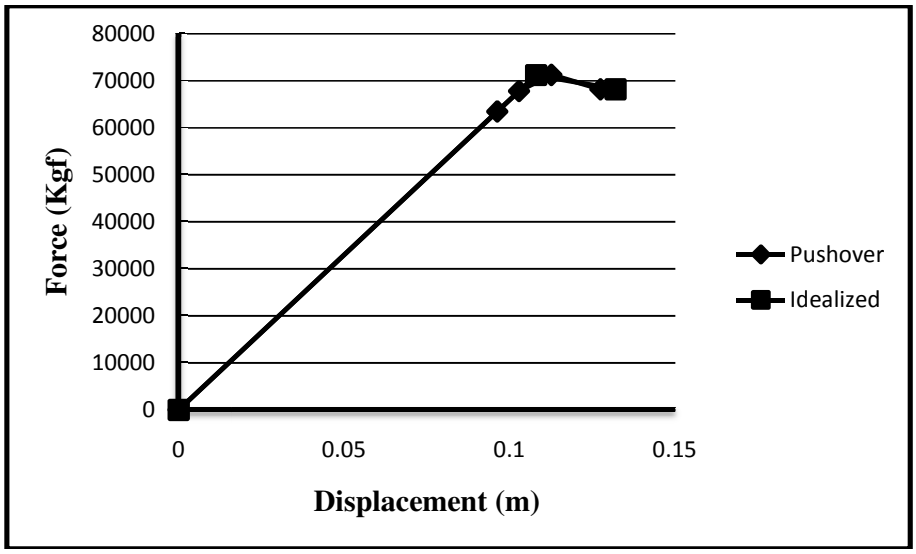

Figure 5.42: Idealized and real structural response curve of 8-story Inverted V-braced frame.

5.4.8 Idealized Response Curve of 8-story Diagonal braced Frame

Table 5.8: Idealizing parameters of structural response curve of 8-story D-braced frame.

Item	Value
C_0	0.7233
C_1	1
C_2	1
S_a	0.4307
T_e	1.3002
T_i	1.3002
K_i (Kgf/m)	786076.8
K_e (Kgf/m)	786076.8
α	0.7245
R	3.8709
V_y (Kgf)	72846.7
D_y (m)	0.0927
Weight (Kgf)	654721.9
C_m	1

Target displacement point of the frame is at the point with displacement of 0.132 m and force of 95283.9 Kgf. Yield and target displacement point of the frame is shown on the idealized response curve of the frame in Figure 5.43.

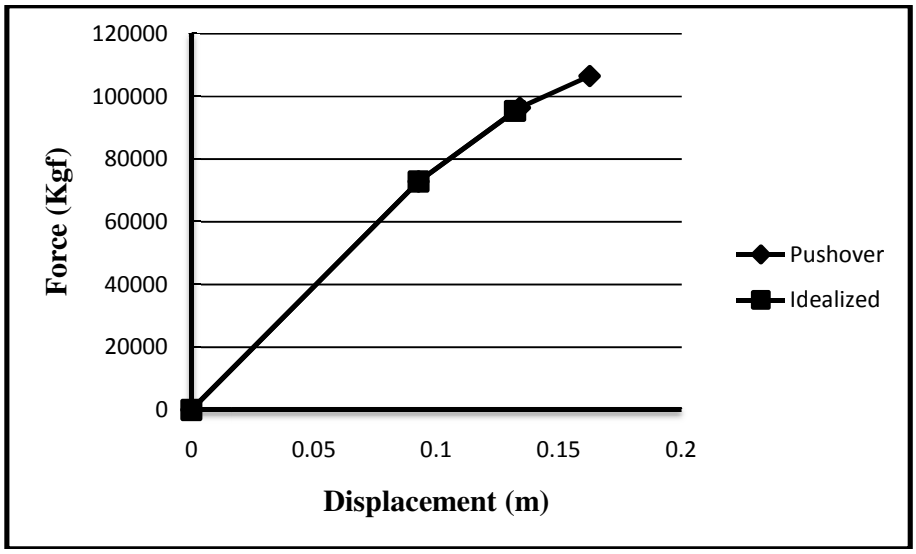

Figure 5.43: Idealized and real structural response curve of 8-story Diagonal braced frame.

5.4.9 Idealized Response Curve of 12-story X-braced Frame

Table 5.9: Idealizing parameters of structural response curve of 12-story X-braced frame.

Item	Value
C_0	0.6571
C_1	1
C_2	1
S_a	0.2673
T_e	2.095
T_i	2.095
K_i (Kgf/m)	271390.41
K_e (Kgf/m)	271390.41
α	0.76
R	3.6652
V_y (Kgf)	48966.37
D_y (m)	0.1804
Weight (Kgf)	671411.3
C_m	1

Target displacement point of the frame is at the point with displacement of 0.193 m and force of 51546.9 Kgf. Yield and target displacement point of the frame is shown on the idealized response curve of the frame in Figure 5.44.

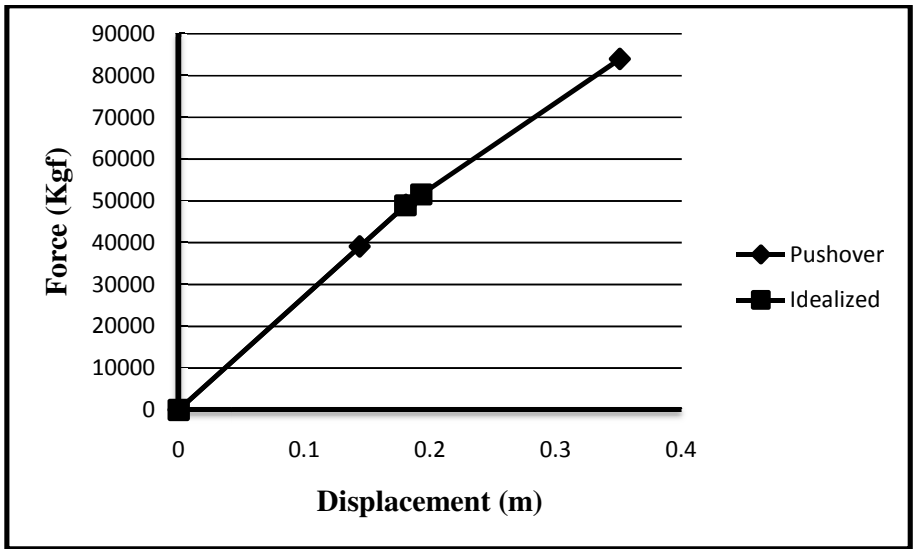

Figure 5.44: Idealized and real structural response curve of 12-story X-braced frame.

5.4.10 Idealized Response Curve of 12-story V-braced Frame

Table 5.10: Idealizing parameters of structural response curve of 12-story V-braced frame.

Item	Value
C_0	0.687
C_1	1
C_2	1
S_a	0.2042
T_e	2.743
T_i	2.743
K_i (Kgf/m)	244394.21
K_e (Kgf/m)	244394.21
α	0.5392
R	3.5799
V_y (Kgf)	55920.29
D_y (m)	0.2288
Weight (Kgf)	980551.6
C_m	1

Target displacement point of the frame is at the point with displacement of 0.264 m and force of 60589.5 Kgf. Yield and target displacement point of the frame is shown on the idealized response curve of the frame in Figure 5.45.

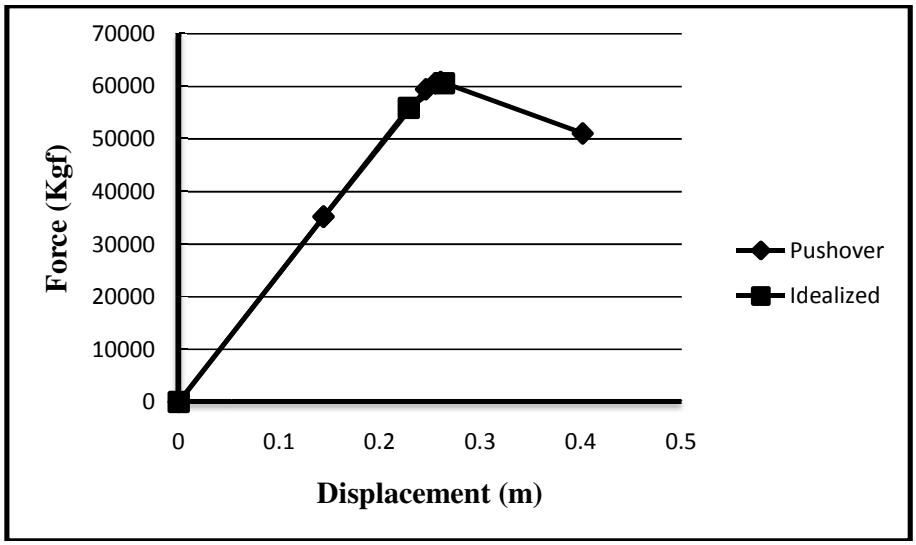

Figure 5.45: Idealized and real structural response curve of 12-story V-braced frame.

5.4.11 Idealized Response Curve of 12-story Inverted V-braced Frame

Table 5.11: Idealizing parameters of structural response curve of 12-story Inverted V-braced frame.

Item	Value
C_0	0.6767
C_1	1
C_2	1
S_a	0.2368
T_e	2.3646
T_i	2.3646
K_i (Kgf/m)	318955
K_e (Kgf/m)	318955
α	0.9567
R	4.6826
V_y (Kgf)	49572.53
D_y (m)	0.1554
Weight (Kgf)	980142.6
C_m	1

Target displacement point of the frame is at the point with displacement of 0.224 m and force of 70630.8 Kgf. Yield and target displacement point of the frame is shown on the idealized response curve of the frame in Figure 5.46.

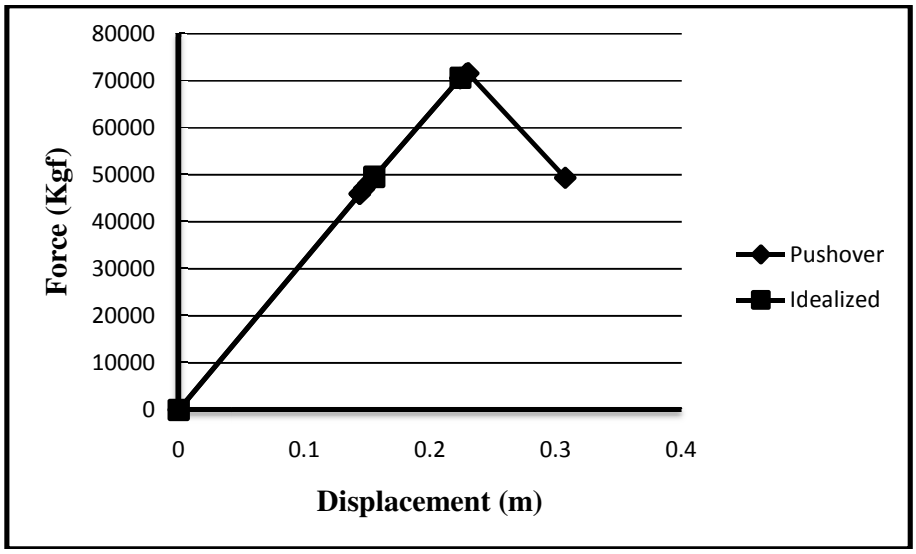

Figure 5.46: Idealized and real structural response curve of 12-story Inverted V-braced frame.

5.4.12 Idealized Response Curve of 12-story Diagonal braced Frame

Table 5.12: Idealizing parameters of structural response curve of 12-story Diagonal braced frame.

Item	Value
C_0	0.6794
C_1	1
C_2	1
S_a	0.2626
T_e	2.1324
T_i	2.1324
K_i (Kgf/m)	400930.8
K_e (Kgf/m)	400930.8
α	0.9664
R	4.4558
V_y (Kgf)	58120.52
D_y (m)	0.145
Weight (Kgf)	986136.3
C_m	1

Target displacement point of the frame is at the point with displacement of 0.203 m and force of 80490.1 Kgf. Yield and target displacement point of the frame is shown on the idealized response curve of the frame in Figure 5.47.

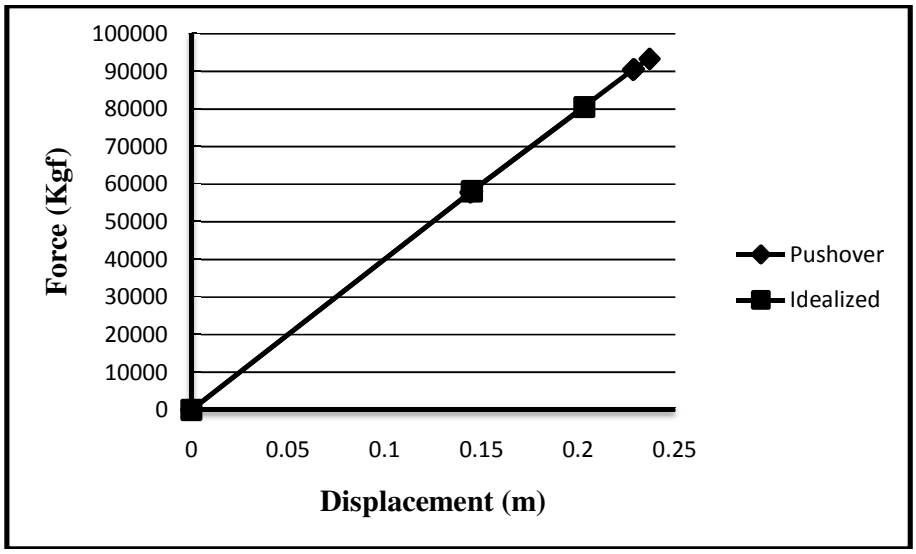

Figure 5.47: Idealized and real structural response curve of 12-story Diagonal braced frame.

5.5 Categorizing Idealized Pushover Curves by Number of Stories

Idealization procedure, results and its effect on the real structural response curve has been given before. In this part, Idealized response curves of frames with the same number of stories are categorized in three parts similar to those in part 5.2 in order to do quantitative discussion on the effect of bracing system on the nonlinear response of structures.

5.5.1 Idealized Response Curves of 4-story Frames

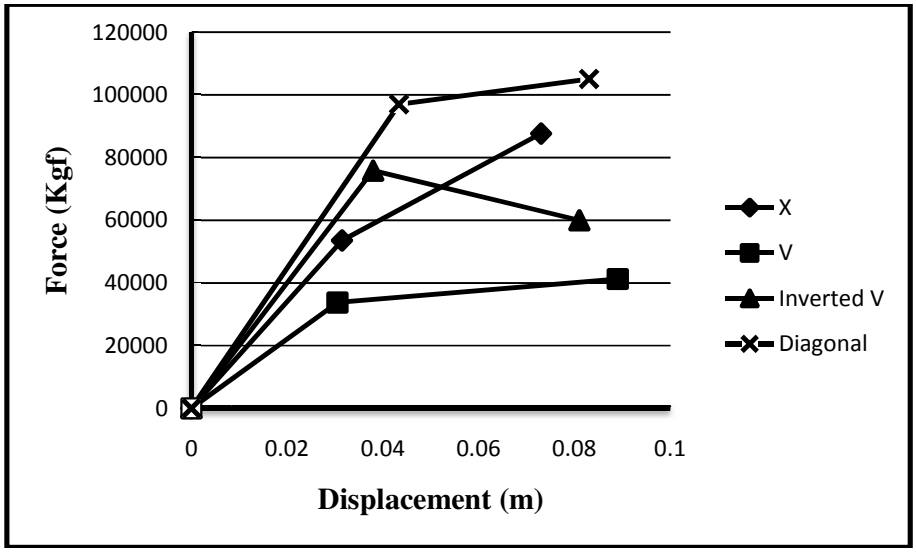

Figure 5.48: Idealized response curve of 4-story frames.

Figure 5.48 shows the effect of bracing system on the nonlinear performance of 4-story frames. Table 5.13 provides the information about the yield and target displacement points of each frame for quantitative comparison.

Table 5.13: Force and Displacement quantity of yield and target displacement points of 4-story frames.

Bracing \ Parameter	Dy	Vy	D	V	Energy
X	0.031	53527.5	0.073	87619.0	3774.6
V	0.030	33771.0	0.089	41232.1	2709.21
Inverted V	0.037	75856.5	0.081	60000.6	4363.83
Diagonal	0.043	97011.8	0.083	105039.7	6109.84

Figure 5.48 and Table 5.13 show that the order of highest to lowest values of lateral elastic stiffness are for the Diagonal, Inverted V, X- and V braced frames respectively. The yielding amounts also vary in the same format with elastic stiffness (the stiffer bracing type has higher yield force demand). Though, in the post-yield region, variables change. It can be seen that the X-braced frames has the least reduction in plastic stiffness. Diagonal and V-braced frames also continue to

have positive plastic stiffness (with a higher rate of reduction compared to X-braced frame). The Inverted V-braced frame is the only 4-story structure with negative post-yield stiffness. The highest values of α (The ratio of plastic to elastic structural stiffness) are for the X-braced, V-braced, Diagonal and Inverted V-braced frames. V-braced frame has the largest displacement before its target displacement point. It should be noted that complete information about the values of α and other idealizing parameters of all of the frames, which is referred to in here and part 5.6, is available in Tables 5.1 through 5.11 in part 5.4. These results show the efficiency of post-yield region of these frames.

5.5.2 Idealized Response Curves of 8-story Frames

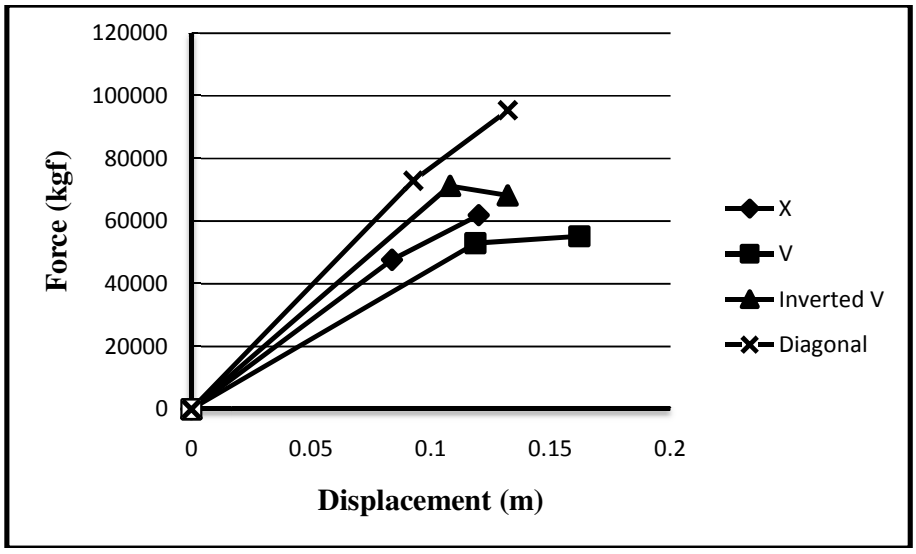

Figure 5.49: Idealized response curve of 8-story frames.

Figure 5.49 shows the effect of bracing system on the nonlinear performance of 8-story frames. Table 5.14 provides the information about the yield and target displacement points of each frame for quantitative comparison.

Table 5.14: Force and Displacement quantity of yield and target displacement points of 8-story frames.

Bracing \ Parameter	D_y	V_y	D_δ	V_δ	Energy
X	0.083	47671.1	0.120	61893.7	3981.7
V	0.118	52989.6	0.162	55167.2	5490.1
Inverted V	0.107	71198.4	0.132	68188.4	5518.1
Diagonal	0.092	72846.7	0.132	95283.9	6681.5

According to Figure 5.49 and Table 5.14, in 8-story frames, the highest value of lateral elastic stiffness is for the Diagonal braced frames. Elastic stiffness continues to decrease in Inverted V, X-, and V braced frames respectively (as the case in 4-story frames). Though, in this case, the yielding values do not vary in the same manner as before for the elastic stiffness. V-braced frame, having the least elastic stiffness yields in the highest displacement (comparing with others). The yield points, from required yielding force point of view, sorted from the highest to the lowest, are for Diagonal, Inverted V-, V- and X-braced frames respectively. The highest target displacement point is again for the V-braced frame. The highest to the lowest α values are for Diagonal, X-, V- and Inverted V-braced frame. Inverted V-braced frame is once again the only structure with negative post-yield stiffness.

5.5.3 Idealized Response Curves of 12-story Frames

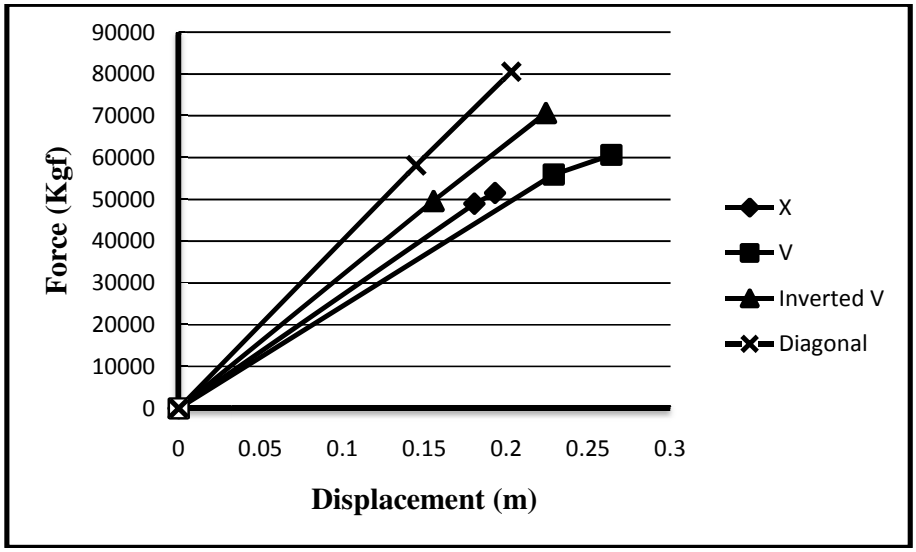

Figure 5.50: Idealized response curve of 12-story frames.

Figure 5.50 shows the effect of bracing system on the nonlinear performance of 12-story frames. Table 5.15 provides the information about the yield and target displacement points of each frame for quantitative comparison.

Table 5.15: Force and Displacement quantity of yield and target displacement points of 8-story frames.

Bracing \ Parameter	D_y	V_y	D	V	Energy
X	0.180	48966.3	0.193	51546.9	5049.2
V	0.228	55920.2	0.264	60589.5	8447.4
Inverted V	0.155	49572.5	0.224	70630.8	7973.9
Diagonal	0.144	58120.5	0.203	80490.1	8234.8

In 12-story frames, elastic stiffness values have a pattern similar to those previously mentioned for shorter frames. The highest to lowest values of lateral elastic stiffness are for the Diagonal, Inverted V, X- and V braced frames respectively. But in the post-yield region, contrary to the great similarity in the response of 4- and 8-story frames, 12-story frames demonstrate a different character. The reasons of this will be studied comprehensively in part 5.6. V-braced frame has the highest displacement

when target displacement points are concerned. All of the frames are showing positive post-yield stiffness. The highest to lowest values of α are for Diagonal, Inverted V-, V- and X-braced frames respectively.

5.6 Categorizing Idealized Pushover Curves by Bracing System

The effect of number of stories on the inelastic response of frames can best be done by comparing the idealized pushover curves of each bracing system with different number of stories. This task is done in this part. The rough comparison done on this subject in part 5.5 will also be discussed further in this section.

For the reasons mentioned in part 5.3, the idealized responses of the frames are shown in Force-Drift curves instead of Force-Displacement curves since in a Force-Displacement curve, the stiffness is a factor of force over displacement. The heights of the frames with different number of stories (that are compared in one figure) are not the same. Therefore, comparing the slopes of curves of different systems can not be a correct way of comparing the stiffness. Instead, the slopes of the response curves of Force-Drift curves are true demonstrators of lateral stiffness because drift is calculated by dividing the displacements over height. In this way, the height differences are properly taken into account.

5.6.1 Idealized Response Curves of X-braced Frames

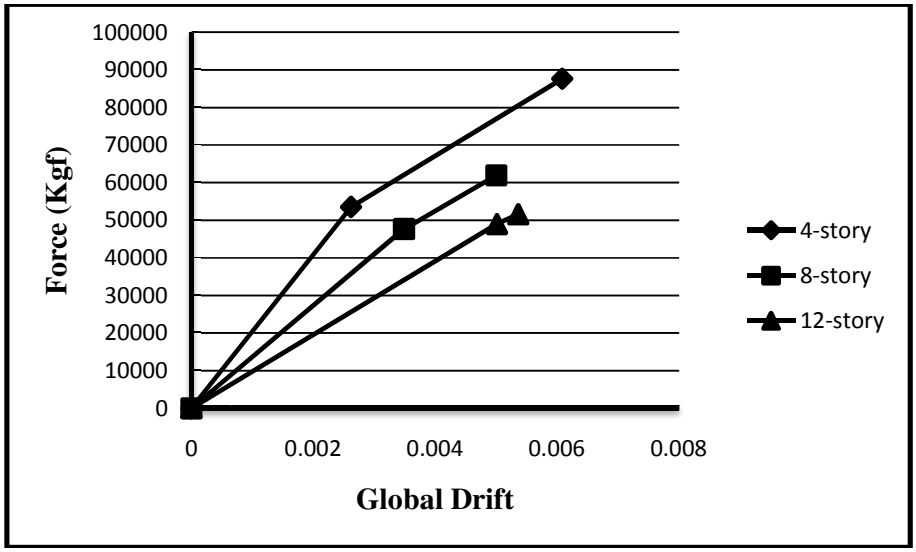

Figure 5.51: Idealized response curves of X-braced frames.

In X-braced frames, elastic lateral stiffness decreases as the number of stories increase. This is similar to the initial stiffness reduction as the number of stories increase. For other variables, it should be mentioned that maximum elastic drift ratio increases while post-yield drift limit decreases as the number of stories increase. Stiffness hardening is subject to a little increase with the number of stories. Maximum total global drift (elastic plus post-yield global drift) may not follow any special rule, but it decreases from 4- to 8-stories and again increases from 8- to 12-stories (but does not reach to the maximum global drift of 4-story frame). Overall, the behaviors are similar and generally predictable for different story heights.

5.6.2 Idealized Response Curves of V-braced Frames

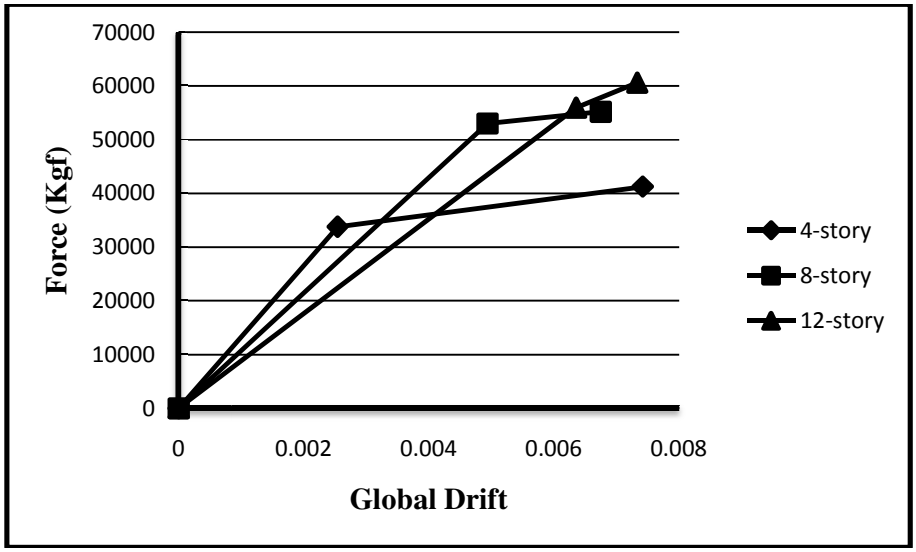

Figure 5.52: Idealized response curves of V-braced frames.

This case is very similar to the X-braced frames; elastic lateral stiffness decreases as the number of stories increase (similar to the initial stiffness decrease when number of stories increase). Elastic drift ratio increases while post-yield drift limit decreases as the number of stories increases. Stiffness hardening is subject to little increase (but more than X-braced frames) with the increase in the number of stories. The behaviors are similar and generally predictable for different story heights. Maximum total global drift is for the 4-, 12- and 8-story frames respectively. This is also similar to X-braced frames.

5.6.3 Idealized Response Curves of Inverted V-braced Frames

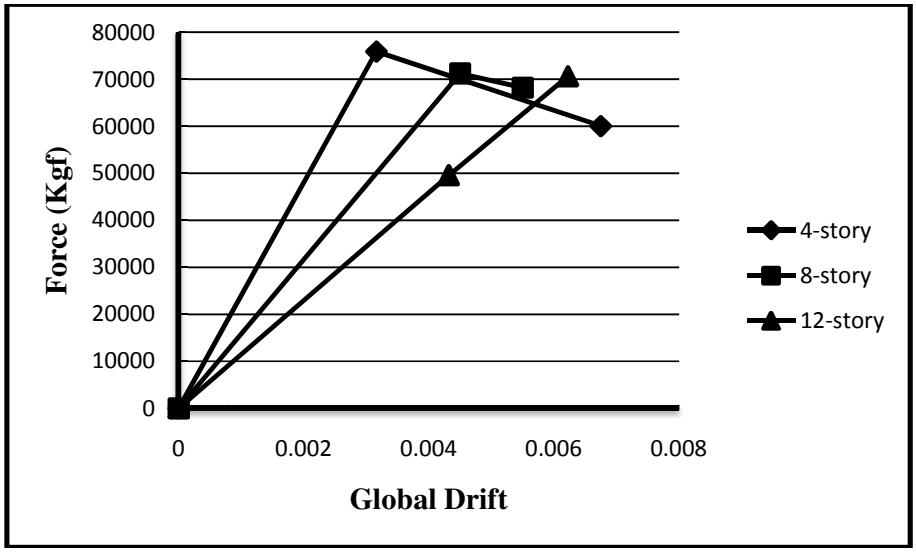

Figure 5.53: Idealized response curves of Inverted V-braced frames.

Behavior is similar to the X- and V-braced frames because elastic lateral stiffness decreases as the number of stories increase (similar to the initial stiffness decrease with number of stories increase). Elastic drift ratio increases while post-yield drift limit decreases as the number of stories increases. The change in the post-yield stiffness follows the previous rule but is subject to greater increases with the number of stories when compared to X- and V-braced frames. The behaviors are again similar and generally predictable for different story heights. Even the maximum total global drift follows the previous rule (decreases from 4- to 8- and increases from 8- to 12-story frames).

5.6.4 Idealized Response Curves of Diagonal braced Frames

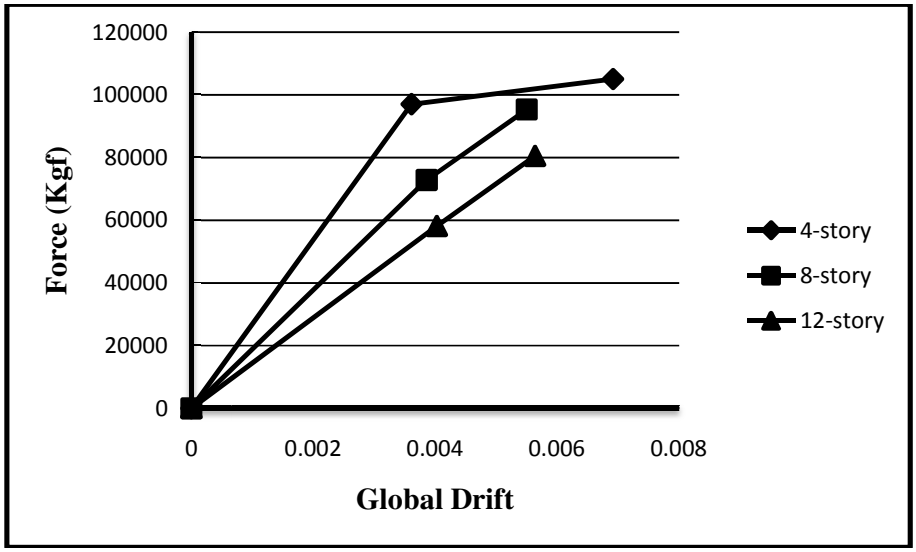

Figure 5.54: Idealized response curves of Diagonal braced frames.

Similar to the case of initial stiffness change due to frame height, elastic lateral stiffness also decreases as the number of stories increase. Elastic drift ratio increases while post-yield drift limit decreases as the number of stories increases. The post-yield stiffness increases with the number of stories. Maximum total global drift decreases from 4- to 8- and increases from 8- to 12-story frames (the highest value of maximum total global drift is for 4-, 8- and 12-story frames). The behaviors are generally similar and predictable for different story heights by the mentioned rules. The explicit demonstration of all of these changes by the selected frames shows the sensitivity of the studied frames (that are selected from past relevant studies of well-known researches) to nonlinear response parameters.

5.7 Idealizing Disadvantageous Effects

As it was discussed in the previous parts, idealization is the only way to get access to numerical nonlinear parameters of structures. The effect of idealization process on the response parameters of the frame is not always advantageous. Besides, it might

reduce the precision of the results due to simplification. It should be tried to minimize these effects as much as possible but it is not possible to fully omit them. As it is given in part 5.4, the idealized curves mach the real response curves in shorter frames better than the 12-story frames. One reason for this is the site characters of the structure including seismicity and soil type. The frames studied in this research are not placed in a special location with special seismicity and soil behaviors. Instead, average values are chosen in chapter IV as per the FEMA 356 (2000) and Kim and Choi (2005) in order to estimate the most appropriate results which are not highly dependent on the site characters. According to Jain and Navin (1995) and Kim and Choi (2005), seismicity of the site, where the structure is located, may lead to a change of 450%-500% on the nonlinear parameters of the frame. Therefore, Kim and Choi (2005) have suggested future researches on nonlinear response of structures to be studied on average-seismic sites. By using the mentioned suggestion regarding the effect of different site characteristics on idealization, it is expected that this study has minimized the side effects of idealization.

5.8 Discussion on Weight Results

Four different methodologies were introduced in chapter III for weight comparison of bracing systems among which the second methodology is the one that has been used by the past researchers for the same purpose and the fourth methodology that is proposed by this study and has been chosen as the most appropriate one among others. The second methodology is found to be undermining the weight differences significantly. This might not be appropriate for the general use of design engineers. In this part, comparison of bracing systems is done with both the second and fourth

methodology in order to clarify the existing problem. The first and third methodologies are not compared because the former is out of use (the recent and past studies did not use it) and the latter is proposes by this study and evolved in the fourth methodology later on. Full details of these four methodologies are available in the third chapter. In this part, weight results are only categorized by the height of the frames but not by the bracing system type because for one building with a specific height, the design engineers are usually capable of deciding on the bracing system type while they can not decide on the number of stories of the frame since this is provided by the architect. Thus, categorizing the frames by their bracing system type will be useless and is not done in this study.

Normalized curves according to X-braced frame are accompanied with each comparison for better clarification of differences in ratios. It can be seen in Figures 5.55 to 5.66 that weight differences of bracing systems are little affected by number of stories. Because of this, the numeral differences are brought totally in a table with their mean values and maximum and minimum and standard deviations.

5.8.1 Weight Results comparison of 4-story Frames

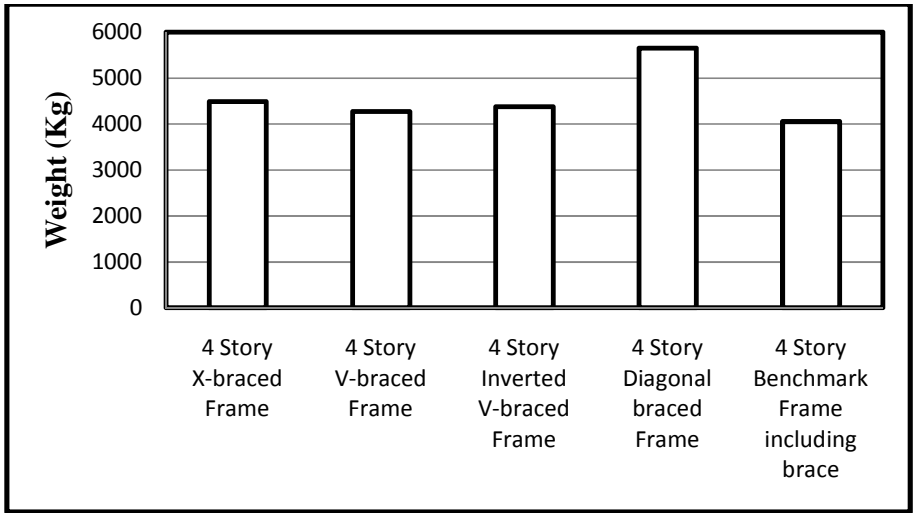

Figure 5.55: Gross Weight of 4 story Frames (2nd Weight Comparison Method).

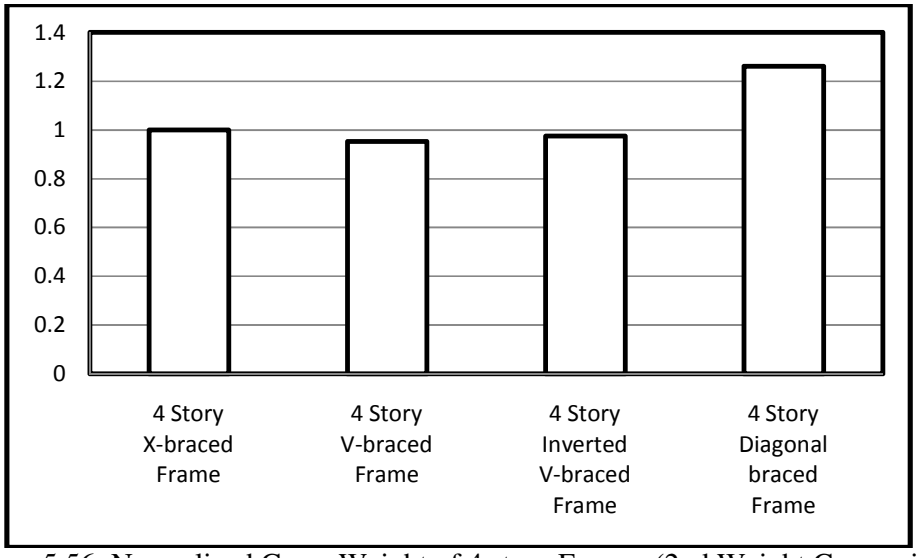

Figure 5.56: Normalized Gross Weight of 4 story Frames (2nd Weight Comparison Method).

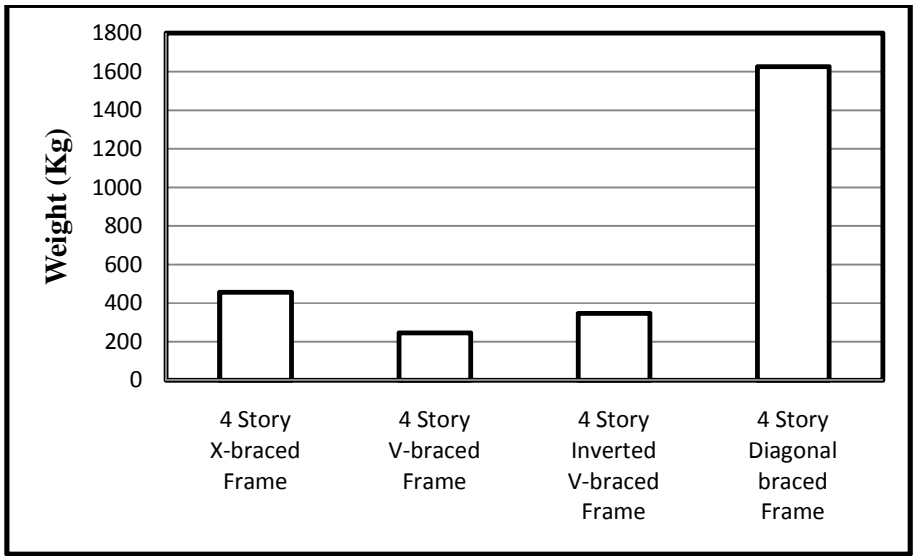

Figure 5.57: Net Bracing Weight of 4-story Frames (4th Weight Comparison Method).

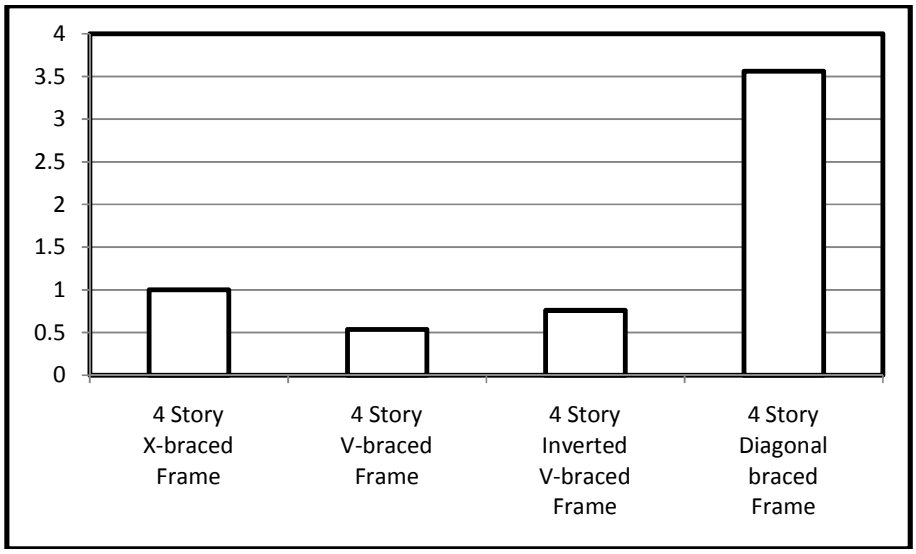

Figure 5.58: Normalized Net Bracing Weight of 4-story Frames (4th Weight Comparison Method).

5.8.2 Weight Results comparison of 8-story Frames

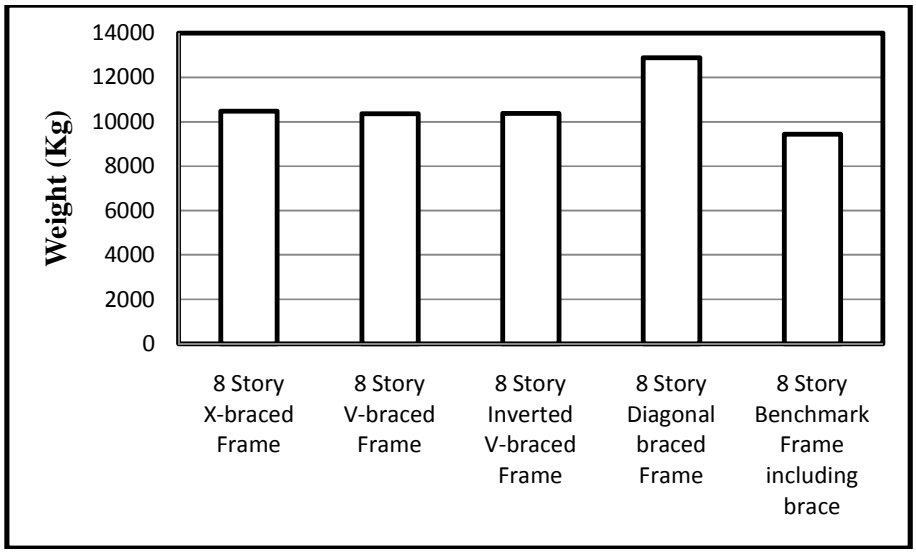

Figure 5.59: Gross Weight of 8 story Frames (2nd Weight Comparison Method).

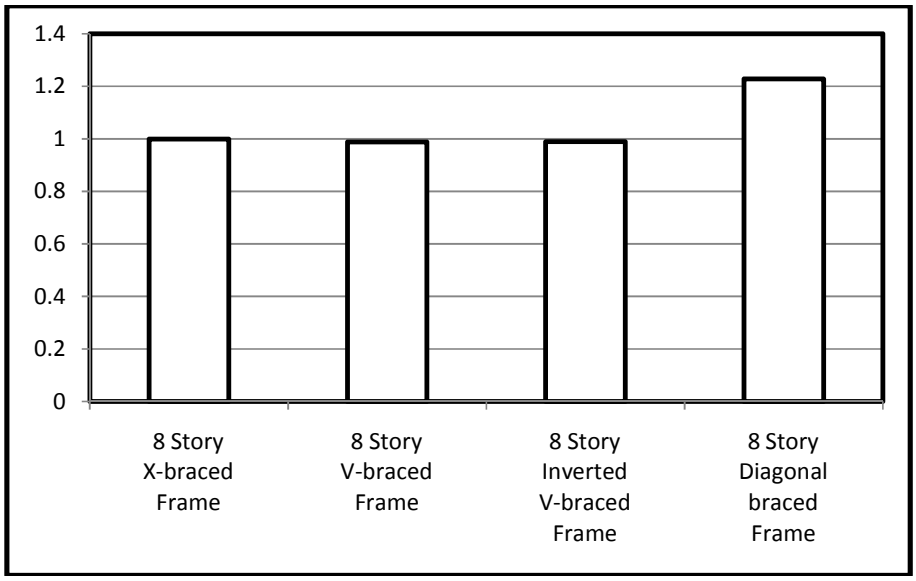

Figure 5.60: Normalized Gross Weight of 8 story Frames (2nd Weight Comparison Method).

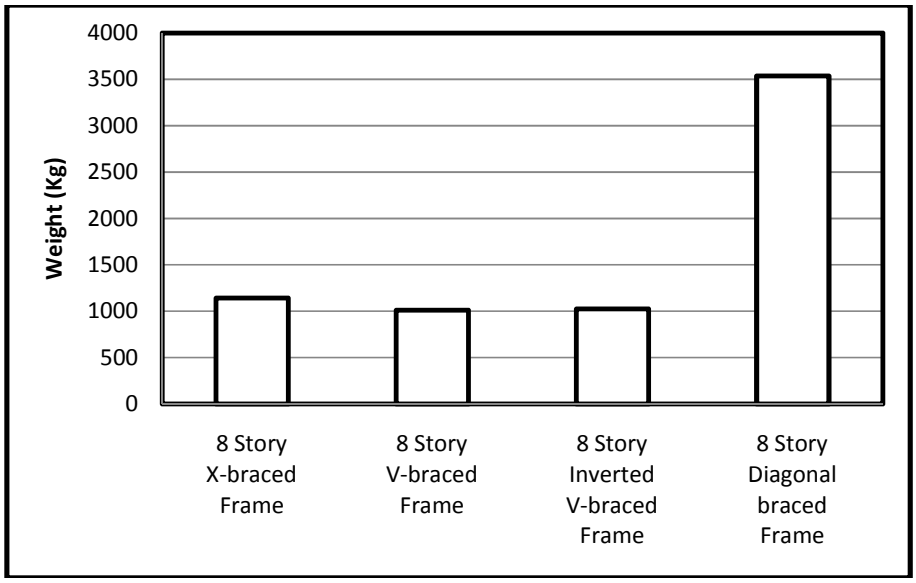

Figure 5.61: Net Bracing Weight of 8-story Frames (4th Weight Comparison Method)

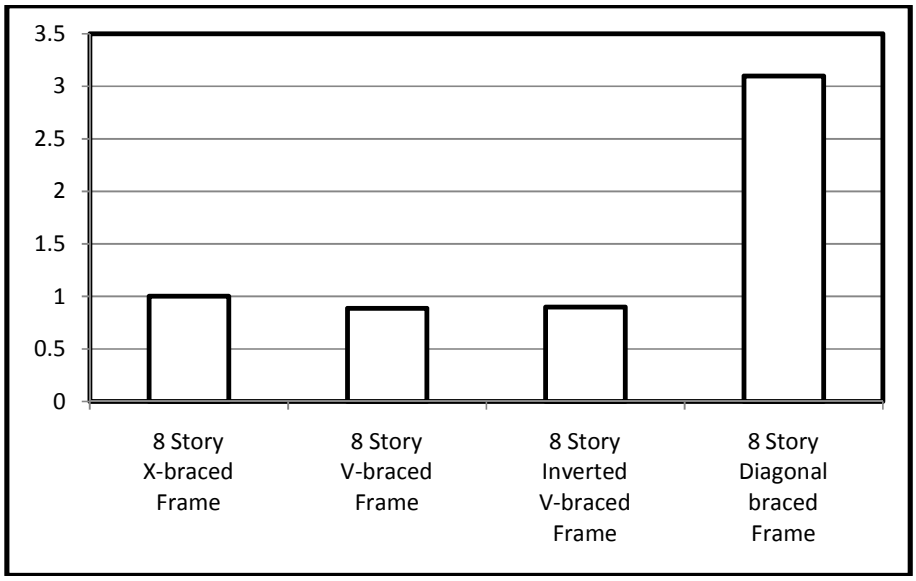

Figure 5.62: Normalized Net Bracing Weight of 8-story Frames (4th Weight Comparison Method)

5.8.3 Weight Results comparison of 12-story Frames

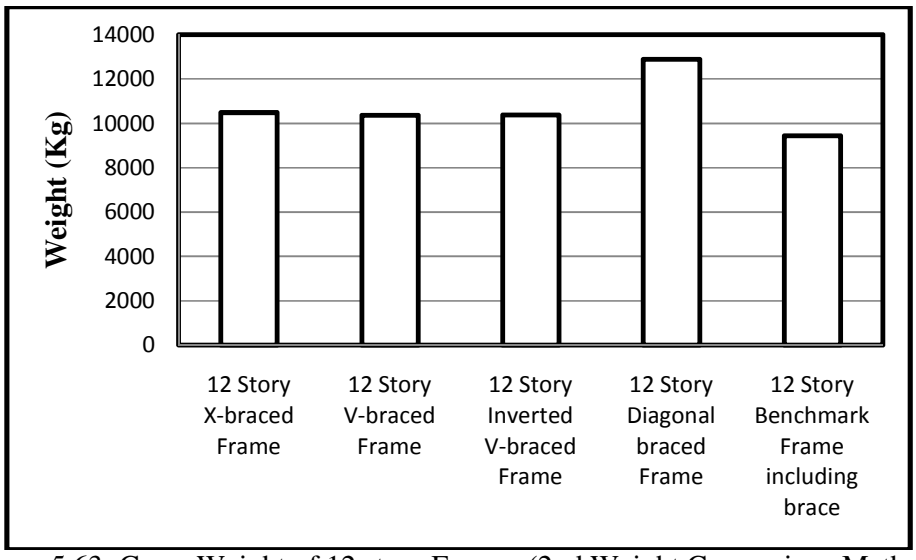

Figure 5.63: Gross Weight of 12 story Frames (2nd Weight Comparison Method).

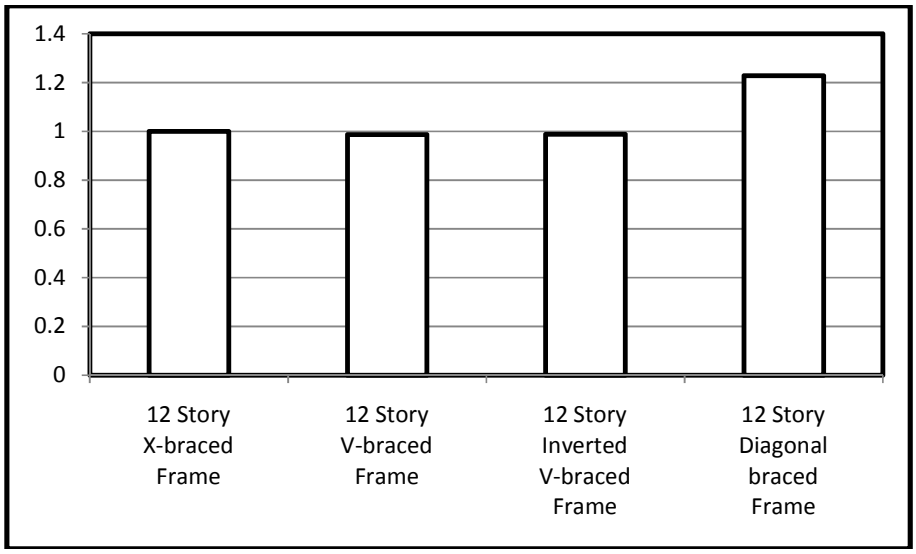

Figure 5.64: Normalized Gross Weight of 12 story Frames (2nd Weight Comparison Method).

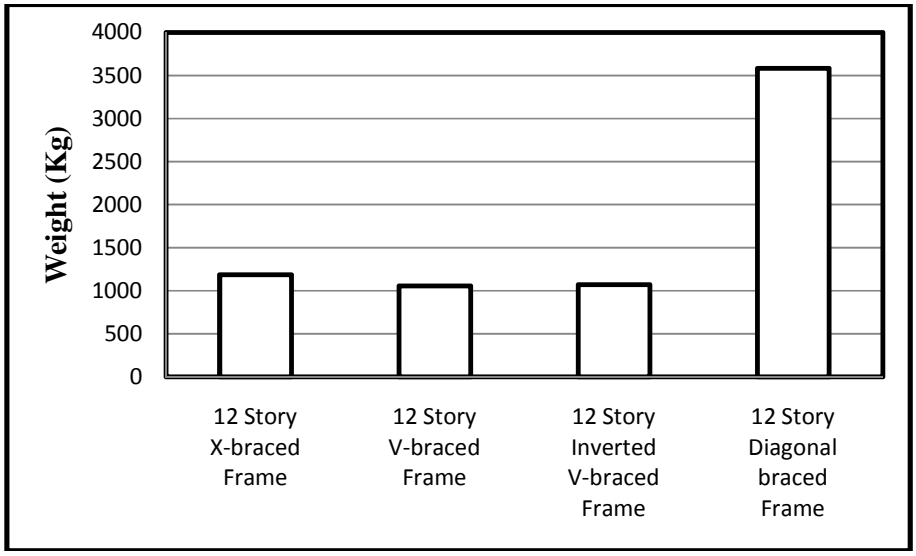

Figure 5.65: Net Bracing Weight of 12-story Frames (4th Weight Comparison Method).

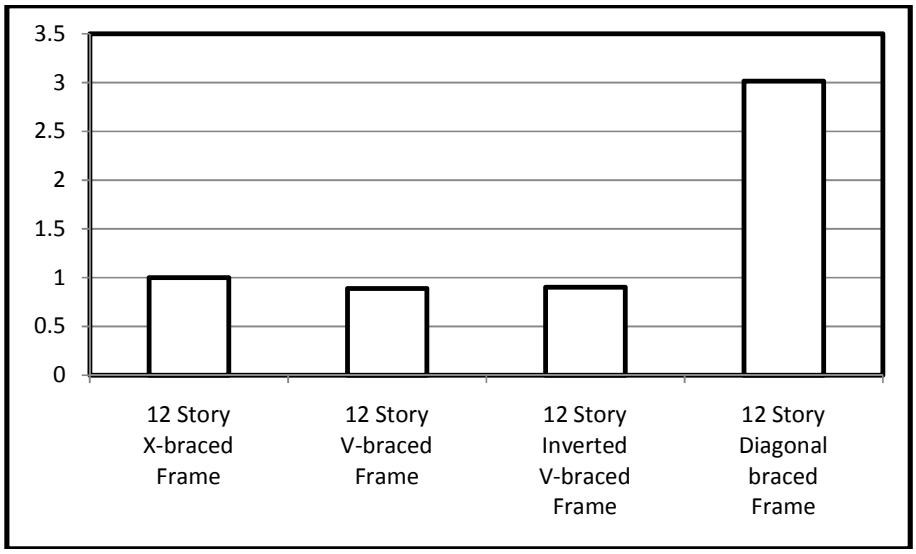

Figure 5.66: Normalized Net Bracing Weight of 12-story Frames (4th Weight Comparison Method).

Table 5.16: Comparison of Normalized Weight Results with second methodology.

No. of Stories	X	V	Inverted V	Diagonal
4	1	0.952	0.975	1.261
8	1	0.988	0.989	1.228
12	1	0.987	0.989	1.228
μ	1	0.976	0.984	1.239
σ (%)	0	2.838	1.101	2.669
Variation	0	0.035	0.013	0.033

From the variation and standard deviation of normalized weight results, it can be noticed that, contrary to the inelastic response of the bracing systems, the economical aspect of them are influenced very little by frame height. The maximum relative standard deviation of bracing system weight made by frame height is less than three percent. Because of this, instead of comparing the weights of bracing systems by their story height and having three different comparison categories of 4-, 8- and 12-story frames, leading to almost the same results, only the mean value of the relative weight results are compared herein. The second weight comparison methodology compares the total weight of the frames with different bracing systems. According to this methodology, relative to X-braced frame as normalized weight of

one, V-braced frame is the lightest frame, being 2.4% lighter. The second lightest frame is Inverted V-braced frame being 1.6% lighter than X-braced frame. Diagonal braced frame is dramatically heavier than other frames, 23.9% heavier than the X-braced frame.

Table 5.17: Comparison of Normalized Weight Results with fourth methodology.

No. of Stories	X	V	Inverted V	Diagonal
4	1	0.537	0.758	3.562
8	1	0.886	0.897	3.099
12	1	0.890	0.901	3.016
μ	1	0.771	0.852	3.226
σ (%)	0	28.676	11.548	41.609
Variation	0	0.353	0.143	0.546

Contrary to the results of second methodology, the comparison of the results by using the fourth methodology indicates greater differences. This was predicted correctly in chapter III. The differences in the weights of the bracing system due to frame height are more significant for this time. The largest standard deviation due to differences in frame height is 41% which is about 14 times more than the second methodology. V- (the lightest) and Inverted V-bracing systems are 23% and 15% lighter than X-bracing system. Diagonal bracing system is 3.2 times heavier than X-bracing system. The greatest differences are for the 4-story frames where Diagonal bracing system (the heaviest) is 3.5 times heavier and V-bracing system which is about half of the weight of X-bracing system. The dramatic differences clearly show the necessity of proposal of the fourth methodology for better economical comparison of bracing systems.

CHAPTER VI

SUMMARY AND CONCLUSION

6.1 Summary

Lateral instability leads to loss of lives of thousands of people during major earthquakes. Over the years different lateral load resisting systems have been invented for steel structures among those are concentrically braced frames (CBFs).

Although the usage and behavior of bracing systems have been studied in the past decades, the current changes in the analysis procedures and design codes especially after major earthquakes explicitly show that further study is required in this field. The necessity was clearly demonstrated by the release of FEMA P695 on seismic performance of structures after IBC 2006 code of practice.

Although inelastic response of buildings is influenced by their structural system and height, these effects are not taken into account for concentrically braced frames in current design codes. In other words, response parameter factors of all CBFs (including X-, V-, Inverted V- and Diagonal braced frames) are assumed to be equal regardless of the building height.

On the other hand, the economical comparison of steel bracing systems being conducted in the past studies has been based on their elastic response only, regardless of their sequential plastic range. Only very few researchers studied the nonlinear behavior and weight comparison of bracing systems simultaneously and

there is very limited research in this field (only one eccentric bracing system type). Such studies are still missing for concentrically braced frames.

The simplifications made by the design codes regarding inelastic behavior of CBFs and the past researches conducted on the economical comparison of steel bracing systems were investigated in the current study in order to reach to a more comprehensive and also more realistic results regarding concentric bracing systems. In other words, this work was aimed to conduct two studies; Assessment of inelastic behaviors and comparison of weights of different CBFs (X-, V-, Inverted V- and Diagonal braced frames).

The assessment of nonlinear response of the frames was done by the most updated nonlinear static (pushover) analysis procedure (FEMA 440) which was comprehensively discussed in the literature review. Actual structural response curves were determined and compared by story level and bracing system. In the next step, the actual capacity curves were idealized using FEMA 440 improved coefficient method in order to find the structural nonlinear response parameters and to do a quantitative comparison between the inelastic responses of the structures. Then, the idealized pushover curves were also compared by their number of stories and bracing system type, similar to the actual response curves.

Finally, the weights of different bracing systems were compared. For this step, the methodology used by previous researchers was found out to be insufficient. In order to find a more suitable method, two available methodologies (evaluation of the bracing members weight and evaluation of total braced frame weight) were reviewed. Two other methodologies were then proposed by this study in order to cover the shortcomings of the previous methods (being used by other studies).

Finally, the fourth methodology was evaluated to give the most accurate results (comparing the weight of the frames with a benchmark X-braced frame which is not subjected to any lateral load). Thus, economical comparison of the bracing systems was carried out according to a methodology which was proposed by this study. At the end of the results of economical comparison of bracing system, a comparison was also done between the results of the methodology of other studies and the one proposed by this study.

6.2 Major Findings

After conducting the works summarized in section 6.1, the following results were obtained.

6.2.1 Failure Progresses

Generally, buckling of compressive bracing members is the main failure reason of concentrically braced frames leading to a dramatic reduction in the structural stiffness. This issue might be accompanied by less severe plastifications in columns or tensile bracing member. Usually, all of the compressive braces are buckling and reaching a collapse level plastic hinge at lower and medium level stories. The vulnerability of the compressive bracing members to buckle is low for the first two stories, increases in the higher stories and again decreases in about tenth story. To be more specific, each bracing system has its special failure progress which is summarized here.

In X-braced frames, one or two plastic hinges occur in the first or second story compressive column. The severity of plastification decreases in the higher story levels.

In V-braced frames, immediate occupancy plastic hinges exist in tensile bracing members of medium level stories causing very efficient energy dissipation. No plastic hinge has occurred in beams or columns or in the first story bracing members.

Inverted V-braced frames, have a similar failure pattern to the V-braced frames but without plastic hinges in tensile bracing members. The shear beams are observed to be too strong to yield and absorb energy since they are heavier to carry the entire gravity load.

In Diagonal braced frames, failure of the frame is due to a few plastic hinges in the compressive members of bracing system and efficient energy dissipation is thus less than the other ones. This problem is amplified with the increase in the number of stories.

6.2.2 Actual Structural Response Curve Conclusions

Diagonal, Inverted V-, X- and V-braced frames generally have the highest to the lowest initial stiffness respectively. Diagonal braced frame has the highest values of shear capacity per displacement and also collapse point. Inverted V-braced frame faces a dramatic decrease in its post-elastic region, which sometimes reaches a low level stiffness when compared to the X-braced frame. V-braced frame has the least values of shear capacity per displacement. These differences are generally amplified by the increase in the number of stories of the frame.

6.2.3 Idealization Conclusions

Generally, the idealized response curves of the frames are closer to the actual curves in the shorter frames. The difference between the actual and idealized response curve usually increases with the frame height.

The highest to the lowest values of lateral elastic stiffness are for the Diagonal, Inverted V, X- and V braced frames respectively. But in the post-yield region, there are various behavior types which are completely described in section 5.5. V-braced frame has the greatest displacement in its target displacement point. The frames sometimes show positive or negative post-yield stiffness.

6.2.4 The effect of number of stories

Typically, the response curves and failure progresses are more influenced by the bracing type, rather than the number of stories. As the number of stories increases, there is a predictable decrease in the initial, elastic and post-elastic stiffness of the frames.

The maximum elastic drift ratio increases while post-yield drift limit decreases as the number of stories increases. Stiffness hardening is subject to a little increase with the increase in the number of stories. Maximum total global drift (elastic plus post-yield global drift) decreases from 4- to 8- and again increases from 8- to 12-stories (but does not reach to the maximum global drift of 4-story frame). Overall, the behaviors are similar and generally predictable for different story heights. The differences between the values of 12- and 8-story frames are more than those of 4- and 8-story frames.

6.2.5 Economical Comparison

V-, Inverted V-, X- and Diagonal braced frames were found to be the lightest to heaviest systems respectively. The two methodologies being used by the previous studies (using the total frame weight instead of the bracing system weight which is explained explicitly in section 3.1.1.2) and being proposed and used by this study (subtracting the weight of a benchmark frame from the frame weights to calculate the pure bracing system weight which is explained thoroughly in section 3.1.1.4) were compared. The previous methodology was found to be dramatically undermining the differences in the weights of bracing systems. This might lead to mistakes in the selection of the bracing system.

6.2.6 Overall Conclusions

Diagonal braced frames give the highest yield values (in linear response range). By nonlinear analysis, it was observed that Diagonal braced frame still possesses the highest value of lateral force per displacement for the whole response range. However, these findings alone can not be a great advantage for this system when compared to others, because it is more than four times heavier than V-braced frame while the response curves do not show great (more than twice) differences between the capacity of these two systems.

The efficiency of the weight comparison methodology can be clearly observed at this stage. If the use of the total frame weight instead of the bracing system had been used in this study (as in section 3.1.1.2), the weight differences would have been reduced into only less than 30% instead of 400%. As a result, Diagonal bracing system might have been chosen as the most appropriate one while it is not.

6.3 Final Conclusion

The final discussion is made by comparing the energy dissipation of each frame (section 5.5) over the pure weight of the bracing system estimated by the methodology of section 3.1.1.4 proposed by this study (section 5.8) in order to find out the efficiency of the bracing systems. This study proposes Global Energy Dissipation Density for evaluation of efficiency of bracing systems to account for the results of sections 5.5 and 5.8 simultaneously. After dividing the energy dissipation of each frame over its pure weight, the results are normalized by dividing them over the amounts of X-braced frames in each story height for better comparison. The results are given in Table 6.1.

Table 6.1: Normalized energy dissipation over weight of bracing systems.

	X	V	Inverted V	Diagonal
4-story	1	1.33	1.53	0.45
8-story	1	1.56	1.54	0.54
12-story	1	1.88	1.75	0.54

It can be observed that in 4-story frames, the most efficient types of concentric bracing systems in order are Inverted V-, V-, X- and Diagonal bracing systems. In 8-story frames, the order has changed to V-, Inverted V-, X- and Diagonal bracing systems while it can be stated that the values are quite similar for V- and Inverted V-braced frames. In 12-story frames, the order is again V-, Inverted V-, X- and Diagonal bracing systems, but this time, contrary to the 8-story frames, there is a great difference between V- and Inverted V-bracing system.

Overall, it can be mentioned that

- Diagonal bracing system is the least efficient concentric bracing system for all frame heights.

- Inverted V-bracing system is the most efficient type for 4-story frames.
- Efficiency of V-bracing system increases dramatically with the number of stories comparing to other systems and results in the two following conclusions.
- V- and Inverted V-bracing systems are almost equally the most efficient systems for 8-story frames.
- V-bracing system is the most efficient system for 12-story frames.
- X-bracing can be a third alternative after V- and Inverted V-bracing systems for all story heights, but its efficiency decreases as the number of stories increases.

6.4 Recommendations for Future Studies

The efficiency of concentrically braced frames has been studied by assessing their inelastic response and weight simultaneously. The same study is recommended to be conducted on eccentric bracing systems and on the other lateral load resisting systems which are described in chapter II.

This study has been carried out on the average values of site-dependent values such as seismicity and soil characteristics. Similar studies on other site characteristics are recommended in the case of necessity of such results in a special region.

The final words are willed to be quoted from an unknown source:

"Earthquakes do not kill people,
poorly designed structures do."

REFERENCES

ACI Committee 318, Building code requirements for structural concrete (ACI 318-05) and commentary (ACI 318R-05), American Concrete Institute, Detroit, Michigan, 1989.

Akkar S.D. and Miranda, E. (2005). "Statistical evaluation of approximate methods for estimating maximum deformation demands on existing structures," *Journal of Structural Engineering*, American Society of Civil Engineers, Vol. 131, No. 1.

Albanesi, T., Nuti, C. and Vanzi, I. (2000). "A simplified procedure to assess the seismic response of nonlinear structures," *Earthquake Spectra*, Vol. 16, No. 4, Earthquake Engineering Research Institute, Oakland, California, pp. 715-734.

American Institute of Steel Construction (AISC), Manual of Steel Construction, Load and Resistance Factor Design, LRFD, 2nd Edition. 1994.

American Welding Society (AWS), Structural Welding Code – Steel. 2005.

ANSI/AISC 360-05, Seismic Provisions for Structural Steel Buildings, LRFD, 1997.

ANSI/AISC 360-05, Specification for Structural Steel Buildings and Commentary, 2005.

ANSI/AISC 360-05, Specification for Structural Steel Buildings, LRFD, 1999.

Applied Technology Council (ATC), Seismic Evaluation and Retrofit of Concrete Buildings, Rep ATC-40, California, 1996.

Aristizabal-Ochoa, J.D. (1986). "Disposable knee bracing: improvement in seismic design of steel frames," *Journal of Structural Engineering*, **112**(7):1544-1552.

Aschheim, M.A., Maffei, J., and Black, E.F. (1998). "Nonlinear static procedures and earthquake displacement demands," *6th U.S. National Conference on Earthquake Engineering, Seattle, Washington*, Earthquake Engineering Research Institute, Oakland, California.

Assaf A.F., Evaluation of structural overstrength in steel building systems. MSc thesis, Northeastern University, Boston, MA, 1989.

Aydinoğlu, N.M. (2003). "An incremental response spectrum analysis procedure based on inelastic spectral displacements for multi-mode seismic performance evaluation," *Bulletin of Earthquake Engineering*, Vol. 1, Kluwer Academic Publishers, pp.3-36.

Balendra, T., Yu, C.Y., Xiao, Y. (2001). "An economical structural system for wind and earthquake loads," *Engineering Structures*, **23**:491-501.

Bracci, J.M., Kunnath, S.K., and Reinhorn, A.M. (1997). "Seismic performance and retrofit evaluation of reinforced concrete structures," *Journal of Structural Engineering-ASCE* 123 (1): 3-10.

Brognoli, M., Gelfi, P., Zandonini, R., and Zanella, M. (1998). "Optimal Design of Semi-rigid Braced Frames Via Knowledge-based Approach," *Journal of Constructional Steel*; 46:365-366.

Bruneau M., Uang, C., and Whittaker, A., Ductile Design of Steel Structures, McGraw-Hill, 1998.

Chintanapakdee, C., and Chopra, A.K. (2003). "Evaluation of modal pushover analysis using generic frames," *Earthquake Engineering and Structural Dynamics*, Vol. 32, Wiley Publishers, Hoboken, New Jersey, pp. 417–442.

Chopra A.K., Goel, R.K., and Chintanapakdee, C. (2004). "Evaluation of a modified MPA procedure assuming higher modes as elastic to estimate seismic demands," *Earthquake Spectra*, Vol. 20, No. 3, Earthquake Engineering Research Institute, Oakland, California, pp. 757-778.

Chopra, A.K. and Goel, R.K., 2000, "Evaluation of NSP to estimate seismic deformation: SDF systems," *Journal of Structural Engineering*, Vol. 126, No. 4, American Society of Civil Engineers, pp. 482-490.

Chopra, A.K., and Goel, R.K. (1999a). *Capacity- Demand Diagram Methods for Estimating Seismic Deformation of Inelastic Structure: SDF Systems*, Report No. PEER-1999/02, Pacific Earthquake Engineering Center, University of California, Berkeley, California.

Chopra, A.K., and Goel, R.K. (1999b). "Capacity-demand diagram methods based on inelastic design spectrum," *Earthquake Spectra*, Vol. 15, No. 4, Earthquake Engineering Research Institute, Oakland, California, pp. 637-656.

Chopra, A.K., and Goel, R.K. (2001a). *A Modal Pushover Analysis Procedure to Estimate Seismic Demands for Buildings: Theory and Preliminary Evaluation*, Report No. PEER 2001/03, Pacific Earthquake Engineering Research Center, University of California, Berkeley.

Chopra, A.K., and Goel, R.K. (2001b). *A Modal Pushover Analysis Procedure to Estimate Seismic Demands for Buildings: Theory and Preliminary Evaluation*, PEER-2001/03, Berkeley: Pacific Earthquake Engineering Research Center, University of California, 87 pages.

Chopra, A.K., and Goel, R.K. (2002). "A modal pushover analysis procedure for estimating seismic demands for buildings," *Earthquake Engineering and Structural Dynamics*, Vol. 31, pp. 561-582.

Chopra, A.K., Goel, R.K., and Chintanapakdee, C. (2003). "Statistics of single-degree-of-freedom estimate of displacement for pushover analysis of buildings," *Journal of Structural Engineering*, Vol. 129, No. 4, pp. 459-469.

CSI. SAP2000 V-11. Integrated finite element analysis and design of structures basic analysis reference manual. Berkeley (CA, USA): Computers and Structures Inc; 2007.

Di Sarno, L., Elnashai, A.S., and Nethercot, D.A. (2005). "Seismic Response and Design of Stainless Steel Frames."

Di Sarno, L., Elnashai, A.S., and Nethercot, D.A. (2006). "Seismic retrofitting of steel structures with stainless steel," *Journal of Constructional Steel Research*; 62(1):93–104.

DiSarno, L., Elnashai, A.S., and Nethercot, D.A. (2008). "Seismic response of stainless steel braced frames," *Journal of Constructional Steel Research*; 64 (7-8): 914-925.

Fajfar, P., Gaspersic, P. (1996). "The N2 method for the seismic damage analysis of RC buildings," *Earthquake Engineering & Structural*; 25 (1): 31-46.

Fardis, M.N., and Panagiotakos, T.B. (1996) "Hysteretic damping and reinforced concrete elements," *Proceedings of 11*th *World Conference on Earthquake Engineering*, Paper 464, Acapulco, Mexico.

Federal Emergency Management Agency (FEMA), Improvement of Nonlinear Static Seismic Analysis Procedures, Rep FEMA 440, Washington DC, 2005.

Federal Emergency Management Agency (FEMA), NEHRP provisions and commentary for the seismic rehabilitation of buildings, Rep FEMA 273 and 274, Washington DC, 1997.

Federal Emergency Management Agency (FEMA), Prestandard and Commentary for the Seismic Rehabilitation of Buildings, Rep FEMA 356, Washington DC, 2000.

Federal Emergency Management Agency (FEMA), Quantification of Building Seismic Performance Factors, Rep FEMA P695, Washington DC, 2009.

Federal Emergency Management Agency (FEMA). BSSC. NEHRP recommended provisions for seismic regulations for new buildings and other structures; part 1: provisions. FEMA-368, Building Seismic Safety Council, Washington, D.C.; 2001.

Federal Emergency Management Agency (FEMA). Next-Generation Performance-Based Seismic Design Guidelines Program Plan for New and Existing Buildings, Rep FEMA-445, Washington DC, 2006

Federal Emergency Management Agency. NEHRP recommended provisions for seismic regulations for new buildings and other structures; part 1: provisions. FEMA-302, Building Seismic Safety Council, Washington, D.C.; 1997.

FEMA 355, 2000, *State of the Art Report on Systems Performance of Steel Moment Frames Subject to Earthquake Ground Shaking*, prepared by the SAC Joint Venture (a partnership of the Structural Engineers Association of California, the Applied Technology Council, and California Universities for Research in Earthquake Engineering) for the Federal Emergency Management Agency, Washington, D.C.

Freeman, S.A., Nicoletti, J.P. and Tyrell, J.V. (1975). “Evaluations of existing

buildings for seismic risk - a case study of Puget Sound Naval Shipyard, Bremerton, Washington," *Proceedings of U.S. National Conference on Earthquake Engineering*, Berkeley, California, pp. 113-122.

Goel, R.K., and Chopra, A.K. (2004). "Evaluation of modal and FEMA pushover analysis: SAC buildings," *Earthquake Spectra*, Vol. 20, No. 1, Earthquake Engineering Research Institute, Oakland, California, pp. 225-254.

Gupta, A., Krawinkler, H. (2000). "Estimation of seismic drift demands for frame structures," *Earthquake Engineering and Structural Dynamics,*29 (9): 1287-1305.

Hadjian, A.H. (1982). "A re-evaluation of equivalent linear models for simple yielding systems," *Earthquake Engineering and Structural Dyn*amics, Vol. 10, pp. 759-767.

Hernández-Montes, E., Kwon, O.S., and Aschheim, M. (2004) "An energy-based formulation for first- and multiple-mode nonlinear static (pushover) analyses," *Journal of Earthquake Engineering,* Vol. 8, No. 1, pp. 69-88.

Huang, Z., Li, Q., Chen, L. (2005). "Elastoplastic analysis of knee bracing frame." *Journal of Zhejiang University Science*. 6A(8):784-789

Inel, M., Ozmen, H.B., (2006). "Effects of plastic hinge properties in nonlinear analysis of reinforced concrete buildings," *Engineering Structures* 28 (11): 1494-1502.

International Code Council, International Building Code, 2006, 2003, 2000 and commentary, 2003.

Iwan, W.D., and Gates, N.C. (1979). "Estimating earthquake response of simple hysteretic structures," *Journal of the Engineering Mechanics Division*, Vol. 105, EM3, American Society of Civil Engineers, pp. 391-405.

Jacobsen, L.S. (1960). "Damping in composite structures," *Proceedings 2nd World Conference on Earthquake Engineering, Tokyo and Kyoto, Japan*, Vol. 2, pp. 1029-1044.

Jacobsen, L.S., (1930). "Steady forced vibrations as influenced by damping," *Transactions ASME*, Vol. 52 (APM), pp. 169-181.

Jain, S.K., Navin, R. (1995). "Seismic Overstrength in Reinforced Concrete Frames," *Journal of Structural Engineering-ASCE* 121 (3): 580-585.

Jan, T.S., Liu, M.W., and Kao, Y.C. (2004). "An upper bound pushover analysis procedure for estimating the seismic demands of high rise buildings," *Engineering Structures*, Vol. 26, pp. 117-128.

Jennings, P., (1968). "Equivalent damping for yielding structures," *Journal of Engineering Mechanics,* Vol. 94, American Society of Civil Engineers, pp. 103-116.

Kameshki, E.S., Saka, M.P. (2001). "Genetic algorithm based optimum bracing

design of non-swaying tall plane frames," *Journal of Constructional Steel Research* 57 (10): 1081-1097.

Kappos, A.J., (1999). "Evaluation of behavior factors on the basis of ductility and overstrength studies," *Engineering Structures* 21 (9): 823-835.

Kim, J.K., and Choi, H. (2005). "Response modification factors of chevron-braced frames," *Engineering Structures* 27 (2): 285-300.

Krawlinkler, H., and Seneviranta, G.D.P.K. (1998). "Pros and Cons of a Pushover Analysis of Seismic Performance Evaluation," *Engineering Structures* 20(4): 452-464

Kunnath, S.K., and Gupta, B. (2000). "Validity of deformation demand estimates using nonlinear static procedures," *Proceedings of the U.S.-Japan Workshop on Performance-Based Engineering of Reinforced Concrete Building Structures*, Sapporo, Hokkaido, Japan.

Lew, H.S. and Kunnath, S.K. (2000). "Evaluation of analysis procedures for performance-based seismic design of buildings," *Proceedings of 12th World Conference on Earthquake Engineering, Auckland*, Paper 1005, New Zealand Society for Earthquake Engineering, Upper Hutt, New Zealand.

MacRae, G., and Tagawa, H. (2002). *Methods to Estimate Displacements of PG&E Structures*, Report PGE/ PEER Task No. 505, University of Washington, Seattle, Washington.

Maheri, M.R., Akbari, R. (2003). "Seismic behaviour factor, R, for steel X-braced and knee-braced RC buildings," *Engineering Structures;* 25 (12): 1505-1513.

Maheri, M.R., Kousari, R., Razazan, M. (2003). "Pushover tests on steel X-braced and knee-braced RC frames," *Engineering Structures;* 25 (13): 1697-1705.

Maheri, M.R., Safari, D. (2005). "Topology Optimization of Bracing in Steel Structures by Genetic Algorithm," *Advances in Steel Structures*; 277-282.

Miranda, E., and Ruiz-García, J. (2002). "Evaluation of approximate methods to estimate maximum inelastic displacement demands," *Earthquake Engineering and Structural Dynamics,* Vol. 31, pp. 539-560.

Miranda, E., Bertero, V.V. (1994). "Evaluation of strength reduction factors for earthquake-resistant design," *Earthquake Spectra*;10(2):357–79.

Mitchell, D., Paultre, P. (1994). Ductility and Overstrength in Seismic Design of Reinforced Concrete Structures," *Canadian Journal of Civil Engineering;* 21 (6): 1049-1060.

Mofid, M., Khosravi, P. (2000). "Non-linear analysis of disposable knee bracing," *Computers & Structures*, **75**: 65-72.

Moghaddam, H., Hajirasouliha, I. (2006). "An investigation on the accuracy of pushover analysis for estimating the seismic deformation of braced steel frames,"

Journal of Constructional Steel Research; 64 (4): 343-351.

Moghaddam, H., Hajirasouliha, I., Doostan, A. (2005). "Optimum seismic design of concentrically braced steel frames: concepts and design procedures," *Journal of Constructional Steel Research;* 61 (2): 151-166.

Mwafy, A.M., Elnashai, A.S. (2001). "Static pushover versus dynamic collapse analysis of RC buildings," *Engineering Structures;* 23 (5): 407-424.

Mwafy, A.M., Elnashai, A.S. (2002). "Calibration of force reduction factors of RC buildings," *Journal of Earthquake Engineering*; 6(2):239–73.

Ozhendekci, D., Ozhendekci, N. (2008). "Effects of the frame geometry on the weight and inelastic behaviour of eccentrically braced chevron steel frames," *Journal of Constructional Steel Research,* 64 (12): 1540-1540.

Ozhendekci, D., Ozhendekci, N. (2008). Effects of the frame geometry on the weight and inelastic behaviour of eccentrically braced chevron steel frames. *Journal of Constructional Steel Research;* 64 (3): 326-343.

Powell G.H., (2007). A State of the Art Educational Event, Performance Based Design Using Nonlinear Analysis.

Reinhorn, A., 1997, "Inelastic techniques in seismic evaluations," in *Seismic Design Methodologies for the Next Generation of Codes*, Fajfar, P., and Krawinkler, H.,

(Eds.). Bled, Slovenia.

Richards, P.W., P.E., ASCE M. (2009). Seismic Column Demands in Ductile Braced Frames. *Journal of Structural Engineering*: 33-41

Ricles, J.M., Popov, E.P. (1994). Inelastic link element for EBF seismic analysis. *Journal of Structural Engineering*; 120(2):441–63.

Saiidi, M., Sozen, M.A., (1981). Simple Non-linear Seismic Analysis of R-C Structures. *Journal of the Structural Division-ASCE;* 107 (5): 937-952.

Sam, M.T., Balendra, T., Liaw, C.Y. (1995). Earthquake- resistant steel frames with energy dissipating knee elements. *Engineering Structure*, **17**(5):334-343.

Sasaki, K.K., Freeman, S.A., and Paret, T.F. (1998), "Multi-mode pushover procedure (MMP) – a method to identify the effects of higher modes in a pushover analysis," *Proceedings, Sixth U.S. National Conference on Earthquake Engineering, Seattle, Washington*, Earthquake Engineering Research Institute, Oakland, California.

Structural Engineers Association of California (SEAOC). Performance based seismic engineering of buildings. Vision 2000 Committee, Structural Engineers Association of California, Sacramento, CA, 1995.

Tasnimi A., Masoomi, A. (1999). Evaluation of response reinforced concrete frames strengthened with steel bracing. *Proceedings of the 3rd International Conference on*

Seismic and Earthquake Engineering, Iran. (In Farsi).

Tremblay, R. (2002). Inelastic seismic response of steel bracing members. *Journal of Constructional Steel Research;* 58 (5-8): 665-701.

Uang, C.M. (1991). Establishing R (or R_W) and C_d Factors for Building Seismic Provisions. *Journal of the Structural Division-ASCE;* 117 (1): 19-28.

Uniform Building Code. International Conference of Building Officials, Whittier, California, 1997.

Vamvatsikos, D., and Cornell, C.A. (2002). "Incremental dynamic analysis," *Earthquake Engineering and Structural Dynamics*, John Wiley & Sons, Ltd.

William, M.S., Blakeborough, A., Clement, D., and Bourahla, N. (2002). Seismic behavior of knee braced frames. *Proceedings of the Institution of Civil Engineers: Structures and Buildings*, **152**(2):147-155.

Yang, C.S., Leon, R.T., and DesRoches, R. (2008). Design and behavior of zipper-braced frames. *Engineering Structures;* 30 (4): 1092-1100.

Youssef, M.A., Ghaffarzadeh, H., Nehdi, M. (2007). Seismic performance of RC frames with concentric internal steel bracing. *Engineering Structures;* 29 (7): 1561-1568.

Yu, K., Heintz, J., and Poland, C. (2001). "Assessment of nonlinear static analysis

procedures for seismic evaluation of building structures," *Proceedings U.S.-Japan Joint Workshop and Third Grantees Meeting, U.S.-Japan Cooperative Research on Urban Earthquake Disaster Mitigation, 15-16 August 2001*, University of Washington, Seattle, Washington, pp. 431-450.

Zamfirescu, D. and Fajfar, P. (2001). "Comparison of simplified procedures for nonlinear seismic analysis of structures," *Proceedings, 3rd U.S. Japan Workshop on Performance-Based Earthquake Engineering Methodology for Reinforced Concrete Buildings,* Seattle, Washington.

Retrieved March 04, 2009 from the World Wide Web:
http://www.fema.gov/about/index.shtm

Retrieved March 04, 2009 from the World Wide Web:
http://www.nehrp.gov/about/index.htm

Retrieved March 04, 2009 from the World Wide Web:
http://www.atcouncil.org/purpose.shtml

APPENDIX

Table A.1: Table 5-4 of FEMA 356 (Courtesy of Federal Emergency Management Agency).

Table 5-4 Steel Moment Frame Connection Types

Connection	Description[1, 2]	Type
Welded Unreinforced Flange (WUF)	Full-penetration welds between beam and columns, flanges, bolted or welded web, designed prior to code changes following the Northridge earthquake	FR
Bottom Haunch in WUF w/Slab	Welded bottom haunch added to existing WUF connection with composite slab[3]	FR
Bottom Haunch in WUF w/o Slab	Welded bottom haunch added to existing WUF connection without composite slab[3]	FR
Welded Cover Plate in WUF	Welded cover plates added to existing WUF connection[3]	FR
Improved WUF-Bolted Web	Full-penetration welds between beam and column flanges, bolted web[4]	FR
Improved WUF-Welded Web	Full-penetration welds between beam and column flanges, welded web[4]	FR
Free Flange	Web is coped at ends of beam to separate flanges, welded web tab resists shear and bending moment due to eccentricity due to coped web[4]	FR
Welded Flange Plates	Flange plate with full-penetration weld at column and fillet welded to beam flange[4]	FR
Reduced Beam Section	Connection in which net area of beam flange is reduced to force plastic hinging away from column face[4]	FR
Welded Bottom Haunch	Haunched connection at bottom flange only[4]	FR
Welded Top and Bottom Haunches	Haunched connection at top and bottom flanges[4]	FR
Welded Cover-Plated Flanges	Beam flange and cover-plate are welded to column flange[4]	FR
Top and Bottom Clip Angles	Clip angle bolted or riveted to beam flange and column flange	PR
Double Split Tee	Split tees bolted or riveted to beam flange and column flange	PR
Composite Top and Clip Angle Bottom	Clip angle bolted or riveted to column flange and beam bottom flange with composite slab	PR
Bolted Flange Plates	Flange plate with full-penetration weld at column and bolted to beam flange[4]	PR[5]
Bolted End Plate	Stiffened or unstiffened end plate welded to beam and bolted to column flange	PR[5]
Shear Connection w/ Slab	Simple connection with shear tab, composite slab	PR
Shear Connection w/o Slab	Simple connection with shear tab, no composite slab	PR

1. Where not indicated otherwise, definition applies to connections with bolted or welded web.
2. Where not indicated otherwise, definition applies to connections with or without composite slab.
3. Full-penetration welds between haunch or cover plate to column flange conform to the requirements of the AISC (1997) *Seismic Provisions*.
4. Full-penetration welds conform to the requirements of the AISC (1997) *Seismic Provisions*.
5. For purposes of modeling, the connection may be considered FR if it meets the strength and stiffness requirements of Section 5.5.2.1.

Table A.2.a: Part one of Table 5-6 of FEMA 356 (Courtesy of Federal Emergency Management Agency).

Table 5-6 Modeling Parameters and Acceptance Criteria for Nonlinear Procedures—Structural Steel Components

	Modeling Parameters			Acceptance Criteria				
	Plastic Rotation Angle, Radians		Residual Strength Ratio	Plastic Rotation Angle, Radians				
					Primary		Secondary	
Component/Action	**a**	**b**	**c**	**IO**	**LS**	**CP**	**LS**	**CP**
Beams—flexure								
a. $\frac{b_f}{2t_f} \le \frac{52}{\sqrt{F_{ye}}}$ and $\frac{h}{t_w} \le \frac{418}{\sqrt{F_{ye}}}$	$9\theta_y$	$11\theta_y$	0.6	$1\theta_y$	$6\theta_y$	$8\theta_y$	$9\theta_y$	$11\theta_y$
b. $\frac{b_f}{2t_f} \ge \frac{65}{\sqrt{F_{ye}}}$ or $\frac{h}{t_w} \ge \frac{640}{\sqrt{F_{ye}}}$	$4\theta_y$	$6\theta_y$	0.2	$0.25\theta_y$	$2\theta_y$	$3\theta_y$	$3\theta_y$	$4\theta_y$
c. Other	Linear interpolation between the values on lines a and b for both flange slenderness (first term) and web slenderness (second term) shall be performed, and the lowest resulting value shall be used							
Columns—flexure [2, 7]								
For $P/P_{CL} < 0.20$								
a. $\frac{b_f}{2t_f} \le \frac{52}{\sqrt{F_{ye}}}$ and $\frac{h}{t_w} \le \frac{300}{\sqrt{F_{ye}}}$	$9\theta_y$	$11\theta_y$	0.6	$1\theta_y$	$6\theta_y$	$8\theta_y$	$9\theta_y$	$11\theta_y$
b. $d\ \frac{b_f}{2t_f} \ge \frac{65}{\sqrt{F_{ye}}}$ or $\frac{h}{t_w} \ge \frac{460}{\sqrt{F_{ye}}}$	$4\theta_y$	$6\theta_y$	0.2	$0.25\theta_y$	$2\theta_y$	$3\theta_y$	$3\theta_y$	$4\theta_y$
c. Other	Linear interpolation between the values on lines a and b for both flange slenderness (first term) and web slenderness (second term) shall be performed, and the lowest resulting value shall be used							

Table A.2.b: Part two of Table 5-6 of FEMA 356 (Courtesy of Federal Emergency Management Agency).

Table 5-6 Modeling Parameters and Acceptance Criteria for Nonlinear Procedures—Structural Steel Components (continued)

	Modeling Parameters			Acceptance Criteria				
	Plastic Rotation Angle, Radians		Residual Strength Ratio	Plastic Rotation Angle, Radians				
					Primary		Secondary	
Component/Action	**a**	**b**	**c**	**IO**	**LS**	**CP**	**LS**	**CP**
For $0.2 < P/P_{CL} < 0.50$								
a. $\frac{b_f}{2t_f} \le \frac{52}{\sqrt{F_{ye}}}$ and $\frac{h}{t_w} \le \frac{260}{\sqrt{F_{ye}}}$	—[3]	—[4]	0.2	$0.25\theta_y$	—[5]	—[3]	—[6]	—[4]
b. $\frac{b_f}{2t_f} \ge \frac{65}{\sqrt{F_{ye}}}$ or $\frac{h}{t_w} \ge \frac{400}{\sqrt{F_{ye}}}$	$1\theta_y$	$1.5\theta_y$	0.2	$0.25\theta_y$	$0.5\theta_y$	$0.8\theta_y$	$1.2\theta_y$	$1.2\theta_y$
c. Other	Linear interpolation between the values on lines a and b for both flange slenderness (first term) and web slenderness (second term) shall be performed, and the lowest resulting value shall be used							
Column Panel Zones	$12\theta_y$	$12\theta_y$	1.0	$1\theta_y$	$8\theta_y$	$11\theta_y$	$12\theta_y$	$12\theta_y$
Fully Restrained Moment Connections[13]								
WUF[12]	0.051-0.0013*d*	0.043-0.0006*d*	0.2	0.0128-0.0003*d*	0.0337-0.0009*d*	0.0284-0.0004*d*	0.0323-0.0005*d*	0.043-0.0006*d*
Bottom haunch in WUF with slab	0.026	0.036	0.2	0.0065	0.0172	0.0238	0.0270	0.036
Bottom haunch in WUF without slab	0.018	0.023	0.2	0.0045	0.0119	0.0152	0.0180	0.023
Welded cover plate in WUF[12]	0.056-0.0011*d*	0.056-0.0011*d*	0.2	0.0140-0.0003*d*	0.0319-0.0006*d*	0.0426-0.0008*d*	0.0420-0.0008*d*	0.056-0.0011*d*
Improved WUF-bolted web[12]	0.021-0.0003*d*	0.050-0.0006*d*	0.2	0.0053-0.0001*d*	0.0139-0.0002*d*	0.0210-0.0003*d*	0.0375-0.0005*d*	0.050-0.0006*d*
Improved WUF-welded web	0.041	0.054	0.2	0.0103	0.0312	0.0410	0.0410	0.054
Free flange[12]	0.067-0.0012*d*	0.094-0.0016*d*	0.2	0.0168-0.0003*d*	0.0509-0.0009*d*	0.0670-0.0012*d*	0.0705-0.0012*d*	0.094-0.0016*d*
Reduced beam section[12]	0.050 0.0003*d*	0.070 0.0003*d*	0.2	0.0125 0.0001*d*	0.0380 0.0002*d*	0.0500 0.0003*d*	0.0525 0.0002*d*	0.07 0.0003*d*
Welded flange plates								
a. Flange plate net section	0.03	0.06	0.2	0.0075	0.0228	0.0300	0.0450	0.06
b. Other limit states	force-controlled							
Welded bottom haunch	0.027	0.047	0.2	0.0068	0.0205	0.0270	0.0353	0.047
Welded top and bottom haunches	0.028	0.048	0.2	0.0070	0.0213	0.0280	0.0360	0.048
Welded cover-plated flanges	0.031	0.031	0.2	0.0078	0.0177	0.0236	0.0233	0.031

Table A.2.c: Part three of Table 5-6 of FEMA 356 (Courtesy of Federal Emergency Management Agency).

Table 5-6 Modeling Parameters and Acceptance Criteria for Nonlinear Procedures—Structural Steel Components (continued)

	Modeling Parameters			Acceptance Criteria				
	Plastic Rotation Angle, Radians		Residual Strength Ratio	Plastic Rotation Angle, Radians				
					Primary		Secondary	
Component/Action	**a**	**b**	**c**	**IO**	**LS**	**CP**	**LS**	**CP**
Partially Restrained Moment Connections								
Top and bottom clip angle[9]								
a. Shear failure of rivet or bolt (Limit State 1)[8]	0.036	0.048	0.200	0.008	0.020	0.030	0.030	0.040
b. Tension failure of horizontal leg of angle (Limit State 2)	0.012	0.018	0.800	0.003	0.008	0.010	0.010	0.015
c. Tension failure of rivet or bolt (Limit State 3)[8]	0.016	0.025	1.000	0.005	0.000	0.013	0.020	0.020
d. Flexural failure of angle (Limit State 4)	0.042	0.084	0.200	0.010	0.025	0.035	0.035	0.070
Double split tee[9]								
a. Shear failure of rivet or bolt (Limit State 1)[8]	0.036	0.048	0.200	0.008	0.020	0.030	0.030	0.040
b. Tension failure of rivet or bolt (Limit State 2)[8]	0.016	0.024	0.800	0.005	0.008	0.013	0.020	0.020
c. Tension failure of split tee stem (Limit State 3)	0.012	0.018	0.800	0.003	0.008	0.010	0.010	0.015
d. Flexural failure of split tee (Limit State 4)	0.042	0.084	0.200	0.010	0.025	0.035	0.035	0.070
Bolted flange plate[9]								
a. Failure in net section of flange plate or shear failure of bolts or rivets[8]	0.030	0.030	0.800	0.008	0.020	0.025	0.020	0.025
b. Weld failure or tension failure on gross section of plate	0.012	0.018	0.800	0.003	0.008	0.010	0.010	0.015
Bolted end plate								
a. Yield of end plate	0.042	0.042	0.800	0.010	0.028	0.035	0.035	0.035
b. Yield of bolts	0.018	0.024	0.800	0.008	0.010	0.015	0.020	0.020
c. Failure of weld	0.012	0.018	0.800	0.003	0.008	0.010	0.015	0.015
Composite top clip angle bottom [9]								
a. Failure of deck reinforcement	0.018	0.035	0.800	0.005	0.010	0.015	0.020	0.030
b. Local flange yielding and web crippling of column	0.036	0.042	0.400	0.008	0.020	0.030	0.025	0.035

Table A.2.d: Part four of Table 5-6 of FEMA 356 (Courtesy of Federal Emergency Management Agency).

Table 5-6 Modeling Parameters and Acceptance Criteria for Nonlinear Procedures—Structural Steel Components (continued)

	Modeling Parameters			Acceptance Criteria				
	Plastic Rotation Angle, Radians		Residual Strength Ratio	Plastic Rotation Angle, Radians				
					Primary		Secondary	
Component/Action	**a**	**b**	**c**	**IO**	**LS**	**CP**	**LS**	**CP**
c. Yield of bottom flange angle	0.036	0.042	0.200	0.008	0.020	0.030	0.025	0.035
d. Tensile yield of rivets or bolts at column flange	0.015	0.022	0.800	0.005	0.008	0.013	0.013	0.018
e. Shear yield of beam flange connection	0.022	0.027	0.200	0.005	0.013	0.018	0.018	0.023
Shear connection with slab[12]	$0.029-0.0002d_{bg}$	$0.15-0.0036d_{bg}$	0.400	$0.0073-0.0001d_{bg}$	--	--	$0.1125-0.0027d_{bg}$	$0.15-0.0036d_{bg}$
Shear connection without slab[12]	$0.15-0.0036d_{bg}$	$0.15-0.0036d_{bg}$	0.400	$0.0375-0.0009d_{bg}$	--	--	$0.1125-0.0027d_{bg}$	$0.15-0.0036d_{bg}$
EBF Link Beam[10, 11]								
a. $e \le \frac{1.6\,M_{CE}}{V_{CE}}$	0.15	0.17	0.8	0.005	0.11	0.14	0.14	0.16
b. $e \ge \frac{2.6\,M_{CE}}{V_{CE}}$	Same as for beams.							
c. $\frac{.6\,M_{CE}}{V_{CE}} < e < \frac{2.6\,M_{CE}}{V_{CE}}$	Linear interpolation shall be used.							
Steel Plate Shear Walls[1]	$14\theta_y$	$16\theta_y$	0.7	$0.5\theta_y$	$10\theta_y$	$13\theta_y$	$13\theta_y$	$15\theta_y$

1. Values are for shear walls with stiffeners to prevent shear buckling.
2. Columns in moment or braced frames shall be permitted to be designed for the maximum force delivered by connecting members. For rectangular or square columns, replace $b_f/2t_f$ with b/t, replace 52 with 110, and replace 65 with 190.
3. Plastic rotation = 11 $(1-1.7\ P/P_{CL})\ \theta_y$.
4. Plastic rotation = 17 $(1-1.7\ P/P_{CL})\ \theta_y$.
5. Plastic rotation = 8 $(1-1.7\ P/P_{CL})\ \theta_y$.
6. Plastic rotation = 14 $(1-1.7\ P/P_{CL})\ \theta_y$.
7. Columns with $P/P_{CL} > 0.5$ shall be considered force-controlled.
8. For high-strength bolts, divide values by 2.0.
9. Web plate or stiffened seat shall be considered to carry shear. Without shear connection, action shall not be classified as secondary. If beam depth, $d_b > 18$ inches, multiply *m*-factors by $18/d_b$.
10. Deformation is the rotation angle between link and beam outside link or column.
11. Values are for link beams with three or more web stiffeners. If no stiffeners, divide values by 2.0. Linear interpolation shall be used for one or two stiffeners.
12. *d* is the beam depth, d_{bg} is the depth of the bolt group.
13. Tabulated values shall be modified as indicated in Section 5.5.2.4.2, item 4.